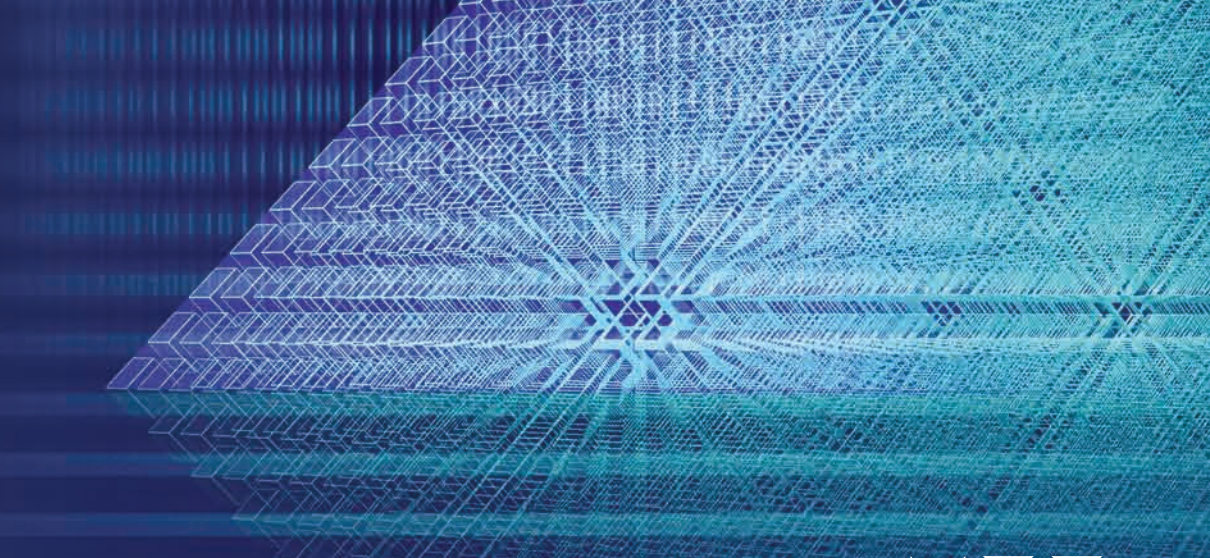

TECHNICAL REPORTS SERIES NO. 457

Dosimetry in Diagnostic Radiology: An International Code of Practice

IAEA
International Atomic Energy Agency

DOSIMETRY IN DIAGNOSTIC RADIOLOGY: AN INTERNATIONAL CODE OF PRACTICE

The following States are Members of the International Atomic Energy Agency:

AFGHANISTAN
ALBANIA
ALGERIA
ANGOLA
ARGENTINA
ARMENIA
AUSTRALIA
AUSTRIA
AZERBAIJAN
BANGLADESH
BELARUS
BELGIUM
BELIZE
BENIN
BOLIVIA
BOSNIA AND HERZEGOVINA
BOTSWANA
BRAZIL
BULGARIA
BURKINA FASO
CAMEROON
CANADA
CENTRAL AFRICAN REPUBLIC
CHAD
CHILE
CHINA
COLOMBIA
COSTA RICA
CÔTE D'IVOIRE
CROATIA
CUBA
CYPRUS
CZECH REPUBLIC
DEMOCRATIC REPUBLIC OF THE CONGO
DENMARK
DOMINICAN REPUBLIC
ECUADOR
EGYPT
EL SALVADOR
ERITREA
ESTONIA
ETHIOPIA
FINLAND
FRANCE
GABON
GEORGIA
GERMANY
GHANA
GREECE
GUATEMALA
HAITI
HOLY SEE
HONDURAS
HUNGARY
ICELAND
INDIA
INDONESIA
IRAN, ISLAMIC REPUBLIC OF
IRAQ
IRELAND
ISRAEL
ITALY
JAMAICA
JAPAN
JORDAN
KAZAKHSTAN
KENYA
KOREA, REPUBLIC OF
KUWAIT
KYRGYZSTAN
LATVIA
LEBANON
LIBERIA
LIBYAN ARAB JAMAHIRIYA
LIECHTENSTEIN
LITHUANIA
LUXEMBOURG
MADAGASCAR
MALAWI
MALAYSIA
MALI
MALTA
MARSHALL ISLANDS
MAURITANIA
MAURITIUS
MEXICO
MONACO
MONGOLIA
MONTENEGRO
MOROCCO
MOZAMBIQUE
MYANMAR
NAMIBIA
NETHERLANDS
NEW ZEALAND
NICARAGUA
NIGER
NIGERIA
NORWAY
PAKISTAN
PALAU
PANAMA
PARAGUAY
PERU
PHILIPPINES
POLAND
PORTUGAL
QATAR
REPUBLIC OF MOLDOVA
ROMANIA
RUSSIAN FEDERATION
SAUDI ARABIA
SENEGAL
SERBIA
SEYCHELLES
SIERRA LEONE
SINGAPORE
SLOVAKIA
SLOVENIA
SOUTH AFRICA
SPAIN
SRI LANKA
SUDAN
SWEDEN
SWITZERLAND
SYRIAN ARAB REPUBLIC
TAJIKISTAN
THAILAND
THE FORMER YUGOSLAV REPUBLIC OF MACEDONIA
TUNISIA
TURKEY
UGANDA
UKRAINE
UNITED ARAB EMIRATES
UNITED KINGDOM OF GREAT BRITAIN AND NORTHERN IRELAND
UNITED REPUBLIC OF TANZANIA
UNITED STATES OF AMERICA
URUGUAY
UZBEKISTAN
VENEZUELA
VIETNAM
YEMEN
ZAMBIA
ZIMBABWE

The Agency's Statute was approved on 23 October 1956 by the Conference on the Statute of the IAEA held at United Nations Headquarters, New York; it entered into force on 29 July 1957. The Headquarters of the Agency are situated in Vienna. Its principal objective is "to accelerate and enlarge the contribution of atomic energy to peace, health and prosperity throughout the world".

TECHNICAL REPORTS SERIES No. 457

DOSIMETRY IN DIAGNOSTIC RADIOLOGY: AN INTERNATIONAL CODE OF PRACTICE

INTERNATIONAL ATOMIC ENERGY AGENCY
VIENNA, 2007

COPYRIGHT NOTICE

Printed by the IAEA in Austria
September 2007
STI/PUB/1294

IAEA Library Cataloguing in Publication Data

Dosimetry in diagnostic radiology : an international code of practice. — Vienna : International Atomic Energy Agency, 2007.
p. ; 24 cm. — (Technical reports series, ISSN 0074–1914 ; no. 457)
STI/DOC/-10/457
ISBN 92–0–115406–2
Includes bibliographical references.

1. Radiation dosimetry. — 2. Radiology, Medical. — 3. Radiation — Measurement. I. International Atomic Energy Agency. II. Series : Technical reports series (International Atomic Energy Agency) ; 457.

IAEAL 07–00477

FOREWORD

International standardization in dosimetry is essential for the successful exploitation of radiation technology. Soon after it was founded, the IAEA initiated a programme on the dosimetry of ionizing radiation, helping Member States develop the calibration and measurement capabilities necessary for the application of radiation in medicine, radiation protection, industry and other applications. The IAEA disseminates standards for radiation measurement, conducts dose audits and comparisons, develops and transfers dosimetry techniques, and provides training and guidance on radiation measurements. Much of this work is carried out through the IAEA/WHO Secondary Standards Dosimetry Laboratory (SSDL) network.

For some time now there has been a growing awareness that radiation dose originating from medical diagnostic procedures in radiology is contributing an increasing proportion of the total population dose. This has been particularly evident for examinations using computed tomography equipment, where increasing usage with patient doses in excess of occupational safety limits is well established. However, diagnostic X ray imaging generally covers a diverse range of examination types, many of which are increasing in frequency and technical complexity. This has resulted in the development of new dosimetric measuring instruments, techniques and terminologies which present challenges to those working in the clinical environment and those supporting them in calibration facilities.

In response to heightened awareness of the importance of patient dose contributed by radiology procedures, there has been a general trend to effect control of patient doses by applying the principles of optimization coupled with an increase in regulatory enforcement. This has been reflected by an increasing demand from Member States for the IAEA to provide assistance in establishing programmes for quality assurance and quality control of X rays used in diagnostic radiology. A high level of dosimetry in radiology departments in Member States cannot be achieved without a systematic and consistent approach.

Following the recommendations of the advisory committee for the IAEA/WHO SSDL network, known as the SSDL Scientific Committee, development of a new Code of Practice for Dosimetry in Diagnostic Radiology was started in 2000 with the appointment of a drafting group that included: G. Alm Carlsson (Sweden), D.R. Dance (United Kingdom), L. DeWerd (United States of America), H.-M. Kramer (Germany), K.-H. Ng (Malaysia), F. Pernička (Czech Republic) and P. Ortiz Lopez (IAEA).

This publication is seen as a continuation of the IAEA's policy of providing guidance in the area of dosimetry of ionizing radiation for medical

physics and follows on from Absorbed Dose Determination in External Beam Radiotherapy: An International Code of Practice for Dosimetry Based on Standards of Absorbed Dose to Water (Technical Reports Series No. 398), which was published in 2000. The Code of Practice for Dosimetry in Diagnostic Radiology addresses issues of dosimetry involving calibrations and measurements from the perspective of both the SSDLs and the clinical users. This Code of Practice has been endorsed by WHO and PAHO.

The IAEA technical officers responsible for the preparation of this report were F. Pernička and I.D. McLean of the Division of Human Health.

CONTENTS

Chapter 1

INTRODUCTION

In 1995, the world celebrated the 100th anniversary of the discovery of X rays by W.C. Röntgen. His discovery was the first to enable the display of human internal anatomical structures and it revolutionized the field of medicine. Since then, the use of X rays has contributed to the diagnosis and treatment of many diseases thereby helping to improve the health of people all over the world. Medical imaging systems have developed from simple units used to image specific anatomical sites to systems that can visualize the whole body, obtain information concerning functional aspects of specific organs and even yield information about the chemistry taking place in organs and tissues. Nowadays, medical imaging equipment is taking advantage of modern digital technology and has become a symbol of 'high technology'.

1.1. FROM SCREEN–FILM RADIOGRAPHY TO DIGITAL TECHNIQUES

Imaging with X rays utilizes a range of techniques. Projection radiography using screen–film technology is the most common imaging modality used in radiology. The X rays are attenuated in the body depending on the type and the thickness of the tissues through which they have to pass. The transmitted X rays are detected by special screens emitting light after interaction with X rays. The emitted light is further detected by the film. Dual screen, dual emulsion film systems are commonly used in radiographic procedures such as chest, abdominal and skull radiography. When high resolution is needed, as in mammography, single screen and single emulsion film systems are used. During the radiography examination, the X ray attenuation information about the human anatomy is projected into the two dimensions of the radiograph. Once the exposed film is chemically processed to create a visible image, it can be displayed on a light box, transported wherever it is needed and kept as an archival record. X ray film systems enable the radiologist to acquire, display, communicate and store image data in a simple way. This technique remains one of the most widely used medical diagnostic tools.

Fluoroscopy is an imaging procedure that allows real time viewing of anatomical structures. As in projection radiography, this is a two dimensional imaging technique but it uses image intensifiers and displays images on a TV

monitor. Fluoroscopic systems have undergone significant technological advances in recent years. For example, they are available with image intensifiers allowing the viewing of the entire abdomen. Depending on the application, these systems are available in a wide variety of modifications (gastrointestinal, angiographic, etc.). Hospitals usually have suites dedicated to specialized applications. The long fluoroscopy times, especially during interventional procedures, may result in local patient doses that cause deterministic effects[1] of radiation in patients. It is important to optimize such investigations to reduce unnecessary exposure of patients and medical staff.

In the 1970s, the development of computed tomography (CT) revolutionized diagnostic radiology. This technique currently utilizes a rotating fan beam of X rays, a corresponding sector of detectors and a computer to reconstruct cross-sectional images of the patient's internal anatomy. Continuing technological developments, such as spiral (or helical) scanning and multislice scanners, have improved both the speed and quality with which images are obtained. Fast scan times and rapid image reconstruction have allowed the development of real time CT scanning. Development of CT was only made possible by a massive development in computer technology. CT started the era of computerized diagnostic methods that are gradually replacing traditional film based diagnostic techniques.

CT also represents one of the earliest forms of digital X ray imaging, in which images are captured and stored in a digital format. More recent developments in digital radiology include digital fluorography employing an image intensifier and computed radiography utilizing a special storage phosphor plate which retains the latent image. Unlike computed radiography, direct digital radiography uses an active matrix detector, typically of amorphous selenium or a phosphor coupled to silicon to convert X ray energy to a digital signal virtually instantaneously with no intermediate operational steps. Digital imaging provides key advantages in the manipulation, storage and transmission of images.

Digital radiological techniques offer the potential for improved image quality and, given the higher sensitivity of its image receptors compared with film, also offers the potential for dose reduction. In practice, however, since image receptors also have a broader dynamic range than film, higher doses are correspondingly possible.

Advances in imaging have facilitated the development of interventional radiological procedures, in which imaging is used to help guide therapeutic

[1] A radiation effect for which generally a threshold level of dose exists above which the effect is manifested. The severity of the effect is greater for a higher dose.

procedures. For example, angioplasty is done fluoroscopically and involves placing and expanding a balloon catheter inside a blood vessel so as to dilate the vessel and improve blood flow. Interventional radiology continues to evolve and other commonly used therapeutic techniques make use of imaging technologies.

In this Code of Practice, separate descriptions of methodology are given for the areas of general radiography, fluoroscopy, mammography, CT and dental radiography. In this context, general radiography implies all radiography apart from the latter four modalities.

1.2. PATIENT EXPOSURES IN RADIOLOGY

Medical ionizing radiation sources provide by far the largest contribution to the population dose from artificial sources and most of this contribution comes from diagnostic X rays (above 90%). One of the reasons for this situation is the large number of X ray examinations performed every year. A report by the United Nations Scientific Committee on the Effects of Atomic Radiation [1.1] estimates that the annual number of all types of medical X ray examination undertaken in the world was about 2100 million in 2000, corresponding to an annual frequency of 360 examinations per 1000 individuals worldwide. This frequency is about 10% higher than the previous estimate of 330 per 1000 for the period 1991–1995 [1.2] indicating an increase in practice. Three quarters of all examinations occur in countries accorded health care level I[2], which account for only one quarter of the world population. Only 1% arises from the lower healthcare levels III and IV, which include one fifth of the world population. However, further growth in medical radiology can be expected in developing countries where facilities and services are often lacking.

The typical highest organ doses in projection radiography, including mammography, range from 1–20 mGy [1.1], but an increasing part of medical radiation exposure is due to the use of X ray procedures. These include CT, fluoroscopy and various interventional procedures. CT procedures result in organ doses in the range of 10–100 mGy, generally below the level required to produce deterministic effects. However, all X ray procedures may give rise to stochastic effects, namely tumour induction or hereditary effects.

Current fluoroscopy machines produce incident air kerma rates of typically less than 0.02 Gy/min in normal mode but can produce 0.2 Gy/min in high dose rate mode. Prolonged use of these machines, especially at high dose

[2] WHO classification.

rate mode, can result in skin doses higher than 2 Gy, the threshold level for some deterministic effects. Such high dose levels may also be reached with CT fluoroscopy. The likelihood and severity of skin injury depends on the dose delivered to a particular portion of skin. It is important to note that fluoroscopy is often performed by non-radiologists with limited knowledge of radiation effects and methods of how to avoid or reduce them. This may increase the chance of producing deterministic effects during interventional procedures.

1.3. QUALITY ASSURANCE AND DOSE MANAGEMENT

Radiologists constantly face the dilemma of trying to minimize patient exposure whenever possible, while still using exposures that are high enough to produce images of good enough quality as to be able to provide a proper diagnosis. Quality assurance provides a framework for achieving this goal. The basic strategy for quality assurance in diagnostic radiology was formulated by the WHO [1.3] and involves various activities, including managerial and technical activities. The International Basic Safety Standards for Protection against Ionizing Radiation and for the Safety of Radiation Sources (BSS) [1.4] provide requirements to establish a quality assurance programme for medical exposures. These principles are further developed in Safety Guide No. RS-G-1.5 [1.5]. It is necessary that a quality assurance programme in diagnostic and interventional radiology include image quality assessment, film reject analysis, patient dose evaluation, measurements of physical parameters of the radiation generators, etc. Various quality control tests are needed to ensure that the radiology machines are working properly.

The BSS also require that guidance levels be established to provide guidance on what is achievable with current good practice. The guidance levels should be derived from the data provided from wide scale surveys. They should be revised as technology and techniques develop. The European Union has adopted a similar approach. In the directive towards “health protection of individuals against the dangers of ionising radiation in relation to medical exposures”, it requires extensive dose measurements [1.6] and establishment of diagnostic reference levels that can be regarded as synonymous with those guidance levels used by the IAEA. It is important to note that optimization in radiology does not always lead to dose reduction. This was documented in the nationwide evaluation of X ray trends [1.7] undertaken in the United States of America. In this context, it is important to stress that the image quality must always be sufficient for the clinical need.

1.4. NEED FOR DOSIMETRY

As stated above, exposures resulting from radiological procedures constitute the largest part of the population exposure from artificial radiation. There is a need to control these doses and therefore to optimize the design and use of X ray imaging systems. It is generally recognized that even a 10% reduction in patient dose is a worthwhile objective for optimization. The main aim of patient dosimetry with respect to X rays used in medical imaging is to determine dosimetric quantities for the establishment and use of guidance levels (diagnostic reference levels) and for comparative risk assessment [1.8]. In the latter case, the average dose to the organs and tissues at risk should be assessed. Only a limited number of measurements serve for potential risk assessment of the examination or intervention. An additional objective of dosimetry in diagnostic and interventional radiology is the assessment of equipment performance as a part of the quality assurance process.

In many situations, it is of interest to make measurements directly on the patient. However, it is preferable to make measurements using a standard phantom to simulate the patient for the control of technical parameters, for the comparison of different systems and for optimization. Various examination techniques are used in X ray diagnostics. In some cases, specialized dosimeters are required, the design and performance of which must be matched to the needs of the clinical measurement. The use of such dosimeters and/or the interpretation of the results obtained may require specialized techniques and knowledge. It is essential to standardize the procedures for the dose measurement in the clinic.

Owing to the increased demand for dosimetry measurements in diagnostic and interventional radiology, it has become important to provide traceability of measurements in this field. The IAEA ensures traceability of radiation measurements through the IAEA/WHO network of Secondary Standards Dosimetry Laboratories (SSDLs). At present, the manner in which calibrations at diagnostic radiation qualities are performed is not properly coordinated. Many laboratories use different radiation qualities and standards, some of which may be unsuitable. Quality control can only work satisfactorily if correct calibrations and measurements are made. This suggests the need for guidance for these laboratories and for those that may wish to join them in the future.

REFERENCES

[1.1] UNITED NATIONS, Sources and Effects of Ionizing Radiation (Report to the General Assembly with Scientific Annexes), Scientific Committee on the Effects of Atomic Radiation (UNSCEAR), UN, New York (2000).

[1.2] UNITED NATIONS, Sources and Effects of Ionizing Radiation (Report to the General Assembly with Scientific Annexes), Scientific Committee on the Effects of Atomic Radiation (UNSCEAR), UN, New York (1996).

[1.3] WORLD HEALTH ORGANIZATION, Quality Assurance in Diagnostic Radiology, WHO, Geneva (1982).

[1.4] FOOD AND AGRICULTURE ORGANIZATION OF THE UNITED NATIONS, INTERNATIONAL ATOMIC ENERGY AGENCY, INTERNATIONAL LABOUR ORGANIZATION, OECD NUCLEAR ENERGY AGENCY, PAN AMERICAN HEALTH ORGANIZATION, WORLD HEALTH ORGANIZATION, International Basic Safety Standards for Protection against Ionizing Radiation and for the Safety of Radiation Sources, Safety Series No. 115, IAEA, Vienna (1996).

[1.5] INTERNATIONAL ATOMIC ENERGY AGENCY, Radiological Protection for Medical Exposure to Ionizing Radiation, IAEA Safety Standards Series No. RS-G-1.5, IAEA, Vienna (2000).

[1.6] EUROPEAN COMMISSION, Council Directive 97/43/Euratom of 30 June 1997 on Health Protection of Individuals Against the Dangers of Ionizing Radiation in Relation to Medical Exposure, and repealing Directive 84/466/Euratom, Off. J. Eur. Comm. Rep. L. 180, Luxembourg (1997) 22–27.

[1.7] SULEIMAN, O.H., STERN, S.H., SPELIC, D.C., Patient dosimetry activities in the United States: The nationwide evaluation of X-ray trends (NEXT) and tissue handbooks, Appl. Radiat. Isot. **50** (1999) 247–259.

[1.8] ZOETELIEF, J., et al., "Dosimetry in diagnostic and interventional radiology: International commission on radiation units and measurements and IAEA activities", Standards and Codes of Practice in Medical Radiation Dosimetry (Proc. Int. Symp. Vienna, 2002), Vol. 1, IAEA, Vienna (2003) 387–404.

Chapter 2

FRAMEWORK

2.1. INTRODUCTION

Dosimetry in diagnostic radiology requires the use of specialized instrumentation, the design and performance of which must be matched to the needs of the clinical situation. The use of this instrumentation and the interpretation of the results obtained may require specialized techniques and knowledge. It is essential to standardize procedures for dose measurements in the clinic. In addition, there are special requirements for the calibration of such instruments so that the measurements are traceable to national or international standards. Clinical needs together with the international programmes that aim at traceability of measurements constitute the two pillars of the framework for dosimetry measurements in diagnostic radiology.

2.2. CLINICAL NEEDS

In radiotherapy it is considered that an accuracy of 5% in the delivery of an absorbed dose to target volume is needed [2.1]. This statement was made in a context where the uncertainty was estimated at the 95% confidence level, and has been interpreted as if it corresponds to approximately two standard deviations. The statement defines goals for calibration of dosimeters used in radiotherapy, calibration of the beams in clinics and calculation of dose distributions and dose delivered to the target volume [2.2]. Dosimetry requirements in radiotherapy are strict but they are needed owing to the critical balance between tumour eradication and complications in healthy tissues.

Assessment of the health effects of radiation from X ray diagnostic examination is subject to considerable uncertainty. The effect of accuracy or precision of diagnostic dosimeters on the overall uncertainty is much lower than the contribution attributable to our incomplete knowledge of risks from exposures to low level ionizing radiations. Nevertheless, it is desirable that the uncertainty associated with the measurements be small.

The issue of required performance of diagnostic dosimeters was formally addressed by the American Association of Physicists in Medicine (AAPM) [2.3], which divided measurements into those used to assess the risk of radiation damage from X ray examinations, those performed as a part of quality assurance programmes and radiation surveys of workplaces and places

occupied by the general public. All statements on accuracy made by the AAPM assumed that uncertainties were estimated at the 99% confidence level, which corresponds approximately to three standard deviations. However, throughout the world, the 95% probability level (approximately two standard deviations) has been adopted for confidence limits of measurements. The original AAPM recommendations on measurement uncertainties discussed here have been corrected following this concept.

If not specifically indicated, throughout this Code of Practice the measurement uncertainties express the 95% confidence limits of the results (coverage factor $k = 2$; see Appendix I).

2.2.1. Dosimetry requirements

2.2.1.1. Risk assessment

Examinations in diagnostic radiology usually result in a limited irradiation of the body. As the doses delivered are relatively low and the uncertainty in the absolute risk for a stochastic effect is high, a required accuracy of 20% in dosimetry measurements for estimating the absolute risk during radiology examination of adults is sufficient. The higher accuracy, similar to the accuracy of dosimetry measurements in radiotherapy, is required for cases where deterministic effects are expected. In this case an accuracy of 7% is more appropriate. The higher accuracy is also required for measurements used to estimate relative risks associated with various procedures, techniques or technologies. It is worthwhile knowing that one technique or technology will produce a lower dose than another, thus enabling a reduction in the risk of radiation induced cancer. It is believed that for comparative dose measurements, the uncertainty of 7% is appropriate.

There is good evidence for increased sensitivity to radiation in younger persons [2.4]. The risks associated with a given absorbed dose of radiation are thus higher for children than for adults. It is believed that an uncertainty of 7% in dosimeter reading is sufficient for assessing the potential risk of paediatric examinations.

Throughout most of pregnancy, the embryo/foetus is assumed to be at about the same level of carcinogenic risk as children. In addition, developmental effects in unborn children are important. These include malformations, growth disturbances and lethal effects. The important factors regarding these effects are the dose and the stage of gestation at which it is delivered. Again, a 7% uncertainty in the measurement is much less than other uncertainties in the estimation of dose to a conceptus and this value should be sufficient.

2.2.1.2. Quality assurance and equipment testing

Quality assurance programmes in diagnostic radiology cover all planned and systematic actions necessary to provide adequate confidence that the optimum quality of the entire diagnostic process, namely, the consistent production of adequate diagnostic information with minimum exposure of patients and personnel, is achieved [2.5]. For a selected imaging technique, the final result depends on the equipment performance and on its use by the operators. Therefore, control of the performance of the imaging equipment is necessary. Measurements of various parameters must be performed on a routine basis to ensure the optimal functioning of the equipment. Some of these measurements require the use of dosimeters. These include measurements of the X ray tube output and its linearity with a tube current or a tube current–exposure time product, reproducibility, etc. The X ray beams are specified in terms of a half-value layer (HVL) that has also to be established. In addition, knowledge of the HVL is important for establishing backscatter factors and conversion coefficients which relate a measured quantity to a quantity used for the estimation of organ dose(s).

The quality assurance measurements can again be divided into two categories: (i) those for the establishment of an absolute value of the investigated parameter and (ii) those that allow comparison with the baseline value established for the same unit or with the value of the parameter established for another unit. In the first case, it is important that the uncertainty of the dose measurement be small enough that the required overall uncertainty of the measured parameter is achieved. In the second case, the same criteria as those for comparative measurement of the risk assessment apply. It is believed that in both cases the 7% uncertainty in dose measurement is sufficient.

2.2.1.3. Radiation surveys

Radiation surveys are performed to identify and quantify exposure levels in areas of potential risk to individuals. In diagnostic radiology, X ray rooms and surrounding public areas are surveyed. Since the uncertainty in the absolute risk for stochastic effects is high, a required accuracy of 20% in dosimetry measurements should be sufficient.

2.2.2. Goals of the Code of Practice

The required accuracy of dosimetry measurements described in this Code of Practice is 7%. This relates to the accuracy of dosimetry quantities directly

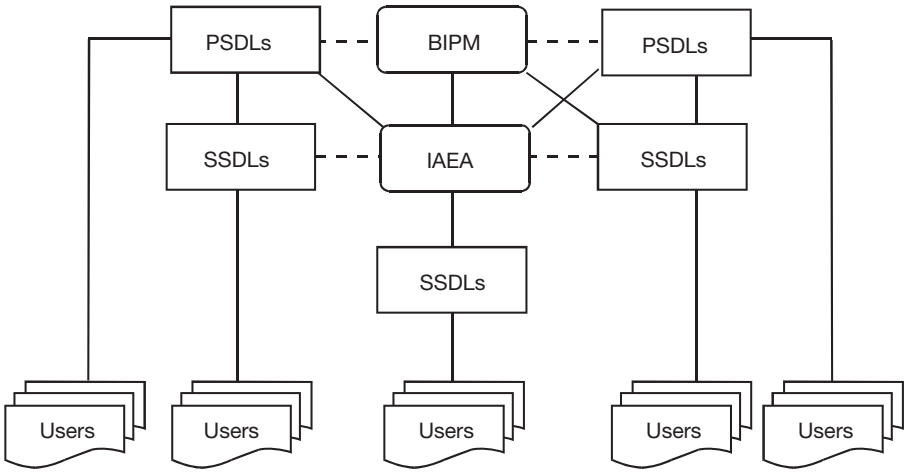

FIG. 2.1. The IMS for radiation metrology, where the traceability of user reference instruments to primary standards is achieved either by direct calibration in a PSDL or, more commonly, in an SSDL with direct link to the BIPM, a PSDL or to the IAEA/WHO network of SSDLs. Most SSDLs from countries not members of the Mètre Convention achieve the traceability of their standards through the IAEA. The dashed lines indicate intercomparisons of primary and secondary standards (adapted from Ref. [2.2]).

measured by the dosimeter and does not include a contribution from sources used to convert the measured quantity to tissue or organ doses. The accuracy corresponds to the 95% confidence level (coverage factor $k = 2$).

An accuracy of 20% is acceptable in cases where the organ dose is low and for radiation survey measurements. The survey measurements are not covered by this Code of Practice. For some investigations (e.g. research), narrower limits of uncertainty may be required.

2.3. THE INTERNATIONAL MEASUREMENT SYSTEM (IMS)

The IMS for radiation metrology constitutes the second pillar of the framework for dosimetry in diagnostic radiology. It provides a mechanism for consistency in radiation dosimetry by disseminating to users calibrations of radiation instruments, which are traceable to primary standards (see Fig. 2.1 and Table 2.1). The IMS consists of the Bureau International des Poids et Mesures (BIPM), national Primary Standards Dosimetry Laboratories (PSDLs), SSDLs and various users performing measurements.

2.3.1. SSDLs

Worldwide, there are only some twenty countries with PSDLs involved in radiation dosimetry and these institutions cannot calibrate the very large number of radiation dosimeters that are in use all over the world. The main role of SSDLs is to bridge the gap between the PSDLs and the users of ionizing radiation by enabling the transfer of calibrations from the primary standard to the user instrument. The SSDLs disseminate calibrations at specific radiation qualities appropriate for the use of the instrument and issue statements regarding the uncertainty of this calibration. In many countries, the SSDLs provide the expert services in dosimetry to end users in hospitals and other institutions involved in the application of ionizing radiation. In some countries, the role of the SSDL is fulfilled by accredited secondary calibration laboratories. As an example one can mention the accredited dosimetry calibration laboratories in the USA. It is required that these laboratories possess a secondary standard calibrated at one of the PSDLs, participate in comparisons and are authorized (accredited) for this activity by the national metrology body.

Historically, the SSDLs have focused mainly on calibrating instruments for use in the measurement of doses in radiation therapy and radiation protection and have paid much less attention to the calibration of instruments used for dosimetry measurements in diagnostic radiology. This was mainly due to a lack of demand in the past. Increasing demand, driven mainly by a need for establishing quality assurance programmes in hospitals, now necessitates expanding calibration services. The SSDLs have to address new metrology issues such as calibrations of mammography and CT dosimeters and also various non-invasive high voltage measuring devices. Nowadays, these services are still deficient in many countries.

In response to the existing situation regarding the calibration of diagnostic radiology dosimetry instruments, some of the equipment manufacturers have taken the initiative and calibrate their products themselves. This Code of Practice does not recommend this practice unless the manufacturer is authorized (accredited) to provide such a service by the national metrology body. Subsequent use of this calibration in other countries requires that it be recognized by the metrological body in the country of use.

2.3.1.1. The IAEA/WHO network of SSDLs

In 1976, a network of SSDLs was established, as a joint effort, by the IAEA and the WHO in order to disseminate calibrations to users by providing the link between users and primary standards, mainly for countries that are not

members of the Mètre Convention. By 2007, the SSDL network included 80 laboratories and 6 SSDL national organizations in 67 countries, of which over half were developing countries. The SSDL network also included 20 affiliated members, mainly the BIPM, several national PSDLs, the International Commission for Radiation Units and Measurements (ICRU) and other international organizations [2.6]. All provide support to the network. Secretariat functions for the SSDL network are shared between the IAEA and the WHO.

The network of SSDLs is responsible for assuring that the services provided by the laboratories follow internationally accepted metrological standards. At present, this is achieved by providing traceable calibrations of SSDL's standards for therapy, radiation protection and diagnostic radiology instruments and for participation in quality audits (comparison programmes). The traceability is accomplished with the transmission of calibration coefficients for ionization chambers from the BIPM or PSDLs through the IAEA dosimetry laboratory. In 2007, about 40% of SSDLs provided calibrations of diagnostic radiology dosimeters; some SSDLs are considering starting these activities.

Membership of the SSDL network is open to laboratories designated by their national competent authority. The privileges, rights and duties of members in the network are specified in the SSDL Network Charter [2.7]. The IAEA publishes an SSDL newsletter biannually, which is distributed to the members of the SSDL network and to the scientific community.

2.3.2. Diagnostic radiology standards

2.3.2.1. Standards of air kerma

All PSDLs employ free air chambers for the realization of the unit of air kerma in low and medium energy X ray beams. Plane parallel and cylindrical types of different designs are in use. A review of the characteristics and design of free air chambers was given by Lee et al. [2.8].

The air kerma determined by the BIPM is used as the key comparison reference value and is therefore of particular importance. Values for the physical constants and correction factors which are used by the BIPM in the determination of the air kerma rate for low and medium energy X rays and their estimated relative standard uncertainties are given in Boutillon et al. [2.9]. The relative combined standard uncertainties associated with the realization of the unit gray for the quantity air kerma of low and medium energy X rays at the BIPM are 0.20% and 0.22%, respectively. The main component is the relative uncertainty of W_{air}/e, which is 0.15% [2.10].

TABLE 2.1. CLASSIFICATION OF INSTRUMENTS AND STANDARDS LABORATORIES (ADAPTED FROM REF. [2.2])

Classification of instruments	Standards laboratories
Primary standard: An instrument of the highest metrological quality that permits determination of the unit of a quantity from its definition, the accuracy of which has been verified by comparison with the comparable standards of other institutions at the same level	PSDL: A national standardizing laboratory designated by the government for the purpose of developing, maintaining and improving primary standards in radiation dosimetry
Secondary standard: An instrument calibrated by comparison with a primary standard	SSDL: A dosimetry laboratory designated by the competent authorities to provide calibration services and which is equipped with at least one secondary standard that has been calibrated against a primary standard
National standard: A standard recognized by an official national decision as the basis for fixing the value in a country of all other standards of the given quantity	
Reference instrument: An instrument of the highest metrological quality available at a given location, from which measurements at that location are derived	
Field instrument: A measuring instrument used for routine measurements whose calibration is related to the reference instrument	

Comparisons of standards for low energy X rays from BIPM and national metrology institutes (NMIs) are usually made directly, i.e. by successively measuring the air kerma rate in the BIPM beam with the two standards. In the low energy region, five different radiation qualities with tube potentials between 10 kV and 50 kV are used. Comparisons of standards for medium energy X rays are usually made indirectly, namely, by employing a transfer standard, which may explain the slightly higher uncertainty of the comparison results of this kind. Four different radiation qualities with tube potentials between 100 kV and 250 kV are used.

Taking into account correlations of uncertainty components between different standards, the relative standard uncertainties in $R_{K,NMI}$, which is the air kerma rate ratio measured with the NMI and BIPM standards, are typically as low as 0.25% and 0.30%. Air kerma comparisons have been made between the standards of the BIPM and those of several Member States of the Mètre Convention maintaining primary standards of this kind. Figure 2.2 shows the current status of the comparison results for low and medium energy X rays. The values are taken from the relevant BIPM reports, which are available on the BIPM web site but which are not referenced separately here. The majority of the results lie within the typical expanded uncertainty claimed for the ratio $R_{K,NMI}$ (indicated in Fig. 2.2 as dotted lines).

2.3.3. Mutual recognition arrangement (MRA)

The globalization of research, development and particularly trade and commerce requires new metrological approaches. Mutual recognition of national measurement standards and calibration certificates is needed for acceleration of exchange of knowledge and goods. In addition, there is enormous economic potential for such an arrangement.

In October 1999, the directors of the NMIs of 38 Member States of the Mètre Convention and representatives of two international organizations signed the MRA [2.11]. The MRA was signed under the auspices of the International Committee for Weights and Measures.

The outcome of the MRA is a determination of the degree of equivalence of national standards and a set of statements on the measurement capabilities of each NMI. These objectives are achieved through a process of:

- International comparisons of measurements, known as key comparisons;
- Supplementary international comparisons of measurements;
- Quality systems and demonstrations of competence by the NMIs.

The MRA provides for the formal recognition of national measurement standards and calibration and measurement capabilities and is expected to become the basis for wider arrangements related to international trade, commerce and regulatory affairs.

2.3.3.1. Relevance of the MRA to the IAEA/WHO SSDL network

The main objective of the SSDL network is to ensure traceability of measurements, for those Member States that do not have access to PSDLs, by

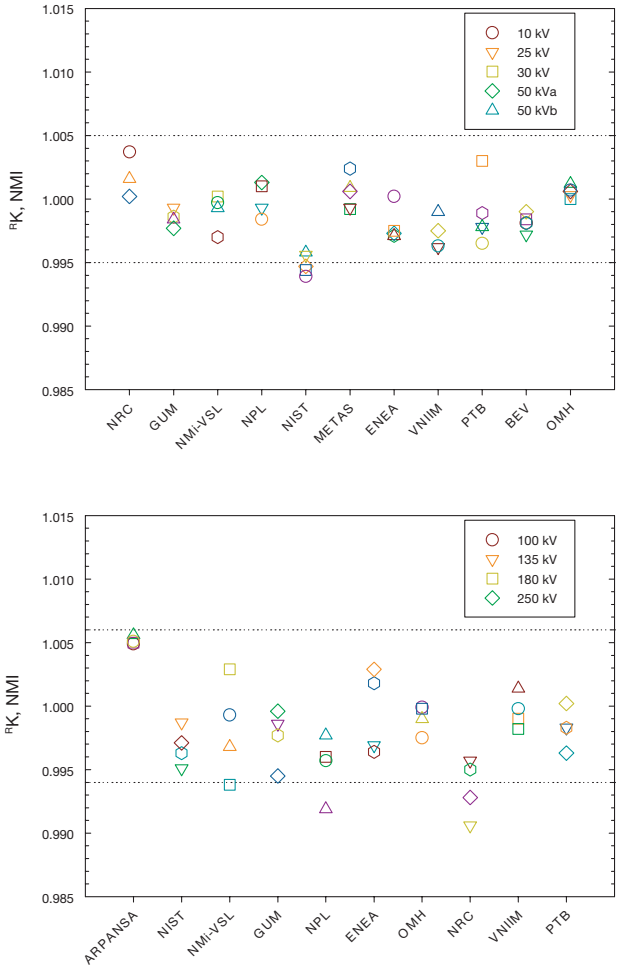

FIG. 2.2. Results of BIPM low (upper) and medium energy (lower) X ray comparisons, expressed as the ratio of the air kerma rate determined with the standard of the NMI to that determined with the BIPM standard. Laboratories: ARPANSA — Australian Radiation Protection and Nuclear Safety Agency (Australia); BEV — Bundesamt für Eich- und Vermessungswesen (Austria); ENEA — Ente per le nuove tecnologie, l'energia e l'ambiente (Italy); GUM — JCGM Working Group on the Expression of Uncertainty in Measurement; METAS — Bundesamt für Metrologie und Akkreditierung Schweiz (formerly OFMET) (Switzerland); NIST — National Institute of Standards and Technology (USA); NMi–VSL — Nederlands Meetinstitut – Van Swinden Laboratorium (Netherlands); NPL — National Physical Laboratory (United Kingdom); NRC — National Research Council (Canada); OMH — Országos Mérésugyi Hivatal (Hungary); PTB — Physikalisch-Technische Bundesanstalt (Germany); VNIIM — D.I. Mendelev Institute for Metrology (Russian Federation).

providing and maintaining the link between the end users of radiation and the international measurement system [2.7]. However, the dissemination of each type of calibration needs to be verified periodically through quality audits and comparisons organized by the IAEA or by a regional metrology organization. By linking to its NMI, any SSDL can take part in a calibration comparison. However, their results cannot be included in the BIPM key comparison database unless their NMI is a signatory to the MRA and the SSDL is specifically mentioned as a designated laboratory for ionizing radiation standards.

There are 48 Member States in the SSDL network which are signatories to the MRA. This leaves a number of NMIs (SSDLs) that will not be able to submit their results to the BIPM key comparison database, nor have their calibration and measurement capabilities been included in Appendix C of the MRA. For these NMIs in particular, traceability of their standards to those of the IAEA and the radiation dosimetry comparisons with the IAEA are both crucial supports for the credibility of their measurement infrastructure.

Each time the IAEA organizes dosimetry comparisons with the SSDLs, it is effectively functioning as an international metrology organization. The IAEA provides a strong link to the MRA for the IAEA Member States that are otherwise excluded. This should bring benefits to those SSDLs in terms of strengthening their position as the dosimetry reference of their country.

REFERENCES

[2.1] INTERNATIONAL COMMISSION ON RADIATION UNITS AND MEASUREMENTS, Determination of Absorbed Dose in a Patient Irradiated by Beams of X or Gamma Rays in Radiotherapy Procedures, ICRU Rep. 24, ICRU, Bethesda, MD (1976).

[2.2] INTERNATIONAL ATOMIC ENERGY AGENCY, Absorbed Dose Determination in External Beam Radiotherapy: An International Code of Practice for Dosimetry Based on Standards of Absorbed Dose to Water, Technical Reports Series No. 398, IAEA, Vienna (2000).

[2.3] AMERICAN ASSOCIATION OF PHYSICISTS IN MEDICINE, Recommendations on Performance Characteristics of Diagnostic Exposure Meters, Report of AAPM Diagnostic X-Ray Imaging Group No. 6, Med. Phys. **19** (1991) 231–241.

[2.4] HALL, E.J., Radiobiology for the Radiologist, 5th edn, Lippincott, Williams and Wilkins, Philadelphia (2000).

[2.5] WORLD HEALTH ORGANIZATION, Quality Assurance in Diagnostic Radiology, WHO, Geneva (1982).

[2.6] INTERNATIONAL ATOMIC ENERGY AGENCY, IAEA Subprogramme in Dosimetry and Medical Radiation Physics, Report for 2004–2005, Report to the SSDL Scientific Committee, IAEA, Vienna (2006).

[2.7] INTERNATIONAL ATOMIC ENERGY AGENCY, The SSDL Network Charter, IAEA, Vienna (1999).
[2.8] LEE, J.-H., et al., The performance of the INER improved free-air ionization chamber in the comparison of air kerma calibration coefficients for medium-energy X-rays, Radiat. Mes. **39** (2005) 1–10.
[2.9] BOUTILLON, M., ALLISY-ROBERTS, P.J., BURNS, D.T., Measuring conditions used for the calibration of ionization chambers at the BIPM, Rapport BIPM-01/04, BIPM, Paris (2001).
[2.10] BOUTILLON, M., PERROCHE-ROUX, A.-M., Re-evaluation of the W value for electrons in dry air, Phys. Med. Biol. **32** (1987) 213–219.
[2.11] ALLISY-ROBERTS, P.J., THOMAS, C., SHORTT, K.R., MEGHZIFENE, A., The organization of the CIPM Mutual Recognition Arrangement and its relevance to the SSDL members of the IAEA/WHO Network, SSDL Newsl. **47** (2003).

Chapter 3

DOSIMETRIC QUANTITIES AND UNITS

In the past, various quantities have been used for specification of the dose in diagnostic radiology and there has been ambiguity because the same name has been used for different quantities. This Code of Practice generally follows ICRU 74 [3.1] on patient dosimetry for X rays used in medical imaging. It divides dosimetric quantities into basic and application specific quantities. Basic quantities are fundamental quantities defined in ICRU 60 [3.2]. Application specific quantities are practical dosimetric quantities that are used for measurements in diagnostic radiology. The notation used in this Code of Practice is based upon that used by ICRU 74 but, after discussion with the ICRU, has been simplified where the generality necessary in ICRU 74 is not required. Terms K_i and K_e are used to denote incident air kerma and entrance surface air kerma instead of $K_{a,i}$ and $K_{a,e}$. For CT dosimetry, all measurements described in this Code of Practice are made with an ionization chamber 100 mm long. An integration length of 100 mm is therefore used for the definitions of all CT air kerma related quantities and the notation modified accordingly.

3.1. BASIC DOSIMETRIC QUANTITIES

3.1.1. Fluence

The fluence, Φ, is the quotient dN by da, where dN is the number of particles incident on a sphere of cross-sectional area da, thus:

$$\Phi = \frac{dN}{da} \tag{3.1}$$

Unit: m^{-2}.

3.1.2. Energy fluence

The energy fluence, Ψ, is the quotient dR by da, where dR is the radiant energy incident on a sphere of cross-sectional area da, thus:

$$\Psi = \frac{\mathrm{d}R}{\mathrm{d}a} \tag{3.2}$$

Unit: J/m^2.

3.1.3. Kerma and kerma rate

The kerma, K, is the quotient $\mathrm{d}E_{\mathrm{tr}}$ by $\mathrm{d}m$, where $\mathrm{d}E_{\mathrm{tr}}$ is the sum of the initial kinetic energies of all the charged particles liberated by uncharged particles in a mass $\mathrm{d}m$ of material, thus:

$$K = \frac{\mathrm{d}E_{\mathrm{tr}}}{\mathrm{d}m} \tag{3.3}$$

Unit: J/kg. The special name for the unit of kerma is gray (Gy).

The kerma rate, $\dot{K}$, is the quotient $\mathrm{d}K$ by $\mathrm{d}t$, where $\mathrm{d}K$ is the increment of kerma in the time interval $\mathrm{d}t$, thus:

$$\dot{K} = \frac{\mathrm{d}K}{\mathrm{d}t} \tag{3.4}$$

Unit: J·kg^{-1}·s^{-1}. If the special name gray is used, the unit of kerma rate is gray per second (Gy/s).

3.1.4. Energy imparted

The mean energy imparted, $\bar{\varepsilon}$, to the matter in a given volume equals the radiant energy, R_{in}, of all those charged and uncharged ionizing particles which enter the volume minus the radiant energy, R_{out}, of all those charged and uncharged ionizing particles which leave the volume, plus the sum, ΣQ, of all changes of the rest energy of nuclei and elementary particles which occur in the volume, thus:

$$\bar{\varepsilon} = R_{\mathrm{in}} - R_{\mathrm{out}} + \Sigma Q \tag{3.5}$$

Unit: J.

For the photon energies used in diagnostic radiology, ΣQ is zero.

In this Code of Practice, the term 'mean energy imparted' is shortened to 'energy imparted'.

3.1.5. Absorbed dose

The absorbed dose, D, is the quotient $\mathrm{d}\bar{\varepsilon}$ by $\mathrm{d}m$, where $\mathrm{d}\bar{\varepsilon}$ is the mean energy imparted to matter of mass $\mathrm{d}m$, thus:

$$D = \frac{\mathrm{d}\bar{\varepsilon}}{\mathrm{d}m} \tag{3.6}$$

Unit: J/kg. The special name for the unit of absorbed dose is gray (Gy).

In diagnostic radiology, the production of bremsstrahlung within low atomic number materials is negligible. For a given material and radiation field, absorbed dose and kerma are then numerically equal when secondary electron equilibrium is established. There will be important numerical differences between the two quantities wherever secondary electron equilibrium is not established (i.e. close to an interface between different materials).

3.2. APPLICATION SPECIFIC DOSIMETRIC QUANTITIES

3.2.1. Rationale for choice of quantities

Several application specific quantities have been found useful in the past for measurements in diagnostic radiology. However, there has been ambiguity in the names of the quantities and their (sometimes incorrect) use. ICRU 74 [3.1] provides a consistent set of quantities, which is adopted in this Code of Practice.

A particular problem has been the use of 'absorbed dose' in situations where this quantity is inappropriate and cannot easily be measured because of a lack of secondary electron equilibrium. Figure 3.1 shows the variation of the air kerma, the polymethylmethacrylate (PMMA) kerma and the absorbed dose to air close to a PMMA–air interface for three diagnostic radiation qualities. It is assumed that an extended parallel beam propagates from left to right. For the sake of simplicity it is assumed that (the relatively small) differences in the stopping powers of air and PMMA are disregarded. Each photon which has undergone an interaction in PMMA or in air is replaced by a new one at the

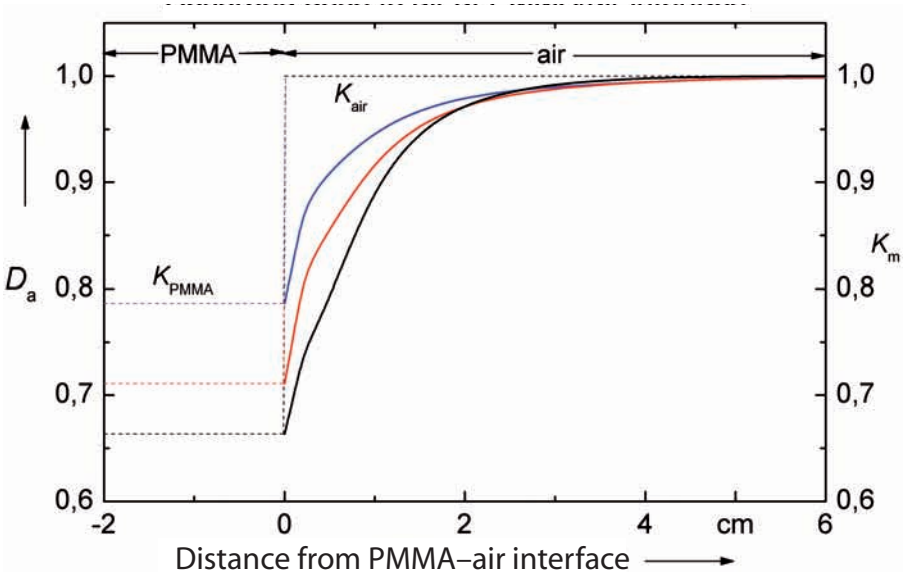

FIG. 3.1. Illustration of the absorbed dose to air (left ordinate, solid lines) and kerma to material m (right ordinate, broken lines, m = air, PMMA) in the vicinity of a PMMA–air interface. All quantities normalized to K_{air} = 1. Black, red and blue curves refer to radiation qualities 70 kV, 2.5 mm Al HVL; 100 kV, 3.97 mm Al HVL and 150 kV, 6.57 mm Al HVL. The kerma to material m (m = air, PMMA) has a discontinuity at the interface. Courtesy: Kramer, H.-M. (2005), private communication.

point of interaction and has the properties of the initial photon. In this way there is no attenuation or scattering in the primary photon beam, while secondary electrons are produced in the usual way. In this model both the air kerma and the PMMA kerma are independent of the distances from the interface. Interestingly, the values of both the air kerma and the PMMA kerma are each unchanged even by a transition from one material to the other.

In contrast, the absorbed dose to air is a physically meaningful quantity only in air. Starting at the interface, the absorbed dose to air displays a gradual buildup. The width of this buildup region is determined by the practical range in air of the most energetic electrons emerging from photon interactions. If, instead of PMMA another material with a higher effective atomic number than air had been chosen, the absorbed dose to air would be decreasing with increasing distance from the interface. A determination of the absorbed dose in the transitional region represents an experimental challenge, irrespective of the kind of adjacent material, even if the most sophisticated equipment is available, such as extrapolation chambers or means for conducting electron spectroscopy.

The experimental expense of a determination of the absorbed dose contrasts with the small value of this information. Owing to the indeterminate nature of the absorbed dose (in the vicinity of interfaces), it is not possible to convert it, for a given radiographic exposure, to, for example, an organ dose by means of just one single conversion factor as is routinely done when starting from an air kerma measurement. For reasons of completeness, it should be noted that there are some exceptional cases in which the absorbed dose close to an interface is at least of general interest. An example is the dose to the tissue surrounding a metal implant. Such questions will not be dealt with in this Code of Practice. In appreciation of the complex nature of the absorbed dose to air, the PSDLs around the world have developed and maintain primary standards for the quantity air kerma and calibrations of dosimeters for use in diagnostic radiology at PSDLs and SSDLs are provided in terms of air kerma. In this Code of Practice, therefore, and in accordance with ICRU 74 [3.1], air kerma is used as the basis of all directly measured application specific quantities.

For dosimetry in CT, both free in air and in phantom measurements have been expressed in terms of a 'CT dose index'. This terminology, however, is misleading. For measurements in phantom using an air kerma calibrated ionization chamber, the measured quantity is air kerma. The absorbed dose to an air cavity within a phantom arises from a situation without secondary electron equilibrium and is difficult to measure and of little interest, as outlined above. For these reasons, the term 'CT air kerma index' is used in this Code of Practice for both free in air and in phantom measurements. All CT air kerma related quantities used correspond directly with those previously referred to as CT dose index related quantities. No change in measurement methods is required.

In the past, the röntgen (R), the old unit of quantity exposure, was used instead of air kerma. Values of exposure in röntgen can be converted to air kerma in gray using the conversion 0.876×10^{-2} Gy/R [3.3].

3.2.2. Incident air kerma

The incident air kerma, K_i, is the kerma to air from an incident X ray beam measured on the central beam axis at the position of the patient or phantom surface (Fig. 3.2). Only the radiation incident on the patient or phantom and not the backscattered radiation is included.

Unit: J/kg. The name for the unit of kerma is gray (Gy).

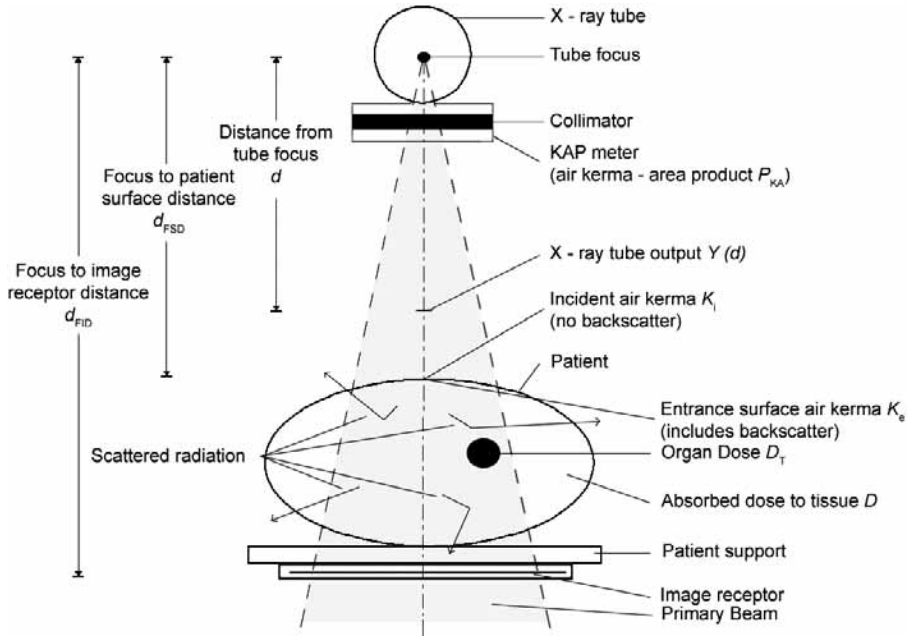

FIG. 3.2. Diagram of the measuring arrangement.

3.2.3. Entrance surface air kerma

The entrance surface air kerma, K_e, is the kerma to air measured on the central beam axis at the position of the patient or phantom surface (Fig. 3.2). The radiation incident on the patient or phantom and the backscattered radiation are included.

Unit: J/kg. The name for the unit of kerma is gray (Gy).

The entrance surface air kerma is related to the incident air kerma by the backscatter factor, B, thus:

$$K_e = K_i B \tag{3.7}$$

3.2.4. X ray tube output

The X ray tube output, $Y(d)$, is defined in ICRU 74 [3.1] as the quotient of the air kerma at a specified distance, d, from the X ray tube focus by the tube current–exposure time product, P_{It}, thus:

$$Y(d) = K(d)/P_{It} \tag{3.8}$$

Unit: $J \cdot kg^{-1} \cdot C^{-1}$. If the special name gray is used, the unit of X ray output is Gy/C or $Gy \cdot A^{-1} \cdot s^{-1}$.

The tube current–exposure time product, P_{It}, is also referred to in this Code of Practice as the tube loading.

3.2.5. Air kerma–area product

The air kerma–area product, P_{KA}, is the integral of the air kerma over the area of the X ray beam in a plane perpendicular to the beam axis (Fig. 3.2), thus:

$$P_{KA} = \int_A K(x, y)\mathrm{d}x\mathrm{d}y \tag{3.9}$$

Unit: $J \cdot kg^{-1} \cdot m^2$. If the special name gray is used, the unit of air kerma–area product is $Gy \cdot m^2$.

The air kerma–area product has the useful property that it is approximately invariant with distance from the X ray tube focus (when interactions in air and extrafocal radiation can be neglected), as long as the planes of measurement and calculation are not so close to the patient or phantom that there is a significant contribution from backscattered radiation.

3.2.6. Air kerma–length product

The air kerma–length product, P_{KL}, is the integral of the air kerma over a line of length, L, thus:

$$P_{KL} = \int_L K(z)\mathrm{d}z \tag{3.10}$$

Unit: $J \cdot kg^{-1} \cdot m$. If the special name gray is used, the unit of air kerma–length product is Gy·m.

In this Code of Practice, the air kerma–length product is applied to the dosimetry of CT and to the dosimetry of dental panoramic examinations.

In the literature for dental panoramic dosimetry, this quantity has been termed the 'dose–width product' [3.4].

3.2.7. Quantities for CT dosimetry

The CT air kerma index, $C_{a,100}$, measured free in air for a single rotation of a CT scanner is the quotient of the integral of the air kerma along a line parallel to the axis of rotation of the scanner over a length of 100 mm and the nominal slice thickness, T (see Glossary)[1]. The integration range is positioned symmetrically about the volume scanned, thus:

$$C_{a,100} = \frac{1}{T}\int_{-50}^{+50} K(z)\mathrm{d}z \tag{3.11}$$

Unit: J/kg. The special name for the unit of CT air kerma index is gray (Gy).

For a multislice scanner with N simultaneously acquired slices of nominal thickness T (nominal width of irradiated beam NT), $C_{a,100}$ becomes:

$$C_{a,100} = \frac{1}{NT}\int_{-50}^{+50} K(z)\mathrm{d}z \tag{3.12}$$

The CT air kerma index is also measured inside PMMA head and body phantoms and is defined similarly to $C_{a,100}$ (Eqs (3.11) and (3.12)). The notation $C_{PMMA,100}$ is used.

The weighted CT air kerma index, C_W, combines values of $C_{PMMA,100}$ measured at the centre and periphery of a standard CT dosimetry phantom [3.5–3.8]. It is given by:

$$C_W = \frac{1}{3}\left(C_{PMMA,100,c} + 2C_{PMMA,100,p}\right) \tag{3.13}$$

[1] It should be noted that the quantity $C_{a,100}$ uses the integration range –50 to +50 mm, whereas the equivalent quantity C_K in ICRU 74 uses the integration range $-\infty$ to $+\infty$.

The quantity $C_{PMMA,100,c}$ is measured at the centre of the standard CT dosimetry phantom and $C_{PMMA,100,p}$ is the average of values measured at four positions around the periphery of the same phantom. A weighted 'CT dose index' was first introduced by Leitz et al. [3.9] and is used in the International Electrotechnical Commission (IEC) [3.8] and the European CT dosimetry protocol [3.6].

The subscript n is used to denote when the value of $C_{a,100}$ or C_W has been normalized [3.6] to unit tube current–exposure time product, P_{It}, thus:

$$ {}_nC_W = \frac{C_W}{P_{It}}; \qquad {}_nC_{a,100} = \frac{C_{a,100}}{P_{It}} \tag{3.14} $$

Unit: $J \cdot kg^{-1} \cdot C^{-1}$. If the special name gray is used, the unit of the normalized weighted CT air kerma index is Gy/C or $Gy \cdot A^{-1} \cdot s^{-1}$.

A further quantity, C_{VOL}, takes into account the helical pitch or axial scan spacing [3.8, 3.10], thus:

$$ C_{VOL} = C_W \frac{NT}{l} = \frac{C_W}{p}; \qquad {}_nC_{VOL} = \frac{C_{VOL}}{P_{It}} \tag{3.15} $$

where N is the number of simultaneously acquired tomographic slices, T is the nominal slice thickness, l is the distance moved by the patient couch per helical rotation or between consecutive scans for a series of axial scans and P_{It} is the tube loading for a single axial scan. The quantity

$$ p = \frac{l}{NT} \tag{3.16} $$

is known as the CT pitch factor (or pitch) for helical scanning.

The CT air kerma–length product determined for the standard CT dosimetry phantom and a complete CT examination, $P_{KL,CT}$, is calculated using

$$ P_{KL,CT} = \sum_j {}_nC_{VOL_j} l_j P_{It_j} \tag{3.17} $$

where the index j represents each serial or helical scan sequence forming part of the examination, l_j is the distance moved by the patient couch between or during consecutive scanner rotations and P_{It_j} is the total tube loading for scan sequence j. This quantity is analogous to the 'dose–length product' introduced in European Commission guidelines [3.6].

3.3. QUANTITIES RELATED TO STOCHASTIC AND DETERMINISTIC EFFECTS

3.3.1. Organ and tissue dose

The mean absorbed dose in a specified tissue or organ is given the symbol D_{T} in ICRU 51 [3.11]. It is equal to the ratio of the energy imparted, $\bar{\varepsilon}_{\mathrm{T}}$, to the tissue or organ to the mass, m_{T}, of the tissue or organ, thus [3.1]:

$$D_{\mathrm{T}} = \frac{\bar{\varepsilon}_{\mathrm{T}}}{m_{\mathrm{T}}} \tag{3.18}$$

The mean absorbed dose in a specified tissue or organ is sometimes simply referred to as the organ dose. This simplification is adopted in this Code of Practice[2].

3.3.1.1. Mean glandular dose

The ICRP [3.12] and ICRU [3.1] recommend the use of the mean dose to the glandular tissues within the breast for breast dosimetry in diagnostic radiology. This quantity has been referred to in the literature as both 'mean glandular dose' and 'average glandular dose'. The term mean glandular dose and the notation D_{G} are used in this Code of Practice.

[2] For stochastic effects, the ICRP [3.13] recommends that that the average absorbed dose in a tissue or organ is the appropriate dosimetric indicator. For deterministic effects, however, the dose to the most heavily irradiated region(s) is more relevant and mean absorbed dose in a localized region of tissue of interest is the required quantity [3.1].

3.3.2. Equivalent dose

The equivalent dose, H_T, to an organ or tissue, T, is defined in ICRP 60 [3.13] and ICRU 51 [3.11]. For a single type of radiation, R, it is the product of a radiation weighting factor, w_R, for radiation R and the organ dose, D_T, thus:

$$H_T = w_R D_T \tag{3.19}$$

Unit: J/kg. The special name for the unit of equivalent dose is sievert (Sv).

The radiation weighting factor, w_R, allows for differences in the relative biological effectiveness of the incident radiation in producing stochastic effects at low doses in tissue or organ, T. For X ray energies used in diagnostic radiology, w_R is taken to be unity.

3.3.3. Effective dose

The effective dose, E, is defined in ICRP 60 [3.13] and ICRU 51 [3.11]. It is the sum over all the organs and tissues of the body of the product of the equivalent dose, H_T, to the organ or tissue and a tissue weighting factor, w_T, for that organ or tissue, thus:

$$E = \sum_T w_T H_T \tag{3.20}$$

The tissue weighting factor, w_T, for organ or tissue T represents the relative contribution of that organ or tissue to the total detriment arising from stochastic effects for uniform irradiation of the whole body.

Unit: J/kg. The special name for the unit of effective dose is sievert (Sv).

The sum over all the organs and tissues of the body of the tissue weighting factors, w_T, is unity.

3.4. CONVERSION COEFFICIENTS FOR THE ASSESSMENT OF ORGAN AND TISSUE DOSES

A conversion coefficient, c, relates the dose to an organ or tissue to a readily measured or calculated dosimetric quantity, thus:

$$c = \frac{\text{organ or tissue dose}}{\text{measured or calculated quantity}} \tag{3.21}$$

Suffixes are added to c to indicate the two quantities that are related, for example the coefficient

$$c_{D_T,K_i} = D_T / K_i \tag{3.22}$$

relates the organ dose, D_T, to the incident air kerma, K_i.

REFERENCES

[3.1] INTERNATIONAL COMMISSION ON RADIATION UNITS AND MEASUREMENTS, Patient Dosimetry for X Rays Used in Medical Imaging, ICRU Rep. 74, ICRU, Bethesda, MD (2006).

[3.2] INTERNATIONAL COMMISSION ON RADIATION UNITS AND MEASUREMENTS, Fundamental Quantities and Units for Ionizing Radiation, ICRU Rep. 60, ICRU, Bethesda, MD (1998).

[3.3] INTERNATIONAL COMMISSION ON RADIATION UNITS AND MEASUREMENTS, Measurements of Dose Equivalents from External Photon and Electron Radiations, ICRU Rep. 47, ICRU, Bethesda, MD (1992).

[3.4] NAPIER, I.D., References doses for dental radiography, Br. Dental J. **186** (1999) 392–396.

[3.5] AMERICAN ASSOCIATION OF PHYSICISTS IN MEDICINE, Recommendations on performance characteristics of diagnostic exposure meters, Report of AAPM Diagnostic X-Ray Imaging Group No. 6, Med. Phys. **19** (1991) 231–241.

[3.6] EUROPEAN COMMISSION, European Guidelines for Quality Criteria for Computed Tomography, Rep. EUR 16262, EC, Luxembourg (2000).

[3.7] FOOD AND DRUG ADMINISTRATION, Computed Tomography (CT) Equipment, Section 1020.33 21 CFR Ch1 (4-1-88 Ed.), Performance Standard for Diagnostic X-ray Systems, US Department of Health and Human Services, FDA, Rockville, MD (1988).

[3.8] INTERNATIONAL ELECTROTECHNICAL COMMISSION, Medical Electrical Equipment Part 2-44: Particular Requirements for the Safety of X-Ray Equipment for Computed Tomography, Rep. IEC-60601-2-44, IEC, Geneva (2002).

[3.9] LEITZ, W., AXELSSON, B., SZENDRO, G., Computed tomography dose assessment — a practical approach, Radiat. Prot. Dosim. **57** (1995) 377–380.

[3.10] MCNITT-GRAY, M.F., Radiation doses in CT, Radiographics **22** (2002) 1541–1553.

[3.11] INTERNATIONAL COMMISSION ON RADIATION UNITS AND MEASUREMENTS, Quantities and Units in Radiation Protection Dosimetry, ICRU Rep. 51, ICRU, Bethesda, MD (1993).
[3.12] INTERNATIONAL COMMISSION ON RADIOLOGICAL PROTECTION, Statement from the 1987 Como Meeting of the ICRP, Publication 52, Pergamon Press, Oxford and New York (1987).
[3.13] INTERNATIONAL COMMISSION ON RADIOLOGICAL PROTECTION, 1990 Recommendations of the International Commission on Radiological Protection, Publication 60, Pergamon Press, Oxford and New York (1991).

Chapter 4

DOSIMETRY FORMALISM

The formalism employed for the determination of dosimetry quantities used in diagnostic radiology is similar to the formalism used in Technical Reports Series No. 398 [4.1] for determination of absorbed dose to water in radiation therapy. In contrast to Technical Reports Series No. 398, where the formalism is based on standards of absorbed dose to water, the formalism in this Code of Practice is based on standards of air kerma.

4.1. N_K BASED FORMALISM

The air kerma, K (air kerma rate, $\dot{K}$), at the reference point in air for a reference beam of quality, Q_0, and in the absence of the dosimeter is given by:

$$K = (M_{Q_0} - M_0) N_{K,Q_0} \tag{4.1}$$

where M_{Q_0} is the reading of the dosimeter under the reference conditions used in the standards laboratory, M_0 the dosimeter reading in the absence of the beam (zero reading) under otherwise unchanged conditions and N_{K,Q_0} is the calibration coefficient of the dosimeter in terms of the air kerma obtained from a standards laboratory. The calibration coefficient refers to reference conditions used at the laboratory and it is the ratio of the conventional true value of the quantity to be measured to the indicated value.

In this equation K represents a generic term for one of the dosimetric quantities K_i, K_e, P_{KA}, P_{KL} or $C_{a,100}$ defined in Chapter 3.

4.1.1. Reference conditions

Reference conditions represent a set of values (reference values) of influence quantities for which the calibration coefficient is valid without further corrections. Examples of influence quantities for calibrations in terms of the air kerma are the beam quality, the ambient temperature, air pressure and relative humidity, direction of radiation incidence, etc.

As the measurement conditions usually do not match the reference conditions used in the standards laboratory, additional corrections to the reference conditions used at the laboratory for the effect of influence quantities are needed.

4.1.2. Influence quantities

Influence quantities are defined as quantities that are not the subject of the measurement, but yet may have an influence on the result of the measurement. They may be of different nature as, for example, ambient pressure and temperature; they may arise from the dosimeter (e.g. leakage, zero drift, warm-up), or they may be quantities related to the radiation field (e.g. beam quality, dose rate, field size, presence of scattered radiation). The influence quantities may have different effects on different types of dosimeter. As an example, the response of a dosimeter with a semiconductor detector is usually not influenced by changes in the atmospheric pressure, whereas ionization chambers are.

During the measurement, as many influence quantities as practicable are kept under control. However, many influence quantities cannot be controlled (e.g. air pressure). It is possible to correct for the effect of these influence quantities by applying correction factors. Assuming that influence quantities act independently of each other, a product of their correction factors, k_i, can be applied to Eq. (4.1). The air kerma in the beam of quality, Q, is given by:

$$K = (M_Q - M_0) N_{K,Q_0} \prod_i k_i \tag{4.2}$$

where M_Q is the instrument reading for a beam quality, Q, and factors k_i represent a correction for the effect of i-th influence quantity. Such correction factors may have to be applied as the calibration coefficient refers, strictly speaking, only to reference conditions. By definition, the value of k_i equals unity if influence quantity, i, assumes its reference value.

In many applications the quantity M_0 can be disregarded as it is of negligible magnitude with respect to M. Equation (4.2) then becomes:

$$K = M_Q N_{K,Q_0} \prod_i k_i \tag{4.3}$$

Under all circumstances it is recommended that a check be made prior to the actual measurement as to whether the zero reading really is negligible in the context of the measurement planned. If not, the instrument reading has to be corrected for this effect as shown in Eq. (4.2). In this Code of Practice, if not explicitly stated, it is assumed that this correction is applied.

4.1.2.1. Correction for density of air

One correction factor that is often applied in measurements with ionization chambers is the one that corrects for changes in the density of air

due to changes in the ambient temperature, T, and pressure, P. The ionization chambers considered in this Code of Practice are vented, which means that they are designed so that the air in the collecting volume communicates with the ambient air in the room where the measurement is performed. As a chamber reading depends on the mass of the air in the collecting volume, it also depends on the temperature and pressure of air as given by:

$$k_{\mathrm{TP}} = \left(\frac{273.2 + T}{273.2 + T_0}\right)\left(\frac{P_0}{P}\right) \tag{4.4}$$

where P_0 and T_0 are the reference pressure and temperature. Both P and P_0 are expressed in kPa, the unit of T and T_0 is °C.

In this Code of Practice, the reference pressure P_0 = 101.3 kPa and the reference temperature T_0 = 20°C are used. In principle, deviations of the relative humidity of the air from its reference value of 50% relative humidity also need to be taken into account by a correction factor. For the purpose of this Code of Practice and certainly for the range of relative humidity between 30% and 80% this correction may be disregarded [4.2].

4.1.2.2. Correction for radiation quality of the beam

A deviation from the reference beam quality, Q_0, used to calibrate an ionization chamber may require the use of a correction. Assuming that other influence quantities are kept at their reference values, the measured air kerma in a beam of quality, Q, different from the beam quality, Q_0, used during the calibration is given by:

$$K_Q = M_Q N_{K,Q_0} k_{Q,Q_0} \tag{4.5}$$

where the factor k_{Q,Q_0} corrects for the effects of the difference between the reference beam quality, Q_0, and the actual quality, Q, during the measurement.

The correction factor, k_{Q,Q_0}, is generally provided by the calibration laboratory but some SSDLs prefer to report calibration coefficients, $N_{K,Q}$, for all beam qualities, Q, measured. If this is the case, the correction factor, k_{Q,Q_0}, can be calculated as:

$$k_{Q,Q_0} = \frac{N_{K,Q}}{N_{K,Q_0}} \tag{4.6}$$

Equation (4.5) can be also written as:

$$K_Q = \frac{M_Q}{R_Q} \tag{4.7}$$

where $R_Q = (N_{K,Q_0} k_{Q,Q_0})^{-1}$ is the response of the dosimeter[1] for the beam quality, Q. The beam quality correction factor, k_{Q,Q_0}, is defined as the ratio of the dosimeter response for beam qualities Q_0 and Q, respectively:

$$k_{Q,Q_0} = \frac{R_{Q_0}}{R_Q} = \frac{M_{Q_0}/K_{Q_0}}{M_Q/K_Q} \tag{4.8}$$

In practice, Q_0 is often omitted in the symbol for the beam quality correction. Instead, the symbol k_Q is used. This is logical for applications in radiotherapy and radiation protection where usually a single radiation quality is used as a reference (^{60}Co radiation in radiotherapy and ^{137}Cs in radiation protection). In diagnostic radiology, various reference qualities are used depending on the modality. There are different reference beams used for mammography, general radiography and CT. When using a simpler symbol for a beam quality correction, the correction factor appropriate for a given modality has to be applied. The reference radiations for various modalities are described in Chapter 6.

4.1.2.3. Other corrections

There are a number of further quantities that have an influence on the result of the measurement. Some of them are common to all measurement methods (e.g. non-linearity of the measuring assembly, positioning of the detector, field non-homogeneity, field size); some of them are technique specific. For example, the response of an ionization chamber may be influenced by the recombination of charge carriers of opposite sign, scattering of radiation by the stem or by microphony in a cable. Thermoluminescence detectors may have a different response depending on the time of their evaluation after

[1] Response of the dosimeter is the ratio between its indication and the conventional true value of the measured quantity. Under reference conditions, the response equals the inverse of the calibration coefficient.

irradiation, on storage temperature, etc. Some of these effects are discussed in Chapters 5–7.

Generally, corrections should be made for deviations from reference conditions. In some cases, such as when the effect of an influence quantity is small, it can also be included in the uncertainty of the measurement. It is suggested that a value (limit) for the smallest uncertainty that should be considered be chosen and those smaller than this limit disregarded. The value of 0.1% is regarded as a reasonable choice.

Discussion of various corrections and their uncertainties is given in Chapter 5 and in Appendix II.

4.2. CROSS-CALIBRATION OF DOSIMETERS

The IMS described in Chapter 2 assumes that user's dosimeters are calibrated in one of the calibration laboratories, typically in an SSDL. However, this is not the case all of the time and some users calibrate their field dosimeters themselves and subsequently use them for practical measurements. There are various reasons for this and these can be summarized as follows:

(a) In some countries, this practice has been historically established and is followed in the majority of institutions.
(b) Some users serve a large number of departments/hospitals and therefore need more dosimeters to perform required measurements. A calibration of all dosimeters in an SSDL would be too costly.
(c) It is not possible to calibrate some dosimeters in an SSDL. The kerma–area product (KAP) meter, which is part of a defined mechanical set-up in the X ray equipment, is one example.

Generally, cross-calibration of a field instrument refers to its direct comparison in a suitable user's beam of a quality, Q_{cross}, against a reference instrument that has been calibrated at an SSDL. Using Eq. (4.5), the calibration coefficient of the field instrument can be written as:

$$N_{K,Q_{\text{cross}}}^{\text{field}} = \frac{M_{Q_{\text{cross}}}^{\text{ref}}}{M_{Q_{\text{cross}}}^{\text{field}}} N_{K,Q_0}^{\text{ref}} k_{Q_{\text{cross}}}^{\text{ref}} \tag{4.9}$$

where 'field' and 'ref' refer to the field and the reference instruments, respectively. The values of readings of the reference and the field instruments $M_{Q_{\text{cross}}}^{\text{ref}}$ and $M_{Q_{\text{cross}}}^{\text{field}}$ have been corrected for the influence of all quantities except that of

beam quality. The calibration coefficient of the field instrument obtained through cross-calibration in the beam quality, Q_{cross}, can be used only for this beam quality. If the beam quality changes, a new cross-calibration in the new beam quality is required.

If a user chooses to adopt the method of cross-calibration it is strongly recommended that a check be made to ensure that the procedure of the cross-calibration leads to correct results. One method of checking consists of exposing both the calibrated chamber and the detector of the field instrument in the plane of measurement in a position about 5 cm off-axis to each side of the point of measurement. Using radiation quality, Q_{cross}, the readings (M_i^{ref} and M_i^{field}) i = 1, 2, 3 from three exposures of the two dosimeters should be taken, the positions of the two chambers be swapped and readings i = 4, 5, 6 from three further exposures be taken. The result of the measurement of the air kerma with the field instrument

$$\left(K^{\text{field}} = N_{K,Q_{\text{cross}}}^{\text{field}} \sum_{i=1}^{6} M_i^{\text{field}} \right)$$

should agree with the result of the measurement taken with the calibrated dosimeter

$$\left(K^{\text{ref}} = N_{K,Q_0}^{\text{ref}} k_{Q_{\text{cross}}} \sum_{i=1}^{6} M_i^{\text{ref}} \right)$$

to within 1%. For ionization chambers used in diagnostic radiology (unsealed type), no corrections for possible changes in air density are required in this procedure. If the field instrument has a solid state detector, it may become necessary in cases of rapid temperature or pressure changes to correct the reading of the reference chamber for variations in the density of air. When the conditions are stable, but not the reference conditions, a correction is also necessary.

It is important to note that a cross-calibration procedure often does not result in establishing traceability of the measurement. In addition to an unbroken chain of comparisons, traceability is characterized by a number of additional essential elements such as a statement of measurement uncertainty, evidence of competence, documentation, etc. All of these requirements may not be fulfilled when cross-calibrating the dosimeter in the hospital. In this Code of Practice, it is recommended that, when feasible, users should calibrate their dosimeters in an SSDL.

REFERENCES

[4.1] INTERNATIONAL ATOMIC ENERGY AGENCY, Absorbed Dose Determination in External Beam Radiotherapy: An International Code of Practice for Dosimetry Based on Standards of Absorbed Dose to Water, Technical Reports Series No. 398, IAEA, Vienna (2000).

[4.2] ROGERS, D.W.O., ROSS, C.K., The role of humidity and other correction factors in the AAPM TG-21 dosimetry protocol, Med. Phys. **15** 1 (1988) 40–48.

Chapter 5

SELECTION OF INSTRUMENTATION

Doses from diagnostic radiological examinations are small and usually do not approach thresholds for deterministic effects. Exceptions are found for interventional procedures in radiology and cardiology that may involve high doses to the patient's skin. Severe skin injuries have been documented [5.1–5.3]. Even ignoring the high doses found for interventional procedures, it needs to be realized that the greatest source of exposure of the population to artificial ionizing radiation is from diagnostic radiology. The doses delivered in diagnostic radiological procedures should therefore be accurately determined in order to maintain a reasonable balance between image quality and patient exposure. Dosimetric methods should be used that ensure appropriate levels of accuracy and long term stability.

5.1. INTRODUCTION

Various examination techniques are employed in X ray diagnostic radiology. They include fluoroscopy, interventional radiological procedures, mammography, CT, and dental and general radiography[1]. X ray beams with tube voltages from about 20 kV to 150 kV are used. The tube voltages in fluoroscopy, CT, and dental and general radiography cover the range 50–150 kV, the anode material usually being tungsten. Mammographic examinations are conducted with tube voltages between 22 kV and 40 kV and various combinations of anode and filtration materials are used, the most common materials being molybdenum anode and molybdenum filtration. An accurate measurement of dose requires correct calibration of the instrumentation in radiation fields of known properties. In diagnostic radiology, the specification of radiation qualities is important as the response of all dosimeters depends, at least to a certain extent, on the spectral distribution of the X rays employed. Radiation qualities are usually specified in terms of the X ray tube voltage first and possibly HVL second.

[1] In this publication the term general radiography is used to cover all X ray imaging modalities other than dental radiography, fluoroscopy, mammography and CT.

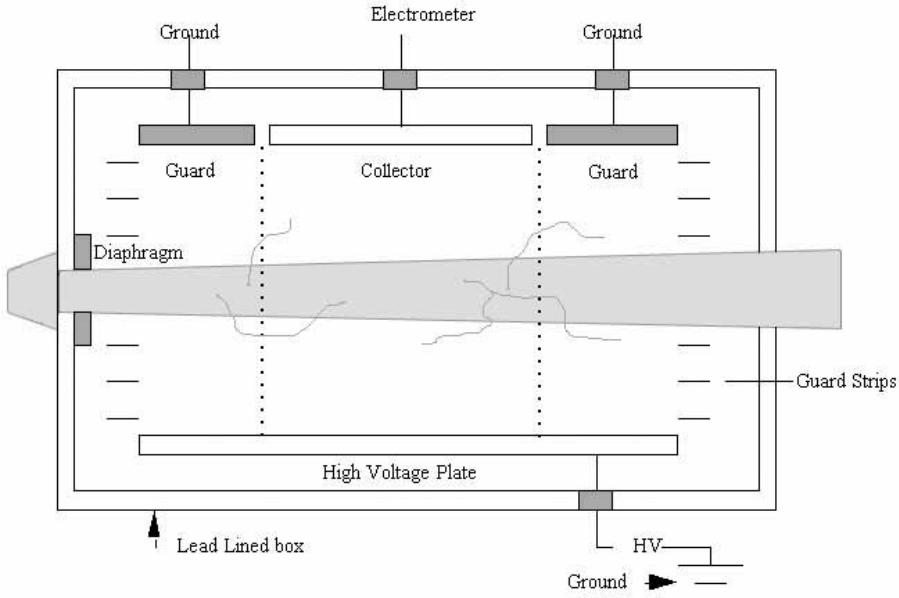

FIG. 5.1. Schematic diagram of free air ionization chamber.

5.2. DOSIMETERS

5.2.1. Ionization chambers

5.2.1.1. Free air chamber

In the energy region considered, the free air chamber (Fig. 5.1) is the primary standard for realizing the unit gray for the quantity air kerma [5.4]. Various PSDLs and some SSDLs use free air chambers to determine the air kerma (rate) in X ray beams. Comparisons of measurements with free air chambers from different institutes usually agree to within 0.5%, which is within the limit of the uncertainty involved in the comparisons [5.5]. Once the air kerma (rate) of a beam has been established, the reference class dosimeter is calibrated using the substitution method (see Chapter 7).

5.2.1.2. Cylindrical and plane parallel chambers

The most common type of ionization chamber for diagnostic radiological measurement of air kerma is a plane parallel chamber. Plane parallel ionization chambers (also known as parallel plate chambers) use two parallel, flat

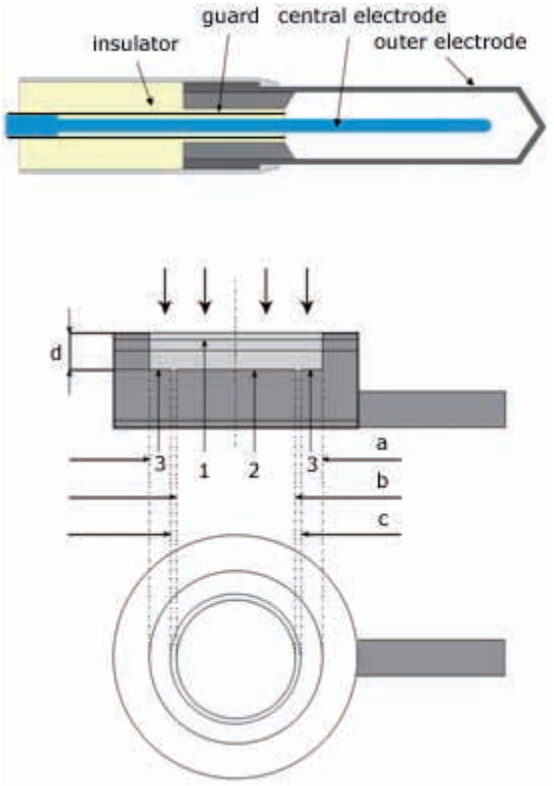

FIG. 5.2. Schematic diagram of cylindrical (upper) and plane parallel (lower) ionization chambers. 1: polarizing electrode; 2: measuring electrode; 3: guard ring. (a) is the diameter of the polarizing electrode; (b) is the diameter of the collecting electrode; (c) is the width of the guard ring; and (d) is the height (electrode separation) of the air cavity (adapted from Ref. [5.6]).

electrodes, separated by a few millimetres. They are calibrated with their plates oriented perpendicular to the beam axis, which is also the orientation in which they should be used. Some of these chambers have different entrance and exit windows, in which case it is important that the entrance window faces the X ray focal point. On the other hand, the response of cylindrical chambers is symmetrical with respect to the chamber axis. They are usually oriented with the cylindrical axis of the chamber perpendicular to the X ray beam. Irrespective of their geometrical design, ionization chambers used in diagnostic radiology should be of the vented type, i.e. their sensitive gas volume should communicate with the atmosphere.

5.2.1.3. CT chamber

Ionization chambers are made in different designs for specialized applications. For example, a lengthened version of a cylindrical chamber results in a unique design for CT. A CT chamber is often termed a pencil chamber because its active volume comprises a thin cylinder 100 mm in length or sometimes longer. While most chambers are designed to be immersed in a uniform beam for proper measurement, the CT chamber is designed for non-uniform exposure from a single scan or a number of scans. Typically, the chamber is inserted inside a phantom (also usually cylindrical in shape) that is used to attenuate the primary beam and to generate scattered X rays, simulating conditions when a patient is in the field. For the measurement of the air kerma–length product, P_{KL}, the chamber is positioned parallel to the rotation axis of the scanner either free in air or inside a cylindrical phantom. For a single scan (except for a multislice), the primary beam does not usually cover more than about 10% of the full length of the chamber. At the same time, the CT chamber detects the scattered radiation generated in the phantom by the primary beam, thereby allowing quantification of the total exposure of a patient. This unique use of the CT chamber requires that the response of the active volume be uniform along its entire axial length, a restriction that is not required of other cylindrical full immersion chambers.

5.2.1.4. Transmission ionization chambers

In examinations using fluoroscopy, irradiation geometry (field size, focus skin distance, projection) and irradiation times vary individually from patient to patient. If the detector mounted on the tube housing is 'transparent' to X rays, then both focal and extrafocal radiation will pass through its sensitive volume. If attenuation in the air can be neglected, those X rays transmitted through the detector will pass every plane perpendicularly to the beam central axis downstream of the beam. If the integration of air kerma over beam area is extended over the entire plane, the air kerma–area product will be invariant with distance from the X ray tube provided the beam is contained by the KAP meter. In this situation, the air kerma–area product offers a convenient quantity for monitoring patient exposure. A detector possessing such properties is termed the transmission ionization chamber [5.7].

The transmission ionization chamber generally consists of layers of PMMA coated with conductive material. Graphite, a commonly used coating material, is close to air equivalent and introduces low energy dependence for air kerma measurements. Graphite coating is, however, inconvenient in transmission chambers since it is non-transparent to light. Light transparent

materials are therefore mostly used. These materials contain elements of high atomic number such as indium and tin, giving rise to relatively strong energy dependence compared to graphite coated chambers [5.8, 5.9].

Transmission ionization chambers are used as detectors for dose–area product or KAP meters. In this Code of Practice, the quantity of interest is the air kerma–area product so a term KAP meter is used throughout. Requirements on performance of this equipment are set in IEC 60580 [5.10].

Besides fluoroscopy, KAP meters are also widely used in general radiography and are being increasingly installed on modern dental radiography equipment.

5.2.2. Solid state dosimeters

Dosimeters other than ionization chambers exist and these have been used for diagnostic measurements [5.11–5.13]. Dosimeters with thermoluminescence and semiconductor detectors are considered here. Real time measurements may be conveniently accomplished with semiconductor dosimeters; the small size of thermoluminescence dosimeters (TLDs) allows their application for conducting measurements on patients.

Traditionally, the main disadvantage of these devices has been their energy dependence of response which differs considerably from that of ionization chambers. These types of dosimeter have found many applications in postal audits or in routine clinical measurements in hospitals. They are not used for calibrations of other dosimeters in SSDLs.

5.2.2.1. TLDs

Some materials, on absorption of radiation, retain part of the absorbed energy in metastable states that are a result of defects in the material lattice. These trapped electrons or holes remain at the metastable state until they are excited to recombine and emit the energy in the form of light. If the method of excitation is heat, then the process is termed thermoluminescence. The amount of light emitted is proportional to the radiation absorbed in the material and thus to the mass of the active phosphor present.

Thermoluminescence has found great use in dosimetry. TLDs are available in various forms (e.g. powder, chips, rods, ribbons) and made of various materials. Dosimeters most commonly used in medical applications are based on lithium fluoride doped with magnesium and titanium (LiF:Mg,Ti) but other materials such as LiF:Mg,Cu,P; $Li_2B_4O_7$:Mn; $CaSO_4$:Dy and CaF_2:Mn have also been used. Table 5.1 gives basic characteristics of these materials.

TABLE 5.1. DOSIMETRIC CHARACTERISTICS OF SELECTED THERMOLUMINESCENT MATERIALS [5.14, 5.15]

Thermo-luminescent material	Form	Glow peak (°C)	Emission maximum (nm)	Z_{eff}	Relative sensitivity	Linear range (Gy)	Fading	Annealing (Temperature and time)
LiF:Mg,Ti	Powder, chips, rods, discs	210	425	8.14	1	5×10^{-5} to 1	<5% per year	400°C, 1 h + 80°C, 24 h
LiF:Mg,Ti,Na	Powder, discs	220	400	8.14	0.5		NA	500°C, 0.5 h
LiF:Mg,Cu,P	Powder, discs	232	310(410)	8.14	15–30	10^{-6} to 10	<5% per year	240°C, 10 min
$Li_2B_4O_7$:Mn	Powder	210	600	7.4	0.15–0.4	10^{-4} to 3	5% in 2 months	300°C, 15 min
Al_2O_3:C	Powder, discs	250	425	10.2	30	10^{-4} to 1	3% per year	300°C, 30 min
$CaSO_4$:Dy	Powder, discs	220	480(570)	15.3	30–40	10^{-6} to 30	7–30% in 6 months	400°C, 1 h
CaF_2:Dy	Powder	200(240)	480(575)	16.3	16	10^{-5} to 10	25% in 4 weeks	600°C, 2 h
BeO	Discs	180–220	330	7.13	0.7–3	10^{-4} to 0.5	7% in 2 months	600°C, 15 min

There are many processes that can affect the thermoluminescence measurement and great care must be taken to be consistent in dosimeter use. For example, the annealing regime, which is the method used to deplete the population of trapped charges or to change the trap structure to prepare the material for reuse, can affect the dose measurement. Some thermoluminescent materials have specified annealing regimes to eliminate low temperature glow peaks without affecting the higher temperature peak. This can be accomplished by conducting a low temperature preheat before reading, which removes charges from low temperature traps while having an insignificant effect on charges in the high temperature traps. Only well-established annealing cycles should be used. Their reproducibility is important for accurate dosimetry.

The trapped charges are also slowly released at room temperature. This process is called fading and the effect must be corrected for when evaluating TLDs long after irradiation. Special attention has to be paid to situations where dosimeters are stored at higher temperatures. Such situations may occur when using TLDs for postal audits. Extensive descriptions of various thermoluminescent materials and procedures for their preparation, handling and evaluation can be found in Refs [5.14, 5.16].

During readout, the thermoluminescence detector emits light the intensity of which is proportional to the energy deposited during irradiation. The electrical signal derived from the emitted light must be converted to one of the quantities of interest in diagnostic radiology defined in Chapter 3. For a given X ray beam, this problem can be overcome by calibrating the dosimeter in a beam of that type, itself already calibrated through some other means.

It is important to note that there are many factors that influence the final result of a thermoluminescence measurement. These include factors related to the performance of the instrument and those related to procedures of dosimeter preparation and handling. When calibrating the dosimeter, the whole system has to be considered. A review of the application of a thermoluminescent method for dosimetry in diagnostic radiology was recently done by Zoetelief et al. [5.15].

5.2.2.2. Semiconductor dosimeters

The small size of TLDs makes them suitable for conducting measurements on patients, but they do not provide real time information about patient exposure. Semiconductor detectors are also small and respond instantaneously to their irradiation thus combining both advantages of solid state detectors. They produce large signals from modest amounts of radiation, they are rigid and do not require pressure correction, which makes them suitable for some clinical applications.

The simplest of semiconducting devices is the diode, which based on a p–n junction between the p-type and n-type parts of a semiconductor. As ionizing radiation strikes the semiconductor, electron hole pairs are induced. This causes the junction to become conductive and the current increases with the rate of ion production. The size of the signal generated depends on the ionizing properties of the radiation and on its ability to penetrate to the junction. The amount of ionization reaching the junction may also depend on the cross-sectional area of the junction in relation to the incidence of the beam. Thus, there may be some energy dependence and some directional sensitivity to these devices. Manufacturers mainly use metal filters to compensate for the energy dependence of the signal of solid state detectors. Another possibility is to compensate for this effect electronically.

Ceasing irradiation terminates ion production and the diode recovers to its original state, except for any possible permanent alteration in the structural properties of the junction. From radiation therapy it is known that repeated exposure of a semiconductor detector to radiation may cause damage to the structure of the detector. This may lead to changes in sensitivity over a period of time. As doses in diagnostic radiology are considerably smaller than those in radiation therapy and as the radiation energy in diagnostic radiology is lower than that used in therapy the occurrence of structural damage is less likely for instruments used in diagnostic radiology. However, no general statement on ageing effects can be made at this stage. Therefore, it is recommended that the dosimeter response be checked at regular intervals.

5.2.3. Dosimeter energy dependence

A diagnostic dosimeter should be calibrated at the appropriate radiation qualities (see Chapter 7). Over the energy range of use, the energy dependence of response should be determined. The quality of diagnostic X ray beams is fully characterized by their spectrum. However, X ray spectrometry requires considerable expertise and thus simpler methods are used the express beam quality. Parameters such as tube voltage, the first and the second HVLs (HVL_1 and HVL_2), total filtration and their combinations are used for this purpose. All detectors show some variation of response with varying HVL. As an example, Fig. 5.3 shows the energy dependence of the relative response of two ionization chambers, where the chamber wall thickness is of particular importance owing to the low energy of the radiation. One is a cylindrical design with a thick wall and the other a plane parallel design with a thin entrance window [5.12]. If the variation of response is not properly taken into account, this leads to an error in the measurement of air kerma. The mean glandular dose is the quantity of interest in mammography. It is obtained by multiplying

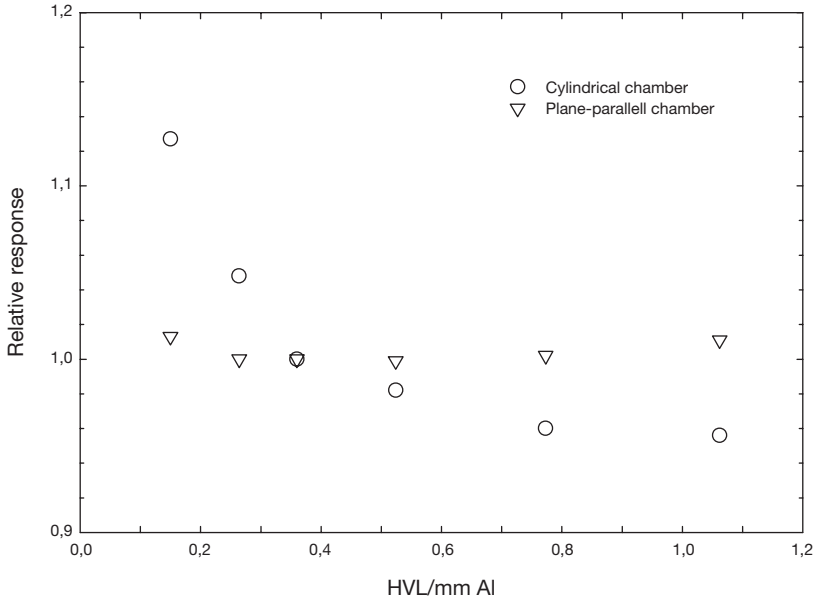

FIG. 5.3. Variation of relative response of a plane parallel chamber and a cylindrical chamber as a function of first HVL of low energy X ray beams.

the value of the air kerma by a conversion coefficient which itself depends on the HVL. As the energy dependence of response also results in an error in the HVL measurement, the result of the determination of the mean glandular dose depends on the energy dependence of the response of the detector employed.

There are also dosimeters in which the energy dependence is electronically compensated [5.12]. The electronic compensation of such dosimeters needs to be checked regularly.

In this Code of Practice, the energy dependence of dosimeters is indicated by the SSDL by reporting the correction factor, k_Q, (see Chapter 4) or the air kerma calibration coefficient, $N_{K,Q}$, for all the energies measured by the SSDL. The value of k_Q for each beam is the ratio of $N_{K,Q}$ to the reference beam air kerma calibration coefficient, N_{K,Q_0}, where:

$$k_Q = \frac{N_{K,Q}}{N_{K,Q_0}} \tag{5.1}$$

5.2.4. Other considerations

The detector and measuring assembly both need to be calibrated. Generally, they are calibrated as a system; if the detector and measuring assembly are calibrated individually, the calibration coefficient of the entire system is the product of the calibration coefficients of the detector and of the assembly[2]. Dosimetry formalism, which was discussed in Chapter 4, assumes that the calibration coefficient under reference conditions, N_{K,Q_0}, and the beam quality correction factor, k_Q, were established at the calibration laboratory. It also discusses the case where the SSDL provides the calibration coefficient, $N_{K,Q}$, for each beam quality. If the user wishes to use a separate calibration coefficient for a beam other than a calibration beam at the SSDL, interpolation of either N_{K,Q_0} and k_Q or $N_{K,Q}$, for a beam quality, Q, should be performed. For KAP meters it may become necessary to consider the use of total filtration, tube voltage and (or) HVL as beam quality specifiers. For details see Pöyry et al. [5.19]. Data for spectra of the same type should be used (tungsten or molybdenum anode). The relationship of $N_{K,Q}$ to N_{K,Q_0} is via k_Q as:

$$N_{K,Q} = N_{K,Q_0} k_Q \tag{5.2}$$

In the case of ionization chambers, it is also important to measure the temperature and pressure at the time and place of measurement. There are some dosimeters that measure temperature and pressure and automatically correct for their influence. The use of such instruments can result in problems caused by their improper operation. If there is such a correction, it is recommended that checks be made periodically to ensure it is being made correctly (see Chapter 6).

The use of dosimeters for measurements in diagnostic radiology requires a correct set-up so that a free in air measurement is performed. In practical situations, the measurement geometry may be far away from the geometry

[2] The standard ISO 31-0 [5.17], 'Quantities and Units', has provided guidelines with regard to the use of the term 'coefficient', which should be used for a multiplier possessing dimensions, and 'factor', which should be reserved for a dimensionless multiplier. The more recent standard IEC-60731 [5.18] is not consistent, however, with the International Organization for Standardization (ISO) vocabulary and still provides a definition of the term 'calibration factor'. In this Code of Practice, the term 'calibration coefficient' will be used throughout.

used for a free in air measurement. The effect of scattered radiation on the energy response of dosimeters is usually not well known, which may result in large inaccuracies in the measurement. The uncertainties of measurements of quantities other than the incident air kerma are discussed in Chapter 8.

5.3. REQUIREMENTS ON USER DOSIMETRIC EQUIPMENT

For the purpose of this Code of Practice and when employing an active dosimeter, the user should make sure that the dosimeter is in compliance with IEC 61674 [5.20]. As IEC 61674 applies both to dosimeters equipped with ionization chambers and to semiconductor detectors, the user should consider which type of instrument is most suitable for the kind of measurement required.

In IEC 61674 [5.20], limits of variations are given for the effects of influence quantities on the response of the whole dosimeter. Using these data an uncertainty budget consistent with the Guide for the Expression of Uncertainties in Measurements [5.21] can be established. Uncertainty budgets for various scenarios are given in Table 8.2 (see Chapter 8). These scenarios are based on uncertainty values achieved through an SSDL calibration. An example of a full treatment of uncertainties according to the Guide for the Expression of Uncertainties in Measurements for a calibration of a user instrument at an SSDL is given in Appendix II.

5.4. REQUIREMENTS ON THE DOSIMETRIC EQUIPMENT OF SSDLs

For the calibration of user's dosimeters at an SSDL, reference class instruments should be employed. The primary advantage of ionization chambers is that they can be constructed in such a way that they exhibit only a small variation of response with varying radiation energy. Furthermore, they are known to have good long term stability. However, care needs to be taken as not all instruments in compliance with IEC 61674 are considered as reference class instruments. Table 5.2 gives guidance on what performance is considered to be adequate for a reference class dosimeter.

TABLE 5.2. RECOMMENDED SPECIFICATIONS OF DETECTORS OF A REFERENCE CLASS DOSIMETER (BY APPLICATION)

Application	Type of detector	Range of X ray tube voltage	Intrinsic error	Maximum variation of energy response	Range of air kerma rate	
					Unattenuated beam	Attenuated beam
		(kV)	(%)	(%)		
General radiography	Cylindrical or plane parallel	60–150	3.2	±2.6	1 mGy/s – 500 mGy/s	10 μGy/s – 5 mGy/s
Fluoroscopy	Cylindrical or plane parallel (preferable)	50–100	3.2	±2.6	10 μGy/s – 10 mGy/s	0.1 μGy/s – 100 μGy/s
Mammography	Plane parallel	22–40	3.2	±2.6	10 μGy/s – 10 mGy/s	
CT*	Cylindrical (pencil type)	100–150	3.2	±2.6	0.1 mGy/s – 50 mGy/s	
Dental radiography	Cylindrical or plane parallel	50–90	3.2	±2.6	1 μGy/s – 10 mGy/s	

* The dosimeters must have no greater variation in their sensitivity than ±3% along the active length.

REFERENCES

[5.1] BERLIN, L., Malpractice issues in radiology: Radiation-induced skin injuries and fluoroscopy, Am. J. Roentgenol. **177** (2001) 21–25.

[5.2] KÖNIG, T.R., WOLFF, D., METTLER, F.A., WAGNER, L.K., Skin injuries from fluoroscopically guided procedures, 2. Review of 73 cases and recommendations for minimizing dose delivered to patient, Am. J. Roentgenol. **177** (2001) 13–20.

[5.3] KÖNIG, T.R., WOLFF, D., METTLER, F.A., WAGNER, L.K., Skin injuries from fluoroscopically guided procedures, 1. Characteristics of radiation injury, Am. J. Roentgenol. **177** (2001) 3–11.

[5.4] ATTIX, F.H., Introduction to Radiological Physics and Radiation Dosimetry, John Wiley & Sons, New York (1986).

[5.5] INTERNATIONAL COMMITTEE FOR WEIGHTS AND MEASURES, The BIPM Key Comparison Database (KCDB), BIPM, Sevres, Paris (1999).

[5.6] INTERNATIONAL ATOMIC ENERGY AGENCY, Radiation Oncology Physics: A Handbook for Teachers and Students, (PODGORSAK, E.B., Ed.), IAEA, Vienna (2005).

[5.7] CARLSSON, C.A., Determination of integral absorbed dose from exposure measurements, Acta Radiol. **1** (1963) 433–457.

[5.8] BEDNAREK, D.R., RUDIN, S., Comparison of two dose-area-product ionization chambers with different conductive surface coating for over-table and under-table tube configurations, Health Phys. **78** (2000) 316–321.

[5.9] LARSSON, J.P., PERSLIDEN, J., SANDBORG, M., ALM CARLSSON, G., Transmission ionization chambers for measurements of air kerma integrated over beam area: Factors limiting the accuracy of calibration, Phys. Med. Biol. **41** (1996) 2381–2398.

[5.10] INTERNATIONAL ELECTROTECHNICAL COMMISSION, Dose Area Product Meters, Rep. IEC-60580, 2nd edn, IEC, Geneva (2000).

[5.11] BRENIER, J.P., LISBONA, A., Air kerma calibration in mammography of thermoluminescence and semiconductor dosemeters against an ionization chamber, Radiat. Prot. Dosim. **80** (1998) 239–241.

[5.12] DEWERD, L.A., WAGNER, L.K., Characteristics of radiation detectors for diagnostic radiology, Appl. Radiat. Isot. **50** (1999) 125–136.

[5.13] MEYER, P., et al., Feasibility of a semiconductor dosimeter to monitor skin dose in interventional radiology, Med. Phys. **28** (2001) 2002–2006.

[5.14] MCKEEVER, S.W.S., MOSCOVITCH, M., TOWNSEND, P.D., Thermoluminescence Dosimetry Materials — Property and Uses, Nuclear Technology Publishing, Ashford, UK (1994).

[5.15] ZOETELIEF, J., JULIUS, H.W., CHRISTENSEN, P., Recommendations for Patient Dosimetry in Diagnostic Radiology Using TLD, Rep. EUR 19604, European Commission, Luxembourg (2000).

[5.16] HOROWITZ, Y.S., Thermoluminescence and Thermoluminescent Dosimetry, 3 vols, CRC Press, Boca Raton, FL (1984).

[5.17] INTERNATIONAL ORGANIZATION FOR STANDARDIZATION, Quantities and Units — Part 0: General Principles, Rep. ISO 31-0, ISO, Geneva (1992).
[5.18] INTERNATIONAL ELECTROTECHNICAL COMMISSION, Medical Electrical Equipment — Dosimeters with Ionization Chambers as Used in Radiotherapy, Rep. IEC-60731, IEC, Geneva (1997).
[5.19] PÖYRY, P., KOMPPA, T., KOSUNEN, A., "X ray beam quality specification for kerma area product meters", Quality Assurance and New Techniques in Radiation Medicine (Proc. Int. Conf. Vienna, 2006), IAEA, Vienna.
[5.20] INTERNATIONAL ELECTROTECHNICAL COMMISSION, Medical Electrical Equipment — Dosimeters with Ionization Chambers and/or Semiconductor Detectors as Used in X-Ray Diagnostic Imaging, Rep. IEC-61674, IEC, Geneva (1997).
[5.21] INTERNATIONAL ORGANIZATION FOR STANDARDIZATION, Guide to the Expression of Uncertainty of Measurement, ISO, Geneva (1995).

Chapter 6

ESTABLISHMENT OF A DIAGNOSTIC SSDL CALIBRATION FACILITY

6.1. INTRODUCTION

This chapter discusses the equipment and X ray apparatus necessary for an SSDL to perform calibrations of diagnostic dosimeters. In many aspects, the requirements and procedures for setting up the calibration facility do not differ from those used for the calibration of radiotherapy equipment described in Ref. [6.1]. This report can be used to provide basic guidance for the SSDL planning to establish a diagnostic calibration facility. In addition, each particular application (mammography, CT, etc.) may have special requirements. After a general introduction, the particular requirements of these applications are discussed.

6.2. GENERAL CONSIDERATIONS

The full characterization of X ray beams is based upon measurement of the photon fluence spectrum. However, in practice, an X ray beam can be characterized by measurement of the first and second HVL in order to obtain a qualitative description of the diagnostic X ray field. The X ray tube voltage should be measured in terms of the practical peak voltage [6.2, 6.3], preferably with an invasive device or, alternatively, with a non-invasive one. HVL measurements are usually performed with ionization chambers. To ensure the accuracy of these measurements, the calibration and the energy dependence of the response of these chambers must be known to the SSDL. When measurements in mammographic X ray beams are to be performed, the response of the detector may also be influenced by the materials of the anode and the filtration.

The reading for the secondary standard is converted to the air kerma or the air kerma rate by means of the calibration coefficient as supplied by the PSDL or the IAEA. The calibration coefficient should have a form appropriate to the nature of the reference dosimeter. If the charge or the current delivered by the dosimeter is displayed, the calibration coefficient should have the dimension of gray per coulomb. If the air kerma or air kerma rate is directly displayed the calibration coefficient should be dimensionless. In practice, a number of correction factors may have to be applied. Examples are the

correction factor for the density of air, k_{TP}, incomplete charge collection, k_s, etc. Usually these correction factors have values close to unity.

Calibration of a dosimeter involves the detector and the electrometer being used to measure the charge or current produced during the exposure. Recommendations for the calibration and use of ionization chambers have been proposed by Wagner et al. [6.4]. The characteristics of radiation detectors for diagnostic radiology have been described by DeWerd and Wagner [6.5]. The following sections outline what should be present in an SSDL for such calibrations.

All measuring equipment used for calibration at the SSDL should be of reference class and be available in duplicate. This includes ionization chambers, electrometers, thermometers, barometers and devices to measure the relative humidity of the air. For calibration purposes, the only detector that is considered by the Code of Practice to be a reference class dosimeter is an ionization chamber. For different applications, Table 5.2 gives recommendations on the upper limit of the variation in the response of detectors with radiation energy. Each reference class chamber should have a valid calibration traceable to a PSDL or to the IAEA. The chambers should be calibrated at a number of radiation qualities sufficient to cover the laboratory's goals. Regular (e.g. monthly) measurements should be made to check the stability of the reference chambers.

The time interval between periodic calibrations of the standard instrument should be within the acceptable period defined by national regulations. Where no such regulations exist, the time interval should not exceed two years.

6.3. ENVIRONMENTAL CONDITIONS

The SSDL's calibration facilities should be accommodated in an acclimatized room. The temperature should be controlled in such a way that it remains within the range 18–24°C. The stabilization of the temperature to the above stated range may not be sufficient for performing calibrations, for example, if there are rapid temperature changes. Usually, it should be sufficient if temperature changes are limited to a maximum of about ±1°C/h. If more rapid temperature changes do occur, special attention is required to correct the measurement for the temperature of the air inside any ionization chambers used, including the monitor chamber, secondary standard and the instrument to be calibrated.

At the time of a calibration the relative humidity should be below 80%. If the chamber geometry does not change under the influence of air humidity and

no substantial leakage currents are induced, the effect of humidity on the chamber response can be ignored [6.6].

6.4. APPARATUS

6.4.1. Dosimetry equipment

6.4.1.1. Ionization chamber

For each category of measurements, the laboratory should have two reference class ionization chambers. Each reference chamber (or set of reference chambers) should provide a useful operating range of radiation qualities applicable to all radiation qualities approved for that category. A chamber is considered suitable for a given series of radiation qualities when its variation of response is in compliance with Table 5.2. The leakage current of a suitable reference chamber should be below 10^{-14} A. Each chamber should have a wall thickness sufficient for completion of buildup and calibration coefficients consistent with the overall accuracy goals of the laboratory. The chambers should have high stability and should be ruggedly constructed of material that will minimize change of response with age, temperature, humidity and moderate mechanical force. Any chamber may qualify for more than one series of radiation qualities as long as it meets the requirements of each series. The laboratory must have standard ionization chambers calibrated at radiation qualities sufficient to cover the laboratory's beam qualities. The SSDL should only provide calibrations with the chambers and radiation qualities for which it has a traceable calibration.

Air communication of vented chambers

The laboratory may decide to check the atmospheric communication of ionization chambers. A vacuum container connected to a fore pump in which the chamber can be irradiated at normal atmospheric and at somewhat reduced pressure is satisfactory. A measurement is made in the beam at normal pressure. Subsequently, the pressure is reduced by about 10% and the signal of the chamber is checked to see if it is reduced proportionally to within 0.5%. If a chamber/electrometer system has corrections for pressure, its accuracy should be determined. In this case the same procedure as above is followed and the resultant reading should be the same to within 0.5%.

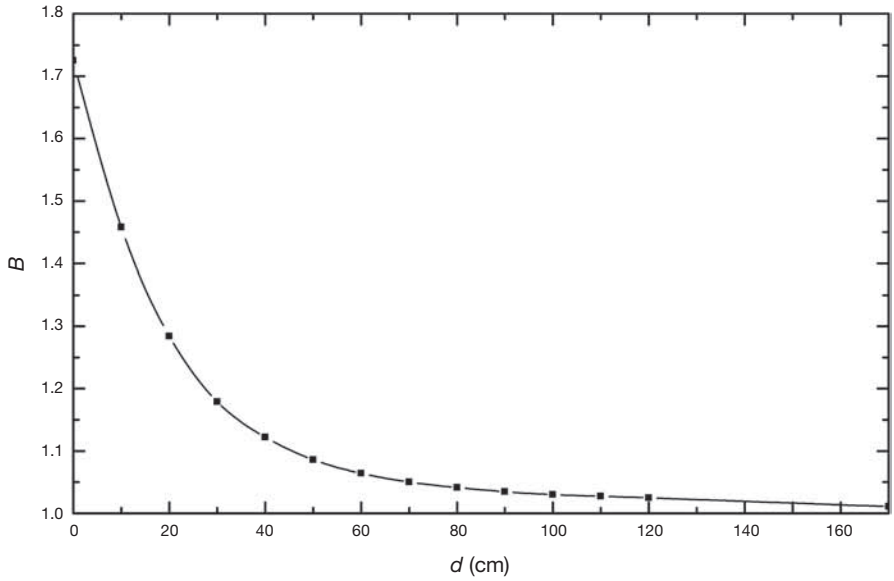

FIG. 6.1. An upper limit for the backscatter factor, B, as a function of the distance, d, from the surface of the backscattering wall. Radiation quality RQR 10, field size 600 mm × 600 mm, backscattering material Perspex (PMMA) of at least 100 mm thickness.

6.4.1.2. Detector positioning

A detector positioning device is required for each detector type. This device should be of a type and quality adequate to restrict detector positioning error to a level consistent with uncertainty goals. The point of test should be located so that scattered radiation does not introduce an uncertainty inconsistent with uncertainty goals.

The magnitude of the effect of scattered radiation at the test position depends essentially on the scattering material, the radiation quality and the field size. Also, the energy dependence of the dosimeter response may be important for practical measurements. In a typical set-up for calibration of diagnostic dosimeters, backscattering potentially forms the strongest component of scattered radiation. Figure 6.1 shows the upper limit on the magnitude of backscattering. It refers to conditions for which the backscattering is most pronounced, i.e. radiation quality RQR 10 (see Section 7.5.2), a field size of 600 mm × 600 mm and a thick (d > 100 mm) Perspex (PMMA) backscattering material. For a further increase of the field size, the backscatter factor remains essentially constant and a further increase in X ray tube voltage leads to a reduction of the backscatter factor. From Fig. 6.1 it can be seen that

the contribution of scattered radiation to the air kerma at the point of measurement is below 3% providing there is no material less than 1 m beyond the point of test.

6.4.1.3. High voltage supply

For chamber polarization, one high voltage supply for the monitor chamber and another for the reference ionization chamber are required. The voltage output should be known to within 1% and be stable to within 0.05% ($k = 2$). Short term stability should be within 1 mV/s. If a voltage supply for the dosimeter to be calibrated is required, it should be of a similar quality. If the combination of detector and readout device is calibrated, the internal voltage supply should be used. This internal voltage supply needs to be checked, if possible, to determine that it is operating properly.

6.4.1.4. Electrometer

At least two electrometers, each capable of measuring charge and current are required. Each should be of sufficient quality to meet the laboratory's accuracy goals for the calibration at all kerma rates. Electrometers should be calibrated according to the information provided in the following paragraphs.

Charge scale calibration of an electrometer may be performed using a set of calibrated capacitors, a calibrated DC voltmeter and a variable voltage source. A precisely known voltage is introduced onto one side of the capacitor standard. The other side of the capacitor standard is connected to the electrometer input. The charge introduced to the electrometer is the product of the voltage and capacitance ($Q = CV$).

The electrometer displays the injected charge value and a calibration coefficient is computed from the ratio of known charge (Q) to the value displayed by the electrometer. This procedure is repeated for a number of different charge values that span the range of the scale. The calibration coefficient of the electrometer, N_C, is obtained by Eq. (6.1):

$$N_C = \frac{C\Delta V}{\Delta M} \tag{6.1}$$

where ΔM is the increment in the reading of the electrometer caused by a voltage increment ΔV. The average of the calibration coefficients determined across the range of the scale should be taken. When the electrometer displays

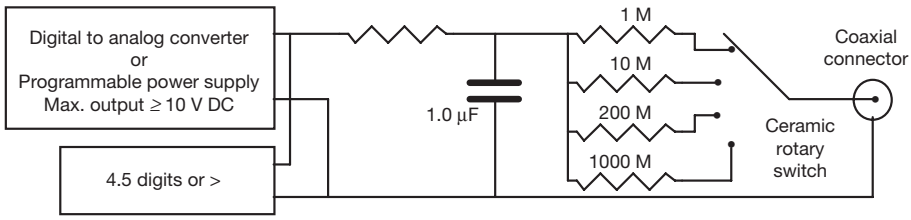

FIG. 6.2. Circuit diagram to apply charge injection to capacitors in Fig. 6.4.

charge in coulombs, the calibration coefficient (N_C) is dimensionless. If the electrometer display is in scale units, then N_C is in units of coulomb/scale unit.

A convenient method of applying the voltage is with a computer controlled digital to analog converter or programmable power supply as illustrated in Fig. 6.2.

A T-filter is inserted between the digital to analog converter and standard capacitor to slow the rise of the voltage and thus reduce the rate of the charge injection. Electrometers that digitize or sample the input signal may require a lower rate of injection than those units with the classic analog integrator preamplifier. The output side of the filter provides for the selection of one of four different resistance values. The selected resistance is dependent on the capacitance of the standard capacitor and the rate limitations of the electrometer. The four resistors are mounted on a ceramic rotary switch. The entire assembly is mounted inside a metal enclosure for electromagnetic shielding purposes and is isolated from earth.

If using a digital analog converter is not an option, then different voltage levels can be produced with a voltage divider circuit (see Fig. 6.3). In Fig. 6.3, four different voltage levels can be produced with a four position rotary switch and a four resistor network. Additional voltage levels would be preferable to give a larger selection of voltage steps. The voltage step size, along with the T-filter selection, determines the rate of charge injection. Electrometers that digitize or sample the signal have a rate limitation.

As illustrated in Fig. 6.4, the standard capacitor is mounted in a separate metal enclosure so that it may be calibrated independently of the other circuitry. The output of the T-filter is connected to the input of the standard capacitor via a coaxial cable. The output of the standard capacitor is connected to the electrometer via a low noise triaxial cable. It should be noted that the triaxial cable is terminated with a coaxial connector and 'pigtail' (outer shield) on the input side and a triaxial connector on the output side. The pigtail may be connected to the standard capacitor enclosure, although for most electrometers this is not necessary.

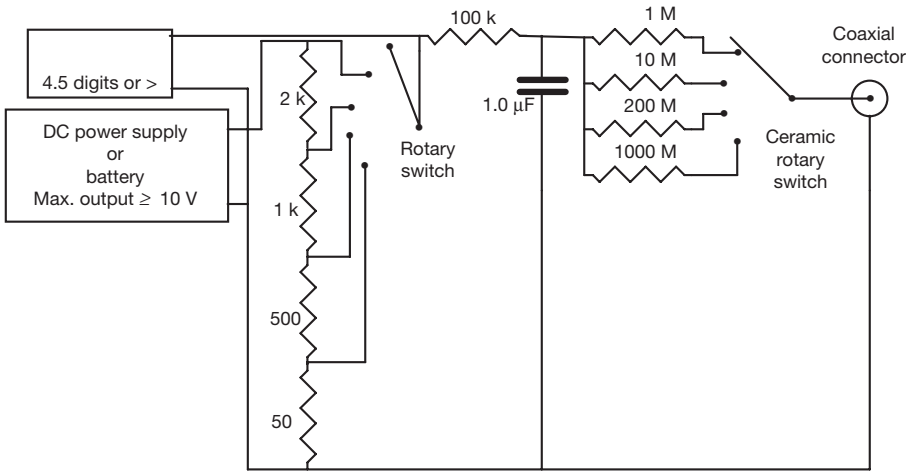

FIG. 6.3. Voltage divider circuit that can be used in place of the digital to analog converter of Fig. 6.2.

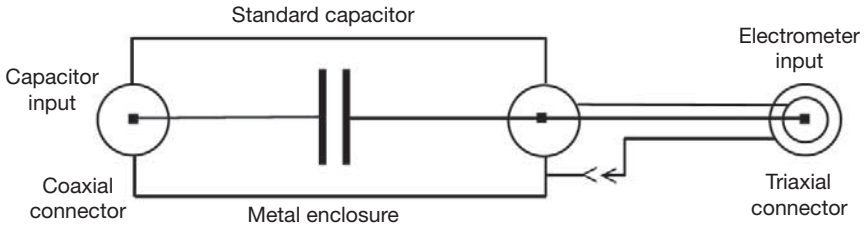

FIG. 6.4. Example of standard capacitor connected to electrometer input.

The standard capacitor should be hermetically sealed and preferably made of polystyrene film. The metal case of the capacitor should be mounted in physical contact with the metal enclosure. The useable capacitance range for this type of capacitor is approximately 0.001–1.0 µF. This standard capacitor will require calibration.

Several capacitors could be mounted in a single enclosure, each terminated with separate coaxial connectors. Alternatively, a ceramic rotary switch could be used to switch several capacitors through a single set of coaxial connectors. It should be noted that the distributive capacitance of a switch may be significant relative to a capacitor with a capacitance near the lower end of the useable range (i.e. 0.001 µF). Owing to the high impedance levels involved, relays or other switching devices have not been found to work satisfactorily.

6.4.2. X ray equipment

The laboratory should use X ray equipment dedicated to calibration use. The range of radiation qualities provided by the laboratory should be consistent with beam qualities as specified in IEC 61267 [6.7]. To perform calibrations of dosimetric equipment in radiation qualities appropriate to conventional diagnostic radiology, the use of a high voltage generator delivering a constant X ray tube voltage at least over the range 50–120 kV is recommended. An X ray tube voltage over the range 20–40 kV is required for mammography applications. Modern high voltage generators do not usually produce a truly constant voltage, it having a certain amount of high frequency ripple. Ripple is expressed as a percentage and is 100 times the ratio of the difference between the highest and lowest values of a rectified waveform during a cycle of potential to the highest value.

For the purpose of this Code of Practice it will be assumed that the X ray tube voltage ripple is less than 10% for conventional applications and less than 4% for mammography applications. It is preferable to use a high voltage generator having as low a ripple as possible. X ray units are commercially available that have a ripple of <l%. It should be possible to display the value of the tube potential to within 1%. For producing the radiation qualities required for diagnostic radiology, the target of the X ray tube should be of the reflecting type. The anode angle should not be larger than 27°. It is preferable that the X ray tube should be of the liquid cooled anode type. This limits its heat dissipation to the environs of the tube and allows its continuous operation.

X ray tubes for calibrations of dosimeters for conventional radiology and CT should have a tungsten target. Requiring tungsten as a target material does not refer to pure tungsten but to a tungsten rich alloy. For technological reasons, for example, alloys are used containing up to 10% rhenium. X ray tubes for calibrations of mammography dosimeters should have a molybdenum target, but having a rhodium target adds to a laboratory's capability [6.8, 6.9]. The number of calibration laboratories with X ray beams from a rhodium target is currently limited. In addition, there are laboratories that use X ray tubes with a tungsten target also for calibrations of mammography dosimeters. This can be done for reference class mammography dosimeters but the possible consequences should be investigated when applying this procedure to dosimeters with marked energy dependence [6.10].

Figure 6.5 shows a schematic drawing of the principal set-up for performing calibrations. The radiation leaves the X ray tube through its exit window. It is important that the exit window adds as little filtration as possible to the inherent filtration of the X ray tube. Too strong a filtration may result in some radiation qualities not being realized. Frequently, the window is made of

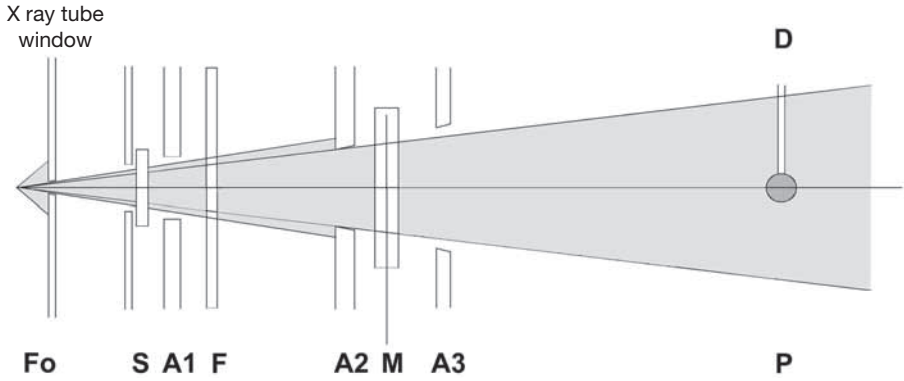

FIG. 6.5. Schematic drawing of the calibration set-up. Fo: focal spot; S: shutter; A1, A2, A3: apertures; F: added filtration; M: monitor chamber; D: detector; P: point of test.

beryllium, in which case the beam hardening is negligible. The inherent filtration, namely, the filtration in the X ray tube and possibly in the radiation protection housing, should always be less than 2.5 mm Al quality equivalent filtration.

6.4.3. Shutter and apertures

The next component in the beam is the X ray beam shutter, S, followed by an aperture, A1, in the radiation protection wall surrounding the X ray tube. The next component is the added filtration, F, which is followed by one, preferably monolithic, assembly of a field limiting aperture, A2, a monitor chamber, M, and a further aperture, A3, the purpose of which is to reduce the impact of backscattering into the monitor chamber from the various types of detector. The secondary standard, the instrument to be calibrated or the detector for performing HVL measurements, denoted by the word detector, is located at the point of test, P, at the reference distance from the focal spot, Fo. To minimize scatter, the apertures A2 and A3 should be constructed according to Fig. 6.6.

The opening angle of the conical aperture needs to be chosen with care. In order to keep the transmission at the 'edge' side of the aperture as small as possible, the angle should be small, but sufficiently large that no radiation emitted by the X ray tube is capable of hitting the inner cone of the aperture. For the determination of the opening angle, the final size of the focal spot as well as extrafocal radiation should be considered. Generally, it can be assumed that any source of X rays lies within a radius of 3 cm of the beam axis.

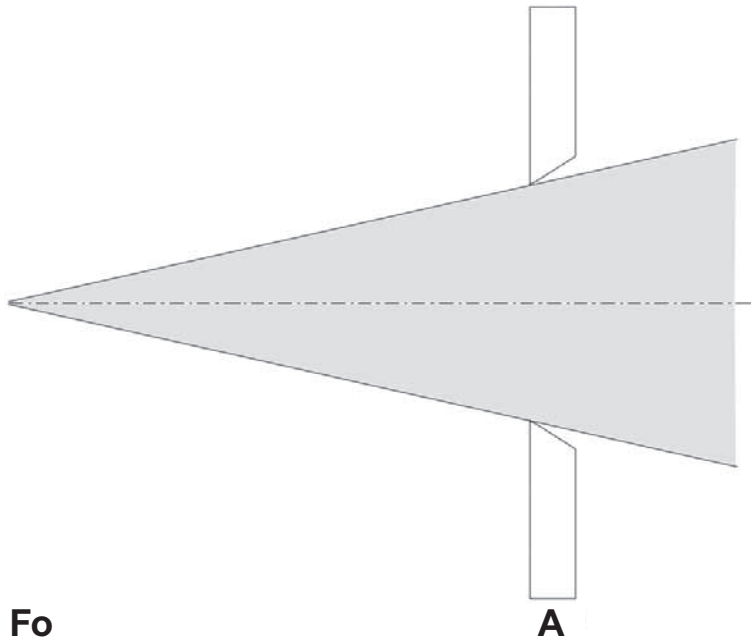

FIG. 6.6. Schematic drawing of apertures designed for low scatter contributions. Fo: focal spot, A: aperture.

The shutter situated between the X ray tube and the monitor chamber must be thick enough to reduce the transmitted air kerma rate to 0.1% for the radiation quality with the highest mean energy to be used. For an X ray tube voltage of 150 kV, a lead thickness of 2 mm is sufficient.

The aperture A2 should be placed after and close to all the added filtration to limit the beam area to the required size. The beam area should be large enough to ensure that both the standard chamber and the detector to be calibrated are irradiated completely and should be small enough so that a minimum of the chamber stem and its support are irradiated. In all directions in the reference plane of the X ray field, the linear dimensions of the field should be at least 1.5 times larger than the corresponding linear dimension of the sensitive volume of the secondary standard or of the detector to be calibrated. Over the central 80% of the calibration field, the air kerma rate should not vary by more than 2% with respect to its maximum value. The beam size must remain constant during a given calibration.

6.4.4. Monitor chamber

A monitor chamber should be positioned in the beam after and close to the field limiting aperture (A2). The monitor chamber should be an unsealed transmission ionization chamber assembly with an associated measuring assembly. The part of the monitor chamber through which the beam passes should be of homogeneous construction and should be large enough to allow the beam with the largest cross-sectional area to pass. The monitor chamber should add as little filtration to the beam as possible. The ionization collection efficiency of this chamber should not be less than 99% for all kerma rates used. The leakage current of the monitor chamber should be less than 2% of the maximum indication in the most sensitive current range and corrections should be applied for leakage current as appropriate. The performance specifications of the monitor chamber and the associated measuring assembly should be similar to that of the standard instrument.

If, for a given radiation quality, the ratio of the indication of the monitor chamber to the indication of the standard instrument can be shown to be stable with time, that is, to change by no more than 0.3% over a specified period, the monitor chamber may be used as a transfer device for that period without further comparison.

The high stability of modern X ray generators does not necessarily require the use of a monitor chamber. Nevertheless, it may be useful to employ a monitor chamber, even for such generators. For highly stable generators, the function of a monitor chamber is primarily focused on quality assurance issues. In a simple approach, the monitor provides information on beam on/off status. In a more sophisticated set-up, the ratio of the monitor current to the X ray tube current may be used. This ratio depends critically on the amount of filtration and on the field size. Agreement, within given limits, between the actual value of this ratio and its nominal value can be used to document the correct choice of filter and field size.

6.4.5. Filters and attenuators

The bremsstrahlung spectrum generated in the target covers the range of energies from zero to the maximum energy corresponding to the X ray tube voltage. Filters, which in diagnostic radiology are usually made of aluminium, are used to modify the primary spectrum by preferentially suppressing its low energy region. This part of the spectrum causes a high dose to the superficial tissues of the patient without contributing to the image.

For conventional radiology beams generated from the tungsten anode at tube voltages of 40 kV and above, the aluminium and/or copper filters, F, to be

used in position between the shutter and the aperture A2 should have a certified purity of at least 99.9%. Their thickness should be known to within 10 μm and be homogeneous over their entire cross-sectional area.

In order to be able to measure attenuation curves over the thickness range 0–31.75 mm, it is recommended to have one of each of the aluminium attenuators with the following nominal thicknesses: 0.05, 0.1, 0.2, 0.4, 0.8, 1.6, 3.2, 6.4, 12.8 and 25.6 mm. The material of these attenuation layers should be aluminium of at least 99.9% purity. The requirements on their homogeneity and the tolerance limits in thickness are the same as for the filters. The geometrical size of the attenuation layers should be large enough to intercept the full radiation beam intended to be used for the calibration.

In mammography, photons with a much lower energy than in conventional radiology are employed to obtain good contrast of the soft tissue. Suitable spectra are produced by combinations of selected target materials and K-edge filters that cut off the low energy end of the bremsstrahlung spectrum and leave much of the bremsstrahlung spectrum at energies above the K-edge. Molybdenum with the K-edge at 20.00 keV and rhodium with the K-edge at 23.22 keV have found widespread application. In order to be able to characterize the radiation quality for such a system reasonably well in terms of HVL, good accuracy with respect to the thickness of filters and HVL attenuators is required. Wagner et al. [6.11] reported 4% changes in measured HVLs for attenuators whose thickness was evaluated using two different methods.

It is recommended that the actual thickness of attenuators be uniform over their entire cross-sectional area and be known with an uncertainty not exceeding 10 μm for X rays of 40 kV and above and 5 μm for mammography applications. The purity of the aluminium attenuators should be at least 99.9%.

6.4.6. X ray tube voltage measuring devices

Preferably an invasive device is used to assess the accuracy and stability of the X ray tube voltage measured as the practical peak voltage. This device should be able to measure the practical peak voltage to within 1.5% or 1.5 kV (k = 2), whichever is the larger. Alternatively, a non-invasive device can be used. Requirements regarding the specifications for non-invasive X ray tube voltage measuring devices are given in IEC 61676 [6.12]. Non-invasive instruments used for measuring the X ray tube voltage in this Code of Practice should comply with IEC 61676.

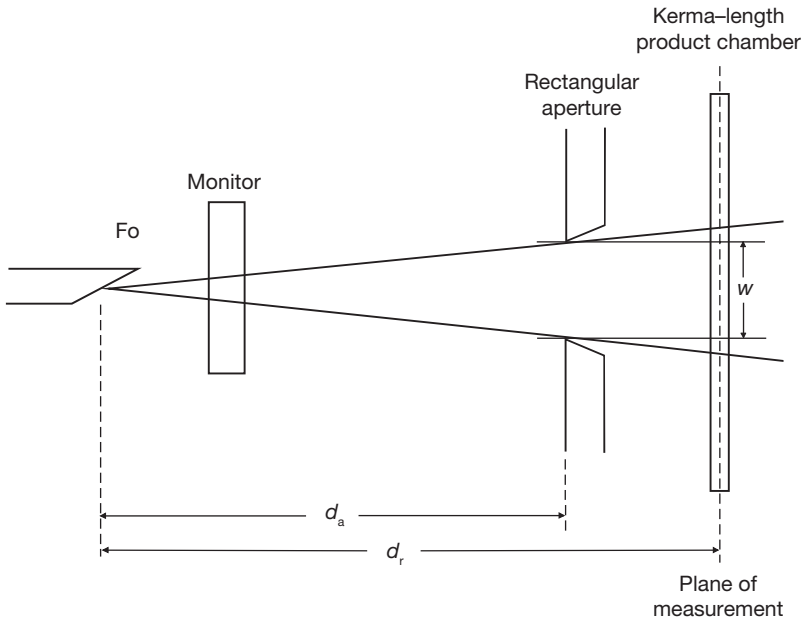

FIG. 6.7. Schematic arrangement for the calibration of CT chambers: d_r is the distance between the focal spot (Fo) and the point of test; d_a is the distance between the focal spot and the plane of the aperture.

6.4.7. Equipment for the calibration of CT chambers

A rectangular lead aperture should be available with a known width (in the direction of the chamber axis) of between 20 and 50 mm and a height corresponding to about two chamber diameters. The laboratory should be able to position the aperture in front of the CT chamber, a suitable separation being 50 mm. This set-up should be used for calibrating the chamber. For the calibration procedure see Section 7.4.6. A schematic arrangement for the calibration of CT chambers is given in Fig. 6.7.

In order to limit the production of scattered radiation at the aperture and given the close proximity between aperture and detector, it is particularly important that the aperture design is in line with the requirements given in Section 6.4.3.

6.4.8. Equipment for the calibration of KAP chambers

A circular or square lead aperture should be available with a known diameter or width between about 40 and 60 mm. The laboratory should be able

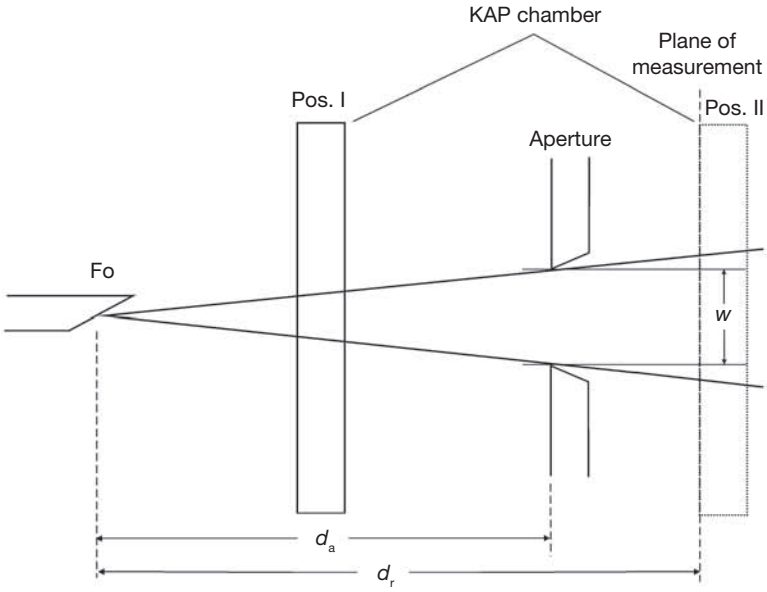

FIG. 6.8. Schematic drawing of the geometrical arrangement for the calibration of KAP chambers. For simplicity, the beam collimator, the filter and the monitor unit are not shown. The arrangement shown in Fig. 6.3 may be used.

to position this aperture in front of the plane of measurement. A suitable distance between the aperture and plane of measurement is 50 mm. Provision should be made to locate the KAP chamber in positions I and II (Fig. 6.8). The exact location of the KAP chamber in position I is not critical. The only requirement is that it should be somewhere between the monitor chamber and the square aperture at a distance d_a from the focal spot.

In position I, there is no need to connect the KAP chamber electrically. Its purpose in the beam is to allow the air kerma (air kerma rate) to be measured behind the KAP chamber, i.e. attenuated by the KAP chamber. This calibration method ensures that the KAP meter, when used in the clinic, measures the air kerma–area product in the beam behind the KAP chamber (measures transmitted radiation). If it is desired that the instrument measures the air kerma–area product for radiation incident on the detector, the KAP chamber is located only in position II during the calibration.

In position II, the entrance plane of the KAP chamber, which is considered to be the KAP chamber's reference plane, should be placed in the plane of measurement at a distance d_r from the focal spot. Recommended values for the distances d_a and d_r are 950 mm and 1000 mm. For the measurement of the air kerma (rate) in the plane of measurement with the

KAP chamber in position I, a reference chamber should be available whose cross-sectional area is smaller than the cross-sectional area of the aperture. For the calibration of KAP meters, the radiation qualities of the RQR series should be used.

In order to limit the production of scattered radiation at the aperture and given the close proximity between aperture and detector, it is particularly important that the aperture design conforms to the requirements given in Section 6.4.3.

6.5. ESTABLISHING RADIATION QUALITIES

6.5.1. General

The most complete specification of X ray beams is given by their spectral distribution. Since the spectrometry of X rays requires considerable expertise and is time consuming to perform, a description of radiation qualities in terms of the X ray tube voltage and the first and second HVLs are usually employed. The description followed in this Code of Practice is a compromise between the mutually conflicting requirements of avoiding excessive effort to establish a radiation quality and of ensuring the complete absence of any ambiguity in the definition of the radiation quality. Owing to differences in the design and the age of X ray tubes (in terms of anode angle, anode roughening and inherent filtration), two radiation qualities produced at a given X ray tube voltage having the same first HVL can still have quite different spectral distributions.

Radiation qualities used for calibrations for diagnostic radiology are shown in Table 6.1 together with their possible applications. The qualities should be established according to IEC 61267 [6.7]. The method of measurement of the first and second HVLs (as described in Appendix V) should be used. This method follows the recommendation given in Ref. [6.13]. Narrow beam geometry should be used for determining the HVLs. The diameter of the beam at the detector location should be just sufficient to irradiate it completely and uniformly. The aluminium absorbers should be located equidistant from the monitor chamber and from the detector. The distance from the aluminium absorbers to the detector should be at least five times the diameter of the beam at the detector. This arrangement ensures that the production of scattered radiation in the absorber does not lead to an unnecessarily large contribution of scattered radiation to the signal of the monitor chamber or the reference chamber. Details of HVL measurements that apply to the SSDL as well as to clinical measurements are given in Appendix V.

TABLE 6.1. RADIATION QUALITIES FOR CALIBRATIONS OF DIAGNOSTIC DOSIMETERS

Radiation quality	Radiation origin	Material of an additional filter	Application
RQR	Radiation beam emerging from X ray assembly	No phantom	General radiography, fluoroscopy and dental applications (measurements free in air)
RQA	Radiation beam with an added filter	Aluminium	Measurements behind the patient (on the image intensifier)
RQT	Radiation beam with an added filter	Copper	CT applications (measurements free in air)
RQR-M	Radiation beam emerging from X ray assembly	No phantom	Mammography applications (measurements free in air)
RQA-M	Radiation beam with an added filter	Aluminium	Mammography studies

6.5.2. Standard radiation qualities RQR

The following describes how the radiation qualities RQR according to IEC 61267 should be established. These radiation qualities represent the beam incident on the patient in general radiography, fluoroscopy and dental applications. They can be realized by means of a tungsten anode X ray tube. The characteristics of the radiation qualities of the RQR series are given in Table 6.2.

Preferentially, the X ray tube voltage should be measured with a voltage divider connected in parallel to the X ray tube. The X ray tube voltage should be specified in terms of the practical peak voltage. The overall uncertainty (coverage factor $k = 2$) of the X ray tube voltage measurement should not be greater than 5% or 2 kV, whichever is the greater.[1] If an invasive X ray tube voltage measuring system is not available, a non-invasive device may be used as

[1] According to IEC 61267, the uncertainty of the high voltage measurement should not exceed 1.5% or 1.5 kV ($k = 2$), whichever is the greater. This can be achieved only with invasive measurements. To facilitate the application of this Code of Practice, non-invasive techniques can also be applied but these have a greater uncertainty.

TABLE 6.2. CHARACTERIZATION OF RADIATION QUALITY SERIES RQR

Radiation quality	X ray tube voltage (kV)	First HVL (mm Al)	Homogeneity coefficient (h)
RQR 2	40	1.42	0.81
RQR 3	50	1.78	0.76
RQR 4	60	2.19	0.74
RQR 5*	**70**	**2.58**	**0.71**
RQR 6	80	3.01	0.69
RQR 7	90	3.48	0.68
RQR 8	100	3.97	0.68
RQR 9	120	5.00	0.68
RQR 10	150	6.57	0.72

* This value is generally selected as the reference radiation quality for unattenuated beams for general radiography applications.

an alternative. The X ray tube voltage should be adjusted to the value given in column 2 of Table 6.2. The next step consists of determining the amount of filtration needed to establish the radiation qualities RQR. This is done by measuring an attenuation curve with aluminium attenuation layers. The attenuation curve should provide for an attenuation factor of at least six.

6.5.2.1. Determination of additional filtration

A simple way of determining the additional filtration necessary to achieve the desired radiation quality is as follows:

(a) Plot the attenuation curve. Use a linear scale on the abscissa for the attenuation layer thickness and a logarithmic scale on the ordinate for the attenuation factor.
(b) Prepare a rectangular template, preferably transparent, the height and width of which, both in the respective units of the diagram, are given by a factor of four and by the first HVL of the standard radiation quality to be realized multiplied by $(1 + 1/h)$, respectively, where h is the homogeneity coefficient of the standard radiation quality.

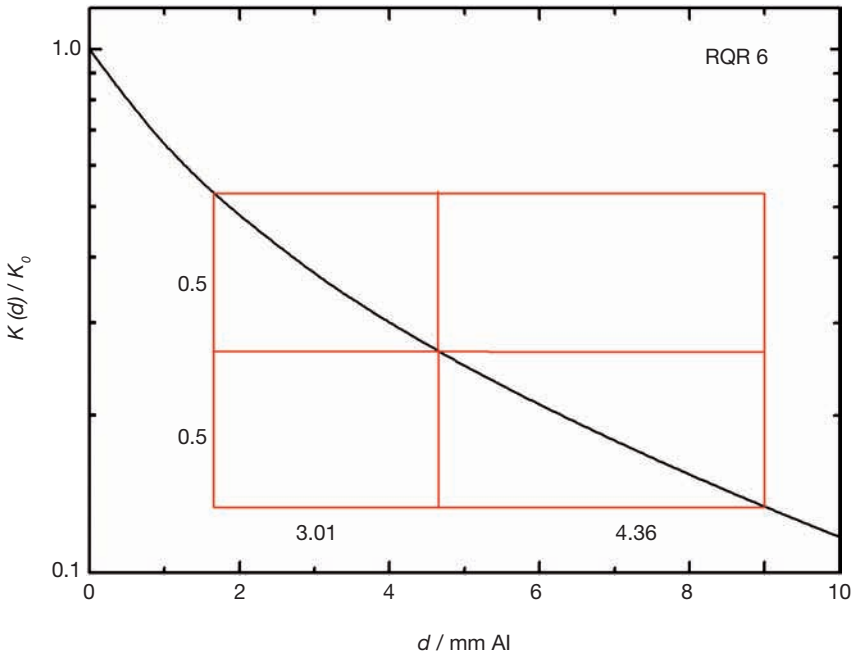

FIG. 6.9. An example of the attenuation curve for the beam RQR 6 expressed as the ratio of the air kerma, K(d), behind a filtration of thickness, d, to the air kerma, K_0, of the unattenuated beam.

(c) Make an auxiliary horizontal line on the template, dividing it into two parts of equal size, and another vertical line at a distance from the left edge of the template corresponding to the first HVL.

(d) Try to position this template on the attenuation curve in such a way that the edges of the template are parallel to the axes of the diagram and that the upper left and the point of intersection of the two auxiliary lines coincide with points on the attenuation curve (see Fig. 6.9). The difference between the position of the left edge of the template and the ordinate gives the amount of additional filtration required to establish the radiation quality RQR.

The algorithm described above has a meaningful solution only as long as the total filtration of the X ray tube and its assembly is less than the filtration required to obtain the desired HVL. If the filtration is too large the template cannot be positioned on the attenuation curve in the required way. In this case a match between the attenuation curve and the template can be achieved by

positioning the template in such a way that the second HVL is matched, i.e. the intersection of the two auxiliary lines and the bottom right corner should lie on the attenuation curve. By doing this the left side of the template will be on the left side of the ordinate. This indicates that a removal of filtration is required, a procedure which usually cannot be carried out. In such a situation the X ray tube is not suited to produce the radiation qualities of the RQR series. However, the RQA radiation qualities, which have a much stronger filtration, can be established as described in Section 6.5.3.

The next step is to add the additional filtration determined above. Finally, the HVL achieved with the modified filtration should be verified by measuring the air kerma or air kerma rate with and without an aluminium attenuation layer of the thickness given in column 3 of Table 6.2. If the ratio of air kerma (rate) values lies between 0.485 and 0.515 the desired radiation quality is established.

Since the establishment of the correct HVL is a non-linear procedure, it may be necessary to repeat the steps described in this section starting with the measurement of the attenuation curve. If the ratio of air kerma (rate) lies slightly outside the range 0.485–0.515, the required filtration can be determined through trial and error measurements. If the ratio of the air kerma is below 0.485, the additional filtration needs to be increased and vice versa.

The amount of additional filtration required to establish each of the radiation qualities RQR will not be identical for each radiation quality. If the difference between the largest and smallest value of the additional filtration is not greater than 0.5 mm, one single additional filter with a thickness close to the arithmetic mean of all values of additional filtration may be used to establish all radiation qualities RQR. This criterion can also be applied to a group of radiation qualities.

The primary beam specifying quantities are the X ray tube voltage and the first HVL. These two quantities should be adjusted as closely as possible to the values given in Table 6.2. The homogeneity coefficient is a secondary beam specifying quantity. The actual value of the homogeneity coefficient associated with the appropriate radiation quality RQR should lie within 0.03 of the value given in column 4 of Table 6.2. A periodic check on the HVL of the beams should be carried out in order to verify that possible changes with respect to prior values do not exceed 3%.

6.5.3. Standard radiation qualities RQA and RQT

The radiation qualities of the RQA series represent simulations of the radiation field behind a patient and those of the RQT series simulate the unattenuated beam used in CT. Once the radiation qualities of the RQR series

are established, the radiation qualities of the RQA series and those of the RQT series are readily obtained by adding the additional filtration given in columns 3 of Tables 6.3 and 6.4 to corresponding RQR radiation qualities.

If there is no need or if the inherent filtration of the X ray tube is too high to establish the radiation qualities of the RQR series, standard radiation qualities RQA can be directly established from the determination of the inherent filtration described in Section 6.5.2. If the left edge of the template matching the attenuation curve is on the right hand side of the ordinate, RQA qualities are established by adding an Al filtration amounting to the sum of the

TABLE 6.3. CHARACTERIZATION OF RADIATION QUALITY SERIES RQA

Radiation quality	X ray tube voltage (kV)	Added filtration (mm Al)	Nominal first HVL (mm Al)
RQA 2	40	4	2.2
RQA 3	50	10	3.8
RQA 4	60	16	5.4
RQA 5*	**70**	**21**	**6.8**
RQA 6	80	26	8.2
RQA 7	90	30	9.2
RQA 8	100	34	10.1
RQA 9	120	40	11.6
RQA 10	150	45	13.3

* This value is generally selected as the reference radiation quality for attenuated beams for general radiography applications.

TABLE 6.4. CHARACTERIZATION OF RADIATION QUALITY SERIES RQT

Radiation quality	X ray tube voltage (kV)	Added filtration (mm Cu)	Nominal first HVL (mm Al)
RQT 8	100	0.2	6.9
RQT 9*	**120**	**0.25**	**8.4**
RQT 10	150	0.3	10.1

* This value is generally selected as the reference radiation quality for CT.

values given in column 3 of Table 6.3 and the additional filtration determined with the help of Fig. 6.9. If the left edge of the template is on the left of the ordinate the Al filtration to be added is obtained from the value in column 3 minus the absolute value of the difference between the left side of the template and the ordinate.

The procedure described in the last paragraph cannot be applied for establishing standard radiation qualities RQT without having first established radiation qualities RQR. In this case, the RQT radiation qualities may be established by trial and error. It is recommended that the amount of copper filtration given in column 3 of Table 6.4 be provided and then the HVL achieved with the modified filtration verified by measuring the air kerma or air kerma rate with and without an aluminium attenuation layer of the thickness given in column 4 of Table 6.4. If the ratio of air kerma (rate) values lies between 0.485 and 0.515, the desired radiation quality, the RQT series, is established. If the ratio is outside this range, the copper filtration needs to be increased or decreased depending on the actual value of the ratio.

6.5.4. Standard radiation qualities RQR-M and RQA-M

For mammography dosimeters, a molybdenum anode tube with molybdenum filtration and an X ray machine capable of generating radiation qualities with a first HVL as shown in Tables 6.5 and 6.6 should be used.

The radiation qualities of the RQR-M series are established by adjusting the X ray tube voltage to the values given in column 2 of Table 6.5. The X ray tube voltage should be measured, preferably with an invasive voltage divider, in terms of the practical peak voltage. Alternatively, a non-invasive device may be used. If not already contained in the inherent filtration of the X ray tube, a

TABLE 6.5. CHARACTERIZATION OF RADIATION QUALITY SERIES RQR-M

Radiation quality	X ray tube voltage (kV)	Nominal first HVL (mm Al)
RQR-M 1	25	0.28
RQR-M 2*	**28**	**0.31**
RQR-M 3	30	0.33
RQR-M 4	35	0.36

* This value is generally selected as the reference radiation quality for mammography (both RQR-M and RQA-M series).

TABLE 6.6. CHARACTERIZATION OF RADIATION QUALITY SERIES RQA-M

Radiation quality	X ray tube voltage (kV)	Added filtration (mm Al)	Nominal first HVL (mm Al)
RQA-M 1	25	2	0.56
RQA-M 2	28	2	0.60
RQA-M 3	30	2	0.62
RQA-M 4	35	2	0.68

molybdenum filter with a thickness of 0.032 ± 0.002 mm should be brought into the beam at a location close to the X ray tube. For the purpose of verification, an HVL thickness measurement should be conducted. Dosimeters with a variation of response over the range of mammographic radiation qualities in compliance with specifications in Table 5.2 are suitable for measuring HVLs in all beams (i.e. RQR-M and RQA-M) and also for all other target/filter combinations routinely used in mammography [6.10]. If the result of the HVL measurement is within 0.02 mm of the values given in column 3 of Table 6.5, the desired radiation quality is established. If the measured HVL differs more than 0.02 mm from the value in Table 6.5, the laboratory should acquire a molybdenum filter of suitable thickness.

The radiation qualities of the RQA-M series simulate the radiation fields behind the patient during mammography. They are established by adding 2 mm of aluminium to the corresponding RQR-M radiation qualities.

The SSDL should establish at least three radiation qualities in the range 20–35 kV.

6.5.5. Other radiation qualities for mammography

Radiation qualities not specified in IEC 61267 have come into use for mammography. This has given rise to the question of whether SSDLs should develop calibration capabilities employing all or most radiation qualities and target/filter combinations used in practice. Experience shows that reference class instruments yield good response in different beams without being specifically calibrated in these beams. Various chambers were measured by DeWerd et al. [6.14] and results showed that only two chambers had a distinguishable difference in response between beams from a rhodium target with rhodium

filtration (Rh/Rh beams[2]) and beams generated from a molybdenum target and filtered by molybdenum (Mo/Mo beams). The differences in the two beams for these two chambers were 2.5% and 4.3%, respectively. The difference between a Mo/Mo beam operated at 28 kV and the beam from a tungsten target filtered by aluminium (W/Al beam) operated at 30 kV was within 1.2%. A comprehensive study of the effect of X ray beam spectra on the response of mammography dosimeters was also done as part of a EUROMET project [6.10]. Conclusions of this study were similar to those of DeWerd et al. [6.14].

The results of both studies show that good mammography dosimeters (reference class chambers (see Chapter 5, Table 5.2)) can be calibrated with almost any of the beams studied with an HVL in the mammography range. If the SSDL does not possess an X ray tube with a molybdenum target, a good compromise would be to use an X ray tube with a tungsten target and molybdenum or rhodium filter. The next option would be to use the X ray tube with a tungsten target and aluminium filters to produce beams with HVLs in the mammography range. An X ray tube with a tungsten target will limit the types of dosimeter that can be calibrated by the SSDL. The mammography radiation qualities with a rhodium filter and/or rhodium target established in the IAEA dosimetry laboratory are shown in Table 6.7 [6.9]. Characteristics of these radiation qualities are similar to those measured for the qualities used at the National Institute of Standards and Technology [6.15].

6.6. CALIBRATION OF NON-INVASIVE X RAY TUBE VOLTAGE MEASURING INSTRUMENTS

6.6.1. Establishing the value for the practical peak voltage

In this Code of Practice, the X ray tube voltage is specified in terms of the practical peak voltage. The rationale for using this quantity and the mathematical procedure for its determination are given in Appendix IV.

The practical peak voltage is the result of achieving a quantity that is measurable and which can be standardized. The problem with all other quantities used to measure the voltage of an X ray generator is the presence of ripple in the electrical waveform. For carrying out calibrations of non-invasive high voltage measuring devices, the SSDL needs to be equipped with suitable

[2] The beam codes used for mammography beams are a combination of the chemical symbol of a target and a filtration followed by the potential of the tube in kilovolts and a letter 'x' to indicate beams attenuated by 2 mm of aluminium (see Table 6.7).

TABLE 6.7. MAMMOGRAPHY RADIATION QUALITIES WITH A RHODIUM FILTER AT THE IAEA DOSIMETRY LABORATORY

Radiation quality	Tube potential (kV)	Added filtration (mm)	First HVL (mm Al)	Homogeneity coefficient (h)
Mo anode				
Mo/Rh-28	28	0.025 Rh	0.417	0.82
Mo/Rh-32	32	0.025 Rh	0.449	0.84
Rh anode				
Rh/Rh-25	25	0.025 Rh	0.362	0.78
Rh/Rh-30	30	0.025 Rh	0.444	0.76
Rh/Rh-35	35	0.025 Rh	0.504	0.78
Rh/Rh-40	40	0.025 Rh	0.548	0.78
Rh/Rh-30x	30	0.025 Rh + 2 Al	0.814	0.94
Rh/Rh-35x	35	0.025 Rh + 2 Al	0.883	0.92

means for calibrating the voltage delivered by the generator to the X ray tube. This should be done under operating conditions, i.e. with the tube current usually used. The best method employs an appropriately calibrated and frequency compensated resistor chain connected parallel to the generator and the X ray tube (see Fig. 6.10). A voltage divider is a common device used to accomplish this method. From the readings of this device the practical peak voltage should be calculated according to Appendix IV from the voltage waveform. In the presence of ripple, it is important that the measurements are performed in such a way that the correct phase relationship between the two outputs is maintained. This can either be achieved by a direct measurement between the two output points of the voltage divider or, alternatively, the voltage of each branch may be measured with respect to ground potential. In the latter case, a correct determination of the voltage difference requires the combination of the two signals from the output points of the divider in their correct phase relationship. If the SSDL follows this procedure, the details of the arrangement actually used must be considered at depth in order to arrive at the uncertainty of the high voltage measurement.

If the above method is not available, one of the following two options should be used: (i) a non-invasive device is employed, which measures the practical peak voltage and has been calibrated by another SSDL or other calibration laboratory; (ii) the X ray tube voltage should be measured with

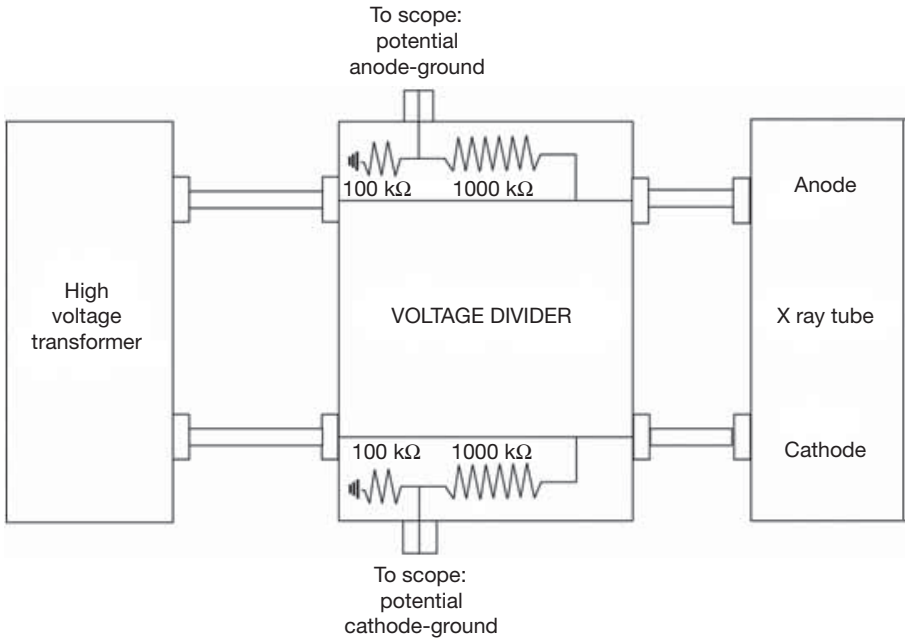

FIG. 6.10. Schematic drawing of a measuremen set-up with a voltage divider.

a non-invasive high voltage measuring device possessing an analog and/or a digital output from which the variation of the high voltage can be taken as a function of time of the X ray beam. After having calibrated the analog or digital output of the non-invasive measuring device with the help of an X ray generator delivering a constant potential, the output signal can be converted to the practical peak voltage by means of the data provided in Appendix IV. It is recommended that the calibration at constant X ray tube voltage be performed by an accredited laboratory.

Unlike for calibration of dosimeters, the uncertainty budget for the calibration of non-invasive high voltage measuring devices is governed by one single component, i.e. the uncertainty of the reference instrument. For a good quality frequency compensated invasive measuring device with an appropriate calibration an uncertainty of 1.5% or 1.5 kV ($k = 2$), whichever is greater, may be achieved. When a non-invasive device for measuring the practical peak voltage according to IEC 61676 is employed, it can be inferred from Table 2 in IEC 61676 that an uncertainty of measurement of about 5% ($k = 2$) is a reasonable estimate for all modalities in diagnostic radiology. In this estimate, the limits of variation associated with the various influence quantities have been converted to a standard uncertainty by dividing the limits of variation by

$\sqrt{3}$ and by summing the standard uncertainties obtained in this way in quadrature.

Over the voltage range of 10–160 kV, the accuracy and stability of the dividing ratio of the voltage divider should be within ±1% for DC and for frequencies up to 100 Hz, and ±5% for higher frequencies up to 100 kHz. The temperature coefficient of the divider should be better than 30 ppm/°C. The output of the invasive voltage divider used for calibrations should be connected to a digitizer (computer). Most of the standard readouts provided with the invasive voltage divider only give an indication of the peak voltage and not the waveform. This is not sufficient. It is best to digitize the waveform and then determine the practical peak voltage as given in Appendix IV. The digitizing system selected should have a conversion depth of at least 12 bits and be able to measure a noise not exceeding the least important two bits when a constant voltage is applied. The sampling rate for the waveform should be fast; this requirement can be considered to be met if it is at least five times higher than the generator frequency. The SSDLs are advised to obtain a calibration certificate for the invasive voltage divider at the time of purchase so that it only has to be shipped once.

6.7. CALIBRATION UNCERTAINTIES AT THE SSDL

A statement of the laboratory goals for each category of calibration should be made by the SSDL. The goals should specify the uncertainties to be achieved. The uncertainty budget should be established on the basis of the Guide for the Expression of Uncertainty of Measurement [6.16]. An example of an uncertainty budget evaluation is given in Appendix II. The uncertainties should also include those stated by the primary laboratory for the secondary standard chamber calibration and this may be itemized separately. The expanded uncertainty should fall within the values given in Table 6.8 (coverage factor $k = 2$).

NOTE: The uncertainties given in Table 6.8 represent realistic values for calibrations of diagnostic dosimeters. An SSDL employing the usual equipment should generally be in a position to establish an uncertainty budget within the frame given in the table. The value for $N_{K,Q}$ or $N_{K,Q_0}k_Q$ has to be taken from the calibration certificate of the secondary standard.

NOTE: Another example of an uncertainty budget may be found in ICRU 74 [6.17]. The differences between the two examples highlight

the fact that there is no 'universal' uncertainty budget and that different contributions may have to be taken into account depending on the nature of the facility and on the type of instrument(s) involved in the calibration.

TABLE 6.8. AN EXAMPLE OF AN UNCERTAINTY BUDGET FOR CALIBRATIONS AT SSDLs

Influence quantity/parameter	Relative standard uncertainty ($k = 1$) (%)
Dosimeters	
$N_{K,Q}$ or $N_{K,Q_0}k_Q$	1.0
Radiation quality (i.e. differences between PSDL and SSDL)	0.3
Kerma rate	0.3
Direction of radiation incidence	0.3
Air pressure	0.3
Temperature and humidity	0.3
Electromagnetic compatibility	0.5
Field size/field homogeneity	0.5
Operating voltage	0.5
Long term stability of reference instrument	0.5
Relative combined standard uncertainty of the reference value of the air kerma ($k = 1$)	1.57
Additional contribution for the calibration of user's instrument	
Uncertainty associated with transfer	0.3*
Relative combined uncertainty of N_K or $N_K k_Q$ of user's instrument ($k = 1$)	1.6
Relative expanded uncertainty of $N_{K,Q}$ or $N_{K,Q_0}k_Q$ of user's instrument ($k = 2$)	**3.2**
Relative expanded uncertainty of electrometers ($k = 2$)	**0.6**
Relative expanded uncertainty of non-invasive X ray tube voltage measuring instruments ($k = 2$)	**5.0**

Note: All uncertainties listed in this table other than the one marked * are type B uncertainties (see Appendix I).

6.8. QUALITY MANAGEMENT SYSTEM

The need for high quality measurements in diagnostic radiology requires that high quality calibration services be provided by SSDLs. The primary goal of any SSDL is to disseminate standards with the smallest possible uncertainty. This is accomplished through the calibration of end user instruments. In order to attain the required level of quality in calibrations, it is necessary to institute procedures for the management of quality in laboratory operations. Although the establishment of a systematic approach to quality assurance is primarily the responsibility of the laboratory's management, all laboratory staff members should share the common goal of achieving the required degree of quality.

The quality assurance system should comply with ISO 17025 [6.18], which documents all the requirements that calibration and testing laboratories have to meet if they wish to demonstrate that they operate a quality assurance system, are technically competent and are able to disseminate technically valid results. The scope of the quality assurance system should be appropriate to the level of quality required and the system should be designed to demonstrate that the required level of performance has been achieved. The basic elements of the quality system are described in a quality manual and the degree of detail included in the manual should be appropriate to the size and complexity of the laboratory. The manual should create trust in the quality of the services provided by the laboratory.

The quality manual describes the level of quality to be expected and the methods the laboratory will employ to achieve the stated goals. Typically, it starts with a description of the main activities of the laboratory, the organizational details and the management structure. It contains the address and organizational charts and lists the responsibilities of the staff members working in the laboratory. It describes the elements of the quality system, including the quality policy, quality objectives and a structure of the quality system as well as document control and services to the client. It further describes procedures for handling client complaints, control of non-conforming measurements or calibration work and the resulting corrective and preventive actions. It also includes remarks on internal and external audits and management quality reviews. The manual describes technical activities, including measurement and calibration methods, equipment, measurement traceability and calibration, measurement uncertainty, quality control and reporting of the results. It also gives examples of calibration certificates and lists controlled documents, the related bibliography and the revision history of the quality manual.

In addition to the quality manual, documents such as relevant regulations, standards, specifications and instruction manuals for all equipment should be available at the laboratory. In this way, the quality system documentation may

be used to demonstrate compliance with applicable standards, regulations and legal requirements.

Once the quality system is established, the laboratory should maintain and update it as necessary, in accordance with the experience gained during operation of the service and internal or external audits. Laboratories working in the same area can also discuss their common problems and compare the results. 'Round robin' comparisons are recommended to ensure consistency among the laboratories. These comparisons may consist of exchanging measuring devices and performing measurements in agreed radiation fields [6.19]. They may also involve the dispatch of passive dosimeters to the participating laboratories in order to be irradiated in agreed radiation fields [6.20, 6.21]. Peer reviews of laboratory procedures may also be useful to foster increased communication and encourage suggestions for improving quality.

The development of a quality system is a complex task that involves various activities. It is not possible to specify precise values for the timescale spent with different activities because they require different amounts of time for completion. Some of the activities require completion of other activities but some of them also overlap or are ongoing tasks. Experience shows that the development of the quality assurance programme requires from one to two years.

As stated above, ISO 17025 provides a basic guide on elements of the quality system. Additional guidance may be found in Refs [6.22–6.24]. A quality assurance programme has been established at the IAEA Dosimetry Laboratory [6.25]. The quality system deals with two main services provided by the laboratory: dosimetry calibration and TLD auditing services. The system was reviewed by external panel in early 2004. The developed documentation may be used as guidance for other laboratories in the IAEA/WHO network of SSDLs that attempt to establish their own quality system.

REFERENCES

[6.1] INTERNATIONAL ATOMIC ENERGY AGENCY, Calibration of Dosimeters Used in Radiotherapy, Technical Reports Series No. 374, IAEA, Vienna (1994).

[6.2] BAORONG, Y., KRAMER, H.-M., SELBACH, H.-J., LANGE, B., Experimental determination of practical peak voltage, Br. J. Radiol. **73** (2000) 641–649.

[6.3] KRAMER, H.-M., SELBACH, H.-J., ILES, W.J., The practical peak voltage of diagnostic X-ray generators, Br. J. Radiol. **71** (1998) 200–209.

[6.4] WAGNER, L.K., et al., Recommendations on the performance characteristics of diagnostic exposure meters: Report of AAPM Diagnostic X-Ray Imaging Task Group No. 6, Med. Phys. **19** (1992) 231–241.
[6.5] DEWERD, L.A., WAGNER, L.K., Characteristics of radiation detectors for diagnostic radiology, Appl. Radiat. Isot. **50** (1999) 125–136.
[6.6] INTERNATIONAL COMMISSION ON RADIATION UNITS AND MEASUREMENTS, Average Energy Required to Produce an Ion Pair, ICRU Rep. 31, ICRU, Bethesda, MD (1979).
[6.7] INTERNATIONAL ELECTROTECHNICAL COMMISSION, Medical Diagnostic X-Ray Equipment — Radiation Conditions for Use in the Determination of Characteristics, Rep. IEC-61267, IEC, Geneva (2005).
[6.8] COLETTI, J.G., PEARSON, D.W., DEWERD, L.A., O'BRIEN, C.M., LAMPERTI, P.J., Comparison of exposure standards in the mammography X-ray region, Med. Phys. **24** (1997) 1263–1267.
[6.9] PERNIČKA, F., ANDREO, P., MEGHZIFENE, A., CZAP, L., GIRZIKOWSKY, R., Standards for Radiation Protection and Diagnostic Radiology at the IAEA Dosimetry Laboratory, SSDL Newsletter 41, IAEA, Vienna (1999) 13–21.
[6.10] WITZANI, J., et al., Calibration of dosemeters used in mammography with different X-ray qualities: Euromet Project No. 526, Radiat. Prot. Dosim. **108** (2004) 33–45.
[6.11] WAGNER, L.K., ARCHER, B.R., CERRA, F., On the measurement of half-value layer in film-screen mammography, Med. Phys. **17** (1990) 989–997.
[6.12] INTERNATIONAL ELECTROTECHNICAL COMMISSION, Medical Electrical Equipment — Dosimetric Instruments Used for Non-invasive Measurements of X-Ray Tube Voltage in Diagnostic Radiology, Rep. IEC 61676, IEC, Geneva (2002).
[6.13] INTERNATIONAL COMMISSION ON RADIATION UNITS AND MEASUREMENTS, Physical Aspects of Irradiation, National Bureau of Standards Handbook 85, ICRU Rep. 10b, ICRU, Bethesda, MD (1964).
[6.14] DEWERD, L.A., et al., The effect of spectra on calibration and measurement with mammographic ionization chambers, Med. Phys. **29** (2002) 2649–2654.
[6.15] LAMPERTI, P.J., O'BRIEN, M., Calibration of X-Ray and Gamma-Ray Measuring Instruments, NIST Special Publication SP 250-58, National Institute of Standards and Technology, Gaithersburg, MD (2001) 250–258.
[6.16] INTERNATIONAL ORGANIZATION FOR STANDARDIZATION, Guide to the Expression of Uncertainty of Measurement, Rep. ISO 98:1995, ISO, Geneva (1995).
[6.17] INTERNATIONAL COMMISSION ON RADIATION UNITS AND MEASUREMENTS, Patient Dosimetry for X Rays Used in Medical Imaging, ICRU Rep. 74, ICRU, Bethesda, MD (2006).
[6.18] INTERNATIONAL ORGANIZATION FOR STANDARDIZATION, General Requirements for the Competence of Testing and Calibration Laboratories, Rep. ISO 17025, ISO, Geneva (1999).

[6.19] MEGHZIFENE, A., CZAP, L., SHORTT, K.R., "Comparison of calibration coefficients in the IAEA/WHO network of secondary standards dosimetry laboratories", Standards and Codes of Practice in Medical Radiation Dosimetry (Proc. Conf. Vienna, 2002), IAEA, Vienna (2004) 375–384.
[6.20] PERNIČKA, F., et al., "Comparison of TLD air kerma measurements in mammography", Standards and Codes of Practice in Medical Radiation Dosimetry (Proc. Conf. Vienna, 2002), IAEA, Vienna (2004) 449–455.
[6.21] PERNIČKA, F., MEGHZIFENE, A., TOELLI, H., IZEWSKA, J., IAEA TLD based audits for radiation protection calibrations at SSDLs, Radiat. Prot. Dosim. **101** (2002) 275–278.
[6.22] INTERNATIONAL ATOMIC ENERGY AGENCY, The SSDL Network Charter, IAEA, Vienna (1999).
[6.23] INTERNATIONAL ATOMIC ENERGY AGENCY, Calibration of Radiation Protection Monitoring Instruments, Safety Reports Series No. 16, IAEA, Vienna (2000).
[6.24] INTERNATIONAL ORGANIZATION FOR STANDARDIZATION, Measurement Management Systems — Requirements for Measurements Processes and Measuring Equipment, Rep. ISO 10012, ISO, Geneva (2003).
[6.25] INTERNATIONAL ATOMIC ENERGY AGENCY, Agency's Dosimetry Laboratory Quality Manual DOLQM.001, IAEA Rep. Internal DMRP-2003-02, IAEA, Vienna (2003).

Chapter 7

CODE OF PRACTICE FOR DIAGNOSTIC CALIBRATIONS AT SSDLs

7.1. INTRODUCTION

The equipment and its characteristics, such as generators, X ray tubes, filtration and the resulting radiation qualities, as well as the types of chamber allowed and the energy dependence of response of the detectors, have been discussed in Chapter 6. Special attention must be given to the area of application. However, some general procedures for all areas are discussed first. The beam qualities for each area need to be established for a minimum of three beams covering the energy region of interest.

Reference [7.1] describes the basic principles of calibration of dosimeters used in radiation therapy. Many of these principles are of a general nature and can be applied to the calibration of dosimeters used in other applications of ionizing radiation, such as diagnostic radiology. Specific procedures used are described in this section.

7.2. GENERAL CONSIDERATIONS

This section applies to all diagnostic dosimeters except those with a CT ionization chamber and KAP ionization chamber for which special considerations apply. The calibrations should be done by the 'substitution method' using a transmission monitor chamber as illustrated in Fig. 6.3. Firstly, measurements are made with the reference ionization chamber in the beam and then with the detector to be calibrated. The reference point of the reference ionization chamber should be indicated in the calibration certificate issued by the PSDL or the IAEA. If there is a conflict between the specification of this point in the documentation provided by the chamber manufacturer and that in the calibration certificate, then the specification made in the certificate should be adopted.

The characteristics of the transmission monitor chamber are given in Chapter 6. A transmission monitor chamber is usually mounted permanently in the beam. Note that this contributes to the beam hardening in the context of establishing radiation qualities. A temperature correction to the transmission monitor chamber reading may be necessary to account for effects resulting from heat generated by the X ray tube. The dosimetry system of the monitor

chamber should have a precision for each beam quality in accordance with the accuracy goals of the laboratory. Corrections for deviations between the measurement conditions and the reference conditions must be made to the monitor chamber measurement system. The reading of the monitor chamber should be taken as soon as practicable after irradiation has been completed. If the leakage current is significant it must be taken into account.

Detector positioning devices are required and should be of a type and quality necessary to ensure the detector positioning uncertainty at the distance of calibration is consistent with uncertainty goals. The positioning device should be capable of easily holding each detector of the diagnostic dosimeter. An appropriate detector positioning device must be designed so that it is able to position the reference point of each detector at the point of test. The point of test should be on the axis of the X ray beam and preferably at a minimum distance of 1000 mm from the focal spot of the X ray tube. However, the distance from the tube is influenced by the sizes of the detectors of the reference instrument and of the instrument to be calibrated. Whichever is the larger of the two detectors should not cover more than 80% of the cross-sectional area of the beam in the application plane. The variation of kerma rate over this fraction of the beam area should be less than 2% and the contribution of scattered radiation to the total kerma rate should be less than 5%. The field homogeneity should be checked along two mutually perpendicular axes by means of a thimble type ionization chamber of not more than approximately 1 cm^3.

The goal for the maximum overall uncertainty of calibrations at SSDLs should be 3.2% ($k = 2$) including the uncertainty of the reference dosimeter calibration (see Table 6.8).

For the instrument to be calibrated, the reference point of the detector should be chosen in accordance with the specifications provided by the manufacturer. If such information is not available, the SSDL should choose the reference point with regard to the nature of the detector. This point should be stated in the calibration certificate issued by the SSDL. The reference point of a spherical chamber should be the centre of the sphere, of a plane parallel chamber for general radiography the centre of the collecting volume, and of a plane parallel chamber for mammography the inner proximal front surface of the window and the centre of the circle for the front window of the chamber.

For calibrations in terms of air kerma rate or with long X ray exposure times, the shutter transit time can be ignored. For calibrations in terms of air kerma with the irradiation time determined by the operation of a shutter, it may be necessary to correct the irradiation time for the transit time of the shutter. The shutter transit time, Δt, can be determined by using the 'multiple exposure technique'. In this technique, a nominal irradiation time, t, and two

apparent air kerma values of K_1 and K_n are determined, where K_1 refers to a single irradiation having a nominal duration of t, in seconds, and K_n refers to the sum of n irradiations, each having a nominal duration of t/n seconds. The shutter transit time, Δt, is therefore given by the following formula:

$$\Delta t = t \frac{\left(K_1 - K_n\right)}{\left(K_n - nK_1\right)} \tag{7.1}$$

7.3. USE OF DETECTORS

There are specific precautions that need to be observed when operating instruments in radiation fields appropriate for diagnostic radiology. These are discussed below.

7.3.1. Secondary standard

The secondary standard should be a reference type instrument (see Chapter 5). The mode of operation of the secondary standard should be in accordance with the instrument calibration certificate and the instrument instruction manual. The time interval between periodic calibrations of the standard instrument should be within the period defined by national regulations. Where no such regulations exist, the time interval should usually be two years.

Regular (e.g. monthly) measurements should be made to check that the stability of the reference chamber, using either an appropriate radioactive check source or calibrated radiation fields, is within 0.3%. Corrections should be applied for the radioactive decay of the source and for changes in air pressure and temperature from the reference calibration conditions.

NOTE: For a multirange instrument, the check source may test only a particular range of the instrument. If the check source is to be used to test more than one range, the range that provides the greatest precision for the reading of the indication should be used.

Alternatively, for a given X ray beam and a given aperture arrangement, if the ratio of the readings of the transmission monitor chamber and those of the reference chamber can be shown to be constant within 0.3% over a period of more than one month, both the reference chamber and the transmission monitor can be considered to be stable.

7.3.2. Instrument to be calibrated

The SSDL should calibrate instruments designed to measure the radiation levels produced by X ray machines used in the various applications of diagnostic radiology covered in this report (see Table 6.1). It is preferable to calibrate the combination of detector and readout device (system calibration). However, upon request of the user, calibrations of the detector and the readout device may be carried out separately (component calibration). In this case, the calibration coefficient of the system is the product of the component calibration coefficients. The calibration of the readout device should be traceable to appropriate electrical standards.

Each ionization chamber submitted for calibration should be tested for atmospheric communication if possible. A device such as that described in Chapter 6 should be used. If the chamber cannot be tested for atmospheric communication, this fact must be stated in the calibration certificate. Some systems used have automatic corrections for temperature and pressure. If operable, this automatic correction should be checked in the apparatus mentioned in the above paragraph. It is generally preferable to calibrate the system with this feature turned off if possible so that any additional uncertainties are not involved in the calibration. The automatic correction feature can then be turned on after calibration and checked to ensure it is operating correctly.

For instruments designed to measure the air kerma rate, the leakage current of the measurement assembly in the absence of radiation other than background radiation should be less than 2% of the maximum indication on the most sensitive scale. For instruments designed to measure air kerma, the accumulated leakage indication should correspond to less than 2% of the indication produced by the reference radiation over the time of measurement. Correction should be made for leakage currents, if significant. The following are examples of sources of leakage currents:

(a) *Post-irradiation leakage*: This effect, produced by the radiation, arises in the chamber insulator and in part of the stem or cable that is irradiated in the beam. The effect continues after the radiation has ceased and commonly decreases exponentially with time.
(b) *Insulator leakage in the absence of radiation*: These currents may be produced either on the surface or within the volume of insulating materials used for the construction of the chamber, cables, connectors and high impedance input components of the electrometer and/or the preamplifier.

(c) *Polarity leakage effects*: Instruments in which the signal from the chamber is digitized may not indicate leakage currents of polarity opposite to that produced by ionization within the chamber. The magnitude of the leakage current cannot, in this case, be determined unless appropriate radiations of known kerma rate or known ratios of kerma rate are available.
(d) *Cable microphony*: A coaxial cable may generate electrical noise whenever it is flexed or otherwise deformed. A low noise, non-microphonic cable should be used and sufficient time should elapse for the mechanically induced currents to subside.
(e) *Preamplifier induced signal*: The preamplifier should, whenever possible, be positioned outside the area of the radiation beam to eliminate induced leakage currents. If this is not possible, then the preamplifier should be adequately shielded.

7.4. CALIBRATION PROCEDURES

The following calibration procedures should be followed either for measurements with the reference ionization chamber or the user's dosimeter.

7.4.1. Generalized protocol for calibration

The following is a check list for the calibration procedure of the user's instruments:

(a) Allow sufficient time for acclimatization of both the reference dosimeter and the dosimeter to be calibrated.
(b) Check the functionality of both systems.
(c) Position the reference ionization chamber with the reference point at the point of test.
(d) Measure temperature, pressure and humidity.
(e) Take four measurements, recording results for monitor chamber and reference chamber. Measurements should not monotonically increase or decrease.
(f) Determine the conventional true value of the air kerma/air kerma rate.
(g) Position the detector of user's dosimeter with the reference point at the point of test.
(h) Measure temperature, pressure and humidity.

(i) Take four measurements, recording results for the monitor chamber and the user's detector/instrument. Measurements should not monotonically increase or decrease.
(j) Determine the calibration coefficient of the user's detector/instrument as the ratio of the conventional true value and the reading of the user's detector/instrument.
(k) Produce the calibration certificate.

7.4.2. Procedures preceding calibration

All detectors to be calibrated, including the reference ionization chamber, need to be acclimatized to the X ray room by being put in there for at least two hours before beginning the calibration. It is desirable to have the detectors stored in the X ray room overnight.

Laser lines are useful for indicating the point of test. If laser lines are not available, the SSDL should have the means to ensure the same position is obtained for the reference points of both the reference ionization chamber and the user's detector.

The orientation of the chambers or detectors with respect to the incident radiation will, in general, have an influence on the result of the measurement. The uncertainty associated with the imprecise orientation should be as small as possible but should not exceed the value given in Table 6.8. The reference orientation of the detector should be stated in the certificate.

Sufficient time should be allowed for stabilization of the instruments after being switched on and before any measurements are performed.

7.4.3. Procedures during calibration

For measuring air kerma rates, the time interval between successive readings should not be less than five times the value of the effective time constant associated with the measuring range in use. If a set zero control is provided, it should be adjusted for the instrument range in use, with the detector connected. A zero shift may be significant on the more sensitive measurement ranges and should, where necessary, be corrected for, or preferably, excluded by appropriate measurement techniques.

The calibration procedure involves using the reference dosimeter first. The user's detector is then placed at the point of test. At least four readings should be taken for each instrument. There may be cases in which the number of readings need to be increased in order to achieve the desired standard deviation of the mean value. The measurements are only acceptable if the ratio of the two successive readings is not monotonically increasing or decreasing by

more than 0.2%. After the calibration cycle is complete, the SSDL may choose to confirm the conventional true value by repeating the measurements with the reference chamber. In this case, three readings may be sufficient to demonstrate that the ratio of the readings of the monitor and of the reference chamber agrees with the value determined originally to within 0.3%. If this is not the case, it is recommended that the discrepancy be investigated and the calibration repeated.

A sample data sheet is included in Appendix III. Since the effects of stem scatter and radiation induced currents in the stem under the calibration condition are included in the calibration coefficient for the standard instrument, no correction factor for these effects should be applied unless the beam area is significantly different from that used to calibrate the standard. The effect of stem scatter may be found from measurements with and without a replicate stem in appropriate geometrical conditions.

NOTE: Stem scatter is a function of the reference radiation quality and the beam area. However, the effect of scattered radiation on subsequent use of the beams to calibrate instruments will be dependent on the type of instrument and the method of its support unless the standard and the instrument are identical.

If there is more than one detector/instrument to be calibrated, it may be sufficient to determine the conventional true value once. The calibration coefficients of a series of detectors/instruments may then be obtained from this conventional true value. At the end of the cycle, the SSDL should verify that the conventional true value has not changed by more than 0.3%. For changes smaller than 0.3%, the average value of the two reference chamber measurements can be taken as the conventional true value.

Regarding the temperature and atmospheric pressure, the readings of the dosimeters refer to reference conditions. For air communicating ionization chambers, deviations from reference conditions are taken into account by the correction factor, k_{TP}, discussed in Chapter 4, where:

$$k_{TP} = \left(\frac{273.2 + T}{273.2 + T_0} \right) \left(\frac{P_0}{P} \right) \tag{7.2}$$

where: P_0 is the reference air pressure (P_0 = 101.3 kPa in this Code of Practice);
T_0 is the reference air temperature (T_0 = 20°C in this Code of Practice);
P is the air pressure during measurement;
T is the air temperature during measurement.

The above correction for air density should be applied for any differences between the conditions during measurement and reference calibration conditions as appropriate. For semiconductor detectors, the correction factor for air density should be taken as $k_{TP} = 1$.

If the measuring volume of an ionization chamber is not influenced by the humidity, the chamber response varies by less than 0.15% in the range 30–80% relative humidity [7.2]. Therefore, the correction factor, k_h, for difference in relative humidity between the reference calibration conditions and conditions during measurement can usually be neglected.

NOTE: It is possible to adjust temperature and humidity within the range of values given for the standard test conditions. This is not the case for pressure. Working outside the range of values given in this Code of Practice may result in reduced accuracy, or special treatment of the correction factors may be required.

7.4.4. Calibration by the substitution method using a monitor chamber

The substitution method denotes a calibration procedure in which first the measurement is made by positioning the secondary standard with its reference point at the point of test and conducting a measurement of the air kerma (rate). In the second step, the secondary standard is replaced by the instrument to be calibrated and the calibration coefficient, N_{K,Q_0}, is obtained from the air kerma (rate), K, prevailing at the point of test and from the instrument's indication, M, by $N_{K,Q_0} = K/M$. As the output from an X ray tube may vary with time it is recommended that use be made of a monitor chamber for the calibration of diagnostic dosimeters. Thus, moderate variations in the air kerma rate with time can be corrected. The readings M^{ref} and M^{user} for the reference instrument and the user's dosimeter whose detectors are located one after the other at the point of test should be related to the values for the monitor chamber. For the reference radiation qualities RQR 5, RQA 5, RQR-M2 and RQT 9 (see Chapter 6), the calibration coefficient, N^{user}_{K,Q_0}, of the instrument to be calibrated can be obtained by:

$$N^{user}_{K,Q_0} = N^{ref}_{K,Q_0} \left(\frac{\left(Mk_{TP}\right)^{ref}}{\left(mk_{TP}\right)^{ref}} \right) \left(\frac{\left(mk_{TP}\right)^{user}}{\left(Mk_{TP}\right)^{user}} \right) \tag{7.3}$$

where:

N_{K,Q_0}^{ref} is the calibration coefficient of the reference standard;
m is the measured value of the monitor chamber (for irradiation of the reference instrument and the calibrated instrument);
k_{TP} is the correction for temperature and pressure (in principle, this should be established separately for the monitor and detectors in the test point).

NOTE: In practice, if the irradiations of the standard instrument and the dosimeter to be calibrated are performed quickly, one after another, the ambient conditions of the monitor chamber remain the same and corrections of the indicated value of the monitor chamber to reference conditions are unnecessary.

NOTE: In cases where the monitor chamber has a good long term stability, i.e. better than 0.3% (k = 1), it may serve as the reference instrument after having been calibrated by the standard instrument.

7.4.5. Determination of the correction factor k_Q using a monitor chamber

Similar measurements to the above should be made for other energies. Equation (7.3) as modified below to Eq. (7.4) can then be used to determine $N_{K,Q}$:

$$N_{K,Q}^{\text{user}} = N_{K,Q}^{\text{ref}} \left(\frac{\left(Mk_{\text{TP}}\right)_Q^{\text{ref}}}{\left(mk_{\text{TP}}\right)_Q^{\text{ref}}} \right) \left(\frac{\left(mk_{\text{TP}}\right)_Q^{\text{user}}}{\left(Mk_{\text{TP}}\right)_Q^{\text{user}}} \right) \tag{7.4}$$

For radiation qualities other than RQR 5, RQA 5, RQR-M2 and RQT 9 (see Chapter 6), the correction factor can then be determined by:

$$k_Q^{\text{user}} = \frac{N_{K,Q}^{\text{user}}}{N_{K,Q_0}^{\text{user}}} \tag{7.5}$$

7.4.6. CT

The use of length in the calibration of CT ionization chambers involves special consideration. The following procedure should be followed for calibration of these chambers. With the reference ionization chamber, an air

kerma measurement is first made in the plane of measurement for the RQT radiation qualities (see Fig. 6.7). Then the lead rectangular aperture is positioned in front of the user's chamber, behind the transmission monitor chamber. The design of the aperture should conform to that given in Fig. 6.6. The aperture should be centered about the length of the chamber and located as described in Chapter 6. The separation of the lead aperture from the point of test must be known precisely. The width of the aperture should be between 20 and 50 mm and be known to within 0.01 mm. The height of the aperture should correspond to about twice the chamber diameter. The outer dimensions of the aperture assembly should be large enough to shield the whole of the chamber. In the plane of measurement, the width of the field is larger than the width of the aperture owing to beam divergence. This is accounted for by the ratio d_r/d_a (see Eq. (7.6)).

The chamber is calibrated in its centre. The calibration coefficient of this chamber is determined by Eq. (7.6):

$$N_{P_{KL},Q} = \frac{Kwd_r}{Md_a} \tag{7.6}$$

where: M is the reading of the chamber corrected to reference temperature and pressure;
K is the air kerma at the point of test;
w is the aperture width;
d_r is the distance between the focal spot and the point of test;
d_a is the distance between the focal spot and the plane of the aperture;
$N_{P_{KL},Q}$ is the air kerma–length product calibration coefficient for the radiation quality Q.

When a monitor chamber is employed for the calibration of CT ionization chambers, the calibration coefficient is obtained by Eq. (7.7):

$$N_{P_{KL},Q} = N_Q^m \left(\frac{wd_r}{d_a}\right)\left(\frac{mk_{TP}^m}{Mk_{TP}^{CT}}\right) \tag{7.7}$$

where: N_Q^m is the calibration coefficient of the monitor chamber in terms of air kerma for radiation quality Q in the plane of measurement;
mk_{TP}^m is the reading of the monitor chamber corrected to reference temperature and pressure;
Mk_{TP}^{CT} is the reading of the CT chamber corrected to reference temperature and pressure.

From an air kerma measurement with a secondary standard chamber positioned on the beam axis in the plane of measurement, N_Q^m, is obtained by:

$$N_Q^m = N_Q^{\text{ref}} \frac{M^{\text{ref}} k_{\text{TP}}^{\text{ref}}}{m k_{\text{TP}}^m} \tag{7.8}$$

NOTE: Although the monitor chamber remains in its usual position in this calibration procedure, the calibration coefficient, N_Q^m, is in terms of air kerma at the position of the secondary standard chamber.

7.4.7. KAP meters

7.4.7.1. Calibration in terms of air kerma–area product for transmitted radiation

This section describes the calibration of KAP meters in terms of the air kerma–area product for radiation transmitted through the chamber. This type of calibration is applicable for KAP meters for clinical use. As with the calibration of kerma–length product meters, the calibration of KAP meters requires special consideration. The calibration of KAP meters or KAP chambers is a two step process. The first step consists of determining, in the plane of measurement at a distance d_r from the focal spot, the air kerma, K (air kerma rate, $\dot{K}$) in the beam with the KAP chamber in position I as indicated in Fig. 6.8.

In the second step, the KAP chamber is removed from position I and brought to position II, i.e. its entrance plane is located in the plane of measurement. The calibration coefficient for radiation quality Q, $N_{P_{\text{KA}},Q}$, is obtained from the reading M of the KAP chamber by:

$$N_{P_{\text{KA}},Q} = \frac{KA(d_r/d_a)^2}{M_{\text{KAP}} k_{\text{TP}}^{\text{KAP}}} \tag{7.9}$$

where M_{KAP} is in units of charge or air kerma–area product and by:

$$N_{P_{\text{KA}},Q} = \frac{\dot{K}A(d_r/d_a)^2}{M_{\text{KAP}} k_{\text{TP}}^{\text{KAP}}} \tag{7.10}$$

where M_{KAP} is in units of current or air kerma–area product rate.

In Eqs (7.9) and (7.10), k_{TP} is the density of air correction applied to the reading M_{KAP} of the KAP meter. The symbol A stands for the cross-sectional area of the aperture.

If a monitor chamber providing a reading m is employed, the calibration coefficient of the KAP chamber is, in analogy to Eq. (7.4), given by:

$$N_{P_{KA},Q} = N_Q^m A \left(\frac{d_r}{d_a}\right)^2 \left(\frac{\left(mk_{TP}\right)_Q^{KAP}}{\left(Mk_{TP}\right)_Q^{KAP}}\right) \tag{7.11}$$

where N_Q^m is obtained by Eq. (7.8) and the symbols have the same meaning as above.

7.4.7.2. Calibration in terms of air kerma–area product for incident radiation

This section describes the calibration of KAP meters in terms of the air kerma–area product for radiation incident on the KAP chamber. This type of calibration is applicable for KAP meters intended to be used for the calibration of KAP meters installed in clinical X ray machines. This also includes devices which determine the air kerma–area product on the basis of X ray generator data (tube current and voltage) and the setting of the diaphragm. The procedure to be employed is similar to that described in Section 7.4.7.1, with the exception that the measurement of the air kerma should be done in the absence of the KAP chamber. Equations (7.9) and (7.10) should be used.

7.5. CALIBRATION OF NON-INVASIVE X RAY TUBE VOLTAGE MEASURING INSTRUMENTS

In this Code of Practice, three methods were discussed for the establishment of the quantity practical peak voltage (see Section 6.6.1). The first and preferable method is to use an invasive voltage divider, which can then be used to calculate a value of the quantity practical peak voltage at the same time that the non-invasive device is placed in the beam to give a reading. The other two methods involve a calibration device which measures the practical peak voltage of the X ray tube at the same time as the non-invasive device is being calibrated.

7.5.1. Use of a voltage divider to calibrate a non-invasive device

The invasive voltage divider is a traceable standard. It can be used when sampling the waveform of the X ray generator to derive the practical peak voltage, as described in Appendix IV. Such a device has the potential for displaying the X ray tube voltage waveform and it is considered to have the greatest accuracy. The capacitance of the additional cables needed for connecting the voltage divider will have an influence on the X ray tube voltage. In order to minimize this effect, these cables should be kept as short as possible. Also, in order to keep propagation effects along the cables to a minimum, the branching point for integrating the divider into the circuit should be close to the X ray tube. The voltage waveform from the voltage divider has been converted to the practical peak voltage as described in Appendix IV.

This method requires the use of an analog to digital converter, which should be supplied with a calibration certificate from which information concerning its accuracy and linearity can be obtained. The specifications of the analog to digital converter should be in line with the uncertainty goals of the SSDL. If it is not supplied with such information then the SSDL should derive this information from measurements performed with the voltage supply and the digital voltmeter used for determining the calibration coefficient of the electrometers as described in Section 6.4.1.

7.5.2. Use of non-invasive devices to calibrate non-invasive devices

The user's instrument is calibrated by comparison of its reading with that of the SSDL's calibrated non-invasive device. The best procedure is to irradiate the calibrated device to obtain an analysis of the waveform at the same time that the user's non-invasive device is irradiated. However, depending on the stability of the X ray source, the substitution technique could be used. In this case, the voltage may change between successive X ray exposures and this increases the uncertainty.

Firstly, the SSDL may have a device with an analog or digital output that tracks the X ray tube voltage waveform from the radiation output. This device would then be placed in the X ray beam at the same time as the non-invasive device to be calibrated, unless a substitution method is used. Depending on the kind of application (conventional or mammography), the voltage waveform is converted to the practical peak voltage by means of a computer code program realizing Eqs (IV.1–IV.5) in Appendix IV. The conversion rate of the analog to digital converter should be sufficiently high in view of the generator frequency. A conversion rate five times higher than the generator frequency is recommended.

Secondly, a non-invasive instrument previously calibrated that is capable of measuring the practical peak voltage and which should be in compliance with IEC 61676 [7.3, 7.4] is used. The prior calibration and the reading of practical peak voltage are assumed to be correct. Again, this device is placed in the X ray beam at the same time as the non-invasive device to be calibrated, unless a substitution method is used.

7.6. PROCEDURES FOLLOWING CALIBRATION

Once the calibration is completed measurements should be evaluated and a calibration certificate issued. Before producing the calibration report the laboratory should evaluate the uncertainty budget applicable to the calibration performed.

7.6.1. Uncertainty budget

A laboratory should develop a procedure to estimate the uncertainty of the calibration taking into account all important components of the uncertainty. These include uncertainties related to:

(a) The laboratory standard;
(b) The instrument to be calibrated;
(c) The laboratory set-up;
(d) The evaluation procedure.

An example of a detailed derivation of the uncertainty budget is given in Appendix II.

7.6.2. Calibration certificate

The calibration certificate should include [7.5] at least the following information:

(a) The name and address of the calibration laboratory;
(b) The name and address of the customer;
(c) A description and an unambiguous identification of the calibrated dosimeter;
(d) Indication of the method used for the calibration;
(e) The calibration result, including the uncertainty and units of measurement;

(f) The name, function and signature of the person authorizing the calibration certificate.

A hard copy of the calibration certificate should include the page number and the total number of pages. It is recommended that laboratories include a statement to the effect that the calibration certificate should not be reproduced except in full and not without written approval of the calibration laboratory.

It is important that the calibration certificate gives a clear description of the calibration geometry and the radiation conditions employed (radiation quality, air kerma rate). Information should be provided on:

(a) Temperature, pressure and relative humidity;
(b) Field size in the plane of measurement;
(c) Distance between focal spot and point of measurement;
(d) Potential of collecting and polarizing electrodes (with sign);
(e) Radiation quality dependent information given in Tables 7.1 and 7.2;
(f) Air kerma rate at which the calibration is carried out.

TABLE 7.1. RADIATION QUALITY DEPENDENT INFORMATION TO BE PROVIDED IN THE CALIBRATION CERTIFICATE FOR LABORATORIES STATING N_{K,Q_0} AND k_Q

Radiation quality	Added filtration[a]	HVL	Air kerma rate	N_{K,Q_0}	k_Q	Relative expanded uncertainty ($N_{K,Q_0}k_Q$) ($k = 2$)
	(mm Al)	(mm Al)	(mGy/min)	(Gy/C)		(%)
RQA 2	6.5	2.24	0.59		1.012	0.77
RQA 3	12.5	3.80	0.63		1.018	0.77
RQA 4	18.5	5.35	0.60		1.012	0.77
RQA 5[b]	**23.5**	**6.75**	**0.62**	**5.341×10^5**	**1.000**	**0.77**
RQA 6	28.5	8.10	0.60		0.995	0.77
RQA 7	32.5	9.18	0.63		0.990	0.77
RQA 8	36.5	10.09	0.64		0.987	0.77
RQA 9	42.5	11.52	0.62		0.988	0.77
RQA 10	47.5	13.36	0.63		0.991	0.77

[a] Additional filtration to that obtained during the establishment of RQR qualities (see Section 6.5.2).

[b] This beam is generally selected as the reference radiation quality for attenuated beams in general radiography.

TABLE 7.2. RADIATION QUALITY DEPENDENT INFORMATION TO BE PROVIDED IN THE CALIBRATION CERTIFICATE FOR LABORATORIES STATING $N_{K,Q}$

Radiation quality	Added filtration*	HVL	Air kerma rate	$N_{K,Q}$	Relative expanded uncertainty ($N_{K,Q}$) ($k = 2$)
	(mm Al)	(mm Al)	(mGy/min)	(Gy/C) ($\times 10^5$)	(%)
RQA 2	6.5	2.24	0.59	5.405	0.77
RQA 3	12.5	3.80	0.63	5.437	0.77
RQA 4	18.5	5.35	0.60	5.405	0.77
RQA 5	**23.5**	**6.75**	**0.62**	**5.341**	**0.77**
RQA 6	28.5	8.10	0.60	5.314	0.77
RQA 7	32.5	9.18	0.63	5.288	0.77
RQA 8	36.5	10.09	0.64	5.272	0.77
RQA 9	42.5	11.52	0.62	5.277	0.77
RQA 10	47.5	13.36	0.63	5.293	0.77

* Additional filtration to that obtained during the establishment of RQR qualities (see Section 6.5.2).

The certificate should state the expanded uncertainty of the calibration coefficient, $N_{K,Q}$, or of the product of $N_{K,Q_0}k_Q$ based on a coverage factor of $k = 2$. A typical uncertainty budget for SSDL calibration is shown in Tables 7.1 and 7.2.

REFERENCES

[7.1] INTERNATIONAL ATOMIC ENERGY AGENCY, Calibration of Dosimeters Used in Radiotherapy, Technical Reports Series No. 374, IAEA, Vienna (1994).

[7.2] ROGERS, D.W.O., ROSS, C.K., The role of humidity and other correction factors in the AAPM TG-21 dosimetry protocol, Med. Phys. **15** 1 (1988) 40–48.

[7.3] BAORONG, Y., KRAMER, H.-M., SELBACH, H.-J., LANGE, B., Experimental determination of practical peak voltage, Br. J. Radiol. **73** (2000) 641–649.

[7.4] KRAMER, H.-M., SELBACH, H.-J., ILES, W.J., The practical peak voltage of diagnostic X-ray generators, Br. J. Radiol. **71** (1998) 200–209.

[7.5] INTERNATIONAL ORGANIZATION FOR STANDARDIZATION, General Requirements for the Competence of Testing and Calibration Laboratories, Rep. ISO/IEC 17025, ISO, Geneva (2005).

Chapter 8

CODE OF PRACTICE FOR CLINICAL MEASUREMENTS

8.1. INTRODUCTION

This section provides the Code of Practice for clinical dosimetry in general radiography, fluoroscopy, mammography, CT and dental radiography. As far as possible, the methods described are based on well-established techniques, but the opportunity has been taken to introduce recent developments where appropriate. For each radiological modality, the procedures for conducting phantom measurements are described first, followed by the procedures for measurements on patients. In each case the description of the method is preceded by a background discussion describing dosimetric quantities and the equipment used. Worked examples, worksheets and an analysis of experimental uncertainties are provided for each modality. The worksheets are developed just for one examination and only those parameters that are necessary to interpret the measurement are listed in the worksheets. Detailed questionnaires aimed at obtaining comprehensive information on the diagnostic equipment, examination technique and the patient may be useful for interpretation of unexpected exposures. Users of the worked examples, worksheets and analysis of uncertainties should be aware that they require adaptation to local needs. The recommended types of measurement and measured dosimetric quantities for each modality are summarized in Table 8.1.

The Code of Practice does not always specify the number of readings that should be taken for measurements with phantoms or on patients. For measurements on individual patients, only a single reading is often possible unless multiple dosimeters are used (e.g. TLDs). For individual measurements with phantoms, it is sometimes only practicable to obtain a single reading. For example, when performing measurements as part of a quality control programme only limited time may be available for a series of different but related measurements. This simplification will introduce additional uncertainties into the measurement owing to the uncertainty of X ray exposure reproducibility and the uncertainty resulting from the precision of the measuring equipment. Their magnitudes have to be estimated using procedures described in the quality assurance programme of the radiology department. For situations where the user wishes to make additional readings, the worksheets presented here may need to be adjusted accordingly.

Measurement methods using ionization chambers, semiconductor detectors and/or TLDs are described. In some situations, the type of dosimeter

TABLE 8.1. DOSIMETRY QUANTITIES AND MEASUREMENT METHODOLOGY USED IN THIS CODE OF PRACTICE

Modality	Measurement subject	Measured quantity	Comments
General radiography	Phantom	Incident air kerma	Methodology for using chest and abdomen/lumbar spine phantoms is described.
	Patient	Incident air kerma	Calculated from exposure parameters and measured tube output.
		Entrance surface air kerma	Measurements on patient's skin.
		Air kerma–area product	Methodology same as for fluoroscopy.
Fluoroscopy	Phantom	Entrance surface air kerma rate	Measured directly on a phantom or calculated from the incident air kerma rate using backscatter factors.
	Patient	Air kerma–area product	Maximum skin dose is also measured. As the methods are not standardized they are not included in this Code of Practice.
Mammography	Phantom	Incident air kerma	Mean glandular dose is the primary quantity of interest. It is calculated from measured incident air kerma.
		Entrance surface air kerma	When this is measured (using TLDs) the backscatter factors are used to calculate the incident air kerma.
	Patient	Incident air kerma	Mean glandular dose is the primary quantity of interest. It is calculated from the incident air kerma estimated from measurements of tube output by using the exposure parameters for the examination.
CT	Phantom	CT air kerma indices	Measurements in air or in PMMA head and body phantoms.
	Patient	CT air kerma–length product	Direct measurements on patients are not described in this Code of Practice. Instead, a CT air kerma–length product is calculated from patient exposure parameters and results of phantom measurements.
Dental radiography	Patient	Incident air kerma	Calculated from exposure parameters and measured tube output for bitewing projection.
		Air kerma–length product	Used for calculation of the air kerma–area product for a panoramic projection.

is specified. However, where the use of a 'diagnostic dosimeter' or 'dosimeter' is described, this may be either an ionization chamber or semiconductor detector conforming to the IEC 61674 [8.1] specification.

Dosimeters should be calibrated by a calibration laboratory. The time elapsing between periodic calibrations of instruments should be within the period defined by national regulations. Where no such regulations exist, the time interval should be determined by factors such as instrument properties, frequency and conditions of use, manufacturer's recommendations, cost of recalibration, likelihood of drift and the use of stability checks, including cross-calibration of dosimeters (see Section 4.2), but should usually not exceed two years. Calibration laboratories usually specify calibration coefficients of diagnostic dosimeters for three beam qualities (see Chapter 7). It is a responsibility of the user to establish the calibration coefficient using interpolation for the beam quality used. This requires knowledge of the HVL of the beam. Its value does not have to be measured each time and it is sufficient if the value measured during quality control is used. For completeness, a 'recipe' for the HVL measurement is given for each modality. More details can be found in Appendix V.

Background material relevant to the methodology recommended for each modality is given in Appendix VII, which addresses the basis and limitations of the methodologies used. Backscatter factors for use in general radiography and fluoroscopy are given in Appendix VIII and field calibrations of KAP meters and TLDs are described in Appendix IX.

It is assumed that all X ray equipment for which dose is measured is properly maintained, checked as part of regular quality control and performs according to specification. One of the assumptions is that the tube output is linear with respect to the tube loading. If not, additional measurements will be required.

The values of the measured doses will reflect the practice used and for phantom exposures the user may also wish to expose a film or record a digital image. Procedures for this are not explicitly described.

8.2. SELECTION OF PATIENTS

Dosimetry measurements with phantoms are very useful for the purpose of quality control and to effect an intercentre comparison of a 'standard patient' but they cannot provide a direct estimate of the average dose for a given patient population. Nor can they indicate the dose variations seen in practice because of differences in patient size, variations in technique or skill between the individuals performing the examination and differences in

exposure factors that may be selected manually or automatically. Such information can only be obtained by measuring the patient dose for a sample of patients, or deducing its value from patient exposure parameters.

It is important that the size of a sample of patients is sufficiently large as to avoid large statistical variations of the mean value of the measured quantity. Care has to be paid also to the selection of patients according to their anatomical parameters (e.g. weight, breast thickness). A range of 10–50 patients for the sample size can be found in the literature [8.2–8.8]. Selection of patients so that the mean weight of the sample lies within 5 kg of 70 kg [8.9] or within 5 kg of 60 kg in some geographical regions [8.10] has been shown to be sufficient for the average value of the doses to be a good indication of the typical dose to an average patient. Reference [8.8] requires that the compressed breast is between 40 and 60 mm thick with a mean value 50 ± 5 mm.

This Code of Practice does not give specific values for the number of patients or their size to be used for a particular study. The user should select the sample that best represents the population studied. The sample size should be large enough to avoid statistical fluctuations caused by a small number of patients and large variations in measured doses. If the patient throughput is not sufficient to provide a sufficiently large sample within given anatomical limitations, deviations from these limitations can be made and the dose for a typical patient can be determined by interpolation from doses for patients within an appropriate range of the anatomical parameter [8.8]. It would be prudent, at least for frequent examinations, to exclude those patients from the sample whose weights lie outside the 20 kg limit on the required mean weight.

8.3. DOSIMETRY FORMALISM

In this Code of Practice, air kerma is used as the basis of directly measured application specific quantities. All other quantities are derived from measured application specific quantities using conversion coefficients and procedures described further in this section.

8.3.1. Determination of application specific quantities

The formalism for the determination of air kerma based dosimetry quantities in diagnostic radiology is described in Chapter 4. The general equation by means of which the reading, M_Q, of the dosimeter at a beam quality, Q, is converted to the measured quantity, K_Q, is:

$$K_Q = \left(M_Q - M_0\right) N_{K,Q_0} \prod_{i=1}^{n} k_i \tag{8.1}$$

In Eq. (8.1), K_Q represents a generic term for one of the application specific dosimetric quantities defined in Chapter 3, N_{K,Q_0}[1] is the calibration coefficient of the dosimeter at the reference beam quality, Q_0, M_0 is the reading of the dosimeter in the absence of the radiation under otherwise unchanged conditions, usually referred to as leakage current, and

$$\prod_{i=1}^{n} k_i$$

is the product of correction factors by means of which deviations between reference conditions and conditions of measurement are taken into account. Examples of influence quantities are beam quality; ambient temperature, pressure and relative humidity; and direction of radiation incidence.

In many applications, the quantity M_0 can be disregarded as it is of a negligible magnitude with respect to M. Equation (8.1) then becomes:

$$K_Q = M_Q N_{K,Q_0} \prod_{i} k_i \tag{8.2}$$

8.3.2. Uncertainties in quantities directly measured by diagnostic dosimeters

The uncertainty associated with dosimetry measurements in diagnostic radiology depends on numerous factors: the kind of dosimeter used, a priori information on the radiation quality, the use of such information for determining the value of k_Q for the prevailing radiation quality, the accuracy with which the dosimeter is located at the measurement point, etc. Requirements for the measurement uncertainty as recommended by this Code of Practice are given in Chapter 2. They relate to measurements as described by Eq. (8.2). Uncertainties in quantities other than those described by Eq. (8.2) will be higher and their actual value will depend on additional sources that contribute to the overall uncertainty.

[1] The calibration coefficient N_{K,Q_0} is related to the calibration coefficient at the beam quality, Q, as $N_{K,Q} = N_{K,Q_0} k_Q$, where k_Q corrects for the energy dependence of the dosimeter response in the beam quality, Q, compared to the response in the quality, Q_0.

In practice, it is recommended that the user select the desired uncertainty level for a given task and then take appropriate measures to achieve it. Guidance on uncertainty levels achievable for quantities measured directly by diagnostic dosimeters are given in Table 8.2. Three scenarios for a user's uncertainty budget are presented, which require, from scenario 1 to scenario 3, increasing attention to parameters of measurement.

Scenario 1, which corresponds to IEC 61674 [8.1], refers to the case where the user employs an instrument in compliance with IEC 61674 (see second column in Table 8.2). It should be noted that the requirements in IEC 61674 constitute a minimum level of performance, which may be exceeded considerably by 'good' instruments. In the IEC scenario, the value of the measured quantity is obtained by multiplying the dosimeter reading by the calibration coefficient. In this scenario, it is sufficient to apply an air density correction based on the normal pressure at the altitude above sea level at the location where the measurement is performed and on the average temperature in the room of measurement. No further corrections are applied. This is acceptable as

TABLE 8.2. EXAMPLES OF TYPICAL UNCERTAINTY BUDGETS FOR QUANTITIES DIRECTLY MEASURED BY DIAGNOSTIC DOSIMETERS

Influence quantity	IEC 61674 L (±%)	Uncertainty (k = 1)/%		
		Scenario 1	Scenario 2	Scenario 3
Intrinsic error, $N_{K,Q}$ or $N_{K,Q_0} k_Q$	5	2.89	1.6	1.6
Radiation quality, i.e. differences between SSDL and user	5	2.89	1.5	0.5
Kerma rate	2	1.15	0.5	0.5
Direction of radiation incidence	3	1.73	1.0	0.5
Air pressure	2	1.15	0.5	0.5
Temperature and humidity	3	1.73	0.5	0.5
Electromagnetic compatibility	5	2.89	1.5	1.0
Field size/field homogeneity	3	1.73	1.0	1.0
Operating voltage	2	1.15	1.2	1.0
Long term stability of user's instrument	2	1.15	1.0	0.5
Relative combined standard uncertainty (k = 1)		6.3	3.5	2.7
Relative expanded uncertainty (k = 2)		**12.6**	**7.0**	**5.4**

there is an upper limit on the range over which the response of a dosimeter may vary when an influence quantity deviates from its respective reference value. The upper limits are converted to standard deviations by assuming that there is a rectangular distribution, within the limits, i.e. by dividing by $\sqrt{3}$.

Scenario 2 describes the case where a reference class dosimeter is used, the performance of which exceeds the requirements of IEC 61674. The properties of a reference dosimeter are shown in Table 5.2. In this scenario, the air density correction needs to be applied using the actual values of pressure and temperature taken at the time of measurement. Beyond that, the procedures in scenario 2 correspond to those of scenario 1. The reduction in uncertainty from scenario 1 to scenario 2 is achieved by reducing the intrinsic error through a calibration by an SSDL and by using a detector with a small energy dependence of response (see Table 5.2).

Finally, scenario 3 describes the case where the conditions of exposure are tightly controlled (i.e. in terms of radiation quality, direction of radiation incidence, air density, etc.) and where corrections for the relevant influence quantities are made. For example, a calibration coefficient or k_Q is interpolated from the values for qualities surrounding the user beam quality and then allowance is made for the energy response of the dosimeter. A reference class dosimeter is used for measurements in this scenario.

Scenarios 2 and 3 require the use of a reference dosimeter with reduced uncertainties for the effect of influence quantities. The actual values used have to be supported by their evidence. This can be achieved by using the values specified by the manufacturer, or better, by deriving them from quality control tests on the measuring equipment.

8.3.3. Uncertainties in quantities derived from directly measured quantities

In many cases, it is the objective of clinical dosimetry to determine quantities other than those directly measured by the dosimeter. In general, additional contributions to the uncertainty of these quantities need to be taken into account.

As an example, consider the determination of the entrance surface air kerma. It may be determined from an air kerma measurement on the surface of a phantom or the patient. In this case, both the kerma contributions associated with the incident and the backscattered radiation need to be taken into account. Alternatively, the result of a measurement of the incident air kerma is multiplied by the backscatter factor appropriate to the conditions prevailing, i.e. tube voltage, filtration, field size, anode material and angle.

Regardless of which of the two methods is employed, contributions beyond those given in Table 8.2 need to be taken into account. The component

of the backscattered radiation has a spectral and angular distribution differing from that of the incident radiation. As a consequence the response of the dosimeter to the backscattered component may be different from that to the incident component. In the second alternative, the backscatter factor is also associated with some uncertainty.

No attempts are made in this Code of Practice to describe the methods to be employed for estimating the uncertainty of measurement when quantities different from directly measured quantities are to be determined. The conditions chosen in a given case will cover such a large variety that, at least for the time being, it seems impossible to give guidance applicable to all cases.

Nevertheless, persons conducting clinical measurements are strongly encouraged to make estimates of the contributions to the uncertainty going beyond those given in Table 8.2. The user should follow principles given in Appendix I. Examples of typical uncertainties associated with measurements in diagnostic radiology are given in the text.

8.3.4. Uncertainties in thermoluminescence measurements

Zoetelief et al. [8.11] recommend that the thermoluminescence measurements in diagnostic radiology be done with the relative combined standard uncertainty better than 12.5%. This gives the relative expanded uncertainty ($k = 2$) of 25%. As there are many factors that influence measurements with TLDs, it is not a simple matter to give a specific figure for the resultant uncertainty. Besides factors relating to the measurement technique, those factors relating to the performance of the instrument and to procedures for dosimeter preparation and handling should be considered. When calibrating the TLD, the whole system has to be considered.

The standard uncertainty of a calibration coefficient for TLDs must be higher than the uncertainty for the reference instrument, which is usually the ionization chamber. The value of 3% is achievable for the relative combined standard uncertainty ($k = 1$) of a TLD calibration. Additional sources of uncertainties come from various correction factors, e.g. the energy dependence of the TLD response, dosimeter fading, linearity of response.

Zoetelief et al. [8.11] show an example of an uncertainty budget for thermoluminescence measurements. The relative combined standard uncertainty ($k = 1$) of about 5% was derived for typical values of uncertainties from various sources. It is used for the estimation of the relative combined standard uncertainty of thermoluminescence measurements (equivalent values for measurements with diagnostic dosimeters are given in Table 8.2) in this Code of Practice. The relative expanded uncertainty ($k = 2$) for thermoluminescence measurements is 10%. This value is realistic provided that measurements

are well controlled. The user should establish the actual uncertainty of the measurement using principles described in Appendix I.

8.4. GENERAL RADIOGRAPHY

8.4.1. Choice of dosimetric quantities

In this Code of Practice, the principal quantities to be measured for use in general radiography are the incident air kerma, the entrance surface air kerma and the air kerma–area product. For phantoms, the incident air kerma is measured but for patient exposures it is determined using recorded exposure parameters. Additionally for patients, the entrance surface air kerma may be determined from measurements with TLDs and the air kerma–area product can be measured using a KAP meter.

8.4.2. Measurements using phantoms

For general radiography, the incident air kerma is measured for standard phantoms utilizing the X ray exposure parameters for an average sized adult patient. The methodology is described for three common imaging tasks: chest, abdomen and lumbar spine. The recommended phantoms for the determination of incident air kerma are the Center for Devices and Radiological Health (CDRH) chest and abdomen/lumbar spine phantoms (see Appendix VII). The general procedure used can be applied to other situations where suitable phantoms are available.

8.4.2.1. List of equipment

The equipment comprises:

(a) Diagnostic dosimeter calibrated for general radiography beam qualities;
(b) CDRH chest phantom;
(c) CDRH abdomen/lumbar spine phantom;
(d) Set of aluminium attenuators and lead diaphragm for HVL measurements;
(e) Loaded cassette (for screen–film and computed radiographic systems);
(f) Tape measure or ruler;
(g) Thermometer and barometer (for measurements with an ionization chamber).

8.4.2.2. Methods

For the measurement of incident air kerma in general radiography, the chest or abdomen/lumbar spine phantom is centred in the beam at the focus to film distance used clinically, with the beam size adjusted to the phantom edges. The exposure parameters (automatic exposure control (AEC) and tube voltage) chosen should be those used clinically for a postero–anterior chest, an antero–posterior abdomen or lumbar spine examination of an average sized adult patient.

A detector of the diagnostic dosimeter is positioned at a sufficient distance from the entrance surface of the phantom to avoid backscatter and the incident air kerma is calculated from the measurement at the detector position using the inverse square law. Measured data and exposure parameters should be recorded using a worksheet.

The HVL of the X ray beam is measured for the tube voltage and filtration used for the exposure. The methodology applies equally to X ray systems employing screen–film, computed radiographic or other digital receptors.

Incident air kerma measurement

The procedure for measurement of incident air kerma is as follows:

(1) Set up the X ray equipment for the chosen examination of a normal adult patient, including the selection of exposure parameters (AEC and tube voltage) and grid (or air gap), focus–skin distance and collimation.
(2) Position the phantom so that it rests directly against the front plate of the vertical Bucky or the table top as appropriate (see Fig. 8.1). For screen–film systems, the technologist should already have positioned the tube and collimated the beam as they normally would, without the phantom in place.
(3) Centre the phantom transversely (across the patient, left to right).
(4) Position the phantom vertically (head to foot), such that all relevant AEC detectors are covered. The phantom may thus not be centred vertically, but shifted up slightly in order to cover the AEC detectors.
(5) For computed radiography and other digital receptors, adjust the X ray field size to the front edges of the phantom (see Fig. 8.2).
(6) Measure and record the distance between the X ray tube focus and the vertical Bucky or table top, d_{FTD} (see Fig. 8.2).
(7) Place the dosimeter in the probe holder. The dosimeter should be sufficiently above the phantom surface to reduce backscatter and positioned

FIG. 8.1. Experimental set-up for measurements using a CDRH abdomen/lumbar spine phantom on the table top with the ionization chamber positioned above the phantom.

outside the AEC detectors. A distance of about 240 mm is recommended for dosimeters that respond to backscattered radiation. For dosimeters that are not sensitive to backscattered radiation (such as the many dosimeters based on a semiconductor detector) this distance could be smaller. The slightly off-axis arrangement enables the AEC detectors to function without any obstruction from the dosimeter. The dosimeter should be placed as close to the central axis as possible to minimize the influence of the heel effect.

(8) Measure and record the distance, d_m, between the reference point of the dosimeter and the table top (see Fig. 8.2).

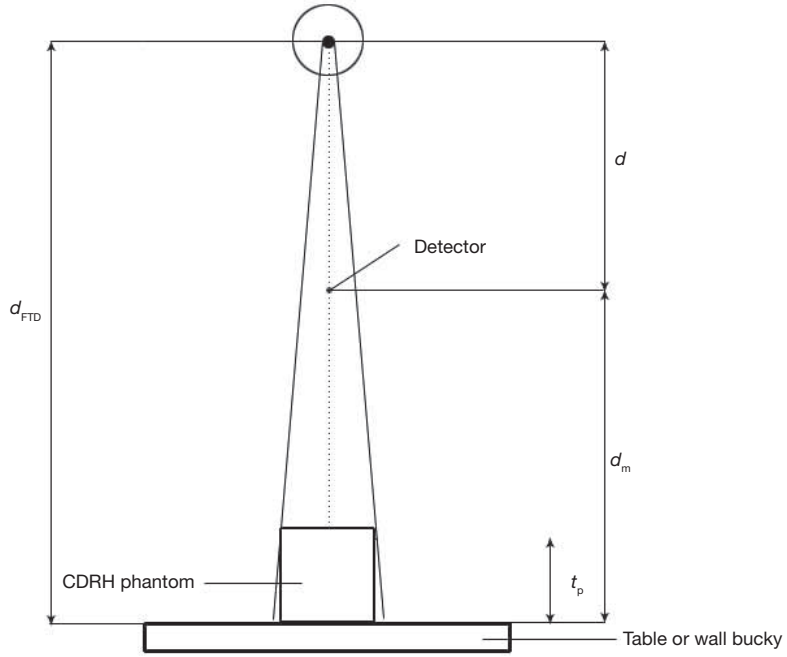

FIG. 8.2. Geometry used for the calculation of incident air kerma for general radiography, where d_{FTD} is the distance between the tube focus and the patient support, d is the distance between detector and the tube focus, d_m is the distance between detector and the patient support and t_P is the thickness of a patient simulated by the phantom. The value of t_P used in the NEXT study [8.5, 8.6] is 225 mm for the standard chest patient and 230 mm for the abdomen/lumbar spine patient. The value of d_m is measured but for the special case of the dosimeter and support used in the NEXT study with these phantoms, where d_m = 509 mm.

(9) For systems using screen–film or computed radiographic receptors, obtain a loaded cassette of the appropriate type and size and insert into the Bucky/cassette holder.
(10) Expose the chamber three times under AEC, or manual control, and record the dosimeter readings, M_1, M_2 and M_3, and exposure parameters used (tube voltage and tube loading or tube current and exposure time).
(11) If a dosimeter with an ionization chamber is used, record the temperature and pressure.

HVL measurement

Measurement of the HVL proceeds as follows:

(1) Set up the X ray equipment for the chosen examination of a normal adult patient in the manual mode.
(2) Select the tube voltage as used for measurements of the incident air kerma.
(3) Centre the dosimeter in the X ray beam.
(4) Collimate the beam to achieve conditions for narrow beam geometry so as to minimize the influence of scattered radiation. The beam should just cover the detector (see Appendix V).
(5) Select a tube loading so that the dosimeter readings with and without the attenuator are within the rated range of the instrument.
(6) Expose the detector and record the measured value. To achieve higher accuracy, multiple exposures can be done and their mean value recorded.
(7) Repeat step 6 for a set of three aluminium attenuators and the same tube loading as that for measurements made without any attenuator. The thickness of the attenuators is selected so that their value encloses the expected HVL of the beam.
(8) Expose the detector again without an attenuator (steps 5 and 6) and record the measured value.

8.4.2.3. Calculations

Incident air kerma

The geometry of the measurement is shown in Fig. 8.2. The inverse square law is used to calculate the incident air kerma from the air kerma at the position of the dosimeter for the exposure of a standard patient with a postero–anterior chest thickness of 225 mm or an antero–posterior abdomen/lumbar spine thickness of 230 mm. The computational procedure applies to measurements with each of the three receptor types considered. The procedure is as follows:

(1) Calculate the HVL of the beam by interpolating graphically or numerically in the measured signal for various thicknesses of the attenuators (see Appendix V). The HVL measured during a quality assurance programme can also be used.
(2) Calculate the mean value, $\bar{M}$, of the dosimeter readings.

(3) Calculate the air kerma $K(d)$ at the measurement point (at a distance, d, from the X ray focus) from the mean value of dosimeter readings, $\bar{M}$, using Eq. (8.3)[2]. In this equation, k_{TP} is the correction factor for temperature and pressure, N_{K,Q_0} is the dosimeter calibration coefficient and k_Q is the factor which corrects for differences in the response of the dosimeter at the calibration quality, Q_0, and at the quality, Q, of the clinical X ray beam. This quality is indicated by the value of the HVL.

$$K(d) = \bar{M} N_{K,Q_0} k_Q k_{TP} \tag{8.3}$$

The correction factor k_{TP} is unity for dosimeters with semiconductor detectors. For dosimeters with ionization chambers it is given by:

$$k_{TP} = \left(\frac{273.2 + T}{273.2 + T_0} \right) \left(\frac{P_0}{P} \right) \tag{8.4}$$

The quantities T and P are the temperatures and pressures (in ^{o}C and kPa) recorded during the measurement and T_0 and P_0 are their reference values for which N_{K,Q_0} is provided.

(4) Using the inverse square law (Eq. (8.5)), calculate the incident air kerma, K_i, to the standard chest (or abdomen). In this equation, d_{FTD} is the measured tube focus to patient support distance in millimetres and d_m and t_P are the distance from the table top (or a wall Bucky) to the reference point of the chamber at the measurement position and the thickness of a standard chest (or abdomen/lumbar spine) patient, respectively (see Fig. (8.2)).

$$K_i = K(d) \left(\frac{d_{FTD} - d_m}{d_{FTD} - t_P} \right)^2 \tag{8.5}$$

8.4.2.4. Estimation of uncertainties

The uncertainty in the measurement of the incident air kerma for chest and abdomen/lumbar spine examinations in general radiography can be estimated using values of relative uncertainties in the three measurement

[2] It is assumed that the leakage signal of the dosimeter can be neglected and that no correction has been applied for this effect.

TABLE 8.3. FACTORS WHICH CONTRIBUTE TO THE MEASUREMENT UNCERTAINTY IN THE DETERMINATION OF INCIDENT AIR KERMA MEASURED USING THE CDRH CHEST OR ABDOMEN/LUMBAR SPINE PHANTOMS

Source of uncertainty	Uncertainty (k = 1) (%)		
	Scenario 1	Scenario 2	Scenario 3
Measurement scenario (see Table 8.2)	6.2	3.5	2.7
Precision of reading	1.0[a]	0.6[b]	0.6[b]
Uncertainty in measurement position[c]	0.5	0.5	0.5
Relative combined standard uncertainty (k = 1)	6.3	3.6	2.8
Relative expanded uncertainty (k = 2)	**12.6**	**7.2**	**5.6**

[a] One single reading taken.
[b] Standard deviation of the mean of three readings.
[c] Corresponding to 2 mm in positioning of the detector.

scenarios given in Section 8.3.2 and adding contributions arising from factors specific to the procedure employed. Table 8.3 gives examples of standard uncertainties arising from each contribution, their combination in quadrature and the value for expanded uncertainty. For diagnostic dosimeters, the relative expanded uncertainty (k = 2) of measurement is between about 5.5% and 12.5%, depending on the scenario selected.

The user should establish the actual measurement uncertainty using principles described in Appendix I.

8.4.2.5. Examples

Measurement of incident air kerma using a chest phantom

The recorded readings of the dosimeter for the repeat exposure of the standard chest phantom were: 0.293 mGy, 0.291 mGy and 0.290 mGy. The calculated mean value of the dosimeter reading $\bar{M}$ is therefore:

$$\bar{M} = (0.293\ \text{mGy} + 0.291\ \text{mGy} + 0.290\ \text{mGy})/3 = 0.291\ \text{mGy}$$

The calibration coefficient, N_{K,Q_0}, for the dosimeter was 0.988 mGy/mGy, the beam quality correction factor, k_Q, was 0.99 and the temperature and pressure correction, k_{TP}, was 1.00. The air kerma $K(d)$ at the measurement point is therefore given by:

$$K(d) = 0.291 \text{ mGy} \times 0.988 \text{ mGy/mGy} \times 0.99 \times 1.00 = 0.285 \text{ mGy}$$

The dosimeter was positioned at a distance d_m = 509 mm from the wall Bucky and the focus to patient support distance, t_{FTD}, was 1000 mm. The incident air kerma is therefore:

$$K_i = 0.285 \text{ mGy}\left(\frac{1000 - 509}{1000 - 225}\right)^2 = 0.285 \text{ mGy}\left(\frac{491}{775}\right)^2 = 0.114 \text{ mGy}$$

For scenario 3 (reference type detector and all corrections applied), the relative expanded uncertainty ($k = 2$) of the measurement is 5.6%. The incident air kerma is written as:

$$K_i = (0.114 \pm 0.006) \text{ mGy}$$

Calculations for the abdomen and lumbar spine phantoms are similar and are not shown.

8.4.2.6. Worksheets

Determination of incident air kerma using the CDRH chest phantom

User: _____ Date: _____

Hospital or clinic name: _____

1. X ray equipment

X ray unit and model: _____ Room no.:_____

Imaging using screen–film combination *Imaging using digital image receptor*

Screen–film combination:_____ Image receptor model:_____

Film processor model: _____

Developer and fixer (brand name): _____

2. Dosimeter and phantom

Dosimeter model: _____ Serial no.: _____ Date of calib.: _____

Calibration coefficient (N_{K,Q_0})[3]: _____ ☐ mGy/nC ☐ mGy/reading

Reference conditions: HVL (mm Al): _____ Field size: _____

Pressure P_0 (kPa): _____ Temperature T_0 (°C): _____

Manufacturer of phantom: _____ Serial no.:_____

3. Exposure conditions

☐ AEC ☐ Manual AEC setting:_____ mA setting:_____ Tube voltage (kV): ____

Manual or (if available) post-exposure (mA·s): _____

Distance d_{FTD} of vertical Bucky from the X ray focus: _____ mm

Distance d_m of dosimeter from vertical Bucky: _____ mm AP chest thickness (t_P) = 225 mm

4. Dosimeter reading and calculation of incident air kerma

Dosimeter reading (M_1, M_2, M_3): _____ Mean dosimeter reading $\bar{M}$: _____

Pressure P (kPa):___ Temperature T (°C):___ $k_{TP} = \left(\frac{273.2+T}{273.2+T_0}\right)\left(\frac{P_0}{P}\right) =$ _____[4]

HVL (from 5 below) = _____ mm Al $k_Q =$ _____

Calculated value of air kerma $K(d) = \bar{M} N_{K,Q_0} k_Q k_{TP} =$ _____ mGy

Calculated value of incident air kerma $K_i = K(d)\left(\frac{d_{FTD} - d_m}{d_{FTD} - 225}\right)^2 =$ _____ mGy

[3] This is the calibration coefficient for the whole dosimeter, including the detector and the measurement assembly. For systems with separate calibration coefficients for the detector and the measurement assembly, the overall calibration coefficient is calculated as the product of the two separate calibration coefficients.

[4] For dosimeters with a semiconductor detector, $k_{TP} = 1$.

5. Determination of HVL

Dosimeter readings should be obtained for filter thicknesses that bracket the HVL. The first and last readings, M_{01} and M_{02}, are made at zero filter thickness.

Filter thickness (mm Al)	Dosimeter reading (M) (mGy)	Average dosimeter reading, $\bar{M}$, at zero thickness
0.00		$(M_{01} + M_{02})/2$ =_____ mGy
0.00		Interpolated HVL: _____ mm Al

Determination of incident air kerma using the CDRH abdomen/lumbar spine phantom

User: _____ Date: _____

Hospital or clinic name: _____

1. X ray equipment

X ray unit and model: _____ Room no.:_____

Imaging using screen–film combination *Imaging using digital image receptor*

Screen–film combination:_____ Image receptor model:_____

Film processor model: _____

Developer and fixer (brand name): _____

2. Dosimeter and phantom

Dosimeter model: _____ Serial no.: _____ Date of calib.: _____

Calibration coefficient (N_{K,Q_0})[5]: _____ ☐ mGy/nC ☐ mGy/reading

Reference conditions: HVL (mm Al): _____ Field size: _____

Pressure P_0 (kPa): _____ Temperature T_0 (°C): _____

Manufacturer of phantom: _____ Serial no.:_____

3. Exposure conditions

☐ AEC ☐ Manual AEC setting:_____ mA setting:_____ Tube voltage (kV): ____

Manual or (if available) post-exposure (mA·s): _____

Distance d_{FTD} of table top from the X ray focus: _____ mm

Distance d_m of dosimeter from table top: _____ mm AP chest thickness (t_P) = 230 mm

4. Dosimeter reading and calculation of incident air kerma

Dosimeter reading (M_1, M_2, M_3): _____ Mean dosimeter reading $\bar{M}$: _____

Pressure P (kPa):___ Temperature T (°C):___ $k_{TP} = \left(\frac{273.2+T}{273.2+T_0}\right)\left(\frac{P_0}{P}\right) =$ _____[6]

HVL (from 5 below) = _____ mm Al $k_Q =$ _____

Calculated value of air kerma $K(d) = \bar{M} N_{K,Q_0} k_Q\, k_{TP} =$ _____ mGy

Calculated value of incident air kerma $K_i = K(d)\left(\frac{d_{FTD} - d_m}{d_{FTD} - 230}\right)^2 =$ _____ mGy

[5] This is the calibration coefficient for the whole dosimeter, including the detector and the measurement assembly. For systems with separate calibration coefficients for the detector and the measurement assembly, the overall calibration coefficient is calculated as the product of the two separate calibration coefficients.

[6] For dosimeters with a semiconductor detector, $k_{TP} = 1$.

5. Determination of HVL

Dosimeter readings should be obtained for filter thicknesses that bracket the HVL. The first and last readings, M_{01} and M_{02}, are made at zero filter thickness.

Filter thickness (mm Al)	Dosimeter reading (M) (mGy)	Average dosimeter reading, $\bar{M}$, at zero thickness
0.00		$(M_{01} + M_{02})/2$ =_____ mGy
0.00		Interpolated HVL: _____ mm Al

8.4.3. Patient dosimetry

In this Code of Practice, the principal quantities for patient dosimetry in general radiography are the incident air kerma, the entrance surface air kerma and the air kerma–area product. One or more of these quantities may be determined depending upon user requirements.

For each patient, the incident air kerma can be determined by calculation from recorded exposure parameters and the measured tube output. The entrance surface air kerma provides direct assessment of patient dose and can be measured by TLDs. Provided the X ray machine is equipped with a KAP meter, the value of the air kerma–area product can be recorded. The methodology for air kerma–area product measurements is similar to the methodology described in Section 8.5 and is not repeated here.

A detailed questionnaire for patient examination is useful. It provides comprehensive information about the X ray equipment, the examination procedure and the patient and helps the interpretation of the measured doses. As the requirements for the questionnaire vary, an example is not given. Users are encouraged to design a questionnaire to suit the conditions of their own diagnostic facility.

8.4.3.1. List of equipment

The list of equipment for patient dosimetry is as follows:

(a) Diagnostic dosimeter calibrated for general radiography beam qualities;
(b) Chamber support stand;
(c) Aluminium attenuators and lead diaphragm for HVL measurements;
(d) Tape measure or ruler;
(e) Thermometer and barometer (for measurements with an ionization chamber);
(f) Weighing scales.

For thermoluminescence measurements, additional equipment is required:

(a) Thermoluminescence reader (not needed by the user if the readout is done by an external service).
(b) Calibrated TLDs enclosed in sachets. Dosimeters should have established their individual sensitivity correction factors or dosimeters within a selected sensitivity range should be chosen (see Appendix IX).
(c) Cellophane tape (Micropore© or surgical tape).

8.4.3.2. Methods

Two methods are used for establishment of the entrance surface air kerma. The first method uses recorded exposure parameters (tube voltage, tube current–exposure time product, field size, etc.) to estimate the incident air kerma. For this purpose, the X ray tube output is measured at the reference point and the inverse square law is applied as appropriate. The determination of the HVL is also required. The entrance surface air kerma is obtained from the calculated values of the incident air kerma using tabulated backscatter factors.

The second method makes use of thermoluminescence detectors to assess the entrance surface air kerma from measurements on patients.

HVL measurement

The methodology for the HVL measurement is the same as that described in Section 8.4.2.2 with the exception that instead of measuring the HVL for a specific tube voltage, it is measured for a set of X ray tube voltages which adequately sample voltages used for the clinical examinations under consideration.

X ray tube output measurements

For the selected filtration, the X ray tube output is measured for a representative set of tube voltages and tube loadings which adequately sample the patient exposure parameters used. It is suggested that measurements of three or four values of the tube loadings and three or four values of the tube voltage are sufficient. Values for other tube voltages and tube loadings may be found by appropriate interpolation. The geometry of the measurement as described in Fig. 8.2 is used with the exception that the phantom is removed from the patient support. The measurements are conducted as follows:

(1) Select the manual exposure control of the X ray unit and a representative value of tube voltage, loading and field size used in a clinical situation. Record the selected parameters.
(2) Position the detector at a suitable distance, d, from the X ray tube focus and centre it in the beam. Avoid possible influence of backscattered radiation on the response of the detector by placing the detector sufficiently far from the patient support. Measure and record the distance, d.
(3) Expose the chamber three times and record the dosimeter readings M_1, M_2 and M_3.

(4) Repeat step 3 using another tube voltage and/or tube loading.
(5) If a dosimeter with an ionization chamber is used, record the temperature and pressure.

Incident air kerma measurement

The incident air kerma is estimated indirectly from the X ray tube output at the selected distance and exposure parameters using the inverse square law. The measurement geometry shown in Fig. 8.2 is used and t_P becomes the thickness of the individual patient. The measurement is conducted as follows:

(1) Select the type of examination to be conducted and the weight range and number of patients to be investigated.
(2) Position the patient and X ray equipment for the desired examination and set the appropriate exposure parameters.
(3) Measure the patient thickness, t_P, at the centre of the beam.
(4) Record the equipment and patient data.
(5) Expose the patient and record the exposure parameters.
(6) Collect data for at least 10 patients.

Entrance surface air kerma measurement

The entrance surface air kerma can be established indirectly from the incident air kerma using backscatter factors discussed in Appendix VIII or it can be measured directly using TLDs.

Indirect assessment

For each patient, the indirect assessment of the entrance surface air kerma consists of the following steps:

(1) Measure the beam HVL and the X ray tube output (see above).
(2) Establish the incident air kerma for exposure parameters recorded during patient examination (see above).
(3) Establish the entrance surface air kerma from the incident air kerma and an appropriate backscatter factor.

Direct measurement

The entrance surface air kerma is directly measured using sachets of three TLDs taped to the patient's skin. One sachet of TLDs is retained so

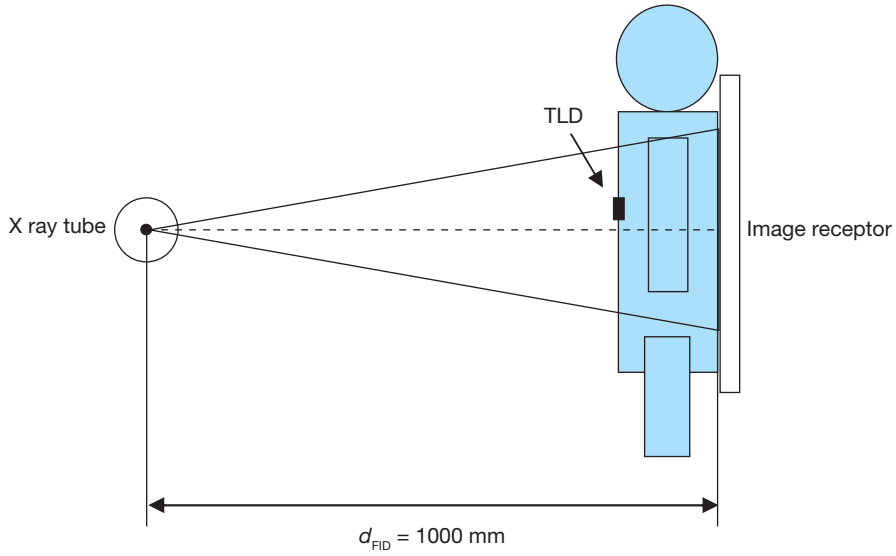

FIG. 8.3. Schematic diagram of the arrangement for measurements with TLDs in general radiography. The TLDs are enclosed in sachets that protect them from dirt and grease and will normally be attached to the patient by the radiographer making the exposure.

that a background correction may be made. The measurement is made as follows:

(1) Select the type of examination to be conducted and the weight range and number of patients to be investigated.
(2) Record the equipment and TLD data.
(3) Set aside a TLD sachet to provide a background reading.
(4) For the required sample of patients follow steps 5–7.
(5) Position the patient and X ray equipment for the desired examination and select the appropriate exposure parameters.
(6) Attach TLDs to the patient's skin (see Fig. 8.3) with cellophane tape (Micropore or surgical tape). The sachet should be attached to the skin as close as possible to the centre of the entrance beam.
(7) Expose the patient. Remove the sachet and record the exposure parameters, date and patient weight on the worksheet. Attach the sachet to the sheet.
(8) Arrange for the TLDs to be read. Record the readings M_1, M_2 and M_3 from the exposed dosimeters and the readings M_{01}, M_{02} and M_{03} from the unexposed dosimeters.

8.4.3.3. Calculations

X ray tube output

The X ray tube output is calculated as follows:

(1) Calculate the HVL of the beam by interpolating graphically or numerically in the measured signal for various thicknesses of attenuator (see Appendix V). The HVL value measured during a quality assurance programme can be also used.
(2) Calculate the mean value of the dosimeter readings, $\bar{M}$.
(3) Calculate the air kerma, $K(d)$, at the measurement point (at a distance, d, from the X ray focus) using Eq. (8.6)[7]. In this equation, k_{TP} is the correction factor for temperature and pressure, N_{K,Q_0} is the dosimeter calibration coefficient and k_Q is the factor which corrects for differences in the response of the dosimeter at the calibration quality Q_0, and at the quality, Q, of the clinical X ray beam. This quality is indicated by the value of the HVL.

$$K(d) = \bar{M} N_{K,Q_0} k_Q k_{TP} \tag{8.6}$$

The correction factor k_{TP} is unity for dosimeters with semiconductor detectors. For dosimeters with ionization chambers it is given by:

$$k_{TP} = \left(\frac{273.2 + T}{273.2 + T_0}\right)\left(\frac{P_0}{P}\right) \tag{8.7}$$

The quantities T and P are the temperatures and pressures (in ^{o}C and kPa) recorded during the measurement and T_0 and P_0 are their reference values for which N_{K,Q_0} is provided.
(4) Calculate the X ray tube output, $Y(d)$, using Eq. (8.8):

$$Y(d) = K(d)/P_{It} \tag{8.8}$$

where P_{It} is the tube loading during the exposure.

[7] It is assumed that the leakage signal of the dosimeter can be neglected and that no correction has been applied for this effect.

Indirect assessment of incident air kerma

The inverse square law is used to calculate the incident air kerma from the X ray tube output and exposure parameters for patient examinations:

(1) For each patient, calculate the incident air kerma from the exposure parameters recorded on the worksheet (tube voltage and tube loading, X ray tube focus to patient support distance, distance of the X ray tube output measurements and patient thickness) using Eq. (8.9):

$$K_{\mathrm{i}} = Y(d) P_{\mathrm{It}} \left(\frac{d}{d_{\mathrm{FTD}} - t_{\mathrm{P}}} \right)^2 \tag{8.9}$$

where:

$Y(d)$ is the X ray tube output measured at a distance, d, from the tube focus;
P_{It} is the tube loading during the exposure of the patient;
d_{FTD} and t_{P} are the tube focus to patient support distance and the patient thickness, respectively.

(2) Repeat step 1 for each patient in series.

Entrance surface air kerma

Indirect assessment

(1) Calculate the incident air kerma for exposure parameters recorded during patient examination (see above).
(2) Calculate the entrance surface air kerma using Eq. (8.10) and the appropriate backscatter factor for water from Appendix VIII. Selection of the backscatter factor is based on the measured HVL and the field size used during the examination:

$$K_{\mathrm{e}} = K_{\mathrm{i}} B \tag{8.10}$$

where K_{i} is the incident air kerma established for a given set of exposure parameters and B is the backscatter factor for water and the selected field size.

Direct measurement using TLDs

(1) Calculate the mean value of the background reading, $\bar{M}_0$, from background dosimeter readings M_{01}, M_{02} and M_{03} ($\bar{M}_0 = (M_{01} + M_{02} + M_{03})/3$).

(2) Calculate the average background corrected dosimeter reading, $\bar{M}$, from the exposed dosimeter readings M_1, M_2 and M_3 as:

$$\bar{M} = \frac{\sum_{i=1}^{3} f_{s,i}\left(M_i - \bar{M}_0\right)}{3} \tag{8.11}$$

where factors $f_{s,i}$ are used to correct for the individual sensitivity of the i-th dosimeter (see Appendix IX)[8].

(3) Calculate the entrance surface air kerma, K_e, from the average background corrected dosimeter reading, $\bar{M}$, using the calibration coefficient, N_{K,Q_0}, of the dosimeter for the reference radiation quality, Q_0, the correction factor, k_Q, for the radiation quality used and the correction factor, k_f, that corrects for the effect of fading of the thermoluminescence signal between irradiation of the dosimeter and its readout:

$$K_e = \bar{M} N_{K,Q_0} k_Q k_f \tag{8.12}$$

(4) Repeat steps 2 and 3 for other patients as appropriate.

8.4.3.4. Estimation of uncertainties

The uncertainty of the measurement of the incident air kerma for patient examinations in general radiography is similar to the uncertainty estimated for measurements with phantoms. For diagnostic dosimeters, the relative expanded uncertainty ($k = 2$) of the incident air kerma is between about 5.5% and 12.5%, depending on the scenario selected (see Table 8.3).

An additional uncertainty in an indirect assessment of the entrance surface air kerma comes from backscatter factors. Considering that the maximum value of the uncertainty for backscatter factors is assumed to be about 3%, it then follows that the relative expanded uncertainty ($k = 2$) of the

[8] $f_{s,i}$ is a constant for dosimeters grouped so that their sensitivity is within a selected range (see Appendix IX).

indirect assessment of the entrance surface air kerma ranges from about 6% to 13%.

The uncertainty of the measurement made with TLDs is discussed in Section 8.3. The relative expanded uncertainty ($k = 2$) of 10% was adopted for this Code of Practice. Additional contributions due to backscatter factors (applied during a calibration of TLDs) and positioning of the dosimeters have to be included in the overall uncertainty. Their values are the same as for measurements made with diagnostic dosimeters. The relative combined standard uncertainty can be calculated as 5.9%. The value of the relative expanded uncertainty ($k = 2$) of measurement of the entrance surface air kerma using TLDs is about 12%.

The user should establish the actual measurement uncertainty using principles described in Appendix I.

8.4.3.5. Examples

Indirect assessment of incident air kerma and entrance surface air kerma

The abdomen examination of an adult 300 mm thick was done with the table at 1000 mm from the tube focus and the machine set to 84 kV and 60 mA·s. The beam HVL was measured as 3.5 mm Al and the X ray tube output at a distance, d, of 500 mm from the tube focus was measured as $Y(d) = 0.075$ mGy/mA·s.

The incident air kerma is:

$$K_i = 0.075\ \text{mGy}(\text{mA}\cdot\text{s})^{-1}\left(\frac{1000-500}{1000-300}\right)^2 60\ \text{mA}\cdot\text{s}$$

$$= 0.075\ \text{mGy}(\text{mA}\cdot\text{s})^{-1}\left(\frac{500}{700}\right)^2 60\ \text{mA}\cdot\text{s} = 6.429\ \text{mGy}$$

For the dosimeter in compliance with IEC 61674 specifications and all corrections applied, the relative expanded uncertainty ($k = 2$) of the measurement is 5.6%. The incident air kerma is written as:

$K_i = (6.43 \pm 0.36)$ mGy

The X ray beam was collimated during examination to 200 mm × 400 mm. The backscatter factor does not vary too much with field size. It is thus reasonable to use the backscatter factor for the maximum field size of 250 mm × 250 mm. The interpolation gives, for an HVL of 3.5 mm Al, a value of the

backscatter factor for water, B, of 1.43. The entrance surface air kerma can be written as:

$$K_e = 6.43 \text{ mGy} \times 1.43 = 9.19 \text{ mGy}$$

Considering the uncertainty of this quantity discussed above, the result and its relative expanded uncertainty of 6% ($k = 2$) are written as:

$$K_e = (9.2 \pm 0.6) \text{ mGy}$$

Direct measurement of entrance surface air kerma

The three exposed TLDs and three background TLDs were read out after the chest examination of a patient. The average readings of the three exposed and three background dosimeters were 776.08 nC and 7.70 nC, respectively. The average background corrected reading is therefore:

$$\bar{M} = 776.08 \text{ nC} - 7.70 \text{ nC} = 768.38 \text{ nC}$$

The calibration coefficient, N_{K,Q_0}, for the TLD was 0.00035 mGy/nC and k_Q for the same tube voltage and filtration setting was 1.0057. The entrance surface air kerma is therefore:

$$K_e = 768.38 \text{ nC} \times 0.00035 \text{ mGy·nC}^{-1} \times 1.0057 = 0.270 \text{ mGy}$$

For an expanded standard uncertainty ($k = 2$) of 12%, the entrance surface air kerma measured by the TLDs is written as:

$$K_e = (0.270 \pm 0.032) \text{ mGy}$$

8.4.3.6. Worksheets and data collection sheets

Determination of X ray tube output

User: _____ Date: _____

Hospital or clinic name: _____

1. X ray equipment

X ray unit and model: _____ Room no.:_____

Imaging using screen–film combination *Imaging using digital image receptor*

Screen–film combination:_____ Image receptor model:_____

Film processor model: _____

Developer and fixer (brand name): _____

2. Dosimeter

Dosimeter model: _____ Serial no.: _____ Date of calib.: _____

Calibration coefficient (N_{K,Q_0})[9]: _____ ☐ mGy/nC ☐ mGy/reading

Reference conditions: HVL (mm Al): _____ Field size: _____

Pressure P_0 (kPa): _____ Temperature T_0 (°C): _____

3. Exposure conditions

Distance, d, of dosimeter from tube focus (mm): _____

4. Dosimeter reading and X ray tube output calculation

Pressure P (kPa):___ Temperature T (°C):___ $k_{TP} = \left(\frac{273.2+T}{273.2+T_0}\right)\left(\frac{P_0}{P}\right) =$ _____[10]

Tube voltage (kV)	Tube loading (P_{It}) (mA·s)	Dosimeter reading M_1, M_2 and M_3	Mean dosimeter reading ($\bar{M}$)	HVL (mm Al)	k_Q	Calculated X ray tube output, $Y(d)$, at distance d (mGy/(mA·s))

X ray tube output, $Y(d)$, is calculated as $Y(d) = \bar{M} N_{K,Q_0} k_Q\, k_{TP} / P_{It}$.

[9] This is the calibration coefficient for the whole dosimeter, including the detector and the measurement assembly. For systems with separate calibration coefficients for the detector and the measurement assembly, the overall calibration coefficient is calculated as a product of the two separate calibration coefficients.

[10] For dosimeters with a semiconductor detector, $k_{TP} = 1$.

5. Determination of HVL

Dosimeter readings should be obtained for filter thicknesses that bracket the HVL. The first and last readings, M_{01} and M_{02}, are made at zero filter thickness.

Tube voltage: ________ kV

Filter thickness (mm Al)	Dosimeter reading (M) (mGy)	Average dosimeter reading, $\bar{M}$, at zero thickness
0.00		$(M_{01} + M_{02})/2$ =________ mGy
0.00		Interpolated HVL: _____ mm Al

Tube voltage: ________ kV

Filter thickness (mm Al)	Dosimeter reading (M) (mGy)	Average dosimeter reading, $\bar{M}$, at zero thickness
0.00		$(M_{01} + M_{02})/2$ =________ mGy
0.00		Interpolated HVL: _____ mm Al

Tube voltage: ________ kV

Filter thickness (mm Al)	Dosimeter reading (M) (mGy)	Average dosimeter reading, $\bar{M}$, at zero thickness
0.00		$(M_{01} + M_{02})/2$ =________ mGy
0.00		Interpolated HVL: _____ mm Al

Data collection sheet for indirect assessment of incident air kerma and entrance surface air kerma

User: _____ Date: _____

Hospital or clinic name: _____

Examination: _____

1. X ray equipment

X ray unit and model: _____ Room no.:_____

Imaging using screen–film combination

Screen–film combination:_____

Film processor model: _____

Developer and fixer (brand name): _____

Imaging using digital image receptor

Image receptor model:_____

2. Collected data

Tube focus to table top distance (d_{FTD}): _____ mm

Date	Patient	Weight (kg)	Tube voltage (kV)	Tube loading (mA·s)	Patient thickness (t_p) (mm)	Field size (mm × mm)

Indirect assessment of incident air kerma and entrance surface air kerma

User: _____ Date: _____

Hospital or clinic name: _____

1. X ray equipment

X ray unit and model: _____ Room no.:_____

Imaging using screen–film combination ☐ *Imaging using digital image receptor* ☐ Examination: _____

Screen–film combination:_____ Image receptor model: _____

Film processor model: _____

Developer and fixer (brand name): _____

Calculated incident air kerma and entrance surface air kerma

Tube focus to table top distance (d_{FTD}): _____ mm Distance, d, of dosimeter from tube focus: _____ mm

Patient	Weight (kg)	Tube voltage (kV)	Tube loading (mA·s)	Patient thickness (t_P) (mm)	Field size (mm × mm)	Backscatter factor (B)	Tube output, $Y(d)$, at distance d [a] (mGy/(mA·s))	Incident air kerma (K_i)[b] (mGy)	Entrance surface air kerma (K_e)[c] (mGy)

[a] The value of $Y(d)$ is interpolated from measured values of tube output.

[b] Incident air kerma $K_i = Y(d) P_{It} \left(\frac{d}{d_{FTD} - t_P} \right)^2 =$ _____ mGy.

[c] Entrance surface air kerma $K_e = K_i B =$ _____ mGy.

K_i Patient: TLD

Determination of the entrance surface air kerma using TLDs

User: _____ Date: _____

Hospital or clinic name: _____

Examination: _____

1. X ray equipment

X ray unit and model: _____ Room no.:_____

Imaging using screen–film combination *Imaging using digital image receptor*

Screen–film combination:_____ Image receptor model:_____

Film processor model: _____

Developer and fixer (brand name): _____

2. TLDs

Identification markings on TLD sachets (if any): _____

Calibration coefficient (N_{K,Q_0}) for TLDs: _____ mGy/reading

Reference beam quality (HVL): _____ mm Al k_Q for measurement set-up: _____

3. Patient data

Sex: ☐ Male ☐ Female Height: _____ cm

Weight: _____ kg Patient thickness at the beam centre: _____ mm

4. Exposure conditions

☐ AEC ☐ Manual AEC setting: _____

Tube voltage (kV): _____ HVL: _____ mm Al

Manual or (if available) post-exposure tube loading: _____ mA·s

5. Dosimeter readings and calculation of entrance surface air kerma

Background dosimeter reading (M_{0i})	Dosimeter reading (M_i)	Average background corrected reading ($\bar{M}$)	Entrance air kerma (K_e) (mGy)

$$\bar{M}_0 = (M_{01} + M_{02} + M_{03})/3 \qquad \bar{M} = \frac{\sum_{i=1}^{3} f_{s,i}\left(M_i - \bar{M}_0\right)}{3} \qquad K_e = \bar{M} N_{K,Q_0} k_Q k_f$$

8.5. FLUOROSCOPY

8.5.1. Choice of dosimetric quantities

In this Code of Practice, the entrance surface air kerma rate is the principal quantity to be measured in fluoroscopy using phantoms. For measurements on patients, the air kerma–area product, a readily measured quantity closely related to the energy imparted to the patient and to the effective dose, is the recommended dosimetric quantity.

Estimation of the maximum entrance surface air kerma on patients during fluoroscopically guided procedures is important. In such procedures, the beam position of the entrance surface of the patient is not fixed and special methods are required to locate the maximum value. Since no standardized method exists, recommendations on how to measure the maximum entrance surface air kerma in interventional procedures will not be given in this Code of Practice.

8.5.2. Measurements using phantoms

For fluoroscopy, the entrance surface air kerma rate is measured using a water phantom or, optionally, a PMMA phantom. It is important that the detector responds to both direct as well as backscattered radiation. Alternatively, for detectors that do not respond to backscattered radiation, the entrance surface air kerma rate can be calculated from the measured incident air kerma rate and an appropriate backscatter factor. Semiconductor detector systems often possess this property.[11]

8.5.2.1. List of equipment

The equipment comprises:

(a) Diagnostic dosimeter calibrated for beam qualities used in fluoroscopy;
(b) Chamber support stand;
(c) Water phantom of 200 mm thickness and cross-section of 300 mm × 300 mm;
(d) Additional water phantom of 100 mm thickness and cross-section of 300 mm × 300 mm for simulation of larger patients;

[11] It should be noted that some semiconductor detectors respond to backscattered radiation. This property of the detector has to be verified before its use.

(e) Rig to support the phantom above the detector;
(f) Ruler;
(g) Thermometer and barometer (for measurements with an ionization chamber).

8.5.2.2. Methods

The 200 mm thick water phantom represents a standard adult. Larger patients are simulated by adding another 100 mm of water. An alternative to using the water phantom is to use a 185 mm thick PMMA phantom and apply a correction factor for the different backscatter properties of water and PMMA (see Appendices VII and VIII).

The fluoroscopic unit should be operated under automatic brightness control. Care should be taken to ensure that the automatic brightness control system has stabilized before each measurement is made. If the dose rate does not stabilize, the reason should be investigated. Measurements should be made for all image intensifier field sizes, dose rates and automatic brightness control options reflecting normal clinical use. The focus to intensifier and focus to chamber distances, tube voltage, tube current and any filtration selected should be recorded for each measurement.

The measurements are strongly dependent on the relative positions of the X ray tube, patient entrance surface and image intensifier. Separate instructions are given below for four different equipment configurations (Fig. 8.4(a–d)).

Measurement of entrance surface air kerma rate for under couch installation

The measurement arrangement is shown in Fig. 8.4(a) and proceeds as follows:

(1) If an anti-scatter grid is used in the clinical situation, make sure it is in position.
(2) Position the phantom on the couch resting on the rig. The space between the couch and the phantom must be sufficient for positioning the detector between the phantom and the couch.
(3) Position the detector in contact with the phantom and at the centre of its entrance surface.
(4) Position the couch so that a space of 100 mm is left between the exit surface of the phantom and the base of the intensifier carriage.
(5) To simulate a larger patient, 100 mm of water is added to the phantom (total thickness 300 mm) so that its exit surface is in contact with the intensifier carriage.

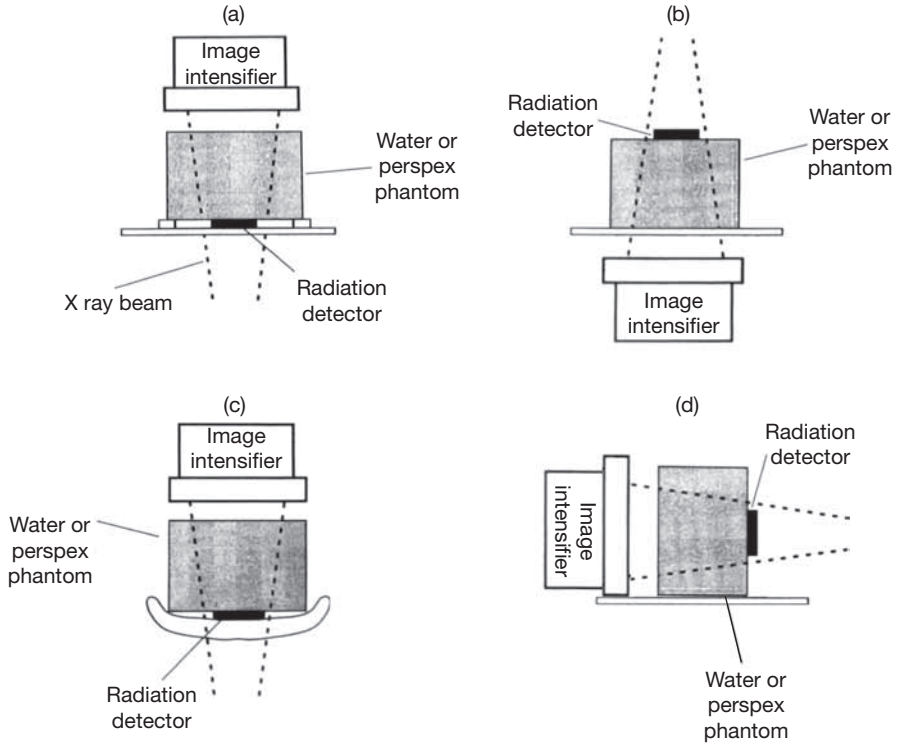

FIG. 8.4. Configuration for measurement of patient entrance surface air kerma: (a) an under couch installation, (b) an over couch installation, (c) a C-arm unit, (d) C-arm unit, lateral exposures or when a couch used clinically is not available (after Martin et al. [8.12]).

(6) Open the collimators fully or to the size of the phantom if this is smaller.
(7) Measure and record the focus to intensifier and focus to detector distances.
(8) Expose the phantom under automatic brightness control and record the dosimeter reading, $\dot{M}$, tube voltage, tube current and the image intensifier settings. Repeat the measurement three times and record dosimeter readings, $\dot{M}_1$, $\dot{M}_2$ and $\dot{M}_3$.
(9) Repeat step 8 for all image intensifier field sizes, dose rates and automatic brightness control options in normal clinical use.
(10) If a dosimeter with an ionization chamber is used, record the temperature and pressure.

Measurement of entrance surface air kerma rate for over couch installation

The measurement arrangement is shown in Fig. 8.4(b) and the measurement is conducted as follows:

(1) If an anti-scatter grid is used in the clinical situation, make sure it is in position.
(2) Position the phantom on the couch.
(3) Position the detector in contact with the phantom and at the centre of its entrance surface.
(4) Set the focus to couch (table top) distance equal to that used in clinical practice. If a standard distance is to be used, set the focus to couch distance equal to 1000 mm or the nearest possible distance to 1000 mm (for comparison of different X ray units).
(5) To simulate a larger patient, 100 mm of water is added to the phantom (total thickness 300 mm).
(6) Open the collimators fully or to the size of the phantom if this is smaller.
(7) Measure and record the focus to intensifier and focus to detector distances.
(8) Expose the phantom under automatic brightness control and record the dosimeter reading, $\dot{M}$, tube voltage, tube current and image intensifier settings. Repeat the measurement three times and record dosimeter readings, $\dot{M}_1$, $\dot{M}_2$ and $\dot{M}_3$.
(9) Repeat step 8 for all image intensifier field sizes, dose rates and automatic brightness control options in normal clinical use.
(10) If a dosimeter with an ionization chamber is used, record the temperature and pressure.

Measurement of entrance surface air kerma rate for C-arm units (fixed and mobile units)

Where the couch used clinically is available

The measurement arrangement is shown in Fig. 8.4(c) and the measurement is conducted as follows:

(1) If an anti-scatter grid is used in the clinical situation, make sure it is in position.
(2) Position the phantom on the couch resting on the rig. Select a position on the couch where the major clinical examinations are performed, e.g. 500 mm from the top of the couch for a cardiology unit.

(3) The space between the couch and the phantom must be sufficient to allow positioning the detector.
(4) Position the detector in contact with the phantom and at the centre of its entrance surface.
(5) Set the distance between the X ray focus and the image intensifier to 1000 mm (if this distance can be varied).
(6) To simulate a larger patient, 100 mm of water is added to the phantom (total thickness 300 mm) so that its exit surface is in contact with the intensifier carriage.
(7) Set the distance between the exit surface of the phantom and the image intensifier assembly to 100 mm.
(8) Measure (if necessary) and record the focus to intensifier and focus to detector distances.
(9) Open the collimators fully or to the size of the phantom if this is smaller.
(10) Expose the phantom under automatic brightness control and record the dosimeter reading, $\dot{M}$, tube voltage, tube current and image intensifier settings. Repeat the measurement three times and record dosimeter readings, $\dot{M}_1$, $\dot{M}_2$ and $\dot{M}_3$.
(11) Repeat step 10 for all image intensifier field sizes, dose rates and automatic brightness control options in normal clinical use.
(12) If a dosimeter with an ionization chamber is used, record the temperature and pressure.

Lateral exposures or where the couch used clinically is not available

The measurement arrangement is shown in Fig. 8.4(d) and the measurement conducted as follows:

(1) If an anti-scatter grid is used in the clinical situation, make sure it is in position.
(2) Position the X ray tube and image intensifier so that the beam is directed horizontally.
(3) Stand the phantom on its side. If a water phantom is used, it should be closed to avoid spillage. Position the detector in contact with the phantom at the centre of its entrance surface.
(4) Set the distance between the X ray focus and the image intensifier to 1000 mm (if this distance can be varied).
(5) To simulate a larger patient, 100 mm of water is added to the phantom (total thickness 300 mm) so that its exit surface is in contact with the intensifier carriage.

(6) Set the distance between the exit surface of the phantom and the image intensifier assembly to 100 mm.
(7) Measure (if necessary) and record the focus to intensifier and focus to detector distances.
(8) Open the collimators fully or to the size of the phantom if this is smaller.
(9) Expose the phantom under automatic brightness control and record the dosimeter reading, $\dot{M}$, tube voltage, tube current and image intensifier settings. Repeat the measurements three times and record dosimeter readings, $\dot{M}_1$, $\dot{M}_2$ and $\dot{M}_3$.
(10) Repeat steps 8 and 9 for all image intensifier field sizes, dose rates and automatic brightness control options in normal clinical use.
(11) If a dosimeter with an ionization chamber is used, record the temperature and pressure.

8.5.2.3. Calculations

Entrance surface air kerma rate

(1) Calculate the mean dosimeter reading, $\bar{\dot{M}}$, from the measurements, $\dot{M}_1$, $\dot{M}_2$ and $\dot{M}_3$.
(2) Calculate the entrance surface air kerma rate, $\dot{K}_e$, from the mean dosimeter reading, $\bar{\dot{M}}$, using Eq. (8.13)[12]. In this equation k_{TP} is the correction factor for temperature and pressure (Eq. (8.14)), N_{K,Q_0} is the chamber calibration coefficient and k_Q is the factor which corrects for differences in the response of the dosimeter at the calibration quality, Q_0, and at the measurement quality, Q. The quantities T and P are the temperature and pressure (in °C and kPa) recorded during the measurement and T_0 and P_0 are their reference values for which N_{K,Q_0} is provided.

$$\dot{K}_e = \bar{\dot{M}} N_{K,Q_0} k_Q k_{TP} \tag{8.13}$$

$$k_{TP} = \left(\frac{273.2+T}{273.2+T_0}\right)\left(\frac{P_0}{P}\right) \tag{8.14}$$

[12] It is assumed that the leakage signal of the dosimeter can be neglected and that no correction has been applied for this effect.

(3) If a PMMA phantom is used, the surface air kerma rate is calculated using Eq. (8.15). In this equation B_w and B_{PMMA} are the backscatter factors in terms of air kerma for water and PMMA, respectively.

$$\dot{K}_e = \bar{\dot{M}} N_{K,Q_0} k_Q k_{TP} \frac{B_w}{B_{PMMA}} \tag{8.15}$$

Values B_w and B_{PMMA} are taken from Table VIII.1 in Appendix VIII.

(4) If a detector has been used that does not respond to backscattered radiation and measures the incident air kerma rate, $\dot{K}_i$, the entrance surface air kerma rate is obtained from Eq. (8.16):

$$\dot{K}_e = \bar{\dot{M}} N_{K,Q_0} k_Q B_w \tag{8.16}$$

(5) If needed, the calculated value of $\dot{K}_e$ is corrected for a difference between the position of the reference point of the detector and the phantom surface using the inverse square law.[13]

8.5.2.4. Estimation of uncertainties

The uncertainty in the measurement of the entrance surface air kerma rate for fluoroscopic installations can be estimated using values of relative uncertainties in three measurement scenarios as given in Table 8.2 and adding contributions arising from factors specific to the procedure employed.

The main source of the additional uncertainty arises from the effect of backscattered radiation from the phantom on the energy response of the detector. The component of the backscattered radiation has a spectral and angular distribution differing from that of the incident radiation. In addition, the effective measurement point of the dosimeter is not on the surface. There are no data available but it is estimated that for ionization chambers these effects may introduce an additional uncertainty of 5%, at most, corresponding to a standard deviation of about 3%. This may be slightly less for systems based on a semiconductor detector but as data are generally not available, the above value for the ionization chambers will also be a good upper estimate of the uncertainty for the semiconductor detectors.

[13] This correction applies strictly to the component of the air kerma from incident radiation. As the component from backscattered radiation is much smaller, the uncertainty introduced by correcting both components will be negligible.

TABLE 8.4. FACTORS WHICH CONTRIBUTE TO THE MEASUREMENT OF UNCERTAINTY IN THE DETERMINATION OF ENTRANCE SURFACE AIR KERMA RATE IN FLUOROSCOPY

Source of uncertainty	Uncertainty (k = 1) (%)		
	Scenario 1	Scenario 2	Scenario 3
Measurement scenario (see Table 8.2)	6.3	3.5	2.7
Precision of reading	1.0[a]	0.6[b]	0.6[b]
Uncertainty in measurement position[c]	0.6	0.6	0.6
Uncertainty in detector response to backscattered radiation	3.0	3.0	3.0
Relative combined standard uncertainty (k = 1)	7.1	4.7	4.1
Relative expanded uncertainty (k = 2)	**14.2**	**9.4**	**8.2**

[a] One single reading taken.
[b] Standard deviation of the mean of three readings.
[c] Corresponding to 2 mm in the positioning of detector at a distance 500 mm from the X ray focus.

Table 8.4 gives examples of the uncertainty arising from each contribution and the value of the relative expanded uncertainty (k = 2) of the measurement that lies between about 8% and 14%, depending on the scenario selected.

The user should establish the actual measurement uncertainty using principles described in Appendix I.

8.5.2.5. Examples

Measurement of the entrance surface air kerma

An entrance surface air kerma rate was measured for an under couch installation using the 200 mm thick water phantom and a plane parallel ionization chamber. The distance of the X ray focus from the image intensifier housing was set to 1000 mm and the water phantom was positioned on the table using a 100 mm thick rig. The distance between the exit surface of the water phantom and the image intensifier housing was 100 mm.

The X ray unit was set to 70 kV with an image intensifier field size of 230 mm × 230 mm and it was operated in a normal mode. The recorded readings of the dosimeter were: 25.3 mGy/min, 25.5 mGy/min and 25.3 mGy/min. The calculated mean value of the dosimeter reading, $\bar{M}$, is therefore:

$\bar{M}$ = ((25.3 + 25.5 +25.3)/3) mGy/min = 25.37 mGy/min

The calibration coefficient, N_{K,Q_0}, for the dosimeter was 0.936, the beam quality correction factor, k_Q, was 1 and the temperature and pressure correction, k_{TP}, was 1.03. The air kerma rate, $\dot{K}$, at the reference point of the detector is therefore given by:

$\dot{K}$ = 25.37 mGy/min × 0.936 × 1.00 × 1.03 = 24.458 mGy/min

The dosimeter was taped to the entrance surface of the phantom with the entry window 5 mm from the phantom. The entrance surface air kerma rate is therefore:

$$\dot{K}_e = 24.458 \text{ mGy/min}\left(\frac{1000-100-200-5}{1000-100-200}\right)^2 = 24.458 \text{ mGy/min}\left(\frac{695}{700}\right)^2$$
$$= 24.109 \text{ mGy/min}$$

For scenario 3 (reference type dosimeter and all corrections applied), the relative expanded uncertainty (k = 2) of the measurement is 8.2%. The entrance surface air kerma is written as:

$\dot{K}_e$ = (24.1 ± 2.0) mGy/min

$\dot{K}_e$ Phantom: Fluoro 1

8.5.2.6. Worksheets

Determination of entrance surface air kerma rate for a fluoroscopy installation

User: _____ Date: _____ UC ☐ OC ☐ C-arm ☐

Hospital or clinic name: _____

1. X ray equipment

X ray unit and model: _____ Room no.:_____

Image intensifier model: _____ Anti-scatter grid ☐ Yes ☐ No

2. Dosimeter and phantom

Dosimeter model: _____ Serial no.: _____ Date of calib.: _____

Calibration coefficient (N_{K,Q_0})[14]: _____ ☐ mGy/nC ☐ mGy/reading

Reference conditions: HVL (mm Al): _____ Pressure P_0 (kPa): ____ Temperature T_0 (°C): _____

Manufacturer of phantom: _____ Serial no.: _____

☐ 200 mm water ☐ 300 mm water ☐ 185 mm PMMA ☐ 278 mm PMMA

3. Exposure conditions for phantom

Focus to intensifier distance: _____ mm Focus to chamber distance: _____ mm

Ambient conditions: Pressure P (kPa): _____ Temperature T (°C): _____ k_{TP} = _____

[14] This is the calibration coefficient for the whole dosimeter, including the detector and the measurement assembly. For systems with separate calibration coefficients for the detector and the measurement assembly, the overall calibration coefficient is calculated as a product of the two separate calibration coefficients.

$\dot{K}_e$ Phantom: Fluoro 2

4. Dosimeter reading and calculation of entrance surface air kerma rate

Selected option	Tube voltage (kV)	Tube current (mA)	Filtration (mm Al)	Manual or automatic mode setting[a]	Field size (mm × mm)	Dosimeter readings ($\dot{M}_1$, $\dot{M}_2$, $\dot{M}_3$) (mGy/min)	Mean dosimeter reading ($\bar{\dot{M}}$) (mGy/min)	k_Q	Entrance surface air kerma rate ($\dot{K}_e$)[b] (mGy/min)

[a] Enter M (manual) or automatic mode details.

[b] For water phantom use formula: $\dot{K}_e = \bar{\dot{M}} N_{K,Q_0} k_Q k_{TP}$, where $k_{TP} = \left(\frac{273.2+T}{273.2+T_0}\right)\left(\frac{P_0}{P}\right)$.

For PMMA phantom use formula: $\dot{K}_e = \bar{\dot{M}} N_{K,Q_0} k_Q k_{TP} \frac{B_w}{B_{PMMA}}$, where $k_{TP} = \left(\frac{273.2+T}{273.2+T_0}\right)\left(\frac{P_0}{P}\right)$; $k_{TP} = 1$ for systems with automatic temperature and pressure corrections and for semiconductor dosimeters.

8.5.3. Patient dosimetry

In examinations using fluoroscopy, irradiation geometry and time vary individually from patient to patient. Effects on patient exposures of these variations are captured by the air kerma–area product (P_{KA}), which is easily measured using a flat transmission ionization chamber (KAP meter) mounted on the collimator housing. The KAP meter does not disturb the examination and gives real time information. The signal can be recorded as a function of time and the course of the examination analysed [8.13].

In this Code of Practice, measurement of the air kerma–area product (P_{KA}) using a transmission ionization chamber (KAP meter) is recommended for monitoring patient exposures in examinations involving fluoroscopy.

The KAP meters should be calibrated for each stand where they are used. In principle, calibrations both in situ and at a standard laboratory are possible. Modern radiology departments usually possess a number of machines that require KAPs. It is not realistic to calibrate each instrument at the SSDL and for built-in KAP meters this is not even possible. It should also be noted that the calibration coefficient provided by the manufacturer should be checked before the instrument is used. Procedures for in situ calibration of KAP meters are described in Appendix IX.

8.5.3.1. List of equipment

The equipment comprises:

(a) Calibrated transmission ionization chamber and electrometer;
(b) Thermometer and barometer.

8.5.3.2. Methods

Measurement of the air kerma–area product

A method for measurement of the air kerma–area product during fluoroscopy is described. It applies to portable KAP meters as well as to instruments that are incorporated into X ray systems. The KAP meters need to be calibrated for transmitted radiation using one of the methods described in Appendix IX. The measurement is conducted as follows:

(1) Mount the KAP meter on the exit surface of the collimator housing of the X ray tube. This step is omitted in the case of a built-in KAP meter.

(2) Record, if possible, the tube voltage and any other machine parameters (e.g. operating mode chosen, tube current and pulse rate if appropriate) used during the examination.
(3) Record the reading, M, of the KAP meter.
(4) If the operating mode is changed during the procedure, it may be helpful to use recorded KAP meter readings (if available) and machine parameters for each stage.
(5) Record the temperature and pressure.

8.5.3.3. Calculations

Air kerma–area product

Calculate the air kerma–area product, P_{KA}, from the KAP meter reading, M, using Eq. (8.17)[15]. In this equation, k_{TP} is the correction for temperature and pressure (Eq. (8.18)) and $N_{P_{KA,Q_0}}$ is the calibration coefficient in terms of the air kerma–area product for the radiation quality, Q_0, used at the calibration temperature and pressure of T_0 and P_0, respectively; T and P are temperature and pressure recorded during the measurement. The factor k_Q corrects for differences in the response of the KAP meter at the calibration quality, Q_0, and at the quality, Q, of the clinical X ray beam. For a total filtration of up to about 3 mm aluminium, this quality can be indicated by the value of the HVL, irrespective of the X ray tube voltage. For beams with stronger filtrations, more comprehensive calibration of the KAP meter may be required. For details of using total filtration, X ray tube voltage and (or) HVL as beam quality specifiers for KAP meters, see Pöyry et al. [8.14].

$$P_{KA} = MN_{P_{KA,Q_0}} k_Q k_{TP} \tag{8.17}$$

$$k_{TP} = \left(\frac{273.2 + T}{273.2 + T_0}\right)\left(\frac{P_0}{P}\right) \tag{8.18}$$

If no information on the response of the KAP chamber to radiation qualities with varying amounts of total filtration is available, the response of the KAP meter may be determined by means of a reference class dosimeter. For all radiation qualities, the KAP chamber is exposed to a given, fixed field

[15] It is assumed that the leakage signal of the KAP meter can be neglected and that no correction for this effect is applied.

size and its indication is measured together with the indication of a reference class dosimeter positioned in the plane of measurement. The calibration coefficient of the KAP meter for radiation quality Q is:

$$N_{P_{\mathrm{KA},Q}} = N_{P_{\mathrm{KA},Q_0}} k_Q^{\mathrm{KAP}} = \frac{M_Q^{\mathrm{ref}}}{M_Q^{\mathrm{KAP}}} N_{K,Q_0}^{\mathrm{ref}} k_Q^{\mathrm{ref}} A_{\mathrm{nom}} \tag{8.19}$$

where M_Q^{KAP} and M_Q^{ref} are readings (corrected for air density) of the KAP meter and the reference chamber for radiation quality Q;
k_Q^{KAP} and k_Q^{ref} are factors expressing the energy dependence of the KAP meter and the reference ionization chamber;
A_{nom} is a measured nominal beam area in the plane of measurement.

For details see Appendix IX.

8.5.3.4. Estimation of uncertainties

IEC 60580 [8.15] specifies acceptable limits of uncertainty in the response of KAP meters when individual exposure parameters (influence quantities) vary to the maximum likely extent. According to this standard, the estimated expanded uncertainty of a measurement with KAP meters is 25% at the 95% confidence interval ($k = 2$). This corresponds to application of a single value for the calibration coefficient representing an average over all influence factors, i.e. all possible doses, dose rates and X ray energies in clinical practice, which are likely to cover the following ranges:

$\dot{P}_{\mathrm{KA}}$	$(10^{-2}$–$1.5 \times 10^4)$ μGy·m^2·s^{-1}
X ray spectrum	(50–150) kV, total filtration 2.5 mm Al

The ranges of temperature and pressure for which the meter will satisfy the tolerance on overall uncertainty should be determined and stated.

If the tube voltage is recorded and calibration coefficients for under and over couch installations are separately determined and applied, the uncertainty can be reduced. If a calibration coefficient has only been established for an over couch situation, it is noted that insertion of a table with a mattress or other filtration in the beam reduces the air kerma incident on the patient by up to 30–40%, depending on the HVL of the beam, beam angulations and table construction [8.13, 8.16, 8.17]. This has to be considered when using the KAP

meter reading to estimate patient exposure (energy imparted to the patient or effective dose).

The uncertainty in the calibration coefficient when the tube voltage and filtration are known and the energy dependence accounted for can be reduced to about 6% at the 95% confidence level. In examinations, including fluoroscopy and automatic brightness control, the tube voltage is likely to vary during the course of the examination. It may be useful to obtain information about the range of actual tube voltages and to adjust the applied calibration coefficient to limit the uncertainty to less than 25%. In the future, X ray units may be capable of automatically applying the correct calibration coefficient to the reading of the KAP meter. In addition, some X ray units currently use KAP indicators, which determine the KAP value based on calculations using exposure and collimations settings.

The user should establish the actual measurement uncertainty using principles described in Appendix I.

8.5.3.5. Examples

Barium enema examination

The single contrast barium enema examination of an adult patient was performed with an X ray unit set to 110 kV. The displayed KAP value for the whole examination was 17.5 Gy·cm^2. The KAP meter was calibrated by the SSDL and its calibration coefficient ($N_{P_{KA,Q_0}} = 1$) was specified for an HVL of 3.7 mm Al. The value for an HVL of 4 mm Al was measured for the X ray stand used for the examination. This gives the value of $k_Q = 1.05$. The temperature and pressure correction factor was calculated as $k_{TP} = 1.03$. The air kerma–area product is therefore:

$$P_{KA} = 17.5 \text{ Gy·cm}^2 \times 1 \times 1.05 \times 1.03 = 18.93 \text{ Gy·cm}^2$$

The relative expanded uncertainty of the measurement was assessed as 15% at $k = 2$. The measured air kerma–area product is written as:

$$P_{KA} = (18.9 \pm 2.8) \text{ Gy·cm}^2$$

8.5.3.6. Worksheet

Determination of air kerma–area product

User: _____ Date: _____

Hospital or clinic name: _____

1. X ray equipment

X ray unit and model: _____ Room no.:_____

Image receptor model: _____

Anti-scatter grid: ☐ Yes ☐ No

2. KAP meter

KAP model: _____ Serial no.: _____ Date of calib.: _____

Under table tube: ☐ Yes ☐ No

Calibration coefficient ($N_{P_{KA,Q_0}}$): _____ ☐ Gy·cm^2·C^{-1} ☐ Gy·cm^2/reading

Reference conditions: Beam quality: _____ HVL (mm Al): _____

Pressure P_0 (kPa): _____ Temperature T_0 (°C): _____

3. KAP reading and calculation of air kerma–area product

Ambient conditions: Pressure P (kPa): _____ Temperature T (°C):_____ k_{TP} = _____

Examination details	Tube voltage (kV)	Automatic brightness control setting	KAP meter reading (M)	k_Q	Air kerma area product (P_{KA})[a] (Gy·cm^2)	Fluoroscopy time (s)

[a] $P_{KA} = MN_{P_{KA,Q_0}} k_Q k_{TP}$, where $k_{TP} = \left(\frac{273.2+T}{273.2+T_0}\right)\left(\frac{P_0}{P}\right)$.

8.6. MAMMOGRAPHY

8.6.1. Choice of dosimetric quantities

In this Code of Practice, three dosimetric quantities are used for mammography: the incident air kerma, K_i, the entrance surface air kerma, K_e, and the mean dose to the glandular tissues within the breast, known as the mean glandular dose, D_G. The latter risk related quantity is the primary quantity of interest and is estimated from the incident air kerma using a conversion coefficient as discussed in Appendix VII. For phantoms, the incident air kerma is measured using a diagnostic dosimeter and the entrance surface air kerma using TLDs. For patient exposures, the incident air kerma is estimated using recorded exposure parameters.

8.6.2. Measurements using phantoms

The phantom used for the determination of incident air kerma and mean glandular dose is a 45 mm thick PMMA phantom which approximately simulates a 'standard' breast of thickness 50 mm and glandularity 50%.

The incident air kerma may be obtained using two alternative methods. The preferred method is to measure the air kerma in the absence of the phantom using a suitable ionization chamber and electrometer or semi-conductor dosimeter. This requires knowledge of the exposure parameters of the phantom. The alternative method uses a measurement of the entrance surface air kerma made with TLDs exposed on the surface of the phantom. The incident air kerma is then calculated by division by the appropriate backscatter factor (see Table 8.8).

The conversion coefficients used to estimate the mean glandular dose from the incident air kerma are quality dependent. It is necessary therefore to note the target/filter combination and tube voltage used and to measure the HVL of the X ray set. Data are provided for situations where measured values of the HVL are not available (see Table 8.7).

If it is required to estimate the incident air kerma and mean glandular dose for other breast thicknesses and compositions, measurements may be made using plastic phantoms of other sizes to simulate the breast. Further information is provided in Appendix VII, where the use of PMMA phantoms is described.

8.6.2.1. List of equipment

The equipment comprises the following:

(a) Calibrated diagnostic dosimeter.
(b) Detector support stand.
(c) Mammographic phantom.
(d) Aluminium attenuators for HVL measurement.
(e) Lead diaphragm or jig for HVL measurement.
(f) Loaded mammographic cassette.
(g) Tape measure or ruler.
(h) Thermometer and barometer (for measurements with an ionization chamber).
(i) Calibrated TLDs may be used as an alternative to the diagnostic dosimeter. Dosimeters should have had their individual sensitivity correction factors established or dosimeters within a selected sensitivity range should be chosen (see Appendix IX).

8.6.2.2. Methods

The mean glandular dose is derived from measurements of the incident air kerma (without backscatter) at the surface of the phantom and of the HVL, using tabulated conversion coefficients. The incident air kerma is measured with a diagnostic dosimeter in the absence of the phantom, using the tube loading required for exposure of the phantom. Alternatively, the incident air kerma is calculated from measurements of entrance surface air kerma made with TLDs. In this case, if the HVL is not measured, a value can be obtained from Table 8.7.

Some X ray equipment uses the thickness of the compressed breast as an aid to the selection of tube voltage and target/filter combination. As the thickness of the phantom will be less than the thickness of the breast being simulated, the user can consider adding an appropriate thickness of a low density material such as expanded polystyrene to the top of the phantom so that the overall thickness is then correct. The polystyrene should be cut away so that it does not cover the AEC system.

The methodology applies equally to X ray systems employing screen–film, computed radiography or other digital receptors. Appropriate time intervals should be allowed between exposures in accordance with the thermal capacity of the X ray tube.

Measurement of incident air kerma using a diagnostic dosimeter

The method consists of two parts: the determination of the tube loading for correct exposure of the phantom and the measurement of the incident air kerma at the mammographic reference point for this tube loading. With suitable modifications, the process described may also be used for the exposure of other breast phantoms. Usually the tube loading is not known in advance because the exposure is made under AEC and the procedure below should be followed.

Determination of tube loading

Clinical exposures are terminated automatically, but the tube voltage and in some cases the materials of the target and filter have to be selected. For some equipment, the selection is made automatically and it is important to check that the automatic selection for the phantom matches that which would be used clinically for the standard breast.

(1) Set up the X ray machine for a cranio-caudal view, with the compression plate in position and a loaded cassette in the Bucky, if a screen–film or computed radiography system is being used.
(2) Place the phantom on the breast table with its longest edge aligned with the chest wall edge of the table and centred laterally.
(3) Bring the compression plate down onto the phantom.
(4) Do not use the magnification mode.

On X ray machines where the tube loading is displayed (those with AEC and post-exposure display of milliampere-seconds):

(5) Expose the phantom for the conditions used clinically for the breast being simulated.
(6) Record the tube loading (P_{It1}), tube voltage and target/filter combination used.
(7) Make two more exposures and record the corresponding tube loadings, P_{It2} and P_{It3}. Calculate the mean tube loading, $P_{It,auto}$.
(8) Record the tube voltage and target/filter combination used.

On X ray machines with AEC but without post-exposure indication of the tube loading:

(5) Position the detector of the diagnostic dosimeter above the entrance surface of the phantom and compression plate in a position that does not shadow the radiation detector for the AEC system.
(6) Expose the phantom under AEC for the conditions used for the breast being simulated.
(7) Record the dosimeter reading, M_1, for conditions using the AEC mode.
(8) Make two more exposures and record the corresponding dosimeter readings, M_2 and M_3. Calculate the mean dosimeter reading ($\bar{M}_{\text{auto}}$).
(9) Select manual exposure mode and a similar tube loading to that used under AEC.
(10) Make sure that the tube voltage (and target and filter if appropriate) for manual operation is the same as that for use with AEC.
(11) Expose the phantom and record the dosimeter reading (M_1) and the tube loading ($P_{\text{It,man}}$) in milliampere-seconds.
(12) Make two more exposures and record the corresponding dosimeter readings (M_2 and M_3) for each. Calculate the mean dosimeter reading ($\bar{M}_{\text{man}}$).
(13) Derive the tube loading for correct exposure of the phantom under AEC ($P_{\text{It,auto}}$) from the following:

$$P_{\text{It,auto}} = \left(\bar{M}_{\text{auto}} / \bar{M}_{\text{man}}\right) P_{\text{It,man}} \tag{8.20}$$

(14) Record the tube voltage and target/filter combination used.

Measurement of the incident air kerma at the relevant tube loading

(1) Remove the phantom and position the reference point of the radiation detector at the mammographic reference point, i.e. 45 mm above the cassette table, 40 mm from the chest wall edge and centred with respect to the lateral direction. The compression plate should be in contact with the detector[16].
(2) Select manual exposure control and the tube loading, tube voltage and target/filter combination determined above. If it is not possible to select the exact tube loading value, choose a loading close to this value.
(3) Make an exposure and record the dosimeter reading (M_1) and the tube loading (P_{It}).

[16] The detector reading will include forward scatter from the compression plate, the error due to this depends on the type of compression plate and detector and may introduce a systematic error [8.18]. This error is acknowledged but ignored.

(4) Make two more exposures and record the corresponding dosimeter readings, M_2 and M_3.
(5) If a dosimeter with an ionization chamber is used, record the temperature and pressure.

Measurement of entrance surface air kerma using TLDs

(1) Set up the X ray machine for a cranio-caudal view, with the compression plate in position and a loaded cassette in the Bucky, if a screen–film or computed radiography system is being used.
(2) Place the phantom on the breast table with its longest edge aligned with the chest wall edge and centred laterally.
(3) Place a sachet containing three TLDs on the surface of the phantom with the centre of the sachet 40 mm from the chest wall edge and centred with respect to the lateral direction. A further sachet of unexposed TLDs is retained for a background reading.
(4) Bring the compression plate down onto the phantom, taking care not to damage the TLDs.
(5) Do not use the magnification mode.
(6) Expose the phantom for the conditions used clinically for the breast being simulated.
(7) Record the tube voltage and target/filter combination used.
(8) Remove the TLD sachet from the phantom and arrange for the dosimeters to be read. Record the readings (M_1, M_2 and M_3) from the exposed dosimeters and the readings (M_{01}, M_{02} and M_{03}) from the unexposed dosimeters.

Measurement of the HVL

The measurement of the HVL should be made with the compression plate in place. It will normally form part of the routine quality control of the equipment. A jig which collimates the beam so that it just covers the detector and which provides support for the aluminium attenuators can be convenient [8.19]. The thickness of the lead diaphragm used to collimate the radiation field should be at least 0.5 mm.

(1) The measurement is performed in so-called 'good geometry', i.e. for narrow beam conditions to minimize the influence of scattered radiation (see Fig. 8.5 and Appendix V).
(2) Do not use the magnification mode.

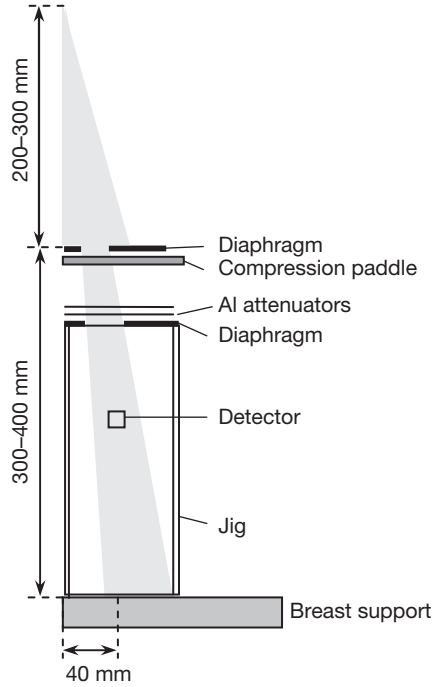

FIG. 8.5. Experimental set-up for the measurement of HVL (not to scale).

(3) Place the radiation detector sufficiently far above the breast support to avoid the influence of backscatter on the measurement. The centre of the detector should be positioned 40 mm from the chest wall edge and centred laterally.
(4) The HVL measurement is performed in the presence of the compression plate. Place the lead diaphragm under the compression plate, in a position approximately halfway between the focal spot and the detector (a measurement jig can be used).
(5) Align the diaphragm in such a way that the radiation beam completely covers the radiation detector and is only slightly larger than necessary. Note that the light field and the radiation beam usually do not coincide. A fluorescent screen can be of help.
(6) Select manual exposure control.
(7) Select the values for tube voltage and typical tube loading that would be used for the routine clinical examination of the breast being simulated. If appropriate, the target and filter should be selected on the same basis. Record the target/filter combination, tube voltage and tube loading.

(8) Perform a sufficient number of exposures to establish repeatability without aluminium attenuators and record the readings of the radiation detector and the tube loading.
(9) Repeat step 8 for a set of three aluminium attenuators and the same tube loading as that for measurements without any attenuator. The thickness of attenuators is selected so that their value encloses the expected HVL of the beam.
(10) Repeat the measurement without the attenuators.

8.6.2.3. Calculations

Measurements with a diagnostic dosimeter

(1) Calculate the HVL of the beam by interpolating graphically or numerically in the measured signal for various thicknesses of attenuator. The HVL measured during a quality assurance programme can also be used.
(2) Calculate the mean dosimeter reading, $\bar{M}$, from the measurements, M_1, M_2 and M_3, of the incident air kerma at the mammographic reference point. If it is possible to select the exact value of the tube loading ($P_{\mathrm{It,auto}}$) recorded under AEC for this measurement, this mean would also be the value of M_{auto}.
(3) If it is not possible to select the exact value of the tube loading recorded under AEC ($P_{\mathrm{It,auto}}$) for the measurement of incident air kerma, calculate the dosimeter reading corresponding to this tube loading using Eq. (8.21):

$$M_{\mathrm{auto}} = P_{\mathrm{It,auto}} \left(\frac{\bar{M}}{P_{\mathrm{It}}} \right) \tag{8.21}$$

(4) Calculate the incident air kerma, K_{i}, for the PMMA phantom from the dosimeter reading M_{auto} using Eq. (8.22)[17]. In this equation, k_{TP} is the correction factor for temperature and pressure, N_{K,Q_0} is the dosimeter calibration coefficient and k_Q is the factor which corrects for differences in the response of the dosimeter at the calibration quality, Q_0, and at the quality, Q, of the clinical X ray beam. This quality is indicated by the value of the HVL.

[17] It is assumed that the leakage signal of the dosimeter can be neglected and that no correction has been applied for this effect.

$$K_{\mathrm{i}} = M_{\mathrm{auto}} N_{K,Q_0} k_Q k_{\mathrm{TP}} \tag{8.22}$$

The correction factor, k_{TP}, is unity for dosimeters incorporating semiconductor devices. For dosimeters employing ionization chambers it is given by:

$$k_{\mathrm{TP}} = \left(\frac{273.2+T}{273.2+T_0}\right)\left(\frac{P_0}{P}\right) \tag{8.23}$$

where T and P are the temperature and pressure (in °C and kPa) recorded during the measurement and T_0 and P_0 are their reference values for which N_{K,Q_0} is provided.

(5) Obtain from Table 8.5, by interpolation if necessary, the conversion coefficient $c_{D_{\mathrm{G50}},K_{\mathrm{i,PMMA}}}$ for the measured HVL and the standard breast of 50 mm thickness and 50% glandularity that is simulated by the 45 mm PMMA phantom. This coefficient converts the incident air kerma at the entrance surface of the PMMA phantom to the mean glandular dose for the standard breast.

TABLE 8.5. CONVERSION COEFFICIENT $c_{D_{\mathrm{G50}},K_{\mathrm{i,PMMA}}}$ USED TO CALCULATE THE MEAN GLANDULAR DOSE TO A 50 mm STANDARD BREAST OF 50% GLANDULARITY FROM THE INCIDENT AIR KERMA FOR A 45 mm PMMA PHANTOM*

HVL (mm Al)	$c_{D_{\mathrm{G50}},K_{\mathrm{i,PMMA}}}$ (mGy/mGy)
0.25	0.149
0.30	0.177
0.35	0.202
0.40	0.223
0.45	0.248
0.50	0.276
0.55	0.304
0.60	0.326
0.65	0.349

* Data taken from Ref. [8.2].

TABLE 8.6. VALUES OF *s* FACTORS FOR DIFFERENT MAMMOGRAPHIC TARGET/FILTER COMBINATIONS*

Target/filter combination	*s* factor
Mo/Mo	1.000
Mo/Rh	1.017
Rh/Rh	1.061
Rh/Al	1.044
W/Rh	1.042

* Data taken from Dance et al. [8.20].

(6) Refer to the spectral correction factor, *s*, for the selected target/filter combination in Table 8.6.

Calculate the mean glandular dose, D_G, to the standard breast from:

$$D_G = c_{D_{G50},K_{i,PMMA}} sK_i \tag{8.24}$$

Measurements with TLDs

(1) Calculate the mean value of the background reading, $\bar{M}_0$, from background dosimeter readings M_{01}, M_{02} and M_{03} ($\bar{M}_0 = (M_{01} + M_{02} + M_{03})/3$).
(2) Calculate the average background corrected dosimeter reading, $\bar{M}$, from the exposed dosimeter readings, M_1, M_2 and M_3, from:

$$\bar{M} = \frac{\sum_{i=1}^{3} f_{s,i}\left(M_i - \bar{M}_0\right)}{3} \tag{8.25}$$

where factors $f_{s,i}$ are used to correct for the individual sensitivity of the *i*-th dosimeter (see Appendix IX)[18].

[18] Factors $f_{s,i}$ are constant for dosimeters grouped so that the sensitivity of dosimeters in a group lies within a selected range (see Appendix IX).

TABLE 8.7. VALUES OF HVL FOR SELECTED TARGET/FILTER COMBINATIONS AT TUBE VOLTAGES IN THE RANGE 24–34 kV*

Tube voltage	Target/filter combination (mm Al)			
(kV)	Mo/Mo	Mo/Rh	Rh/Rh	W/Rh
24	0.317	0.381	0.369	0.507
25	0.326	0.389	0.382	0.516
26	0.336	0.397	0.394	0.525
27	0.345	0.405	0.407	0.534
28	0.355	0.413	0.419	0.543
29	0.365	0.422	0.432	0.552
30	0.374	0.430	0.444	0.561
31	0.384	0.438	0.457	0.571
32	0.394	0.446	0.469	0.580
33	0.403	0.454	0.482	0.589
34	0.413	0.463	0.494	0.598

* Data provided by Young [8.21].

(3) If a measured value of the HVL is not available, refer to the HVL value in Table 8.7 for the target/filter combination and tube voltage used for the exposure. Use linear interpolation to obtain values for tube voltages that are between the tabulated data points.

(4) Obtain from Table 8.8, by interpolation if necessary, the backscatter factor, *B,* for the HVL obtained in step 3 above.

(5) Calculate the incident air kerma, K_i, for the PMMA phantom from the average background corrected dosimeter reading, $\bar{M}$, and the backscatter factor, *B,* using Eq. (8.26). In this equation N_{K,Q_0} is the TLD calibration coefficient for the reference radiation quality used and k_Q is the factor which corrects for differences in the response of the dosimeter at the calibration quality and at the quality, Q, of the clinical X ray beam. This quality is indicated by the value of the HVL. The factor k_f corrects for the effect of fading of the thermoluminescence signal between irradiation of the dosimeter and its readout.

$$K_i = \frac{\bar{M} N_{K,Q_0} k_Q k_f}{B} \tag{8.26}$$

TABLE 8.8. VALUES OF THE BACKSCATTER FACTOR, *B*, FOR MAMMOGRAPHIC BEAM QUALITIES AS A FUNCTION OF HVL*

HVL (mm Al)	0.25	0.30	0.35	0.40	0.45	0.50	0.55	0.60	0.65
B	1.07	1.07	1.08	1.09	1.10	1.11	1.12	1.12	1.13

* Data taken from Ref. [8.2].

(6) Obtain from Table 8.5, by interpolation if necessary, the conversion coefficient $c_{D_{G50},K_{i,PMMA}}$ for the measured HVL and the standard breast of 50 mm thickness and 50% glandularity that is simulated by the 45 mm PMMA phantom. This coefficient converts the incident air kerma to the PMMA phantom to the mean glandular dose for the standard breast.

(7) Refer to the spectral correction factor, *s,* for the selected target/filter combination in Table 8.6.

(8) Calculate the mean glandular dose, D_G, to the standard breast using Eq. (8.27):

$$D_G = c_{D_{G50},K_{i,PMMA}} s K_i \tag{8.27}$$

8.6.2.4. Estimation of uncertainties

Table 8.9 lists the factors which contribute to the measurement uncertainty for the estimation of mean glandular breast dose using the 45 mm PMMA phantom and a diagnostic dosimeter. The table gives examples of standard uncertainties arising from each contribution, their combination in quadrature and the value of the expanded uncertainty. For diagnostic dosimeters, the relative expanded uncertainty (k = 2) of measurement is between about 8% and 14%, depending on the scenario selected.

It is pointed out that the conversion coefficients used are model dependent. The value of the mean glandular dose obtained applies just to the model simulated in the Monte Carlo calculations. Changes in model can produce large differences in the estimate of mean glandular dose [8.22].

The uncertainty in the measurement made with TLDs is discussed in Section 8.3. The relative expanded uncertainty (k = 2) of 10% was adopted for this Code of Practice. Additional contributions from the application of a backscatter factor, positioning of the dosimeters, the uncertainty in conversion coefficients and phantom thickness have to be included in the overall uncertainty. The relative combined standard uncertainty can be calculated as

TABLE 8.9. FACTORS WHICH CONTRIBUTE TO THE MEASUREMENT UNCERTAINTY IN THE DETERMINATION OF MEAN GLANDULAR DOSE USING THE 45 mm PMMA MAMMOGRAPHIC PHANTOM[a]

Source of uncertainty	Uncertainty (k = 1) (%)		
	Scenario 1	Scenario 2	Scenario 3
Measurement scenario (see Table 8.2)	6.3	3.5	2.7
Precision of reading	1.0[b]	0.6[c]	0.6[c]
Uncertainty in measurement position[d]	0.4	0.4	0.4
Precision of tube loading indication	1.0	1.0	1.0
Uncertainty in conversion coefficient due to uncertainty of 3% in HVL measurement	1.7	1.7	1.7
Uncertainty in thickness of phantom of 0.5 mm[e]	1.7	1.7	1.7
Relative combined standard uncertainty (k = 1)	6.9	4.5	3.9
Relative expanded uncertainty (k = 2)	**13.8**	**9.0**	**7.8**

[a] The data are for the use of a diagnostic dosimeter.
[b] One single reading taken.
[c] Standard deviation of the mean of three readings.
[d] Corresponding to ±2 mm at 600 mm focus to surface distance.
[e] Uncertainty due to effect on phantom attenuation [8.23].

6.9%. The value of the relative expanded uncertainty (k = 2) in measurements of the entrance surface air kerma using TLDs is about 14%.

The user should establish the actual measurement uncertainty using the principles described in Appendix I.

8.6.2.5. Examples

Example for measurements with an ionization chamber

An exposure of the 45 mm PMMA phantom employing a mammography unit in the AEC mode, at 28 kV and with a Mo/Mo anode/filter combination required a tube loading of 110 mA·s. It was not possible to set the exact tube loading required under manual exposure control. The mean value of the dosimeter reading at the reference point was 7.98 mGy for a tube loading of 100 mA·s. The calculated value of the dosimeter reading for an exposure under AEC of $P_{\mathrm{It,auto}}$ is therefore (see Eq. (8.21)):

M_{auto} = 110 mA·s × (7.98 mGy/100 mA·s) = 8.778 mGy

The calibration coefficient, N_{K,Q_0}, for the dosimeter was 1.000 and the value of k_Q was 1.037 at this mammographic quality. The correction factor, k_{TP}, for temperature and pressure was 1.031. The incident air kerma is therefore (see Eq. (8.22)):

K_i = 8.778 mGy × 1.000 × 1.037 × 1.031 = 9.385 mGy

The measured HVL was 0.350 mm Al, giving a value of 0.202 mGy/mGy for the conversion coefficient $c_{D_{G50},K_{i,PMMA}}$ from Table 8.5. The target/filter combination was Mo/Mo, giving a value of 1.000 for factor *s* from Table 8.6.

The mean glandular dose is therefore (see Eq. (8.24)):

D_G = 0.202 mGy/mGy × 1.000 × 9.385 mGy = 1.896 mGy

For scenario 3 (reference type detector and all corrections applied), the relative expanded uncertainty (k = 2) of the measurement is 7.8%. The mean glandular dose is written as:

D_G = (1.90 ± 0.15) mGy

Example for measurements with TLDs

The 45 mm PMMA phantom was exposed under AEC at 28 kV using a Mo/Mo target/filter combination. The three exposed TLDs and three background TLDs were read. The average readings of the three exposed and three background dosimeters were 539.85 nC and 5.83 nC, respectively. The average background corrected reading is therefore:

$\bar{M}$ = 539.85 – 5.83 = 534.02 nC

From Table 8.7, the HVL at 28 kV for the Mo/Mo target/filter combination is 0.355 mm Al. From Table 8.8, the backscatter factor at an HVL of 0.355 mm of Al is 1.085. The product of the calibration coefficient, N_{K,Q_0}, and the factor k_Q for the TLD was 0.02048 mGy/nC for this mammographic quality. The incident air kerma is therefore:

K_i = 534.02 nC × 0.02048 mGy/nC ÷ 1.085 = 10.08 mGy

The assumed HVL is 0.355 mm Al, giving a value of 0.212 mGy/mGy for the conversion coefficient $c_{D_{G50},K_{i,PMMA}}$ from Table 8.5. The target/filter combination was Mo/Mo, giving a value of 1.000 for factor *s* from Table 8.6. The mean glandular dose is therefore:

$$D_G = 0.212 \text{ mGy/mGy} \times 1.000 \times 10.08 \text{ mGy} = 2.14 \text{ mGy}$$

For an expanded standard uncertainty ($k = 2$) of 14%, the mean glandular dose measured by the TLDs is written as:

$$D_G = (2.14 \pm 0.30) \text{ mGy}$$

8.6.2.6. Worksheets

Determination of mean glandular dose to the standard breast using the 45 mm PMMA phantom and a diagnostic dosimeter

User: _____ Date: _____

Hospital or clinic name: _____

1. X ray equipment

X ray unit and model: _____ Room no.:_____

Imaging using screen–film combination *Imaging using digital image receptor*

Screen–film combination:_____ Image receptor model:_____

Film processor model: _____

Developer and fixer (brand name): _____

2. Dosimeter and phantom

Dosimeter model: _____ Serial no.: _____ Date of calib.: _____

Calibration coefficient (N_{K,Q_0})[19]: _____ ☐ mGy/nC ☐ mGy/reading

Reference conditions: Beam quality: _____ HVL (mm Al): _____

Pressure P_0 (kPa): _____ Temperature T_0 (°C): _____

Manufacturer of phantom: _____ Serial no.: _____

3. Exposure conditions for phantom

☐ AEC ☐ Manual AEC setting: _____

Tube voltage (kV): ____ Target/filter combination: _____

Tube loadings under AEC (if available) P_{It1}, P_{It2} and P_{It3}: _____ mA·s

Mean tube loading (AEC) $P_{It,auto}$ (if available): _____ mA·s

4. Tube loading for equipment without post-exposure display of mA·s

Dosimeter readings under AEC (M_1, M_2, M_3): _____

Mean dosimeter reading (AEC) $\bar{M}_{auto}$: _____

Dosimeter readings under manual control (M_1, M_2, M_3): _____

Mean dosimeter reading (manual) $\bar{M}_{man}$: _____ at tube loading $P_{It,man}$: _____ mA·s

Calculated value ($P_{It,auto}$) of tube loading under AEC $P_{It,auto} = (\bar{M}_{auto}/\bar{M}_{man})/P_{It,man}$ ____ mA·s

[19] This is the calibration coefficient for the whole dosimeter, including the detector and the measurement assembly. For systems with separate calibration coefficients for the detector and the measurement assembly, the overall calibration coefficient is calculated as a product of the two separate calibration coefficients.

5. Dosimeter reading at tube loading ($P_{\mathrm{It,auto}}$) and calculation of incident air kerma

Dosimeter readings under manual control (M_1, M_2, M_3): _____

Mean dosimeter reading ($\bar{M}$): _____ at tube loading (P_{It}): _____ mA·s

Calculated dosimeter reading (M_{auto}) at $P_{\mathrm{It,auto}}$ ($M_{\mathrm{auto}} = P_{\mathrm{It,auto}}\,(\bar{M}/P_{\mathrm{It}})$): _____ mGy

Pressure P (kPa):___ Temperature T (ºC):___ $k_{\mathrm{TP}} = \left(\frac{273.2+T}{273.2+T_0}\right)\left(\frac{P_0}{P}\right) =$ _____[20]

HVL (from 6 below) = _____ mm Al $k_Q =$ _____

Calculated value of incident air kerma $K_{\mathrm{i}} = M_{\mathrm{auto}} N_{K,Q_0} k_Q k_{\mathrm{TP}} =$ _____ mGy

6. Determination of HVL

Dosimeter readings should be obtained for filter thicknesses that bracket the HVL. The first and last readings are made at zero filter thickness.

Filter thickness (mm Al)	Dosimeter reading (mGy)	Average dosimeter reading, $\bar{M}$, at zero thickness
0.00		$(M_{01} + M_{02})/2 =$_____ mGy
0.00		Interpolated HVL: _____ mm Al

7. Mean glandular dose to the standard breast for 45 mm PMMA phantom

Conversion coefficient $c_{D\mathrm{G50},K\mathrm{i,PMMA}}$ interpolated from Table 8.5 for the measured value of the HVL and factor s from Table 8.6 for the selected target/filter combination.

$c_{D\mathrm{G50},K\mathrm{i,PMMA}}$: _____ mGy/mGy s: _____

Mean glandular dose $D_{\mathrm{G}} = c_{D\mathrm{G50},K\mathrm{i,PMMA}}\, sK_{\mathrm{i}} =$ _____ mGy

[20] For dosimeters with a semiconductor detector, $k_{\mathrm{TP}} = 1$.

Phantom:
MGD - TLD 1

Determination of mean glandular dose to the standard breast using the 45 mm PMMA phantom and TLDs

User: _____ Date: _____

Hospital or clinic name: _____

1. X ray equipment

X ray unit and model: _____ Room no.:_____

Imaging using screen–film combination *Imaging using digital image receptor*

Screen–film combination:_____ Image receptor model:_____

Film processor model: _____

Developer and fixer (brand name): _____

2. TLDs and phantom

Identification markings on TLD sachets (if any): _____

Calibration coefficient (N_{K,Q_0}) for TLDs: _____ mGy/reading

Reference beam quality (HVL): _____ mm Al k_Q for measurement set-up: _____

Manufacturer of phantom: _____ Serial no.: _____

3. Exposure conditions for phantom

☐ AEC ☐ Manual AEC setting: ____ Tube voltage (kV): ____ HVL: ____ mm Al

Target/filter combination: _____ Post-exposure mA·s (if available): _____

4. Dosimeter readings and calculation of incident air kerma

Date of exposure: Date of evaluation: Fading correction (k_f) = _____

Dosimeter reading (uncorrected) (M_i)	Dosimeter reading (background) (M_{0i})	Average corrected reading:
		$\bar{M}$ = _____
		Backscatter factor (B) (Table 8.8): _____

$\bar{M}_0 = (M_{01} + M_{02} + M_{03})/3$ $\qquad \bar{M} = \dfrac{\sum_{i=1}^{3} f_{s,i}\left(M_i - \bar{M}_0\right)}{3}$

Incident air kerma $K_i = \dfrac{\bar{M} N_{K,Q_0} k_Q k_f}{B}$ = _____ mGy

5. Mean glandular dose to the standard breast for measurements with 45 mm PMMA phantom

Conversion coefficient ($c_{D_{G50},K_{i,PMMA}}$) interpolated from Table 8.5 for the measured value of the HVL and factor *s* from Table 8.6 for the selected target/filter combination.

$c_{D_{G50},K_{i,PMMA}}$: _____ mGy/mGy *s*: _____

Mean glandular dose $D_G = c_{D_{G50},K_{i,PMMA}} sK_i$ = _____ mGy

8.6.3. Measurements on patients

The mean glandular dose for a given patient is estimated from the incident air kerma for exposure of that patient using conversion coefficients as discussed in Appendix VII. The incident air kerma for each patient exposure in the required series of patient exposures is estimated using knowledge of the selected exposure parameters and breast thickness and the measured X ray tube output.

The calibration of the breast thickness indication device should be checked before these measurements are made, and if necessary a correction applied to the recorded values of the thickness before the mean glandular dose is estimated.

It is necessary to know the tube loading of the X ray tube for each patient exposure, which will generally be obtained under AEC. In many cases the tube loading for each exposure is displayed on the equipment console after completion of the exposure. If post-exposure display of the tube loading is not available, it will not be possible to measure patient doses using the method described here.

The conversion coefficients used to estimate the mean glandular dose from the incident air kerma are quality dependent. It is necessary therefore to note the target/filter combination and tube voltage used and to measure the HVL of the X ray set. Data are provided for situations where measured values of the HVL are not available.

The selection of the conversion coefficients used to estimate the mean glandular dose from the incident air kerma from the tables supplied requires knowledge of the glandularity of each breast. Two approaches are described. The first uses data for an assumed glandularity of 50% and the second allows the user to make their own estimate of the glandularity.[21]

8.6.3.1. List of equipment

The measuring equipment comprises:

(a) Calibrated diagnostic dosimeter;
(b) Detector support stand;
(c) Aluminium attenuators for HVL measurement;

[21] Conversion coefficients for typical values of glandularity taken from a United Kingdom survey of women aged 50–64 are reported in Dance et al. [8.20]. These are not necessarily appropriate for other populations of women.

(d) Lead diaphragm for HVL measurement;
(e) Tape measure or ruler;
(f) Thermometer and barometer (for measurements with an ionization chamber).

8.6.3.2. Methods

The incident air kerma for each exposure of the left and right breasts in the required series of patient exposures is estimated from recorded details of the selected target/filter combination, the tube voltage, the indicated breast thickness and the tube current–exposure time product. For this purpose, the X ray tube output is measured at the reference point and the inverse square law is applied as appropriate. The determination of the HVL is also required. Separate data should be collected for each radiographic projection. The mean glandular dose is obtained from the calculated values of the incident air kerma using tabulated conversion coefficients.

Appropriate time intervals should be allowed between exposures in accordance with the thermal capacity of the X ray tube.

Measurement of the X ray tube output at the reference point for the relevant target/filter combinations, tube voltages and tube loading(s)

The X ray tube output at the reference point should be determined with the compression plate in place for each target/filter combination in clinical use and for a representative set of tube voltages and tube loadings which adequately sample the patient exposure parameters used. It is suggested that measurements giving three or four values of the tube loading and three or four values of the tube voltage are sufficient for each target/filter combination. Values for other tube voltages and tube loadings may be found by appropriate interpolation.

(1) For each target/filter combination in clinical use, select representative values of the tube voltage which are suitable for the estimation of incident air kerma.
(2) Set up the X ray machine for a cranio-caudal view.
(3) Do not use the magnification mode.
(4) Position the reference point of the radiation detector at the mammographic reference point, i.e. 45 mm above the cassette table, 40 mm from the chest wall edge and centred with respect to the lateral direction. The compression plate should be present between the detector and the X ray tube.

(5) Select manual exposure control.
(6) Select one of the target/filter combinations identified in step 1.
(7) Select one of the tube voltages chosen in step 1 for the selected target/filter combination. Make an exposure and record the target/filter combination, tube voltage, tube loading and dosimeter reading.
(8) Make two more exposures and record the corresponding dosimeter readings.
(9) Repeat steps 7 and 8 for each of the representative values of the tube voltage for the selected target/filter combination.
(10) Repeat steps 6–9 for all target/filter combinations in clinical use.
(11) If a dosimeter with an ionization chamber is used, record the temperature and pressure.

Measurement of the tube focus to breast support plate distance

Measure and record the distance, d_P, between the focus of the X ray tube and the upper surface of the breast support plate.

Measurement of the HVL

The methodology for the HVL measurement is the same as the methodology described in Section 8.6.2.2 with the exception that for each target/filter combination a set of X ray tube voltages is measured which adequately samples the voltages used for clinical examinations.

Collection of patient data

(1) For each patient and patient exposure, record the following data: selected target/filter combination, tube voltage, tube loading (post-exposure (mA·s)) and indicated breast thickness. Data should be recorded separately for left and right breasts and the radiographic projection used for each exposure should be noted.
(2) Collect data for the required series of patients.

8.6.3.3. Calculations

Mean glandular dose

(1) For a given target/filter combination, calculate the mean dosimeter reading, $\bar{M}$, at the mammographic reference point.

(2) Calculate the corresponding X ray tube output at the reference point, Y_{ref}, from the mean dosimeter reading, $\bar{M}$, and the tube loading, P_{It}, using Eq. (8.28)[22]. In this equation, k_{TP} is the correction factor for temperature and pressure, N_{K,Q_0} is the chamber calibration coefficient and k_Q is the factor which corrects for differences in the response of the dosimeter at the calibration quality and at the measurement quality, Q, of the clinical X ray beam. This quality is indicated by the value of the HVL.

$$Y_{ref} = \frac{\bar{M} N_{K,Q_0} k_Q k_{TP}}{P_{It}} \tag{8.28}$$

The correction factor, k_{TP}, is unity for dosimeters with semiconductor devices. For dosimeters with ionization chambers it is given by:

$$k_{TP} = \left(\frac{273.2 + T}{273.2 + T_0} \right) \left(\frac{P_0}{P} \right) \tag{8.29}$$

The quantities T and P are the temperature and pressure (in ^{o}C and kPa) recorded during the measurement and T_0 and P_0 are their reference values for which N_{K,Q_0} is provided.

(3) Repeat steps 1 and 2 for each combination of target/filter and tube voltage measured.

(4) For each patient exposure select the results from step 2 which correspond to the particular target/filter combination used and the tube voltages which straddle that used for the patient exposure. Use these results to calculate by interpolation the X ray tube output at the reference point, Y_{ref}, for the tube voltage used for the patient exposure.

(5) Calculate the incident air kerma, K_i, for the patient exposure using the inverse square law in accordance with Eq. (8.30). In this equation, d_P is the distance from the tube focus to the top of the breast support platform, d_{ref} and d_B are the distances from this platform to the reference point (45 mm) and the top of the breast (the breast thickness), respectively, and $P_{It,pat}$ is the recorded tube loading for the patient exposure:

[22] It is assumed that the leakage signal of the dosimeter can be neglected and that no correction has been applied for this effect.

$$K_i = Y_{ref} \left(\frac{d_P - d_{ref}}{d_P - d_B} \right)^2 P_{It,pat} \quad (8.30)$$

(6) For each patient exposure obtain from Table 8.10, by interpolation if necessary, the conversion coefficient c_{D_{G50},K_i} for the appropriate value of the HVL and the thickness of the breast. The coefficient c_{D_{G50},K_i} converts the incident air kerma to the mean glandular dose for a breast of 50% glandularity. Depending upon the assumptions to be used, set the value of the conversion coefficient $c_{D_{Gg},D_{G50}}$ to unity (if a glandularity of 50% is to be used), or obtain its value from Table 8.11 (if particular values of the glandularity, g, are known). The coefficient $c_{D_{Gg},D_{G50}}$ converts the mean glandular dose for a breast of 50% glandularity to that for a breast of glandularity, g, and of the same thickness.

(7) Refer to the spectral correction factor, s, for the selected target/filter combination in Table 8.6.

(8) Calculate the mean glandular dose using:

$$D_G = c_{D_{G50},K_i} c_{D_{Gg},D_{G50}} s K_i \quad (8.31)$$

TABLE 8.10. CONVERSION COEFFICIENT c_{D_{G50},K_i} IN mGy/mGy USED TO CALCULATE THE MEAN GLANDULAR DOSE TO BREASTS OF 50% GLANDULARITY FROM INCIDENT AIR KERMA*

Breast thickness	HVL (mm Al)						
(mm)	0.30	0.35	0.40	0.45	0.50	0.55	0.60
20	0.390	0.433	0.473	0.509	0.543	0.573	0.587
30	0.274	0.309	0.342	0.374	0.406	0.437	0.466
40	0.207	0.235	0.261	0.289	0.318	0.346	0.374
50	0.164	0.187	0.209	0.232	0.258	0.287	0.310
60	0.135	0.154	0.172	0.192	0.214	0.236	0.261
70	0.114	0.130	0.145	0.163	0.177	0.202	0.224
80	0.098	0.112	0.126	0.140	0.154	0.175	0.195
90	0.086	0.098	0.111	0.123	0.136	0.154	0.172
100	0.076	0.087	0.099	0.110	0.121	0.138	0.154
110	0.069	0.079	0.089	0.099	0.109	0.124	0.139

* Data taken from Dance et al. [8.20, 8.24].

TABLE 8.11. VALUES OF THE CONVERSION COEFFICIENT $c_{D_{Gg},D_{G50}}$ FOR GLANDULARITIES (g) OF 0.1–100% IN THE CENTRAL REGION OF THE BREAST*

HVL	Breast thickness	Breast glandularity (g) (%)				
(mm Al)	(mm)	0.1	25	50	75	100
0.30	20	1.130	1.059	1.000	0.938	0.885
	30	1.206	1.098	1.000	0.915	0.836
	40	1.253	1.120	1.000	0.898	0.808
	50	1.282	1.127	1.000	0.886	0.794
	60	1.303	1.135	1.000	0.882	0.785
	70	1.317	1.142	1.000	0.881	0.784
	80	1.325	1.143	1.000	0.879	0.780
	90	1.328	1.145	1.000	0.879	0.780
	100	1.329	1.147	1.000	0.880	0.780
	110	1.328	1.143	1.000	0.879	0.779
0.35	20	1.123	1.058	1.000	0.943	0.891
	30	1.196	1.090	1.000	0.919	0.842
	40	1.244	1.112	1.000	0.903	0.816
	50	1.272	1.121	1.000	0.890	0.801
	60	1.294	1.132	1.000	0.886	0.793
	70	1.308	1.138	1.000	0.886	0.788
	80	1.312	1.140	1.000	0.884	0.786
	90	1.319	1.145	1.000	0.884	0.786
	100	1.319	1.144	1.000	0.881	0.785
	110	1.322	1.142	1.000	0.882	0.784
0.40	20	1.111	1.054	1.000	0.949	0.900
	30	1.181	1.087	1.000	0.922	0.851
	40	1.227	1.105	1.000	0.907	0.825
	50	1.258	1.120	1.000	0.899	0.810
	60	1.276	1.125	1.000	0.890	0.798
	70	1.292	1.132	1.000	0.887	0.793
	80	1.302	1.136	1.000	0.885	0.790
	90	1.308	1.138	1.000	0.884	0.789
	100	1.311	1.138	1.000	0.883	0.788

TABLE 8.11. VALUES OF THE CONVERSION COEFFICIENT $c_{D_{Gg},D_{G50}}$ FOR GLANDULARITIES (g) OF 0.1–100% IN THE CENTRAL REGION OF THE BREAST* (cont.)

HVL	Breast thickness	Breast glandularity (g) (%)				
(mm Al)	(mm)	0.1	25	50	75	100
0.40	110	1.315	1.140	1.000	0.885	0.791
0.45	20	1.099	1.052	1.000	0.948	0.905
	30	1.169	1.080	1.000	0.924	0.858
	40	1.209	1.102	1.000	0.909	0.829
	50	1.248	1.115	1.000	0.898	0.815
	60	1.267	1.125	1.000	0.891	0.801
	70	1.283	1.129	1.000	0.892	0.797
	80	1.298	1.137	1.000	0.887	0.799
	90	1.301	1.135	1.000	0.886	0.792
	100	1.305	1.138	1.000	0.886	0.791
	110	1.312	1.138	1.000	0.885	0.789
0.50	20	1.098	1.050	1.000	0.955	0.910
	30	1.164	1.078	1.000	0.928	0.864
	40	1.209	1.094	1.000	0.912	0.835
	50	1.242	1.111	1.000	0.903	0.817
	60	1.263	1.120	1.000	0.896	0.807
	70	1.278	1.127	1.000	0.890	0.800
	80	1.289	1.132	1.000	0.889	0.794
	90	1.295	1.134	1.000	0.887	0.793
	100	1.302	1.138	1.000	0.886	0.791
	110	1.303	1.140	1.000	0.885	0.789
0.55	20	1.086	1.043	1.000	0.955	0.914
	30	1.154	1.071	1.000	0.932	0.870
	40	1.196	1.093	1.000	0.918	0.843
	50	1.227	1.105	1.000	0.906	0.824
	60	1.252	1.115	1.000	0.900	0.814
	70	1.267	1.122	1.000	0.896	0.805
	80	1.278	1.125	1.000	0.890	0.800
	90	1.285	1.128	1.000	0.890	0.798

TABLE 8.11. VALUES OF THE CONVERSION COEFFICIENT $c_{D_{Gg},D_{G50}}$ FOR GLANDULARITIES (g) OF 0.1–100% IN THE CENTRAL REGION OF THE BREAST* (cont.)

HVL	Breast thickness	Breast glandularity (g) (%)				
(mm Al)	(mm)	0.1	25	50	75	100
0.55	100	1.290	1.133	1.000	0.889	0.796
	110	1.293	1.134	1.000	0.888	0.793
0.60	20	1.089	1.045	1.000	0.959	0.919
	30	1.142	1.065	1.000	0.933	0.874
	40	1.185	1.090	1.000	0.923	0.850
	50	1.216	1.102	1.000	0.910	0.830
	60	1.238	1.113	1.000	0.904	0.820
	70	1.252	1.120	1.000	0.899	0.812
	80	1.266	1.123	1.000	0.894	0.806
	90	1.272	1.124	1.000	0.893	0.801
	100	1.279	1.125	1.000	0.891	0.797
	110	1.284	1.129	1.000	0.893	0.798

* Data taken from Dance et al. [8.20].

(9) Sort the patient calculations into exposures for the left and right breasts and for each of the X ray projections used. For each group calculate the average value of the mean glandular dose and the breast thickness.

8.6.3.4. Estimation of uncertainties

Table 8.12 lists the factors which contribute to the measurement uncertainty in the estimation of mean glandular breast dose for patients. The table gives examples of standard uncertainties arising from each contribution, their combination in quadrature and, finally, the value of the expanded uncertainty. For diagnostic dosimeters, the relative expanded uncertainty ($k = 2$) in the estimation of the mean glandular dose for a single patient exposure is, at best, between about 14.6% and 18.5%, depending on the scenario selected.

No allowance is made in the estimate for any uncertainty arising from lack of knowledge of the breast glandularity, which will have a significant effect. For example, as can be seen from Table 8.12, for larger breasts an uncertainty of 25% in glandularity can give rise to a difference of 17% in the

TABLE 8.12. FACTORS CONTRIBUTING TO THE MEASUREMENT UNCERTAINTY IN THE DETERMINATION OF MEAN GLANDULAR DOSE FOR INDIVIDUAL PATIENTS

Source of uncertainty	Uncertainty (k = 1) (%)		
	Scenario 1	Scenario 2	Scenario 3
Measurement scenario (see Table 8.2)	6.3	3.5	2.7
Precision of reading	1.0[a]	0.6[b]	0.6[b]
Uncertainty in measurement position[c]	0.4	0.4	0.4
Precision of tube loading indication	1.0	1.0	1.0
Uncertainty in conversion coefficient due to uncertainty of 3% in HVL measurement	1.7	1.7	1.7
Uncertainty in conversion coefficient due to uncertainty in breast thickness of 5 mm[d]	6.4	6.4	6.4
Relative combined standard uncertainty (k = 1), single patient	9.3	7.6	6.4
Relative expanded uncertainty (k = 2), single patient	**18.5**	**15.3**	**14.6**

[a] One single reading taken.
[b] Standard deviation of the mean of three readings.
[c] Corresponding to ±2 mm at 600 mm focus to surface distance.
[d] The error includes an inverse square law correction.

estimate of the mean glandular dose. It is also to be noted that the conversion coefficients used are model dependent. The value of the mean glandular dose obtained applies just to the model simulated in the Monte Carlo calculations. Changes in model and the distribution of glandular tissue within the breast can produce large differences in the estimate of the mean glandular dose [8.25]. Similarly, changes in thickness estimation from flexion in the compression paddle have also been excluded.

The user should establish the actual measurement uncertainty using principles described in Appendix I.

8.6.3.5. Examples

Measurement of the mean glandular dose

An exposure of the left breast of a patient in the cranio-caudal projection employing a mammography unit in the AEC mode, at 29 kV and a Mo/Rh

anode/filter combination required a tube loading of 132 mA·s. The recorded value of the breast thickness was 67 mm. A breast glandularity of 50% is to be assumed.

The mean value of the dosimeter reading at the reference point at 29 kV for the Mo/Rh target/filter combination was 9.83 mGy at 100 mA·s.

The product of the calibration coefficient, N_{K,Q_0}, and k_Q for the dosimeter was 0.950 for mammographic qualities used and the correction k_{TP} for temperature and pressure was 1.023.

The X ray tube output at the reference point is therefore:

$$Y_{ref} = (9.83\ \text{mGy} \times 0.950 \times 1.023)/100\ \text{mA·s} = 0.0955\ \text{mGy·mA}^{-1}\text{·s}^{-1}$$

The focus breast support distance is 640 mm, the reference distance is 45 mm, the breast thickness 67 mm and the tube loading 132 mA·s. The incident air kerma is therefore:

$$K_i = 0.0955\ \text{mGy·mA}^{-1}\text{·s}^{-1} \times 132\ (\text{mA·s}) \times (640\text{-}45)^2/(640\text{-}67)^2 = 13.6\ \text{mGy}$$

The measured HVL for this condition was 0.420 mm Al, yielding a value of 0.161 mGy/mGy for the conversion coefficient c_{D_{G50},K_i} from Table 8.10. The target/filter combination was Mo/Rh, giving a value of 1.017 for the factor s from Table 8.5.

The mean glandular dose is therefore:

$$D_G = 0.161\ \text{mGy/mGy} \times 1.017 \times 13.6\ \text{mGy} = 2.227\ \text{mGy}$$

For scenario 3 (reference type detector and all corrections applied), the relative expanded uncertainty ($k = 2$) of a single measurement is 14.6%. The mean glandular dose is written as:

$$D_G = (2.23 \pm 0.33)\ \text{mGy}$$

8.6.3.6. Worksheets and data collection sheets

Determination of X ray tube output

User: _____ Date: _____

Hospital or clinic name: _____

1. X ray equipment

X ray unit and model: _____ Room no.:_____

Imaging using screen–film combination *Imaging using digital image receptor*

Screen–film combination:_____ Image receptor model:_____

Film processor model: _____

Developer and fixer (brand name): _____

2. Dosimeter

Dosimeter model: _____ Serial no.: _____ Date of calib.: _____

Calibration coefficient (N_{K,Q_0})[23]: _____ ☐ mGy/nC ☐ mGy/reading

Reference conditions: HVL (mm Al): _____ Field size: _____

Pressure P_0 (kPa): _____ Temperature T_0 (°C): _____

3. Exposure conditions

Distance, d, of dosimeter from tube focus (mm): _____

4. Dosimeter reading and X ray tube output calculation

Pressure P (kPa):___ Temperature T (°C):___ $k_{TP} = \left(\frac{273.2+T}{273.2+T_0}\right)\left(\frac{P_0}{P}\right) =$ _____[24]

Tube voltage (kV)	Tube loading (P_{It}) (mA·s)	Dosimeter reading (M_1, M_2 and M_3)	Mean dosimeter reading ($\bar{M}$)	HVL (mm Al)	k_Q	Calculated X ray tube output at the reference point (Y_{ref})* (mGy·mA^{-1}·s^{-1})

* $Y_{ref} = \bar{M} N_{K,Q_0} k_Q k_{TP} / P_{It}$ where $\bar{M}$ is the mean dosimeter reading.

[23] This is the calibration coefficient for the whole dosimeter, including the detector and the measurement assembly. For systems with separate calibration coefficients for the detector and the measurement assembly, the overall calibration coefficient is calculated as the product of the two separate calibration coefficients.

[24] For dosimeters with a semiconductor detector, $k_{TP} = 1$.

5. Determination of HVL

Dosimeter readings should be obtained for filter thicknesses that bracket the HVL. The first and last readings are made at zero filter thickness.

Tube voltage (kV)	Filter thickness (mm Al)	Dosimeter reading (M)	
	0.00		$(M_{01} + M_{02})/2 =$ _______
			Interpolated HVL:
	0.00		_________ mm Al

Tube voltage (kV)	Filter thickness (mm Al)	Dosimeter reading (M)	
	0.00		$(M_{01} + M_{02})/2 =$ _______
			Interpolated HVL:
	0.00		_________ mm Al

Tube voltage (kV)	Filter thickness (mm Al)	Dosimeter reading (M)	
	0.00		$(M_{01} + M_{02})/2 =$ _______
			Interpolated HVL:
	0.00		_________ mm Al

Patient:
MGD Calculation 1

Data collection sheet for the estimation of mean glandular dose for mammographic patient exposures

User: _____ Date: _____

Hospital or clinic name: _____

1. X ray equipment

X ray unit and model: _____ Room no.:_____

Imaging using screen–film combination *Imaging using digital image receptor*

Screen–film combination:_____ Image receptor model:_____

Film processor model: _____

Developer and fixer (brand name): _____

2. Collected data

Date	Initials	L/R breast	Projection	Target/ filter	Tube voltage (kV)	Tube loading (mA·s)	Breast thickness (mm)

Patient:
MGD Calculation 2

Estimation of mean glandular dose for mammographic patient exposures

User: _____ Date: _____

Hospital or clinic name: _____

1. X ray equipment

Patient data collection date: _____

X ray unit and model: _____ Room no.:_____

Imaging using screen–film combination

Screen–film combination:_____

Film processor model: _____

Imaging using digital image receptor

Image receptor model: _____

Developer and fixer (brand name): _____

2 Collected data and calculation of mean glandular dose

L/R breast	Projection	Target/ filter	Tube voltage (kV)	Tube loading ($P_{It,pat}$) (mA·s)	Breast thickness (mm)	Distance (d_P) (mm)	Tube output at reference point (Y_{ref})[a] (mGy·mA^{-1}·s^{-1})	Incident air kerma (K_i)[b] (mGy)	HVL[c] (mm Al)	s-factor	Conversion coefficient (c_{D_{G50},K_i})[d] (mGy/mGy)	Conversion coefficient ($c_{D_{Gg}D_{G50}}$)[d] (mGy/mGy)	Mean glandular dose (D_G)[e] (mGy)

Patient:
MGD Calculation 2

[a] The values of the X ray tube output at the reference point, Y_{ref}, are obtained by interpolation in tube voltage from the measurements made for the particular target/filter combination used.

[b] The incident air kerma, K_i, is obtained by multiplying the tabulated value of the X ray tube output at the reference point by the tube loading for the patient exposure (in mA·s) and using the inverse square law to correct the value to that at the upper surface of the breast.

[c] The HVL corresponding to each patient exposure is obtained by interpolation in tube voltage from the measurements made for the particular target/filter combination used.

[d] Conversion coefficients c_{D_{G50},K_i} and $c_{D_{Gg},D_{G50}}$ are interpolated from Tables 8.10 and 8.11 for the particular breast thickness and glandularity and HVL. If a glandularity of 50% is used $C_{D_G,D_{G50}}$ is equal to unity. The factor s for the selected target/filter combination is obtained from Table 8.5.

[e] Mean glandular dose is calculated using $D_G = c_{D_G,D_{G50}} c_{D_{G50},K_i} s K_i$.

8.7. CT

8.7.1. Choice of dosimetric quantities

In this Code of Practice, the basic quantities used for dosimetry in CT are the CT air kerma indices, $C_{a,100}$ and C_W. A further CT air kerma index, C_{VOL}, is derived from C_W for particular patient scan parameters. Patient doses for a complete examination are described in terms of the CT air kerma–length product, $P_{KL,CT}$.

8.7.2. Measurements using phantoms and free in air

The CT air kerma indices $C_{a,100}$ and C_W are measured with a calibrated pencil ionization chamber[25] specially designed for CT (Fig. 8.6), and an electrometer. The index $C_{a,100}$ is measured free in air and the index C_W is derived from measurements of the CT air kerma indices $C_{PMMA,100,c}$ and $C_{PMMA,100,p}$ in standard head and body CT dosimetry phantoms.

8.7.2.1. List of equipment

For the measurement of $C_{a,100}$ free in air, the equipment comprises:

(a) CT ionization chamber and electrometer calibrated for CT beam qualities;
(b) Chamber support stand;
(c) Thermometer and barometer.

Additionally, for the measurement of $C_{PMMA,100,c}$ and $C_{PMMA,100,p}$ in PMMA, standard head and body CT dosimetry phantoms are employed.

8.7.2.2. Methods

The CT air kerma indices $C_{a,100}$, $C_{PMMA,100,c}$ and $C_{PMMA,100,p}$ should be determined for a single axial rotation of the scanner and the combinations of the pre-patient collimation, beam filter and tube voltage which are used

[25] Active semiconductor detectors and passive solid state detectors (thermoluminescence and optically stimulated luminescence) have also been used for CT dosimetry but their use is limited. CT ionization chambers have found widespread use in the daily practice of CT dosimetry, so their use is described in this Code of Practice.

FIG. 8.6. Pencil ionization chamber used for dosimetry of CT examinations. The active volume of the chamber is 3 cm^3 and the active length 100 mm.

clinically, employing the head or body phantom for the in phantom measurements as appropriate. It is also possible to make measurements for more than one consecutive axial rotation, with the resulting measurements being normalized to a single rotation.

There may be a deliberate overscan in axial mode to reduce movement artefacts. This can be as much as 36° [8.26]. It is important to note that the scan time indicated on the scanner console may be the nominal scan time, not including any overscan. The actual scan time may be greater by up to 10% (scanner dependent) [8.26].

For multislice (multidetector) CT, care should be taken to interpret correctly both *N*, the number of simultaneously acquired slices per rotation (also referred to as the number of data channels used during the acquisition), and *T*, the nominal thickness of each acquired slice (which is not necessarily the same as the nominal width of the reconstructed slice). The product, *NT*, should reflect the total nominal width of the X ray beam.

The values of $C_{a,100}$ and C_W, normalized to unit tube loading, are also calculated.

Measurement of $C_{a,100}$ free in air

For the measurement of $C_{a,100}$, the pencil ionization chamber should be supported in a specially designed stand so that it extends beyond the end of the couch. The measurement arrangement is shown in Fig. 8.7.

FIG. 8.7. Arrangement for the measurement of the CT air kerma index free in air, $C_{a,100}$. The chamber is clamped in a specially designed support and aligned so that it is coaxial with the scanner rotation axis and its sensitive volume is bisected by the scan plane. In this particular example, alignment has been achieved with the aid of lasers.

Measured data and exposure parameters should be recorded on a worksheet. An example is shown in Section 8.7.2.6. The measurement procedure is as follows:

(1) Set the gantry tilt to 0°.
(2) Position the chamber support stand on the couch and fix the chamber in position so that the clamp does not shield its active volume. Adjust the position of the support so that all of the active volume of the chamber extends beyond the end of the couch.
(3) Use the optical alignment aids provided with the scanner to position and align the chamber so that its axis is coincident with the axis of the scanner and the centre of the chamber volume lies on the scan plane.
(4) Select the desired scanner parameters and a single axial rotation.
(5) Record the dosimeter reading, M_1, for a single rotation of the scanner.
(6) Make two more exposures and record the dosimeter readings, M_2 and M_3.

FIG. 8.8. Arrangement for the measurement of the CT air kerma index, $C_{PMMA,100,c}$, in the standard body phantom. The phantom is positioned on the couch top and the chamber is positioned in the central hole of the phantom. A plastic sleeve is placed over the chamber to ensure a good fit within the phantom. The central plane of the phantom has still to be aligned with the position of the scan slice. In practice, the phantom may be secured in position using masking tape.

(7) Record all relevant scanner settings including tube voltage, beam filter, slice thickness and tube loading.
(8) Repeat steps 4–7 for the other appropriate sets of scanner parameters.
(9) Record the temperature and pressure.

Measurement of $C_{PMMA,100,c}$ and $C_{PMMA,100,p}$ using the standard head and body phantoms

For the measurement of $C_{\mathrm{PMMA,100,c}}$ and $C_{\mathrm{PMMA,100,p}}$ (and hence of C_{W}), the ionization chamber is supported by the phantom, which is placed on the couch top. The measurement arrangement is shown in Fig. 8.8.

The standard phantoms should be orientated so that one of the peripheral dose measurement holes corresponds to the position of the maximum air kerma at a depth of 10 mm below the phantom surface [8.27, 8.28]. The location of this position should be provided by the manufacturer. In many examples of these phantoms there are eight dose measuring holes equally spaced around the periphery. Only four equally spaced holes are required.

The distribution of the air kerma at a depth of 10 mm below the phantom surface will not be uniform because of the presence of the patient couch and the effect of any overscan. Voltage ramping at the start of a scan can also give rise to a localized increase. If the position of kerma maximum is not known, it can be located when the equipment is commissioned by using a series of measurements taken with different orientations of the phantom. In some situations, however, the scan start angle may vary from scan to scan, making the position of dose maximum difficult to locate. In this situation, the advice of the IPEM protocol [8.26] is adopted. It may be possible to operate the machine in 'engineer' mode to control the start angle for the scan. If this is not possible, a series of measurements taken for one peripheral hole can be used to determine the range of values. If the position of the maximum varies from scan to scan, a practical approach for routine measurements is to use the fluoroscopy mode and to make the measurements for three complete axial rotations of the scanner.

At least one set of measurements for C_W should be obtained with three sets of readings in each phantom hole to determine reproducibility and to establish whether there is any variation due to overscan. Thereafter, single readings in each phantom hole are used.

Measured data and exposure parameters should be recorded on a worksheet. An example is shown in Section 8.7.2.6. The procedure is as follows:

(1) Set the gantry tilt to 0°.
(2) Position the head phantom in the head holder on the scanner couch. Orientate the phantom so that one of the peripheral measurement bores is at the position of dose maximum.
(3) Use the external markings of the phantom and the optical alignment aids provided with the scanner to position and align the phantom. It should be centred on the scan plane with its axis coincident with the scanner rotation axis. (If the phantom is supplied with alignment inserts, these should be placed in the five measurement bores and the manufacturer's instructions followed for their orientation. Make an axial CT scan of the phantom and check the alignment of the phantom using the imaged alignment tools. If necessary, make adjustments to the phantom position and repeat this process until the phantom is aligned.)
(4) Insert the chamber in its plastic sleeve and place the whole assembly in the central dosimetry hole so that the centroid of the chamber's active volume is in the central plane of the phantom. Make sure that there are PMMA plugs in all other holes in the phantom.
(5) Select the desired scanner parameters and a single axial rotation.
(6) Record the dosimeter reading, M_{1c}, for a single rotation of the scanner.

(7) Make two more exposures and record the dosimeter readings, M_{2c} and M_{3c}.
(8) Repeat this procedure for the four peripheral holes in the phantom to obtain three readings, M_{1p}, M_{2p}, M_{3p}, for each peripheral position.
(9) Record all relevant scanner settings including tube voltage, beam filter, slice thickness and tube loading.
(10) Repeat steps 5–9 for the other appropriate sets of scanner parameters.
(11) Position the body phantom on the couch. Orientate the phantom so that one of the peripheral measurement bores is at the position of dose maximum.
(12) Repeat steps 3–10 for the body phantom.
(13) Record the temperature and pressure.

8.7.2.3. Calculations

Measurement of $C_{a,100}$ free in air

(1) Calculate the mean dosimeter reading, $\bar{M}$, from the free in air measurements, M_1, M_2 and M_3.
(2) Calculate the CT air kerma indices, $C_{a,100}$ and ${}_nC_{a,100}$, from the mean dosimeter reading, $\bar{M}$, and the tube loading, P_{It},[26] using Eqs (8.32) and (8.33)[27]. In Eq. (8.32), T is the nominal slice thickness and N is the number of slices simultaneously exposed (so that the nominal width of the irradiating beam is NT), k_{TP} is the correction factor for temperature and pressure (Eq. (8.34)), N_{P_{KL},Q_0} is the dosimeter calibration coefficient in terms of the air kerma–length product[28] and k_Q is the factor which corrects for differences in the response of the dosimeter at the calibration quality and at the measurement quality, Q, of the clinical X ray beam.

$$C_{a,100} = \frac{1}{NT}\bar{M}N_{P_{KL},Q_0}k_Q k_{TP} \tag{8.32}$$

[26] It should be noted that overscan may occur, as mentioned previously in Section 8.7.2.2.

[27] It is assumed that the leakage signal of the dosimeter can be neglected and that no correction has been applied for this effect.

[28] In CT, the air kerma–length product is generally expressed in units of mGy·cm, whereas slice thickness is often expressed in millimetres. Care must be taken in the application of Eq. (8.32) to ensure that a consistent set of units is used.

$$ {}_{n}C_{\mathrm{a},100} = \frac{C_{\mathrm{a},100}}{P_{\mathrm{It}}} \tag{8.33} $$

The correction factor, k_{TP}, is given by:

$$ k_{\mathrm{TP}} = \left(\frac{273.2 + T}{273.2 + T_0} \right) \left(\frac{P_0}{P} \right) \tag{8.34} $$

(3) Repeat the calculation for all sets of scanner parameters measured.

Measurement of $C_{PMMA,100,c}$ and $C_{PMMA,100,p}$ using the standard head and body phantoms and the calculation of C_W

The measurement procedure is as follows:

(1) Select the measurement set obtained with the head phantom.
(2) For a given set of scanner parameters calculate the mean dosimeter reading, $\bar{M}_{\mathrm{c}}$, from the readings $M_{1\mathrm{c}}$, $M_{2\mathrm{c}}$ and $M_{3\mathrm{c}}$ in the central chamber bore of the standard phantom and the mean dosimeter reading, $\bar{M}_{\mathrm{p}}$, from the twelve readings in the peripheral chamber bores (readings $M_{1\mathrm{p}}$, $M_{2\mathrm{p}}$ and $M_{3\mathrm{p}}$ in each of the four positions).
(3) Calculate the CT air kerma indices, $C_{\mathrm{PMMA},100,\mathrm{c}}$, for the measurement in the central chamber bore and $C_{\mathrm{PMMA},100,\mathrm{p}}$ for the mean of the measurements in the four peripheral chamber bores using the mean dosimeter readings, $\bar{M}_{\mathrm{c}}$ and $\bar{M}_{\mathrm{p}}$, and Eqs (8.35) and (8.36)[29]. In these equations, T is the nominal slice thickness, N is the number of tomographic slices simultaneously exposed (so that the nominal width of the irradiating beam is NT), k_{TP} is the correction factor for temperature and pressure, N_{P_{KL},Q_0} is the dosimeter calibration coefficient in terms of the air kerma–length product[30] and k_Q is the factor which corrects for differences in the response of the dosimeter at the calibration quality and at the measurement quality, Q, of the clinical X ray beam.

[29] It is assumed that the leakage signal of the dosimeter can be neglected and that no correction has been applied for this effect.

[30] In CT, the air kerma–length product is generally expressed in units of mGy·cm, whereas slice thickness is often expressed in millimetres. Care must be taken in the application of Eqs (8.35) and (8.36) to ensure that a consistent set of units is used.

$$C_{\mathrm{PMMA,100,c}} = \frac{1}{NT}\bar{M}_{\mathrm{c}}N_{P_{\mathrm{KL}},Q_0}k_Q k_{\mathrm{TP}} \tag{8.35}$$

$$C_{\mathrm{PMMA,100,p}} = \frac{1}{NT}\bar{M}_{\mathrm{p}}N_{P_{\mathrm{KL}},Q_0}k_Q k_{\mathrm{TP}} \tag{8.36}$$

The correction factor, k_{TP}, is given by:

$$k_{\mathrm{TP}} = \left(\frac{273.2+T}{273.2+T_0}\right)\left(\frac{P_0}{P}\right) \tag{8.37}$$

(4) Calculate the weighted CT air kerma index, C_{W}, and the normalized weighted CT air kerma index, ${}_nC_{\mathrm{W}}$, using:

$$C_{\mathrm{W}} = \frac{1}{3}\left(C_{\mathrm{PMMA,100,c}} + 2C_{\mathrm{PMMA,100,p}}\right) \tag{8.38}$$

$${}_nC_{\mathrm{W}} = \frac{C_{\mathrm{W}}}{P_{\mathrm{It}}} \tag{8.39}$$

where P_{It} is the tube loading for a complete rotation of the scanner.

(5) Repeat the calculation for all sets of scanner parameters measured using the standard phantom.
(6) Select the measurement set obtained with the body phantom.
(7) Repeat steps 2–6 for the measurements obtained with the body phantom.

8.7.2.4. Estimation of uncertainties

Table 8.13 lists the factors which contribute to the measurement uncertainty in the estimation of $C_{\mathrm{a,100}}$ and C_{W} using the ionization chamber/electrometer system. The table gives examples of standard uncertainties arising from each contribution, their combination in quadrature and the value of expanded uncertainty. The uncertainties associated with phantom construction have been estimated from the values of typical in phantom measurements. For ionization chambers, the relative expanded uncertainty ($k = 2$) of measurement for $C_{\mathrm{a,100}}$ is between about 6% and 13%, depending on the scenario selected.

TABLE 8.13. FACTORS CONTRIBUTING TO THE MEASUREMENT UNCERTAINTY IN THE DETERMINATION OF THE CT AIR KERMA INDICES, $C_{a,100}$ AND C_W, USING THE IONIZATION CHAMBER/ ELECTROMETER SYSTEM

Source of uncertainty	Uncertainty (k = 1)(%)		
	Scenario 1	Scenario 2	Scenario 3
Measurement scenario (see Table 8.2)	6.3	3.5	2.7
Precision of reading	1.0[a]	0.6[b]	0.6[b]
Precision of tube loading indication	1.0	1.0	1.0
Precision of chamber/phantom positioning in the centre of the gantry	0.3	0.3	0.3
Uncertainty of 1 mm in phantom diameter and 0.5 mm in depth of measurement bores[c]	0.35	0.35	0.35
Uncertainty in chamber response for in phantom measurements	3.0	3.0	3.0
Relative combined standard uncertainty (k =1) for $C_{a,100}$	6.5	3.7	3.0
Relative expanded uncertainty (k = 2) for $C_{a,100}$	**13.0**	**7.4**	**6.0**
Relative combined standard uncertainty (k = 1) for C_W	7.2	4.8	4.2
Relative expanded uncertainty (k = 2) for C_W	**14.4**	**9.6**	**8.4**

[a] One single reading taken.

[b] Standard deviation of the mean of three readings for $C_{a,100}$. For C_W, the uncertainty is smaller and depends upon the relative magnitudes of the readings in the peripheral and central phantom bores.

[c] This contribution does not apply for in air measurements of $C_{a,100}$.

Additional sources of uncertainty arise from the effect of scattered radiation inside the phantom, beam hardening and other effects which may affect the chamber response for measurements in phantom [8.29]. There are no data available but it is estimated that these effects may introduce an additional uncertainty of 5%, at most, corresponding to a standard deviation of about 3%, and this has been included in Table 8.13. For measurements of C_W in phantoms, the relative expanded uncertainty (k = 2) of measurement is then between about 8.4% and 14.4%, depending on the scenario selected.

The user should establish the actual measurement uncertainty using principles described in Appendix I.

8.7.2.5. Examples

Measurement of $C_{a,100}$ free in air

An exposure of a CT chamber free in air positioned along the axis of the CT scanner gave a mean dosimeter reading of 3.55. The tube loading, P_{It}, was 200 mA·s (200 mA for a 1 s rotation). The scanner collimation was adjusted so that 4 tomographic slices (N), each of nominal thickness 2.5 mm (T), were simultaneously exposed.

The calibration coefficients, $N_{P_{\mathrm{KL},Q_0}}$ and k_Q, for the dosimeter were 10.02 mGy·cm/reading and 1.003, respectively. The correction factor, k_{TP}, for temperature and pressure was 0.984.

The CT air kerma indices, $C_{\mathrm{a},100}$ and ${}_nC_{\mathrm{a},100}$, are therefore:

$$C_{\mathrm{a},100} = [10/(4 \times 2.5)]/\mathrm{cm} \times 3.55 \times 10.02\ \mathrm{mGy{\cdot}cm} \times 1.003 \times 0.984 = 35.0\ \mathrm{mGy}$$

$${}_nC_{\mathrm{a},100} = 35.0\ \mathrm{mGy}/200\ \mathrm{mA{\cdot}s} = 0.175\ \mathrm{mGy{\cdot}mA^{-1}{\cdot}s^{-1}}$$

The factor of 10 in the above calculation is required because the slice thickness is specified in millimetres.

For scenario 3 (reference type detector and all corrections applied), the relative expanded uncertainty ($k = 2$) of the measurement is 6%. The CT air kerma indices are written as:

$$C_{\mathrm{a},100} = (35.0 \pm 2.1)\ \mathrm{mGy} \qquad {}_nC_{\mathrm{a},100} = (0.175 \pm 0.011)\ \mathrm{mGy{\cdot}mA^{-1}{\cdot}s^{-1}}$$

Measurement of $C_{PMMA,100,c}$ and $C_{PMMA,100,p}$ using the standard head and body phantoms; calculation of C_W

Exposures of a 100 mm long CT chamber positioned in turn in the five bores of the standard body phantom gave mean dosimeter readings of 2.130, 1.930, 2.070 and 2.042 for the four peripheral bores and 0.915 for the central bore. The tube loading, P_{It}, was 200 mA·s (200 mA for a 1 s rotation). The scanner collimation was adjusted so that 4 slices (N), each of nominal thickness 2.5 mm (T), were simultaneously exposed.

The calibration coefficients, $N_{P_{\mathrm{KL},Q_0}}$ and k_Q for the dosimeter, were 10.02 mGy·cm/reading and 1.003, respectively. The correction factor, k_{TP}, for temperature and pressure was 0.984.

The CT air kerma indices, $C_{PMMA,100,p}$, $C_{PMMA,100,c}$, C_W and ${}_nC_W$ are therefore:

$$C_{PMMA,100,p} = [10/(4 \times 2.5)]/\text{cm} \times (2.130 + 1.930 + 2.070 + 2.042)/4 \times 10.02\ \text{mGy·cm} \times 1.003 \times 0.984 = 20.20\ \text{mGy}$$

$$C_{PMMA,100,c} = [10/(4 \times 2.5)]/\text{cm} \times 0.915 \times 10.02\ \text{mGy·cm} \times 1.003 \times 0.984 = 9.05\ \text{mGy}$$

$$C_W = [9.05\ \text{mGy} + (2 \times 20.20)\ \text{mGy}]/3 = 16.48\ \text{mGy}$$

$${}_nC_W = 16.48\ \text{mGy}/200\ \text{mA·s} = 0.0824\ \text{mGy·mA}^{-1}\text{·s}^{-1}$$

The factor of 10 in the above calculation is required because the slice thickness is specified in millimetres.

For scenario 3 (reference type detector and all corrections applied), the relative expanded uncertainty ($k = 2$) of the measurement is 8.4%. The CT air kerma indices are written as:

$$C_W = (16.48 \pm 1.38)\ \text{mGy}$$

$${}_nC_W = (0.082 \pm 0.007)\ \text{mGy·mA}^{-1}\text{·s}^{-1}$$

Phantom:
CT 1

8.7.2.6. Worksheets

Measurement of $C_{a,100}$, $C_{PMMA,100,c}$ and $C_{PMMA,100,p}$ and calculation of C_w

User: _____ Date: _____

Hospital or clinic name: _____

1. X ray equipment

CT scanner model: _____ Room no.:_____

2. Ionization chamber, electrometer and phantom

Dosimeter model: _____ Serial no.: _____ Date of calib.: _____

Calibration coefficient (N_{P_{KL},Q_0})[31]: _____ ☐ mGy·cm/nC ☐ mGy·cm/reading

Reference conditions: Beam quality: _____ HVL (mm Al): _____

Pressure P_0 (kPa): _____ Temperature T_0 (°C): ___

Manufacturer of phantom: _____ Serial no.: _____

Conditions during measurement:

Pressure P_0 (kPa): _____ Temperature T_0 (°C): ___ $k_{TP} = \left(\frac{273.2+T}{273.2+T_0}\right)\left(\frac{P_0}{P}\right) =$

[31] This is the calibration coefficient for the whole dosimeter, including the detector and the measurement assembly. For systems with separate calibration coefficients for the detector and the measurement assembly, the overall calibration coefficient is calculated as a product of the two separate calibration coefficients.

Phantom: CT 2

3. CT air kerma index ($C_{a,100}$)

Scanner settings (tube voltage, beam filter, head/body mode, etc.)	Nominal slice thickness (T) (mm)	Number of slices (N)	Tube loading (P_{It}) (mA·s)	Dosimeter readings (M_1, M_2, M_3)	Mean dosimeter reading ($\bar{M}$)	Calculated value of $C_{a,100}$ (mGy)	Calculated value of ${}_nC_{a,100}$ (mGy·mA^{-1}·s^{-1})

The CT air kerma index is calculated using[32]: $C_{a,100} = \frac{10}{NT} M N_{P_{KL},Q_0} k_Q k_{TP}$ and ${}_nC_{a,100} = \frac{C_{a,100}}{P_{It}}$.

[32] The factor of 10 in the formulas for $C_{a,100}$, $C_{PMMA,100,c}$ and $C_{PMMA,100,p}$ takes account of the use of a dosimeter calibration in milligray-centimetres and a slice thickness specified in millimetres.

Phantom: CT 3

4. CT air kerma indices $C_{PMMA,100,c}$, $C_{PPMMA,100,p}$ and C_w for the standard phantom **Head/body:** _____

Scanner settings (tube voltage, beam filter, head/body mode, etc.)	Nominal slice thickness (T) (mm)	Number of slices (N)	Tube loading (P_{It}) (mA·s)	Position	Dosimeter readings (M_1, M_2, M_3)	Mean $\bar{M}_c$ or $\bar{M}_p$	Calculated value of $C_{PMMA,100,c}$ (mGy)	Calculated value of $C_{PMMA,100,p}$ (mGy)	Calculated value of C_w (mGy)	Calculated value of ${}_nC_w$ (mGy·mA^{-1}·s^{-1})
				C						
				P1						
				P2						
				P3						
				P4						
				C						
				P1						
				P2						
				P3						
				P4						
				C						
				P1						
				P2						
				P3						
				P4						

Note: $\bar{M}_c$ is the mean of the three readings* in the central chamber bore (C). $\bar{M}_p$ is the mean of the 12 readings in the peripheral bores (three readings* in each of the bores P1, P2, P3 and P4). The CT air kerma indices are calculated using: $C_{PMMA,100,c} = \frac{10}{NT}\bar{M}_c N_{P_{KL},Q_0} k_Q k_{TP}$; $C_{PMMA,100,p} = \frac{10}{NT}\bar{M}_p N_{P_{KL},Q_0} k_Q k_{TP}$; $C_W = \frac{1}{3}\left(C_{PMMA,100,c} + 2C_{PMMA,100,p}\right)$ and ${}_nC_W = \frac{C_W}{P_{It}}$.

* Three sets of readings required for initial reading, thereafter one set only required.

8.7.3. Measurements on patients

In this Code of Practice, patient dose is specified using measurements made in the standard CT dosimetry phantoms. The CT air kerma index, ${}_nC_W$, is used in combination with the scan parameters to calculate the CT air kerma index, ${}_nC_{VOL}$, and hence the CT air kerma–length product, $P_{KL,CT}$. For the dose for one scanner rotation, the CT air kerma indices, C_W and C_{VOL}, are used. Direct measurements of patient dose are not made.

For multislice (multidetector) CT, care should be taken to interpret correctly both N, the number of simultaneously acquired slices per rotation (also referred to as the number of data channels used during the acquisition), and T, the nominal thickness of each acquired slice (which is not necessarily the same as the nominal width of the reconstructed slice). The product, NT, should reflect the total nominal width of the X ray beam.

Many scanners now use tube current modulation techniques to reduce patient dose so that the tube current may vary continuously as the scanner rotates or may change for each successive rotation. When calculating the air kerma–length product, $P_{KL,CT}$, it is important to use the actual values of the tube loading for the complete helical scan or for each axial scan as appropriate. Alternatively, for helical scans, the product of the average tube current and total scan time can be used.

Care should be taken when recording values of tube current as some scanners give values of an 'effective tube current' which varies with pitch rather than the actual tube current.

It is important to note that there may be differences in air kerma–length product for a single axial scan and that for a single helical rotation. These can arise because of overscan or voltage ramping. For the larger collimation widths available with multislice CT, the overscan required for the interpolation of projection data in helical mode extends the nominal scan region substantially. If the amount of overscan is known, a correction can be calculated. Alternatively, a correction factor can be measured using the CT ionization chamber as described in Ref. [8.26]. The correction factor is obtained by scanning slightly more than the entire length of the chamber in axial and then helical mode. The same collimated beam width is used for both scans; the axial scans should be contiguous and the helical scan should have a pitch of 1. The measurement is made with the chamber positioned along the scanner axis and free in air.

The measurement of the patient dose arising from the scan projection radiograph used to localize the scan volume is not described here, but is discussed in Appendix VII.

8.7.3.1. List of equipment

None

8.7.3.2. Methods

The measurement of C_W and ${}_nC_W$ is described in Section 8.7.2. The index, C_{VOL}, and the CT air kerma–length product, $P_{KL,CT}$, are calculated from ${}_nC_W$ using recorded values of the scan parameters. If the value of the 'dose–length product' indicated on the scanner console is to be used, this value should be recorded as well. The method and calculations presented here assume that manual calculation of the air kerma–length product is to be used.

Data collection

Patient data should be recorded on a worksheet. An example is given in Section 8.7.3.6. The procedure is as follows:

(1) Record all relevant scanner settings for each patient and patient scan, including:
   (a) Tube voltage;
   (b) Beam filter type;
   (c) Number of simultaneously acquired tomographic slices (e.g. 4 for a 4 slice scanner if used in this mode) and nominal thickness of each slice;
   (d) Use of tube current modulation techniques;
   (e) Distance of couch movement between axial rotations or per helical rotation, the distance of table movement per 360° of tube rotation;
   (f) For each axial scan series in the examination procedure, the total tube loading for the scan series (might be obtained from the tube loading(s) for each axial rotation);
   (g) For each helical scan series in the examination procedure, the total tube loading for the series (might be obtained from the average tube current and total scan time or recorded on scanner for series of scans).

   NOTE: When tube current modulation is used, the tube loadings recorded are those delivered rather than those set, though in this situation it may be helpful to record both.

(2) Collect data for the required series of patient exposures.

8.7.3.3. Calculations

Calculation of CT air kerma indices, C_W and C_{VOL}, for specific patient exposures

(1) Obtain the measured value of ${}_nC_W$ for the recorded patient exposure conditions, selecting measurements obtained with the head or body phantom as appropriate. Calculate C_W using Eq. (8.40). In this equation, P_{It} is the tube loading for a single axial scan or a single helical rotation.

$$C_W = {}_nC_W P_{It} \tag{8.40}$$

(2) Calculate C_{VOL} using Eq. (8.41). In this equation, N is the number of simultaneously obtained tomographic slices, T is the nominal slice thickness (so that the nominal width of the irradiating beam is NT) and l is the distance moved by the couch per helical rotation or between consecutive scans for a series of axial scans.

$$C_{VOL} = C_W \frac{NT}{l} \tag{8.41}$$

Calculation of the CT air kerma–length product, $P_{KL,CT}$, for a series of specific patient examinations

(1) For the given patient examination, divide the procedure into one or more axial and/or helical scan sequences obtained with the same scan settings.
(2) For each scan sequence, obtain the measured value of ${}_nC_W$ for the recorded patient exposure conditions, selecting measurements obtained with the head or body phantom as appropriate.
(3) Calculate ${}_nC_{VOL}$ using Eq. (8.42). In this equation, N is the number of simultaneously obtained tomographic slices, T is the nominal slice thickness (so that the nominal width of the irradiating beam is NT) and l is the distance moved by the couch per scanner rotation or between consecutive scans for a series of axial scans.

$${}_nC_{VOL} = {}_nC_W \frac{NT}{l} \tag{8.42}$$

(4) For each helical or axial scan sequence, calculate the CT air kerma–length product, $P_{KL,CT}$, using Eq. (8.43). In this equation, l is the distance moved

by the patient couch between consecutive scanner rotations (table feed) and in this case P_{It} is the tube loading for the complete helical or axial scan sequence. Express the answer in units of milligray-centimetres (see Eq. (3.17)).

$$P_{KL,CT} = {}_nC_{VOL} l P_{It} \tag{8.43}$$

(5) The CT air kerma–length product for the complete examination is obtained by adding together the contributions from the individual scan sequences (see Chapter 3).
(6) Repeat steps 1–5 for each patient.
(7) Using the results from all patients in the sample, calculate the mean value of the CT air kerma–length product for the complete examination.

8.7.3.4. Estimation of uncertainties

Table 8.14 lists the factors which contribute to the measurement uncertainty in the estimation of the CT air kerma–length product, $P_{KL,CT}$, from knowledge of the scan parameters and the measured value of ${}_nC_W$. The table gives examples of the uncertainty arising from each contribution with a coverage factor $k = 1$. The uncertainty in the measurement of ${}_nC_W$ is taken from Section 8.7.2.4. The relative expanded uncertainty ($k = 2$) of measurement for the determination of the CT air kerma–length product, $P_{KL,CT}$, is between about 9% and 15%, depending on the scenario selected.

The user should establish the actual measurement uncertainty using the principles described in Appendix I.

TABLE 8.14. FACTORS CONTRIBUTING TO THE MEASUREMENT UNCERTAINTY IN THE DETERMINATION OF THE CT AIR KERMA–LENGTH PRODUCT, $P_{KL,CT}$

Source of uncertainty	Uncertainty ($k = 1$) (%)		
	Scenario 1	Scenario 2	Scenario 3
Uncertainty in the measurement of ${}_nC_W$ (see Table 8.13)	7.2	4.8	4.2
Precision of tube loading indication	1.0	1.0	1.0
Relative combined standard uncertainty ($k = 1$)	7.3	4.9	4.3
Relative expanded uncertainty ($k = 2$)	**14.6**	**9.8**	**8.6**

8.7.3.5. Examples

High resolution CT for interstitial or obstructive lung disease

A patient was examined with the following scan parameters: axial scans of single slices ($n = 1$) of width 1 mm (T) with 10 mm couch increment (l) between slices. The tube voltage was 120 kV and the tube loading per axial rotation was 90 mA·s. The total scan length was 331 mm.

The measured value of the ${}_nC_W$ in the standard body phantom for these conditions was 0.166 mGy·mA^{-1}·s^{-1}. The CT air kerma indices, C_W, ${}_nC_{VOL}$ and C_{VOL}, are therefore:

$$C_W = 0.166 \text{ mGy·mA}^{-1}\text{·s}^{-1} \times 90 \text{ mA·s} = 14.94 \text{ mGy}$$

$$C_{VOL} = 14.94 \text{ mGy} \times (1 \times 1/10) = 1.494 \text{ mGy}$$

$${}_nC_{VOL} = 1.494 \text{ mGy}/90 \text{ mA·s} = 0.0166 \text{ mGy·mA}^{-1}\text{·s}^{-1}$$

For the scan length of 331 mm there were 34 axial rotations. The CT air kerma–length product, $P_{KL,CT}$, for the complete examination is therefore:

$$P_{KL,CT} = 0.0166 \text{ mGy·mA}^{-1}\text{·s}^{-1} \times (10/10) \text{ cm} \times 34 \times 90 \text{ mA·s} = 50.8 \text{ mGy·cm}$$

The divisor of 10 in the above calculation is required because the couch increment is specified in millimetres.

For scenario 3 (reference type dosimeter and all corrections applied), the relative expanded uncertainty ($k = 2$) in the measurement is 8.6 %. The CT air kerma–length product is written as:

$$P_{KL,CT} = (50.8 \pm 4.4) \text{ mGy·cm}$$

CT of the abdomen

A patient was examined with the following scan parameters: helical scan with the collimation adjusted so that 4 slices (N), each of nominal thickness 2.5 mm (T), were simultaneously exposed. Couch increment (l) per scanner rotation was 12.5 mm. The tube voltage was 120 kV and tube loading per scanner rotation was 200 mA·s. The total scan length was 213 mm and the tube loading for the whole helical scan sequence was 3400 mA·s.

The measured value of ${}_nC_W$ in the standard body phantom for these conditions was 0.080 mGy·mA^{-1}·s^{-1}. The CT air kerma indices, C_W, ${}_nC_{VOL}$ and C_{VOL}, are therefore:

$$C_W = 0.080 \text{ mGy·mA}^{-1}\text{·s}^{-1} \times 200 \text{ mA·s} = 16.0 \text{ mGy}$$

$$C_{VOL} = 16.0 \text{ mGy} \times (4 \times 2.5/12.5) = 12.8 \text{ mGy}$$

$${}_nC_{VOL} = 12.8 \text{ mGy}/200 \text{ mA·s} = 0.064 \text{ mGy·mA}^{-1}\text{·s}^{-1}$$

The CT air kerma–length product, $P_{KL,CT}$, is therefore:

$$P_{KL,CT} = 0.064 \text{ mGy·mA}^{-1}\text{·s}^{-1} \times (12.5/10) \text{ cm} \times 3400 \text{ mA·s} = 272 \text{ mGy·cm}$$

The divisor of 10 in the above calculation is required because the couch increment is specified in millimetres.

For scenario 3 (reference type detector and all corrections applied), the relative expanded uncertainty ($k = 2$) in the measurement is 8.6%. The CT air kerma–length product is written as:

$$P_{KL,CT} = (272 \pm 27) \text{ mGy·cm}$$

Patient:
CT

8.7.3.6. Worksheets

Estimation of $P_{KL,CT}$ for CT patient exposures

User: _____ Date: _____

Hospital or clinic name: _____

1. X ray equipment

CT scanner model: _____ Room no.:_____

Examination details	Patient weight (kg)	Scanner settings (tube voltage, beam filter, etc.)	Nominal slice thickness (T) (mm)	Number of slices (N)	Couch movement per rotation (l) (mm)	Total tube loading, P_{It}, for scan series (mA·s)	${}_nC_w$ (mGy·mA^{-1}·s^{-1})	Calculated value of C_{VOL} (mGy)	Calculated value of $P_{KL,CT}$ (mGy·cm)	Displayed $P_{KL,CT}$ (mGy·cm)

Note: C_{VOL} is calculated using $C_{VOL} = {}_nC_W P_{It}(NT/l)$ and $P_{KL,CT}$ is calculated using $P_{KL,CT} = C_{VOL} l$.

8.8. DENTAL RADIOGRAPHY

8.8.1. Choice of dosimetric quantities

In this Code of Practice, two types of dental radiography examination are considered: intraoral (bitewing projections) and panoramic examinations. For intraoral radiography, incident air kerma, K_i, is the measured quantity. This can be converted to the entrance surface air kerma by multiplication with a suitable backscatter factor. The air kerma–area product, P_{KA}, can be obtained by multiplying K_i with the beam area A, which is well defined by the spacer/director cone.

For panoramic examinations, the air kerma–area product, P_{KA}, has been adopted as the quantity for patient dose measurements. It is obtained from the measured air kerma–length product, P_{KL}, multiplied by the height of the X ray beam, H.

8.8.2. Measurements using phantoms

Phantom measurements in dental radiography are usually performed on anthropomorphic phantoms in order to derive organ doses [8.30–8.34] and thereby determine the effective dose and/or the energy imparted to the patient [8.35, 8.36].

Measurements in anthropomorphic phantoms are performed using TLDs positioned in drilled holes in the phantom. General principles for the use of TLDs should be followed [8.11]. Measurements with anthropomorphic phantoms are not described in this Code of Practice.

8.8.3. Patient dosimetry

In dental radiography, exposure settings are normally fixed and do not vary from patient to patient although different protocols may be used for the different types of teeth of adults and paediatric patients. Patient exposures are therefore surveyed using measurements free in air. Two methods of measurement of the incident air kerma are described in this Code of Practice. They make a use of a diagnostic dosimeter and TLDs. The TLD is a useful tool for postal dose audits when a large number of dental X ray units need to be evaluated.

For patient dose measurements in panoramic projections, the measured quantity is the air kerma–length product, P_{KL}. The P_{KL} is the integral of the free in air profile of the air kerma across the front side of the slit of the secondary collimator. In this Code of Practice, methods using a CT chamber or a stack of

TLDs for the measurement of P_{KL} are described. The air kerma–area product, P_{KA}, is obtained as $P_{KA} = P_{KL}H$, where H is the height of the X ray beam at the secondary collimator.

8.8.3.1. List of equipment

Bitewing projection

The equipment used for bitewing projection comprises:

(a) Calibrated diagnostic dosimeter;
(b) Detector support stand;
(c) Thermometer and barometer (for measurements with an ionization chamber);
(d) Calibrated TLDs (for measurements using TLDs).

Panoramic projection

The equipment used for panoramic projection comprises:

(a) Calibrated cylindrical ionization chamber[33] and electrometer.
(b) Chamber support.
(c) Thermometer and barometer.
(d) TLDs and a jig for mounting the dosimeters in front of the secondary collimator may be used as an alternative to the pencil ionization chamber. Dosimeter thickness and their diameter should be about 1 mm or less and 3 mm, respectively. Dosimeters should have had their individual sensitivity correction factors established or dosimeters within a selected sensitivity range should be chosen (see Appendix IX).
(e) Film and a ruler (for screen–film systems).

[33] A suitable detector is a CT ionization chamber calibrated for dental radiology beam qualities. Pencil shaped semiconductor detectors are being developed but as they have not yet found widespread use their application is not described in this Code of Practice.

8.8.3.2. Methods

Bitewing projection

Measurement of incident air kerma using a diagnostic dosimeter

(1) Position the detector of a calibrated diagnostic dosimeter at the centre of the exit of the spacer/director cone. Make sure that the sensitive volume of the detector is completely covered by the primary X ray beam and that there are no scattering objects nearby in the beam.
(2) Expose the detector three times using standard settings of tube voltage and tube loading and record the dosimeter readings, M_1, M_2 and M_3.
(3) Record the machine parameters (tube voltage and tube loading).
(4) Repeat steps 2 and 3 for all settings used in clinical practice.
(5) If a dosimeter with an ionization chamber is used, record the temperature and pressure.

Measurement of incident air kerma using TLDs

(1) Place a sachet containing three TLDs at the centre of the exit of the spacer/director cone (using an adhesive tape) and make sure that there are no scattering objects nearby in the beam. A further sachet of unexposed TLDs is retained for a background reading.
(2) Expose TLDs using standard settings of tube voltage and tube loading.
(3) Record the machine parameters (tube voltage and tube loading).
(4) Repeat steps 1–3 for all settings used in clinical practice.
(5) Arrange for the TLDs to be read. Record the readings, M_1, M_2 and M_3, from the exposed dosimeters in each exposed sachet and the readings, M_{01}, M_{02} and M_{03}, from the unexposed dosimeters.

Panoramic projection

The air kerma–length product is measured using either a calibrated cylindrical ionization chamber or an array of TLDs. The air kerma–length product is immediately obtained using an ionization chamber whereas use of TLDs requires several procedures before the result is registered. When neither a cylindrical ionization chamber nor TLD is available, direct film could be used as described by Napier [8.37]. The latter method requires calibration of the film in terms of air kerma and careful handling of film development. In this Code of Practice, no explicit advice on film dosimetry is given.

FIG. 8.9. Experimental arrangement for measurements of the air kerma–area product for a dental panoramic unit using a CT chamber.

Measurement of the air kerma–length product using a cylindrical ionization chamber and electrometer

(1) Position the cylindrical ionization chamber in front of the secondary collimator (slit), at the centre of the slit and perpendicular to its length direction (see Fig. 8.9).
(2) Make sure that the space between the chamber and the headrest is sufficient when the secondary collimator is rotated.
(3) Expose the chamber three times using standard settings of tube voltage, tube load and exposure cycle and record the dosimeter readings, M_1, M_2 and M_3.
(4) Repeat step 3 for other standard settings used in the clinic.
(5) Record the temperature and pressure.

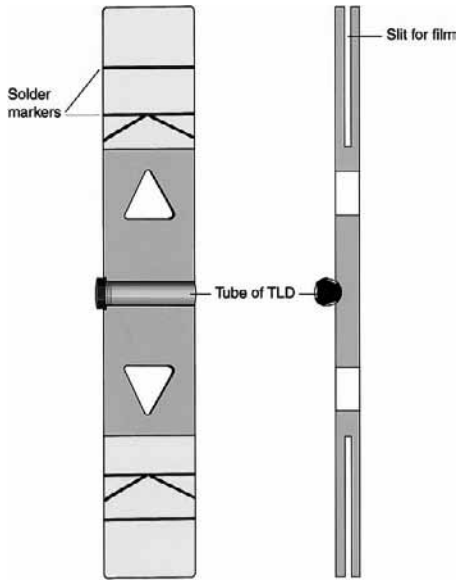

FIG. 8.10. Schematic of the jig used to measure the dose profile across the receiving slit of a panoramic X ray unit using TLDs. Positioning of the jig in front of the receiving slit is facilitated by the triangular windows in the jig, which are centred over the slit. Beam length is measured from the developed films using the image of the solder markers. The inner markers are separated by a distance of 120 mm and the outer markers by 150 mm. The jig is mounted with the diagonal solder markers pointing upwards, as shown, to indicate the orientation of the developed films (after Williams and Montgomery [8.38]).

Measurement of the air kerma–length product using an array of TLDs

(1) Select a set of TLDs with the sum of the thicknesses sufficient to cover a length of three times the slit width. Keep another three dosimeters for measurement of the background signal obtained without irradiation. Label each individual dosimeter so that its readings can be identified in calibrations and measurements.
(2) Pack the chips in a tube of PMMA.
(3) Position the tube with the TLDs in front of the secondary collimator with the tube axis perpendicular to the length of the slit and at its centre. A jig may be used to hold the tube, including insertions for intraoral film for measurement of the height, H, of the X ray beam (see Fig. 8.10).
(4) Expose TLDs using standard settings of tube voltage, tube loading and exposure cycle. Record the settings.

(5) Arrange for the dosimeters to be read. Record the readings, M_1, M_2,…, M_n, from the exposed dosimeters and the readings, M_{01}, M_{02} and M_{03}, from the unexposed dosimeters.
(6) Repeat measurements for other standard settings used in the clinic.

Measurement of the height of the X ray beam at the secondary collimator slit

(1) Position the film in front of the collimator slit, at about the same location as where the ionization chamber was located and expose the film to an optical density of less than 0.5.
(2) Develop the film and measure the height of the X ray beam on the film using a ruler or scanner. The height is defined as the length between points where the optical density is reduced to half its maximum value.

HVL measurement

(1) Set up the X ray equipment for the chosen examination. For panoramic examination, suppress the tube movement if possible.
(2) Select the tube voltage that would be used for a routine clinical examination.
(3) Centre the dosimeter in the X ray beam. The detector should be mounted free in air in such a way as to avoid the effect of scattered radiation.
(4) Collimate the beam to achieve conditions for narrow beam geometry. The beam should just cover the detector (see Appendix V). This may be difficult for the panoramic equipment unless the width of the beam can be increased. In this case, use a detector with a smaller volume and try to cover the maximum area of the detector.
(5) Select a tube loading so that the dosimeter readings with and without the attenuator are within the rated range of the instrument.
(6) Expose the detector three times and record measured values, M_1, M_2 and M_3.
(7) Repeat step 6 for a set of three Al attenuators and the same tube loading as that used for measurements without any attenuator. The thickness of attenuators is selected so that their value encloses the expected HVL of the beam.
(8) Expose the detector again without any attenuator (steps 5 and 6) and record the measured value.

8.8.3.3. Calculations

Bitewing projection

Measurement of incident air kerma using a diagnostic dosimeter

(1) Calculate the HVL of the beam by interpolating in measured signal for various attenuator thicknesses. The HVL value measured during a quality assurance programme can be also used.
(2) Calculate the mean value, $\bar{M}$, of the dosimeter readings.
(3) Calculate the incident air kerma, K_i, from the mean value of dosimeter readings, $\bar{M}$, using Eq. (8.44)[34]. In this equation, k_{TP} is the correction factor for temperature and pressure, N_{K,Q_0} is the dosimeter calibration coefficient and k_Q is the factor which corrects for differences in the response of the dosimeter at the calibration quality Q_0 and at the quality Q of the clinical X ray beam. This quality is indicated by the value of the HVL.

$$K_i = \bar{M} N_{K,Q_0} k_Q k_{TP} \tag{8.44}$$

The correction factor, k_{TP}, is unity for dosimeters with semiconductor detectors. For dosimeters with ionization chambers it is given by:

$$k_{TP} = \left(\frac{273.2 + T}{273.2 + T_0}\right)\left(\frac{P_0}{P}\right) \tag{8.45}$$

Measurement of incident air kerma using TLDs

(1) Calculate the mean value of the background reading, $\bar{M}_0$, from background dosimeter readings, M_{01}, M_{02} and M_{03} ($\bar{M}_0 = (M_{01} + M_{02} + M_{03})/3$).
(2) Calculate the average background corrected dosimeter reading, $\bar{M}$, from the exposed dosimeter readings, M_1, M_2 and M_3, as follows:

$$\bar{M} = \frac{\sum_{i=1}^{3} f_{s,i}\left(M_i - \bar{M}_0\right)}{3} \tag{8.46}$$

[34] It is assumed that the leakage signal of the dosimeter can be neglected and that no correction has been applied for this effect.

where factor $f_{s,i}$ is used to correct for the individual sensitivity of the i-th dosimeter (see Appendix IX)[35].

(3) Calculate the incident air kerma, K_i, from the average background corrected dosimeter reading, $\bar{M}$, using Eq. (8.47). In this equation, N_{K,Q_0} is the TLD calibration coefficient for the reference radiation quality used and k_Q is the factor which corrects for differences in the response of the dosimeter at the calibration quality Q_0 and at the quality Q of the clinical X ray beam. This quality is indicated by the value of the HVL. The factor k_f corrects for the effect of fading of the thermoluminescence signal between irradiation of dosimeters and their readout.

$$K_i = \bar{M} N_{K,Q_0} k_Q k_f \tag{8.47}$$

Panoramic projection

Measurement of the air kerma–length product using a cylindrical ionization chamber and electrometer

(1) Calculate the HVL of the beam by interpolating in measured signal for various attenuator thicknesses. The HVL value measured during a quality assurance programme can be also used.

(2) Calculate the mean value, $\bar{M}$, of the dosimeter readings.

(3) Calculate the air kerma–length product, P_{KL}, from the mean dosimeter reading, $\bar{M}$, using Eq. (8.48)[36]. In this equation, k_{TP} is the correction factor for temperature and pressure, N_{P_{KL},Q_0} is the calibration coefficient for the radiation quality Q_0 obtained at the temperature T_0 and pressure P_0 and k_Q is the correction factor for the radiation quality Q used during the measurement.

$$P_{KL} = \bar{M} N_{P_{KL},Q_0} k_Q k_{TP} \tag{8.48}$$

The correction factor, k_{TP}, is given by:

$$k_{TP} = \left(\frac{273.2 + T}{273.2 + T_0} \right) \left(\frac{P_0}{P} \right) \tag{8.49}$$

[35] Factor $f_{s,i}$ is constant for dosimeters grouped so that the sensitivity of dosimeters in the group lies within a selected range (see Appendix IX).

[36] It is assumed that the leakage signal of the dosimeter can be neglected and that no correction has been applied for this effect.

Measurement of the air kerma–length product using an array of TLDs

(1) Calculate the mean value of the background reading, $\bar{M}_0$, from background dosimeter readings, M_{01}, M_{02} and M_{03} ($\bar{M}_0 = (M_{01} + M_{02} + M_{03})/3$).

(2) For i-th dosimeter (i = 1, …, n), calculate the background corrected dosimeter reading, M_i, from the exposed dosimeter readings, M_i^c, and the mean background dosimeter reading, $\bar{M}_0$, using Eq. (8.49):

$$M_i^c = f_{s,i}\,(M_i - \bar{M}_0) \tag{8.50}$$

where factor $f_{s,i}$ is used to correct for the individual sensitivity of the i-th dosimeter (see Appendix IX)[37].

(3) For i-th dosimeter (i = 1, …, n), calculate the air kerma, K_i, from the background corrected dosimeter reading, M_i^c, using the TLD calibration coefficient, N_{K,Q_0}, for the reference radiation quality, Q_0, the correction factor, k_Q[38], for the radiation quality used and the correction factor, k_f, that corrects for the effect of fading of the thermoluminescence signal between irradiation of the dosimeter and its readout:

$$K_i = M_i^c N_{K,Q_0} k_Q k_f \tag{8.51}$$

(4) Calculate the air kerma–length product, P_{KL}, using Eq. (8.52). In this equation, Δd is the thickness of a single TLD:

$$P_{KL} = \sum_{i=1}^{n} K_i \Delta d \tag{8.52}$$

Establishment of the air kerma–area product

Calculate the air kerma–area product using Eq. (8.53). In this equation, P_{KL} is the air kerma–length product obtained from Eq. (8.52) and H is the height of the X ray beam at the secondary collimator slit:

$$P_{KA} = P_{KL} H \tag{8.53}$$

[37] Factor $f_{s,i}$ is a constant for dosimeters grouped so that the sensitivity of dosimeters in the group lies within a selected range (see Appendix IX).

[38] This correction factor depends on HVL of the beam that should be established using the diagnostic dosimeter.

TABLE 8.15. FACTORS THAT CONTRIBUTE TO THE MEASUREMENT OF UNCERTAINTY IN THE DETERMINATION OF INCIDENT AIR KERMA FOR A BITEWING PROJECTION USING THE DIAGNOSTIC DOSIMETER

Source of uncertainty	Uncertainty (k = 1) (%)		
	Scenario 1	Scenario 2	Scenario 3
Measurement scenario (see Table 8.2)	6.3	3.5	2.7
Precision of reading	1.0[a]	0.6[b]	0.6[b]
Uncertainty in measurement position[c]	1.2	1.2	1.2
Relative combined standard uncertainty (k = 1)	6.5	3.7	3.0
Relative expanded uncertainty (k = 2)	**13.0**	**7.4**	**6.0**

[a] One single reading taken.
[b] Standard deviation of the mean of three readings.
[c] Corresponding to ±2 mm in positioning of a detector at distance 200 mm from the X ray focus.

8.8.3.4. Estimation of uncertainties

The uncertainty in the measurement of the incident air kerma for bitewing projection can be estimated using values of relative uncertainties in three measurement scenarios as given in Table 8.2 and adding contributions arising from factors specific to the procedure employed. Table 8.15 gives examples of the uncertainty arising from each contribution and the value of the relative expanded uncertainty of the measurement, which is in the range 6–13%, depending on the scenario selected.

Similar evaluations can be done for measurements of the air kerma with a cylindrical ionization chamber during panoramic projections. The value of relative expanded uncertainty for measurements of the air kerma–length product is again 6–13%, depending on the measurement scenario selected. Assuming that the maximum difference of a measured slit height from the actual height is 2%, the relative standard uncertainty for this effect is 1.2%. The expanded uncertainty for the measurement of the air kerma–area product using a cylindrical chamber is 6.4–13.2%.

The uncertainty in measurements made with TLDs is discussed in Section 8.3. The relative expanded uncertainty (k = 2) of 10% was adopted for this Code of Practice. Additional contributions from positioning of the dosimeters and measured slit height have to be included in the overall

uncertainty. The value of the relative expanded uncertainty (k = 2) in measurements of the air kerma–area product using TLDs is about 10.5%.

The user should establish the actual measurement uncertainty using the principles described in Appendix I.

8.8.3.5. Examples

Measurement of incident air kerma for bitewing examination

An ionization chamber was used for measurement at the exit surface of a dental unit operated at 70 kV with a 60 mm diameter circular cone. Three repeated exposures gave a mean value of the dosimeter readings of $\bar{M}$ = 2.17.

The calibration coefficients, N_{K,Q_0} and k_Q, for the dosimeter were 1.052 mGy/reading and 0.98, respectively. The correction factor, k_{TP}, for temperature and pressure was 1.003. The measured air kerma is:

$$K_i = 2.17 \times 1.052 \text{ mGy} \times 0.98 \times 1.003 = 2.244 \text{ mGy}$$

For scenario 3 (reference type detector and all corrections applied), the relative expanded uncertainty (k = 2) of the measurement is 6%. The incident air kerma is written as:

$$K_i = (2.24 \pm 0.13) \text{ mGy}$$

Measurement of air kerma–area product for panoramic unit using a CT chamber

A panoramic dental unit is typically operated at 70 kV and 15 mA for a duration of 15 s. The air kerma–length product was measured at a secondary collimator using a calibrated CT chamber. The reading of the dosimeter was 0.923.

The calibration coefficients, N_{P_{KA},Q_0} and k_Q, for the dosimeter were 10.02 mGy·cm/reading and 0.98, respectively. The correction factor, k_{TP}, for temperature and pressure was 1.002. The measured air kerma–length product is:

$$P_{KL} = 0.923 \times 10.02 \text{ mGy·cm} \times 0.98 \times 1.002 = 9.082 \text{ mGy·cm}$$

The height of the X ray beam at the secondary collimator slit was measured as 12.5 cm. The air kerma–area product is thus calculated as:

$$P_{KA} = 9.082 \text{ mGy·cm} \times 12.5 \text{ cm} = 113.53 \text{ mGy·cm}^2$$

For scenario 3 (reference type detector and all corrections applied), the relative expanded uncertainty (k = 2) in the measurement is 6.4%. The air kerma–area product is written as:

$$P_{KA} = (114 \pm 7)\ \text{mGy·cm}^2$$

8.8.3.6. Worksheets

Determination of incident air kerma for bitewing projection using a diagnostic dosimeter

User: _____ Date: _____

Hospital or clinic name: _____

1. X ray equipment

X ray unit and model: _____ Room no.:_____

Type of cone used: _____ Focus to cone tip distance: _____ mm

2. Dosimeter

Dosimeter model: _____ Serial no.: _____ Date of calib.: _____

Calibration coefficient (N_{K,Q_0})[39]: _____ ☐ mGy/nC ☐ mGy/reading

Reference conditions: HVL (mm Al): _____ Field size: _____

Pressure P_0 (kPa): _____ Temperature T_0 (°C): _____

3. Exposure conditions

Tube voltage (kV): ____ Tube loading: ____ mA·s Focus to detector distance: ____ mm

4. Dosimeter reading and calculation of incident air kerma[40]

Dosimeter reading (M_1, M_2, M_3): _____ Mean dosimeter reading $\bar{M}$: _____

Pressure P (kPa):___ Temperature T (°C):___ $k_{TP} = \left(\frac{273.2 + T}{273.2 + T_0}\right)\left(\frac{P_0}{P}\right) =$ _____[41]

HVL (from 5 below) = _____ mm Al $k_Q =$ _____

Calculated value of incident air kerma $K_i = \bar{M} N_{K,Q_0} k_Q k_{TP} =$ _____ mGy

[39] This is the calibration coefficient for the whole dosimeter, including the detector and the measurement assembly. For systems with separate calibration coefficients for the detector and the measurement assembly, the overall calibration coefficient is calculated as a product of the two separate calibration coefficients.

[40] This is an example for one setting. The measurements should be repeated for all settings used in clinical practice.

[41] For dosimeters with a semiconductor detector, $k_{TP} = 1$.

5. Determination of HVL

Dosimeter readings should be obtained for filter thicknesses that bracket the HVL. The first and last readings, M_{01} and M_{02}, are made at zero filter thickness.

Filter thickness (mm Al)	Dosimeter reading (M) (mGy)	Average dosimeter reading, $\bar{M}$, at zero thickness
0.00		$(M_{01} + M_{02})/2$ =_____ mGy
0.00		Interpolated HVL: _____ mm Al

Determination of incident air kerma for bitewing projection using TLDs

User: _____ Date: _____

Hospital or clinic name: _____

1. X ray equipment

X ray unit and model: _____ Room no.:_____

Type of spacer cone used: _____ Focus to spacer cone tip distance: _____ mm

2. Dosimeter

Identification markings on TLD sachets (if any): _____

Calibration coefficient (N_{K,Q_0}) for TLDs: _____ mGy/reading

Reference beam quality (HVL)[42]: _____ mm Al k_Q for measurement set-up: _____

3. Exposure conditions

Tube voltage (kV): ____ Tube loading: ____ mA·s Focus to detector distance: ____ mm

4. Dosimeter readings and calculation of incident air kerma[43]

Date of exposure: Date of evaluation: Fading correction (k_f) = _____

Background dosimeter reading (M_{0i})	Dosimeter reading (M_i)	Average background corrected reading ($\bar{M}$)	Incident air kerma (K_i) (mGy)

$$\bar{M} = \frac{\sum_{i=1}^{3} f_{s,i}\left(M_i - \bar{M}_0\right)}{3} \quad \text{where } \bar{M}_0 = (M_{01} + M_{02} + M_{03})/3 \qquad K_i = \bar{M} N_{K,Q_0} k_Q k_f$$

[42] It is assumed that HVL was obtained from measurements made using a diagnostic dosimeter.

[43] This is an example for one setting. The measurements should be repeated for all settings used in clinical practice.

Determination of the air kerma–length product and the air kerma–area product for panoramic projection using a cylindrical diagnostic dosimeter

User: _____ Date: _____

Hospital or clinic name: _____

1. X ray equipment

X ray unit and model: _____ Room no.:_____

Slit width: _____ mm X ray beam height (H): _____ mm

2. Dosimeter

Dosimeter model: _____ Serial no.: _____ Date of calib.: _____

Calibration coefficient (N_{P_{KL},Q_0})[44]: _____ ☐ mGy·cm/nC ☐ mGy·cm/reading

Reference conditions: HVL (mm Al): _____ Field size: _____

Pressure P_0 (kPa): _____ Temperature T_0 (°C): _____

3. Exposure conditions

Starting tube voltage (kV): _____ Tube current: _____ mA Time _____ *s*

Ambient conditions: Pressure P (kPa): _____ Temperature T (°C): _____ k_{TP} = _____

4. Dosimeter reading and calculation of air kerma–length product and air kerma–area product[45]

Dosimeter reading (M_1, M_2, M_3): _____ Mean dosimeter reading $\bar{M}$: _____

Pressure P (kPa):___ Temperature T (°C):___ $k_{TP} = \left(\frac{273.2+T}{273.2+T_0}\right)\left(\frac{P_0}{P}\right)$ = _____[46]

HVL (from 5 below) = _____ mm Al k_Q = _____

Calculated value of air kerma–length product $P_{KL} = \bar{M} N_{P_{KL},Q_0} k_Q k_{TP}$ = _____ mGy·cm

Calculated value of air kerma–area product $P_{KA} = P_{KL} H/10$ = _____ mGy·cm^2

[44] This is the calibration coefficient for the whole dosimeter, including the detector and the measurement assembly. For systems with separate calibration coefficients for the detector and the measurement assembly, the overall calibration coefficient is calculated as a product of the two separate calibration coefficients.

[45] This is an example for one setting. The measurements should be repeated for all settings used in clinical practice.

[46] For dosimeters with a semiconductor detector, $k_{TP} = 1$.

5. Determination of HVL

Dosimeter readings should be obtained for filter thicknesses that bracket the HVL. The first and last readings, M_{01} and M_{02}, are made at zero filter thickness.

Filter thickness (mm Al)	Dosimeter reading (M) (mGy)	Average dosimeter reading, $\bar{M}$, at zero thickness
0.00		$(M_{01} + M_{02})/2$ =_____ mGy
0.00		Interpolated HVL: _____ mm Al

Determination of the air kerma–area product using an array of TLDs

User: _____ Date: _____

Hospital or clinic name: _____

1. X ray equipment

X ray unit and model: _____ Room no.:_____

Slit width: _____ mm Slit height (H): _____ mm

2. TLDs

Identification markings on TLD sachet (if any): _____

Calibration coefficient (N_{K,Q_0}) for TLDs: _____ mGy/reading

Reference beam quality (HVL): _____ mm Al k_Q for measurement set-up: _____

Dosimeter thickness (Δd): _____ cm

3. Exposure conditions

Tube voltage (kV): _____

4. Dosimeter readings and calculation of the air kerma–area product

Background readings (M_1, M_2, M_3): _____ _____ _____

Mean background $\bar{M}_0 = (M_{01} + M_{02} + M_{03})/3$ = _____ Fading correction (k_f) = _____

No.	dosimeter reading (M_i)	Corrected reading (M_i^c)	Individual sensitivity (k_{si})	Air kerma (K_i)	No.	dosimeter reading (M_i)	Corrected reading (M_i^c)	Individual sensitivity (k_{si})	Air kerma (K_i)

$M_i^c = f_{s,i}(M_i - \bar{M}_0)$ Air kerma, $K_i = M_i^c N_{K,Q_0} k_Q k_f$

Air kerma–length product, $P_{KL} = \sum_{i=1}^{n} K_i \Delta d$ = _____ mGy·cm

Air kerma–area product, $P_{KA} = P_{KL} H/10$ = _____ mGy·cm^2

REFERENCES

[8.1] INTERNATIONAL ELECTROTECHNICAL COMMISSION, Medical Electrical Equipment: Dosimeters with Ionization Chambers and/or Semi-conductor Detectors as Used in X-Ray Diagnostic Imaging, Rep. IEC-61674, IEC, Geneva (1997).

[8.2] EUROPEAN COMMISSION, European Protocol on Dosimetry in Mammography, Rep. EUR 16263, EC, Luxembourg (1996).

[8.3] EUROPEAN COMMISSION, European Guidelines on Quality Criteria for Diagnostic Radiographic Images in Paediatrics, Rep. EUR 16261, EC, Luxembourg (1996).

[8.4] EUROPEAN COMMISSION, European Guidelines for Quality Criteria for Computed Tomography, Rep. EUR 16262, EC, Luxembourg (2000).

[8.5] FOOD AND DRUG ADMINISTRATION, NEXT 2001—Protocol for the Survey of Adult Chest Radiography, Rep. FDA/CDRH (2002), http://www.crcpd.org/free_docs.asp

[8.6] FOOD AND DRUG ADMINISTRATION, NEXT 2002—Protocol for the Survey of A/P Abdomen and Lumbo-Sacral Spine Radiography, Rep. FDA/CDRH (2002), http://www.crcpd.org/free_docs.asp

[8.7] NATIONAL RADIOLOGICAL PROTECTION BOARD, National Protocol for Patient Dose Measurements in Diagnostic Radiology, Report of the Dosimetry Working Party of the Institute of Physical Sciences in Medicine, NRPB, Chilton (1992).

[8.8] STATENS STRÅLSKYDDINSTITUT, The Swedish Radiation Protection Authority's Regulations and General Advice on Diagnostic Standard Doses and Reference Levels Within Medical X-Ray Diagnostics, Rep. SSS FS 2002:2, Swedish Radiation Protection Authority, Stockholm (2002).

[8.9] HART, D., HILLIER, M.C., WALL, B.F., Doses to Patients from Medical X-ray Examinations in the UK—2000 Review, Rep. NRPB-W14, National Radiological Protection Board, Chilton (2002).

[8.10] NG, K.-H., et al., Doses to patients in routine X-ray examinations in Malaysia, Br. J. Radiol. **71** (1998) 654–660.

[8.11] ZOETELIEF, J., JULIUS, H.W., CHRISTENSEN, P., Recommendations for Patient Dosimetry in Diagnostic Radiology Using TLD, Rep. EUR 19604, European Commission, Luxembourg (2000).

[8.12] MARTIN, C.J., SUTTON, D.G., WORKMAN, A., SHAW, A.J., TEMPERTON, D., Protocol for measurement of patient entrance surface dose rates for fluoroscopic X-ray equipment, Br. J. Radiol. **71** (1998) 1283–1287.

[8.13] CARLSSON, C.A., Integral absorbed doses in roentgen diagnostic procedures I: The dosemeter, Acta Radiol. **3** (1965) 310–326.

[8.14] PÖYRY, P., KOMPPA, T., KOSUNEN, A., "X ray beam quality specification for kerma area product meters", Quality Assurance and New Techniques in Radiation Medicine (Proc. Conf. Vienna, 2006), IAEA, Vienna (in preparation).

[8.15] INTERNATIONAL ELECTROTECHNICAL COMMISSION, Dose Area Product Meters, Rep. IEC-60580, 2nd edn, IEC, Geneva (2000).
[8.16] GREWAL, R.K., MCLEAN, I.D., Comparative evaluation of cardiovascular imaging systems within a clinical environment, Australas. Phys. Eng. Sci. Med. **28** 3 (2005) 151–158.
[8.17] HARRISON, D., RICCIARDELLO, M., COLLINS, L., Evaluation of radiation dose and risk to the patient from coronary angiography, Aust. N.Z. J. Med. **28** (1998) 597–603.
[8.18] HEMDAL, B., et al., Average glandular dose in routine mammography screening using a Sectra Microdose mammography unit, Radiat. Prot. Dosim. **114** 1–3 (2005) 436–443.
[8.19] INSTITUTE OF PHYSICS AND ENGINEERING IN MEDICINE, The Commissioning and Routine Testing of Mammographic X-Ray Systems: A Technical Quality Control Protocol, IPEM Rep. 89, 3rd edn, IPEM, York (2005).
[8.20] DANCE, D.R., SKINNER, C.L., YOUNG, K.C., BECKETT, J.R., KOTRE, C.J., Additional factors for the estimation of mean glandular breast dose using the UK mammography dosimetry protocol, Phys. Med. Biol. **45** (2000) 3225–3240.
[8.21] YOUNG, K.C., Royal Surrey County Hospital, Guildford, personal communication, 2003.
[8.22] DANCE, D.R., et al., Computer simulation of X-ray mammography using high resolution voxel phantoms, Med. Phys. **30** (2003) 1456.
[8.23] FAULKNER, K., CRANLEY, K., An investigation into variations in the estimation of mean glandular dose in mammography, Radiat. Prot. Dosim. **57** (1995) 405–408.
[8.24] DANCE, D.R., Monte Carlo calculation of conversion factors for the estimation of mean glandular breast dose, Phys. Med. Biol. **35** (1990) 1211–1219.
[8.25] DANCE, D.R., et al., Breast dosimetry using a high-resolution voxel phantom, Radiat. Prot. Dosim. **114** (2005) 359–363.
[8.26] INSTITUTE OF PHYSICS AND ENGINEERING IN MEDICINE, Measurement of the Performance Characteristics of Diagnostic X-Ray Systems: Computed Tomography X-Ray Scanners, IPEM Rep. 32, Part 3, 2nd edn, IPEM, York (2003).
[8.27] FOOD AND DRUG ADMINISTRATION, Performance Standards for Diagnostic X-Ray Systems—Computed Tomography (CT) Equipment, Federal Register Rules and Regulations Ed 1/4/00 CFR Part 1020.33, FDA/CDRH, Rockville, MD (2000).
[8.28] INTERNATIONAL ELECTROTECHNICAL COMMISSION, Medical Electrical Equipment—Part 2-44: Particular Requirements for the Safety of X-Ray Equipment for Computed Tomography, Rep. IEC-60601-2-44, Consol. Ed. 2.1, IEC, Geneva (2002).
[8.29] INTERNATIONAL COMMISSION ON RADIATION UNITS AND MEASUREMENTS, Patient Dosimetry for X Rays Used in Medical Imaging, ICRU Rep. 74, ICRU, Bethesda, MD (2006).

[8.30] COHNEN, M., KEMPER, J., MOBES, O., PAWELZIK, J., MODDER, U., Radiation dose in dental radiology, Eur. Radiol. **12** (2002) 634–637.
[8.31] HAYAKAWA, Y., KOBAYASHI, N., KUROYANAGI, K., NISHIZAWA, K., Paediatric absorbed doses from rotational panoramic radiography, Dento-Maxillo-Facial Radiol. **30** (2001) 285–292.
[8.32] LECOMBER, A.R., YONEYAMA, Y., LOVELOCK, D.J., HOSOI, T., ADAMS, A.M., Comparison of patient dose from imaging protocols for dental implant planning using conventional radiography and computed tomography, Dento-Maxillo-Facial Radiol. **30** (2001) 255–259.
[8.33] LUDLOW, J.B., DAVIES-LUDLOW, L.E., BROOKS, S.L., Dosimetry of two extraoral direct digital imaging devices: New Tom cone beam CT and Orthophos Plus DS panoramic unit, Dento-Maxillo-Facial Radiol. **32** (2003) 229–234.
[8.34] SCHULZE, D., HEILAND, M., THURMANN, H., ADAM, G., Radiation exposure during midfacial imaging using 4- and 16-slice computed tomography, cone beam computed tomography systems and conventional radiography, Dento-Maxillo-Facial Radiol. **33** (2004) 83–86.
[8.35] STENSTRÖM, B., HENRIKSON, C.O., KARLSSON, L., SARBY, B., Energy imparted from intraoral radiography, Swed. Dent. J. **10** (1986) 125–136.
[8.36] STENSTRÖM, B., HENRIKSON, C.O., KARLSSON, L., SARBY, B., Effective dose equivalent from intraoral radiography, Swed. Dent. J. **11** (1987) 71–77.
[8.37] NAPIER, I.D., Reference doses for dental radiography, Br. Dent. J. **186** (1999) 392–396.
[8.38] WILLIAMS, J.R., MONTGOMERY, A., Measurement of dose in panoramic dental radiology, Br. J. Radiol. **73** (2000) 1002–1006.

Appendix I

UNCERTAINTY OF MEASUREMENT

I.1. INTRODUCTION

The aim of any measurement is to obtain the value of a parameter or quantity, generally termed the measurand. By nature, the difference between the measured value and the 'true' value of the measurand (the error of the measurement), is never zero. It may be small but it may also reach large values and it may be either negative or positive. The error is never precisely known and may have a number of components, each originating from a different source of error. A measure of how the measurement is 'wrong' is expressed by the uncertainty in the measurement. The terms 'error' and 'uncertainty' were used interchangeably in the past but the modern approach, initiated by the International Committee for Weights and Measures [I.1], distinguishes between these two concepts.

An error has both a numerical value and a sign. In contrast, the uncertainty associated with a measurement is a parameter that characterizes the dispersion of the values "that could reasonably be attributed to the measurand". This parameter is normally an estimated standard deviation. An uncertainty, therefore, has no known sign and is usually assumed to be symmetrical. It is a measure of our lack of exact knowledge; after all recognized 'systematic' effects have been eliminated by applying appropriate corrections. If errors were known exactly, the true value could be determined and there would be no problem left. In reality, errors are estimated in the best possible way and corrected for. Therefore, after application of all known corrections, errors do not have to be considered any longer (their expectation value being zero) and the only quantities of interest are uncertainties.

The detailed guide based on this approach was developed by the ISO [I.2]. In this Code of Practice, the ISO guide is followed and it should be consulted for details when needed.

I.2. ISO GUIDE

The ISO's Guide on the Expression of Uncertainty in Measurement [I.2] gives definitions and describes methods of evaluating and reporting uncertainties. It presents a consensus on how the uncertainty in measurement should be treated.

In the past, it was common practice to treat random and systematic contributions to measurement error independently and state them separately in the measurement report. According to the Guide, a description of uncertainties as either random or systematic may be misleading. It may suggest that their nature is random or systematic and not that this behaviour is a consequence of the measurement system. To avoid these problems, the Guide suggests using Type A and Type B uncertainties based on a method of the uncertainty evaluation. Statistical methods are used to evaluate Type A uncertainties as opposed to Type B uncertainties which are determined by other means.

1.2.1. Mean value of measurement

In a series of n measurements, with observed values, x_i, the best estimate of the quantity x is usually given by the arithmetic mean value:

$$\bar{x} = \frac{1}{n}\sum_{i=1}^{n} x_i \tag{I.1}$$

The scatter of the measured values around their mean, $\bar{x}$, can be characterized for an individual result, x_i, by the standard deviation:

$$s(x_i) = \sqrt{\frac{1}{n-1}\sum_{i=1}^{n}(x_i - \bar{x})^2} \tag{I.2}$$

and the quantity $s^2(x_i)$ is called the empirical variance of a single measurement, based on a sample of size n.

The parameter of major interest is often the standard deviation of the mean value, written as $s(\bar{x})$, for which the general relation applies:

$$s(\bar{x}) = \frac{1}{\sqrt{n}}\, s(x_i) \tag{I.3}$$

An alternative way to estimate $s(\bar{x})$ would be based on the outcome of several groups of measurements. If they are all of the same size, the formulas given above can still be used, provided that x_i is now taken as the mean of group i and $\bar{x}$ is the overall mean (or mean of the means) of the n groups. For groups of different size, statistical weightings would have to be used. This

second approach may often be preferable, but it usually requires a larger number of measurements. A discussion of how much the two results of $s(\bar{x})$ may differ from each other is beyond this elementary presentation.

1.2.2. Type A standard uncertainty

The standard uncertainty of type A, denoted by u_A, is described by the standard deviation of the mean value of statistically independent observations, i.e.:

$$u_A = s(\bar{x}) \tag{I.4}$$

This equation shows that a type A uncertainty of the measurement of a quantity can, in principle, always be reduced by increasing the number, n, of individual readings. It must be noted that the reliability of a type A uncertainty estimation according (Eq. (I.4)) must be considered for the low number of measurements ($n < 10$). Other means of estimations, such as the t-distribution may be considered. If several measurement techniques are available, preference should be given to the one which produces the least scatter of the results, i.e. that which has the smallest standard deviation $s(x_i)$, but in practice the possibilities for reduction are often limited. One example is the measurement of ionization currents that are of the same order as the leakage currents, which may also be variable. In order to arrive at an acceptable uncertainty of the result, it is then necessary to take many more readings than would normally be needed were the ionization currents much higher than the leakage currents.

The type A standard uncertainty is obtained by the usual statistical analysis of repeated measurements. It is normally found that the reproducibility of each model of dosimeter is essentially the same from one instrument to the next. Thus, if the type A standard uncertainty of an air kerma rate measurement is determined for one kind of dosimeter, the same value can generally be used for other instruments of that same model, used under the same conditions.

1.2.3. Type B standard uncertainty

There are many sources of measurement uncertainty that cannot be estimated by repeated measurements. These are termed type B uncertainties. These include not only unknown, although suspected, influences on the measurement process, but also little known effects of influence quantities (mechanical deformation of an ionization chamber owing to variations in

temperature and humidity), application of correction factors or physical data taken from literature, experience gained from previous measurements, manufacturer's specifications, etc. A calibration uncertainty, even if derived from type A components, becomes a type B uncertainty when using the calibrated instrument.

In the International Committee for Weights and Measures method of characterizing uncertainties, the type B uncertainties must be estimated so that they correspond to standard deviations; these are termed type B standard uncertainties. Some experimenters claim that they can estimate directly this type of uncertainty, while others prefer to use, as an intermediate step, some type of limit. It is often helpful to assume that these uncertainties have a probability distribution which corresponds to some easily recognizable shape.

If, for example, we are 'fairly certain' of that limit, L, it can be considered to correspond approximately to a 95% confidence limit, whereas, if we are 'quite certain', then it may be taken to correspond approximately to a 99% confidence limit. Thus, the type B standard uncertainty, $u_{B,}$ can be obtained from the equation:

$$u_B = \frac{L}{k} \tag{I.5}$$

where $k = 2$ if we are fairly certain, and $k = 3$ if we are quite certain of the estimated limits $\pm L$. These relations correspond to the properties of a Gaussian distribution and it is usually not worthwhile to apply divisors other than 2 or 3 because of the approximate nature of the estimation [I.3, I.4].

It is sometimes assumed (Fig. I.1) that type B uncertainties can be described by a rectangular probability density, i.e. that they have equal probability anywhere within the given maximum limits $-M$ and $+M$ and their probability is zero outside these limits. It can be shown that with this assumption the type B standard uncertainty u_B is given by:

$$u_B = \frac{M}{\sqrt{3}} \tag{I.6}$$

Alternatively, if the assumed distribution is triangular (with the same limits), the standard uncertainty can be expressed as:

$$u_B = \frac{M}{\sqrt{6}} \tag{I.7}$$

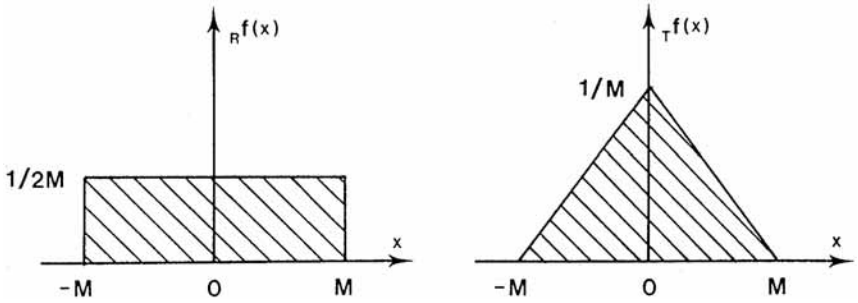

FIG. I.1. The two simple probability density functions, ${}_Rf(x)$ and ${}_Tf(x)$, with a rectangular or triangular shape, may be useful models for unknown distributions.

There are, thus, no rigid rules for estimating type B standard uncertainties and the best available knowledge and experience should be used to estimate them. In practice, very little is usually known about the uncertainty distribution and its choice is somewhat arbitrary. As most uncertainty sources have a Gaussian distribution, it is preferable to use this model when the exact shape of the distribution is unknown. However, this applies only to situations in which the uncertainty is not a dominant part of the overall uncertainty. In such a case, the uncertainty distribution should be reliably estimated [I.3]. The proper use of available information for evaluation of a type B uncertainty requires a good general knowledge and experience.

1.2.4. Combined uncertainties and expanded uncertainties

Type A and type B uncertainties are both estimated standard deviations, so they are combined using the statistical rules for combining variances (which are squares of standard deviations). If u_A and u_B are the type A and the type B standard uncertainties of a quantity, respectively, the combined standard uncertainty, u_C, of that quantity is:

$$u_C = \sqrt{\left(u_A^2 + u_B^2\right)} \tag{I.8}$$

This equation is strictly valid only provided that the uncertainty sources are not correlated. The correlation terms must be considered in the expression for u_C if some of the uncertainties are not completely independent. An example is a difference or ratio of two measurements made by the same instrument. Details of a correlation treatment can be found elsewhere [I.2].

The combined standard uncertainty still has the character of a standard deviation. If, in addition, it is believed to have a Gaussian probability density,

then the standard deviation corresponds to a confidence limit of about 66%. Therefore, it is often felt desirable to multiply the combined standard uncertainty by a suitable factor, termed the coverage factor, k, to yield an expanded uncertainty, U, where:

$$U = ku_C \tag{I.9}$$

Suitable values of the coverage factor are $k = 2$ or 3, corresponding to confidence limits of about 95% or 99%. The approximate nature of uncertainty estimates, in particular those for type B, makes it doubtful that more than one significant figure is ever justified in choosing the coverage factor. In any case, the numerical value taken for the coverage factor should be clearly indicated. The expanded uncertainty is also known as 'overall uncertainty'.

1.2.5. Propagation of uncertainties

The expression 'propagation of errors' was part of statistical terminology before it became customary to distinguish between errors and uncertainties, and it is still occasionally used. In order to be consistent with the present terminology, it is preferable to talk about the propagation of uncertainties. The following is a practical example.

The calibration factor determined by a given calibration laboratory is not only based on various measurements performed at the laboratory, but also on correction factors and physical constants, as well as on a beam calibration traceable to a secondary laboratory, and ultimately, to a primary laboratory. All these numerical values contain uncertainties and they combine to a given final uncertainty in the calibration factor. This situation can be represented in more general terms by considering a variable, y, which is a function of a number of variables, $x_1, x_2, x_3, \ldots$ This can be written in the form:

$$y = f(x_1, x_2, x_3, \ldots) \tag{I.10}$$

In many practical cases, the influence quantities x_1, x_2, $x_3, \ldots$ are independent of each other. Then $u(y)$ can be calculated by the simple formula:

$$u(y) \cong \left[\left(\frac{\partial f}{\partial x_1} \right)^2 u^2(x_1) + \left(\frac{\partial f}{\partial x_2} \right)^2 u^2(x_2) + \left(\frac{\partial f}{\partial x_3} \right)^2 u^2(x_3) + \ldots \right]^{\frac{1}{2}} \tag{I.11}$$

Two special cases should be mentioned in particular since they are of great practical importance and cover most of the usual situations.

If the functional dependence is linear, i.e. for sums (or differences), then:

$$y = c_1x_1 + c_2x_2 + c_3x_3 + \ldots \tag{I.12}$$

where:

$$c_i = \frac{\partial y}{\partial x_i} \tag{I.13}$$

and c_i is the sensitivity coefficient for the input quantity x_i.

Then, the uncertainty on y is:

$$u(y) = \left[c_1^2 u^2\left(x_1\right) + c_2^2 u^2\left(x_2\right) + c_3^2 u^2\left(x_3\right) + \ldots \right]^{\frac{1}{2}} \tag{I.14}$$

Thus, if independent variables are added (or subtracted), the variances also add. In other words, the uncertainty of the sum is obtained by adding in quadrature the 'weighted' uncertainties of the independent variables, where the weights are the squares of the coefficients c_1, c_2, ... (the term 'adding in quadrature' means taking the square root of the sum of the squares).

The other special case concerns a product (or ratio) of independent variables. The functional dependence then is:

$$y = x_1^{\alpha} x_2^{\beta} x_3^{\gamma} \tag{I.15}$$

where the exponents α, β, γ, ... are constants. In this case, from Eq. (I.15) the following expression for the relative uncertainty on y is obtained:

$$r(y) = [\alpha^2 r^2(x_1) + \beta^2 r^2(x_2) + \gamma^2 r^2(x_3) + \ldots]^{\frac{1}{2}} \tag{I.16}$$

where $r(x_1) = u(x_1)/|x_1|$ is the relative uncertainty of x_1, etc.

Thus, for a product (or ratio) of independent variables, the relative weighted variances add, where the weights are the squares of the exponents α, β, γ, etc. A very common case is that of a ratio, $y = x_1/x_2$, where the quantities x_1 and x_2 contain measurements and correction factors. From Eq. (I.16) the relative variance on y is equal to the quadratic sum of the relative uncertainties on x_1 and x_2.

The foregoing discussion applies to type A, type B and combined standard uncertainties, all of which are estimated to correspond to standard deviations. The rules for propagation of uncertainty also apply to expanded uncertainties, provided that everywhere the same coverage factor, k, has been used. The uncertainty on published data is generally in terms of an expanded

uncertainty, or some equivalent terminology. This must then be converted into a standard deviation before using it to calculate an uncertainty. If no coverage factor is stated, it may be assumed to have the value $k = 2$.

It is preferable to tabulate both type A and type B standard uncertainties separately. This makes any later changes easier to perform.

I.3. EXPRESSION OF UNCERTAINTIES AND RESULTS

1.3.1. Common rules for rounding of numbers

Numbers are rounded to remove unwarranted detail in the least significant digits. Rounding involves two steps, a rejection of non-significant digits and an adjustment of the last digit retained. The following general rules apply for rounding numbers:

- Numbers with the first non-significant figure <5 are rounded downwards (1.243 785 is rounded as 1.24);
- Numbers with the first non-significant figure >5 are rounded upwards (3.458 678 is rounded as 3.46);
- There are different ways of rounding figure 5. For the purpose of this Code of Practice, an upwards rounding of figure 5 is recommended (e.g. 2.745 006 is rounded up to 2.75).

1.3.2. Rounding of uncertainty and measured value

When expressing the result of measurement and its uncertainty, the rounding process is first applied on the value of uncertainty. Generally, the value of uncertainty is not a precise number and is not usually known to better than 10–30% [I.3, I.5]. It is recommended that rounding be done in such a way that the resulting rounding error is less than about 10% of the uncertainty. For the process of rounding, the rules described above are used. However, if the rounding brings the numerical value of uncertainty down by more than 5%, the uncertainty should be rounded upwards.

The expression of the uncertainty to more than one or two significant digits is not justified. For the purpose of this Code of Practice, it is recommended that the uncertainty be expressed to:

- One significant figure when the most significant digit (the first non-zero digit from the left) is 5 or more (0.005 46 is rounded to 0.005);
- Two significant figures (0.0235 is rounded to 0.024).

After establishing the value of the uncertainty, the measured value is rounded to match that of the uncertainty. It should be expressed with its least significant digit being the last digit affected by the uncertainty. The numerical value of the result of measurement should be rounded to the least significant figure in the value of the expanded uncertainty assigned to the result.

It is important to note that rounding is done only once, when the final results are expressed. Rounding during the process of manipulation with data may result in accumulation of rounding uncertainties. This effect may become significant.

REFERENCES

[I.1] COMITÉ INTERNATIONAL DES POIDS ET MESURES, Rapport du Groupe de Travail sur l'expression des incertitudes au Comité International des Poids et Mesures, (1981), http://www.bipm.org/utils/en/pdf/mra_2003.pdf

[I.2] INTERNATIONAL ORGANIZATION FOR STANDARDIZATION, Guide to the Expression of Uncertainty of Measurement, ISO, Geneva (1995).

[I.3] BENTLEY, R.E., Uncertainty in Measurement: The ISO Guide, Monograph 1, 6th edn, NML Technology Transfer Series, National Measurements Laboratory, CSIRO, Sydney (2003).

[I.4] INTERNATIONAL ATOMIC ENERGY AGENCY, Calibration of Radiation Protection Monitoring Instruments, Safety Reports Series No. 16, IAEA, Vienna (2000).

[I.5] DUTCH ACCREDITATION COUNCIL, Explanation on ISO/IEC 17025 Calibration Certificates, Rep. RvA-TK-2.10, RvA, Utrecht (2004).

Appendix II

EXAMPLE OF UNCERTAINTY ANALYSIS FOR THE CALIBRATION OF A USER DOSIMETER IN TERMS OF AIR KERMA FOR RADIATION QUALITY, Q_0

The overall aim of this appendix, which is based on Ref. [II.1], is to help in the analysis and reporting of measurement uncertainty. The essential uncertainty components are introduced in the context of a measurement procedure and a series of numerical values. A worked example is illustrated in Table II.1. Although efforts have been made to provide realistic values based on experience, the values given in this example are entirely illustrative and should not be used.

II.1. MEASUREMENT PROCEDURE

For this example, it is assumed that the SSDL reference chamber and measuring assembly were calibrated by the IAEA within the previous two years and that the SSDL checked its stability by monthly measurements. The stability check can be performed either by using a stability check source device or the monitor chamber or by comparison of a number of such chambers [II.2]. The second alternative should only be used if the monitor chamber has been shown to have a long term stability of its response to within 0.5%.

Employing the substitution method, the reference and user chambers were positioned one after the other with their reference points on the beam axis at a distance of 1000 mm (± 0.5 mm) from the focal spot. The chamber orientation (with the mark to the chamber) was checked visually. The ambient humidity was measured with a traceably calibrated humidity meter and found to lie within the range 30–80% relative humidity, over which the humidity correction is constant to within 0.1%. In all measurements with both the reference and user ionization chambers, the chamber was allowed to settle for at least an hour in the measurement room at or close to the point of measurement (temperature stabilization) and the chamber polarizing potential was verified. The leakage and radiation induced leakage currents were found to be less than 0.1% of the current during measurements. Ten readings were taken for each chamber and the calculated standard deviation was less than 0.1% for the reference instrument and less than 0.2% for the user instrument. The long term stability was 0.05% per month for both chambers.

Step 1: Measurements of the air kerma free in air at the desired location are made with the reference standard dosimeter. The reference instrument has a resolution of 0.1% or better.

Step 2: The calibration coefficient of the monitor chamber in terms of air kerma at the point of measurement is determined from the readings of the monitor in the measurements of step 1. The monitor chamber is read with a resolution of 0.01% or better.

Step 3: The reference standard chamber is replaced by the detector of the user instrument such that its reference point coincides with the point of measurement to within 0.5 mm.

Step 4: By comparing the readings of the monitor chamber with those of the user dosimeter, the calibration coefficient of the user dosimeter is obtained. The user dosimeter has a resolution of 0.1% or better.

Corrections to the readings of the monitor chamber and of the reference and user instruments are based on measurements with the same barometer and thermometer.

II.2. MODEL EQUATION

In the first step, the air kerma was determined with the reference instrument according to the equation:

$$K = N_{K,Q_0}^{\text{ref}} \left(M_{Q_0,\text{corr}}^{\text{ref}} - M_0^{\text{ref}} \right) \tag{II.1}$$

In the second step, the calibration coefficient of the monitor chamber in terms of air kerma at the point of measurement is obtained from:

$$n_{K,Q_0} = \frac{K}{\left(m_{Q_0,\text{corr}}^{\text{ref}} - m_0^{\text{ref}} \right)} \tag{II.2}$$

Finally, the calibration coefficient of the user dosimeter is obtained from:

$$N_{K,Q_0}^{\text{user}} = \frac{n_{K,Q_0} \left(m_{Q_0,\text{corr}}^{\text{user}} - m_0^{\text{user}} \right)}{\left(M_{Q_0,\text{corr}}^{\text{user}} - M_0^{\text{user}} \right)} \tag{II.3}$$

where:

N_{K,Q_0}^{ref} is the calibration coefficient for air kerma at radiation quality Q_0 of the reference instrument (determined at a PSDL or the IAEA).

$n_{K,Q0}$ is the air kerma calibration coefficient of the monitor chamber. It relates the reading of the monitor chamber to the air kerma for radiation quality Q_0 at the point of measurement.

K is the air kerma determined with the reference instrument.

$M_{Q_0,\text{corr}}^{\text{ref}}; M_{Q_0,\text{corr}}^{\text{user}}$ are the readings of the reference chamber or the user dosimeter during exposure to radiation of radiation quality Q_0 corrected to reference conditions (see Eq. (II.1)).

$m_{Q_0,\text{corr}}^{\text{ref}}; m_{Q_0,\text{corr}}^{\text{user}}$ are the readings of the monitor chamber during the measurements with the reference chamber or with the user dosimeter at radiation quality Q_0 corrected to reference conditions (see Eq. (II.4)).

$M_0^{\text{ref}}; M_0^{\text{user}}$ are the readings of the reference chamber or the user dosimeter in absence of the beam.

$m_0^{\text{ref}}; m_0^{\text{user}}$ are the readings of the monitor chamber during the measurements with the reference chamber or with the user dosimeter in absence of the beam.

The corrected reading, M_{corr}, is obtained from the value displayed on the readout device, M_{raw}, by:

$$M_{\text{corr}} = M_{\text{raw}} k_{\text{TP}} k_{\text{dist}} k_{\text{other}} \tag{II.4}$$

where M stands for $M_{Q_0}^{\text{ref}}$; $M_{Q_0}^{\text{user}}$; $m_{Q_0}^{\text{ref}}$; $m_{Q_0}^{\text{user}}$; and:

M_{raw} is the mean value of the readings taken after the instrument has settled.

k_{TP} is a factor to correct for departure of air density from reference conditions.

k_{dist} is a factor to correct for deviation of chamber position from the reference position.

k_{other} is a factor that includes all the corrections whose uncertainties are too small to consider individually in the uncertainty budget because they are estimated to be much less than 0.1%.

Factor k_{other} is given by:

$$k_{\text{other}} = k_Q k_{\text{lin}} k_{\text{dir}} k_{\text{emc}} k_{\text{fs}} k_{\text{lt}} k_{\text{ms}} \tag{II.5}$$

where:

k_Q is the correction factor for the energy dependence of the reference chamber. In the context of this example it takes into account differences in the response of the reference instrument in the beams in which it was calibrated and in which it is used in the SSDL.

k_{lin} is a factor to correct for non-linearity in the sensitivity of the measuring assembly.

k_{dir} is a factor to correct for changes in instrument sensitivity caused by any deviation from the reference conditions in respect to the direction of radiation incident upon the reference.

k_{emc} is a factor to correct for the effect of electromagnetic compatibility.

k_{fs} is a factor to correct for departure of field size/field homogeneity from the reference condition.

k_{lt} is the factor correcting for long time variations of response.

k_{ms} is the factor correcting the dependence of the instrument on supply voltage (mains supply or battery).

Combining Eqs (II.1–II.4) gives:

$$N_{K,Q_0}^{\text{user}} = \frac{N_{K,Q_0}^{\text{ref}} \left(M_{Q_0,\text{raw}}^{\text{ref}} k_{\text{TP}}^{\text{ref}} k_{\text{dist}}^{\text{ref}} k_{\text{other}}^{\text{ref}} - M_0^{\text{ref}} \right) \left(m_{Q_0,\text{raw}}^{\text{user}} k_{\text{TP,m}}^{\text{user}} - m_0^{\text{user}} \right)}{\left(M_{Q_0,\text{raw}}^{\text{user}} k_{\text{TP}}^{\text{user}} k_{\text{dist}}^{\text{user}} k_{\text{other}}^{\text{user}} - M_0^{\text{user}} \right) \left(m_{Q_0,\text{raw}}^{\text{ref}} k_{\text{TP,m}}^{\text{ref}} - m_0^{\text{ref}} \right)} \tag{II.6}$$

By replacing k_{TP} with the explicit expression in terms of temperature and pressure and by introducing $k_{\text{dist}} = (d/d_0)^2$, the following expression is obtained:

$$N_{K,Q_0}^{\text{user}} = \frac{N_{K,Q_0}^{\text{ref}} \left(M_{Q_0,\text{raw}}^{\text{ref}} \left(\frac{(273.2 + T^{\text{ref}})101.3}{293.2 P^{\text{ref}}} \right) \left(d^{\text{ref}}/d_0 \right)^2 k_{\text{other}}^{\text{ref}} - M_0^{\text{ref}} \right)}{\left(M_{Q_0,\text{raw}}^{\text{user}} \left(\frac{(273.2 + T^{\text{user}})101.3}{293.2 P^{\text{user}}} \right) \left(d^{\text{user}}/d_0 \right)^2 k_{\text{other}}^{\text{user}} - M_0^{\text{user}} \right)}$$

$$\times \frac{\left(m_{Q_0,\text{raw}}^{\text{user}} \left(\frac{(273.2 + T_{\text{m}}^{\text{user}})101.3}{293.2 P^{\text{user}}} \right) - m_0^{\text{user}} \right)}{\left(m_{Q_0,\text{raw}}^{\text{ref}} \left(\frac{(273.2 + T_{\text{m}}^{\text{ref}})101.3}{293.2 P^{\text{ref}}} \right) - m_0^{\text{ref}} \right)} \tag{II.7}$$

where T^{ref} and T^{user} are the temperatures (in °C) at the point of measurement during the measurement with the reference chamber and the user dosimeter, T_m^{ref} and T_m^{user} are the temperatures at the location of the monitor chamber during the measurement with the reference chamber and the user dosimeter and P^{ref} and P^{user} are the atmospheric pressures (in kPa) during the measurement with the reference chamber and the user dosimeter. It is assumed that there are no pressure gradients in the measuring room.

The overall uncertainty of N_{K,Q_0}^{user} is obtained from the component uncertainties that arise from the influence quantities on the right hand side of Eq. (II.7) in Table II.1. The values of the quantities used for calculating the calibration coefficient of the user instrument are also given in the table. The values provided in this table apply only to this example and must, of course, be replaced by values arising in practice. They are included here for the purpose of illustration only.

II.3. NOTES ON INFLUENCE QUANTITIES AND SOURCES OF UNCERTAINTY

Influence quantities are those quantities that are not the subject of the measurement but yet which influence the quantity being measured (e.g. air pressure, ageing and zero drift of dosimeter, beam quality, dose rate, field size).

In calibrating a dosimeter, as many influence quantities as practicable should be kept under control. However, many influence quantities cannot be controlled (e.g. air pressure, electromagnetic interference) and the corresponding effects should be corrected by applying appropriate factors. In either case an incomplete knowledge about the values of influence quantities and their impact on the final result must be considered in the uncertainty analysis.

For practical reasons a value (limit) should be chosen for the smallest uncertainty desired in the uncertainty analysis. All effects whose uncertainty is smaller than this (reasonably selected) limit would be ignored in the uncertainty budget. However, a check should be made to confirm whether their uncertainties are really below the limit. Nevertheless, mention should be made of such neglected effects in the uncertainty budget in order to document that they were not forgotten. In this Code of Practice the limit for relative standard uncertainties to be considered in the uncertainty budget is 0.1%.

II.3.1. Correction for change in source position

The uncertainty was estimated from a series of measurements of air kerma made on a previous occasion, in which the reference chamber was left in

TABLE II.1. MODEL EQUATION FOR THE SSDL CALIBRATION OF A USER DOSIMETER WITH A REFERENCE DOSIMETER USING A MONITOR CHAMBER

Model equation:
N=Nr*(M1*P0*k1q*k1nl*k1dir*k1emc*k1fh*k1ms*k1lts*d1^2*(273.2+T1)/(d0^2*(273.2+T0)*P1)-M0)
*(M2*k2emc*k2ms*(273.2+T2)*P0/((273.2+T0)*P2)-M3)/((M4*M4r*k4emc*k4ms*k1lts*P0*d4^2*(273.2+T4)/(d0^2*P2*(273.2+T0))–M5)
*(M6*k2emc*k2ms*(273.2+T6)*P0/((273.2+T0)*P1)–M7))

Quantity		Type	Distribution	Value	Unit	Degrees of freedom	Expanded uncertainty	Unit	Coverage factor
Symbol	Name								
N	Result: Calibration coefficient of the user instrument			9.23×10^{7}	Gy/C	62	1.5×10^{6}	Gy/C	2
d0	Reference distance	B	normal	1000	mm	50	0	mm	2
P0	Reference pressure	B	normal	101.3	kPa	50	0.0	kPa	2
T0	Reference temperature	B	normal	20	°C	50	0	°C	2
Nr	Calibration coefficient of the reference instrument	B	normal	1.021×10^{8}	Gy/C	50	0.9	%	2
M1	Raw reading of the reference instrument	A		1.6687×10^{-9}	C	9	0.1	%	1
M0	Leakage of the reference instrument	A		2.2365×10^{-12}	C	1	10	%	1
d1	Distance of the reference chamber	B	rectangular	1000	mm	infinite	0.25[a]	mm	1.73
T1	Temperature of the reference chamber	B	rectangular	23.4	°C	8	0.05[a]	°C	1.73
P1	Pressure during reference measurements	B	normal	102.3	kPa	8	0.1	kPa	1.73
k1q	Correction factor for the radiation quality for the reference chamber	B	normal	1		50	0.3	%	2

TABLE II.1. MODEL EQUATION FOR THE SSDL CALIBRATION OF A USER DOSIMETER WITH A REFERENCE DOSIMETER USING A MONITOR CHAMBER (cont.)

Model equation:
N=Nr*(M1*P0*k1q*k1nl*k1dir*k1emc*k1fh*k1ms*k1lts*d1^2*(273.2+T1)/(d0^2*(273.2+T0)*P1)-M0)
*(M2*k2emc*k2ms*(273.2+T2)*P0/((273.2+T0)*P2)-M3)/((M4*M4r*k4emc*k4ms*k1lts*P0*d4^2*(273.2+T4)/(d0^2*P2*(273.2+T0))–M5)
*(M6*k2emc*k2ms*(273.2+T6)*P0/((273.2+T0)*P1)–M7))

Quantity		Type	Distribution	Value	Unit	Degrees of freedom	Expanded uncertainty	Unit	Coverage factor
Symbol	Name								
k1nl	Correction factor for non-linearity of the reference instrument	B	normal	1		50	0.3	%	2
k1dir	Correction factor for the direction of radiation incidence on the reference chamber	B	normal	1		50	0.3	%	2
k1emc	Correction factor for the electromagnetic compatibility of the reference instrument	B	normal	1		50	0.3	%	2
k1fh	Correction factor for the field size/field homogeneity of the reference chamber	B	normal	1		50	0.5	%	2
k1lts	Correction factor for the long term stability of the reference instrument	B	normal	1		50	0.5	%	2
k1ms	Correction factor for voltage supply of the reference instrument	B	normal	1		50	0.3	%	2
M2	Raw reading of the monitor during measurements with the user instrument	A		3.7659×10^{-8}	C	9	0.2	%	1
M3	Leakage of the monitor during measurements with the user instrument	A		2.8159×10^{-11}	C	1	10	%	1

TABLE II.1. MODEL EQUATION FOR THE SSDL CALIBRATION OF A USER DOSIMETER WITH A REFERENCE DOSIMETER USING A MONITOR CHAMBER (cont.)

Model equation:
N=Nr*(M1*P0*k1q*k1nl*k1dir*k1emc*k1fh*k1ms*k1lts*d1^2*(273.2+T1)/(d0^2*(273.2+T0)*P1)-M0)
*(M2*k2emc*k2ms*(273.2+T2)*P0/((273.2+T0)*P2)-M3)/((M4*M4r*k4emc*k4ms*k1lts*P0*d4^2*(273.2+T4)/(d0^2*P2*(273.2+T0))–M5)
*(M6*k2emc*k2ms*(273.2+T6)*P0/((273.2+T0)*P1)–M7))

Quantity		Type	Distribution	Value	Unit	Degrees of freedom	Expanded uncertainty	Unit	Coverage factor
Symbol	Name								
T2	Temperature of monitor chamber during measurements with the user instrument	B	rectangular	23.4	°C	8	0.05*	°C	1.73
P2	Pressure during measurements with the user instrument	B	normal	102.3	kPa	8	0.1	kPa	1.73
k2ms	Correction factor for voltage supply of the user instrument	B	normal	1		50	0.2	%	2
k2emc	Correction factor for electromagnetic compatibility of the monitor chamber	B	normal	1		50	0.3	%	2
M4	Raw reading of the user instrument	A		1.8302×10^{-9}	C	9	0.2	%	1
M4r	Resolution of the readout of the user instrument	B	rectangular	1		infinite	0.05*	%	1.73
M5	Leakage of the user instrument	A		4.7132×10^{-11}	C	1	10	%	1
T4	Temperature of the monitor during reference measurements	B	rectangular	23.4	°C	8	0.05*	°C	1.73
d4	Distance of the detector of the user instrument	B	rectangular	1000	mm	infinite	0.25*	mm	1.73

TABLE II.1. MODEL EQUATION FOR THE SSDL CALIBRATION OF A USER DOSIMETER WITH A REFERENCE DOSIMETER USING A MONITOR CHAMBER (cont.)

Model equation:
N=Nr*(M1*P0*k1q*k1nl*k1dir*k1emc*k1fh*k1ms*k1lts*d1^2*(273.2+T1)/(d0^2*(273.2+T0)*P1)-M0)
*(M2*k2emc*k2ms*(273.2+T2)*P0/((273.2+T0)*P2)-M3)/((M4*M4r*k4emc*k4ms*k1lts*P0*d4^2*(273.2+T4)/(d0^2*P2*(273.2+T0))–M5)
*(M6*k2emc*k2ms*(273.2+T6)*P0/((273.2+T0)*P1)–M7))

Quantity		Type	Distribution	Value	Unit	Degrees of freedom	Expanded uncertainty	Unit	Coverage factor
Symbol	Name								
k4emc	Correction factor for electromagnetic compatibility of the user instrument	B	normal	1		50	0.3	%	2
k4ms	Correction factor for voltage supply of the user instrument	B	normal	1		50	0.3	%	2
M6	Raw reading of the monitor during reference measurement	A		3.8959×10^{-8}	C	9	0.2	%	1
M7	Leakage of the monitor during reference measurement	A		4.8412×10^{-11}	C	1	10	%	1
T6	Temperature of the monitor chamber during reference measurement	B	rectangular	23.4	°C	8	0.05*	°C	1.73

* Half-width between the limits.

place and the source repeatedly exposed. The standard deviation of the results was calculated and the uncertainty obtained was dominated by the type A contribution from variations in source position. The uncertainty has an effective number of degrees of freedom of about 20. In the present context, this influence quantity makes a contribution to the overall uncertainty of type B: the source is exposed once for the reference measurement and once for the user measurement. Therefore, this uncertainty enters twice and the sensitivity of the overall calibration to the change in source position has a sensitivity coefficient equal to $\sqrt{2}$.

II.3.2. Calibration coefficient of the reference instrument

The calibration coefficient of the reference instrument concerns several aspects:

(a) The uncertainty stated on the calibration certificate from the IAEA is 1.0% with a coverage factor, k, of 2, corresponding to a confidence level of approximately 95%. The effective number of degrees of freedom (50) corresponds to a 'good' estimate of this uncertainty.
(b) Measurements with the stability check source device over an extended period show that the relative change of the calibration coefficient is less than ±0.25% ($k = 1$). It is assumed that this is a 'rough' estimate and so the effective number of degrees of freedom has been set to 8.

II.3.3. Raw reading of the reference instrument

Ten readings were taken and the standard deviation obtained. This standard deviation is used in the table. The number of effective degrees of freedom in this approach is one less than the number of readings.[1]

II.3.4. Raw reading of the instrument to be calibrated

The following procedure was undertaken for the instrument to be calibrated:

[1] Another approach is possible in laboratories that have extensive records of measurements with reference instruments. It is possible to extract from these data a mean value for this standard deviation, i.e. an average over many measurements equivalent to the one made here, and this would mean that the effective number of degrees of freedom would be much larger.

(a) Ten readings were taken and the standard deviation obtained. This standard deviation is used in the table. The number of effective degrees of freedom in this approach is one less than the number of readings.
(b) The resolution of the user instrument is taken into account (type B).

II.3.5. Readings in absence of the beam, leakage current

It is assumed that one measurement of the signal in absence of the beam is made prior to the measurement and another one after the ten measurements have been carried out. This leads to an effective degree of freedom of one. Given the small size of the correction itself and even more so for the uncertainty this seems justified. If the leakage current in one measuring channel is larger it may become necessary to perform a greater number of measurements of the leakage current.

II.3.6. Temperature and pressure measurements

A distinction needs to be made for two cases: (i) both the reference chamber and the detector of the user instrument are unsealed ionization chambers and (ii) the user dosimeter has a detector of a type different from an unsealed ionization chamber.

In case (i), the same thermometer is used for the temperature measurements for the reference and user ionization measurements, and so its calibration cancels in the ratio of temperatures, provided that these temperatures are not greatly different. The temperature sensed, i.e. that of the mercury in the glass bulb of the thermometer which is placed close to the point of measurement, will not be significantly different from that of the air in the chamber cavity and the effect of this difference on the overall uncertainty is neglected. Typically, the sensed temperature will not change over the course of readings taken with either reference or user instrument and so a type A uncertainty does not arise. However, this means that the type B uncertainty arising from the thermometer resolution must be included for both measurements. It is assumed that there is no correlation between the two. Case (i) has been selected in Table II.1.

For case (ii), it is assumed that a user instrument with a semiconductor detector is calibrated. For such a device it is reasonable to assume that the leakage current may depend on temperature but not the response, i.e. the signal per unit dose does not depend on temperature. It is therefore necessary to correct the readings of the reference chamber to normal temperature. In this case both the type A and type B uncertainties associated with the temperature in the measurement with the reference chamber need to be taken into account.

On the other hand, the temperature of the user instrument is no longer contained in the model equation. The correction for the density of air for the monitor chamber is the same in cases (i) and (ii). It should be noted that temperature differences at the position of the monitor and at the point of measurement are quite likely because of the heat dissipation of the X ray tube.

A similar distinction between cases (i) and (ii) needs to be made for pressure measurements and the uncertainties associated with them. In contrast to the temperature, it may be assumed that there are no pressure gradients in the room of measurement. However, there may be variation of pressure between the measurements with reference chamber and user instrument.

II.3.7. Chamber positioning

This calibration is based on a measurement of air kerma with the reference instrument at the chamber's reference point. The chamber should be placed so that its reference point is close to the required point of measurement. In the second step, the detector of the user instrument must be placed so that its reference point is in the same position as that at which the dose rate has been measured. In this approach, the contribution to the overall uncertainty arises only from the deviation in the position of the detector of the user instrument from that of the reference chamber. The deviation of the reference chamber position from the reference depth has a negligible effect on the overall result.

The uncertainty in distance is expressed in millimetres. A change in distance affects the reading approximately by the inverse square law; therefore the sensitivity coefficient is two.

II.3.8. Other influence quantities

The correction factors $k_{\text{other}}^{\text{ref}}$ and $k_{\text{other}}^{\text{user}}$ in the model equation (Eq. (II.7)) subsume all those correction factors in Eq. (II.4) whose value is not known. Given this lack of knowledge, the value is assumed to be unity. The uncertainty of this assumption is, however, taken into account in the model equation.

The factor k_Q enters only for the reference chamber. By definition k_Q is unity for the user instrument and for the monitor chamber.

The factor k_{lin} includes both recombination losses and the non-linearity of the readout device. It enters only for the reference chamber. For the monitor chamber it cancels as the reference and the user instrument measurement should ideally be performed at constant dose rate. For the user instrument it does not enter. The user instrument's calibration coefficient refers to the dose rate at which it has been calibrated.

For the reasons noted above, the uncertainties associated with k_{dir}, k_{lt}, k_{fh} enter only for the reference chamber.

The corrections k_{emc} and k_{ms} apply to the measurements with the reference and the user instruments and to those with the monitor chamber as the impact of these influence quantities occurs in each of these measurements.

II.4. CALIBRATION COEFFICIENT OF THE USER INSTRUMENT

The calibration coefficient of the user instrument is obtained by evaluating the model equation (Eq. (II.7)) directly. For the values given in this example (Table II.1) the result is $N_{K,Q}^{user} = 9.228 \times 10^7$ Gy/C.

The calculation of the uncertainty proceeds in stages. For each source of uncertainty, the standard uncertainty, u_i, and sensitivity coefficient, c_i, are obtained and their product gives the corresponding uncertainty component ($c_i u_i$). These components are summed in quadrature to give the combined standard uncertainty of the result. The effective number of degrees of freedom for this uncertainty is calculated according to the Welch-Satterthwaite formula [II.3] from the uncertainty components and effective degrees of freedom for each influence quantity. The final values are rounded appropriately in the result, but not at any intermediate stages of the analysis.

The combined standard uncertainty ($u_c(N_{K,Q}^{user}) = 0.813\%$) has been multiplied by a coverage factor $k = 2$ to obtain an expanded uncertainty $U = 1.63\%$. This expanded uncertainty has a confidence probability of 95%, which has been calculated from the effective number of degrees of freedom $\upsilon_{eff} = 62$.

REFERENCES

[II.1] INTERNATIONAL ATOMIC ENERGY AGENCY, Implementation of the International Code of Practice on Dosimetry in Radiotherapy (TRS 398): Review of Testing Results, IAEA-TECDOC-1455, IAEA, Vienna (2005).

[II.2] ROZENFELD, M., JETTE, D., Quality assurance of radiation dosage: Usefulness of redundancy, Radiol. **150** (1984) 241–244.

[II.3] BROWNLEE, K.A., Statistical Theory and Methodology in Science and Engineering, John Wiley, New York (1960).

Appendix III

EXAMPLE OF DATA SHEET FOR CALIBRATIONS AT AN SSDL

Table III.1 gives an example of a data sheet for entering the results of the charge, temperature and pressure measurements performed in the calibration of a user instrument at an SSDL.

It is assumed that a measurement of the background current is performed in absence of radiation prior to and after taking a set of five measurements. Pressure measurements are performed both in the reference measurements and in the user instrument measurements at one single location. The results are entered in column 2. The reading of the monitor as taken from the electrometer is given in column 3. Using the pressure and the temperature at the monitor chamber, T_{mon}, the reading corrected to normal air density is given in column 5. Use has been made of Eqs (III.1) and (III.4). Readings of the reference instrument and the user instrument, respectively, are shown in column 6 in the upper and lower parts of the table.

Column 8 contains readings of the reference instrument and the user instrument corrected to normal air density using Eqs (III.2) and (III.5). Temperatures T_{ref} and T_u are given in column 7. In the upper and lower part of column 9, the calibration coefficients of the monitor chamber (in terms of air kerma at the point of measurement) and the user instrument, according to Eqs (III.3) and (III.6), are given together with the respective type A uncertainties of each calibration step. It should be noted that the total type A uncertainty of the calibration coefficient of the user instrument is given by combining the two uncertainties in quadrature.

TABLE III.1. DATA SHEET FOR CALIBRATION OF THE USER DOSIMETER

Reference instrument measurement								
Measurement no.	Pressure (P)	Monitor reading (m)	Monitor temperature (T_{mon})	Corrected monitor reading (m_c)[a]	Reference instrument reading (M_{ref})	Reference temperature (T_{ref})	Corrected reference instrument reading ($M_{c,ref}$)[b]	Monitor calibration coefficient (N_{mon})[c]
	(kPa)	(C)	(°C)	(C)	(C)	(°C)	(C)	(Gy/C)
Background (0)	100.5	2.2197E-13	21.3		2.3175E-13	21.1		
1	100.5	3.2310E-11	21.3	3.2426E-11	8.4011E-10	21.0	8.4933E-10	9.3431E+08
2	100.5	3.2547E-11	21.2	3.2651E-11	8.4398E-10	21.0	8.5316E-10	9.3204E+08
3	100.5	3.2419E-11	21.2	3.2522E-11	8.4189E-10	21.0	8.5105E-10	9.3343E+08
4	100.5	3.1979E-11	21.2	3.2074E-11	8.3918E-10	20.9	8.4794E-10	9.4302E+08
5	100.5	3.2203E-11	21.1	3.2289E-11	8.3956E-10	20.9	8.4832E-10	9.3714E+08
Background (6)	100.5	3.2980E-13	21.1		1.3289E-13	20.9		
								N_{mon} = 9.3599E+08
								$u(N_{mon})$ = 0.46%
User instrument measurement								
No.	Pressure (P)	Monitor reading (m)	Monitor temperature (T_{mon})	Corrected monitor reading (m_c)[d]	User instrument reading (M_u)	User temperature (T_u)	Corrected user instrument reading ($M_{c,u}$)[e]	User instrument calibration coefficient (N_u)[f]
	(kPa)	(C)	(°C)	(C)	(C)	(°C)	(C)	(Gy/C)
Background (7)	100.5	2.8192E-13	21.1		8.8583E-13	20.9		
8	100.5	3.1982E-11	21.0	3.1979E-11	1.5982E-09	20.9	1.6142E-09	1.8543E+07
9	100.5	3.2471E-11	21.0	3.2470E-11	1.6192E-09	20.8	1.6347E-09	1.8592E+07

TABLE III.1. DATA SHEET FOR CALIBRATION OF THE USER DOSIMETER (cont.)

10	100.5	3.2291E-11	21.0	3.2288E-11	1.6129E-09	20.8	1.6283E-09	1.8560E+07
11	100.5	3.2019E-11	20.9	3.2003E-11	1.6017E-09	20.8	1.6170E-09	1.8525E+07
12	100.5	3.2308E-11	20.9	3.2295E-11	1.6136E-09	20.8	1.6290E-09	1.8556E+07
Background (13)	100.5	4.1920E-13	20.9		1.2197E-12	20.7		
								N_u = 1.8555E+07
								u (N_u) = 0.48 %

[a] $$m_c(i) = \left[m(i) - 0.5(m(0) + m(6))\right] \frac{(273.2 + T_{mon}(i))101.3}{293.2P(i)},\ i = 1,\ 5 \quad \text{(III.1)}$$

[b] $$M_{c,ref}(i) = \left[M_{ref}(i) - 0.5(M_{ref}(0) + M_{ref}(6))\right] \frac{\left(273.2 + T_{ref}(i)\right)101.3}{293.2P(i)},\ i = 1,\ 5 \quad \text{(III.2)}$$

[c] $$N_{mon} = \frac{N_{ref}}{5} \sum_{i=1}^{5} \frac{M_{c,ref}(i)}{m_c(i)},\ N_{ref} = 3.5670\text{E+07} \quad \text{(III.3)}$$

[d] $$m_c(i) = \left[m(i) - 0.5(m(7) + m(13))\right] \frac{\left(273.2 + T_{mon}(i)\right)101.3}{293.2P(i)},\ i = 8,\ 12 \quad \text{(III.4)}$$

[e] $$M_{c,u}(i) = \left[M_u(i) - 0.5(M_u(7) + M_u(13))\right] \frac{\left(273.2 + T_u(i)\right)101.3}{293.2P(i)},\ i = 8,\ 12 \quad \text{(III.5)}$$

[f] $$N_u = \frac{N_{mon}}{5} \sum_{i=8}^{12} \frac{m_c(i)}{M_{c,u}(i)} \quad \text{(III.6)}$$

Appendix IV

DETERMINATION OF THE PRACTICAL PEAK VOLTAGE

IV.1. RATIONALE

The measurement of the X ray tube and generator voltage is thought to be consistent. However, there are many definitions of this voltage that are used. The quantities defined in Section IV.2 are either ambiguous or have no relation to the properties of the radiological image. Thus, a new well-defined quantity, the practical peak voltage, has been proposed [IV.1].

The problem with the quantities used hitherto arises because the voltage supplied by the generator is usually not a single value. When the generator does supply a constant voltage the situation is unambiguously described by specifying this (constant) value of the potential difference between the anode and the cathode. However, in the presence of ripple, some form of averaging over the X ray tube voltages occurring during the measurement period needs to be performed in order to be able to specify the (time dependent) X ray tube voltage by just one single value. The quantities defined in Section IV.2 are examples of how the averaging is often done in practice. Only the first of the examples is well defined in terms of physics. It does, however, only weakly correlate with properties of a radiological image. It becomes obvious that the average peak voltage requires further specifications (see Fig. IV.1 (c) and (d)). The third example is related to the properties of the radiological image, although at the cost of introducing an undefined factor which is meant to establish this very relation.

The situation that exists for these quantities is similar to that existing when ionizing radiation was first being measured. In the early years, the method of assessing the 'amount' of radiation was by means skin erythema or erythema dose, which was a 'measurement' of the reddening of the skin caused by ionizing radiation. Erythema dose was not a well-defined physical quantity by which ionizing radiation could be measured. It is not a physical quantity and was based also upon biological response. It was realized that a physical quantity was necessary and a large step forward was made when, in 1928, the 2nd International Congress of Radiology adopted the roentgen, the quantity based upon ionization of air, as the unit of exposure. Similarly, the voltage for X ray units being measured in terms of practical peak voltage is expected to be a step forward.

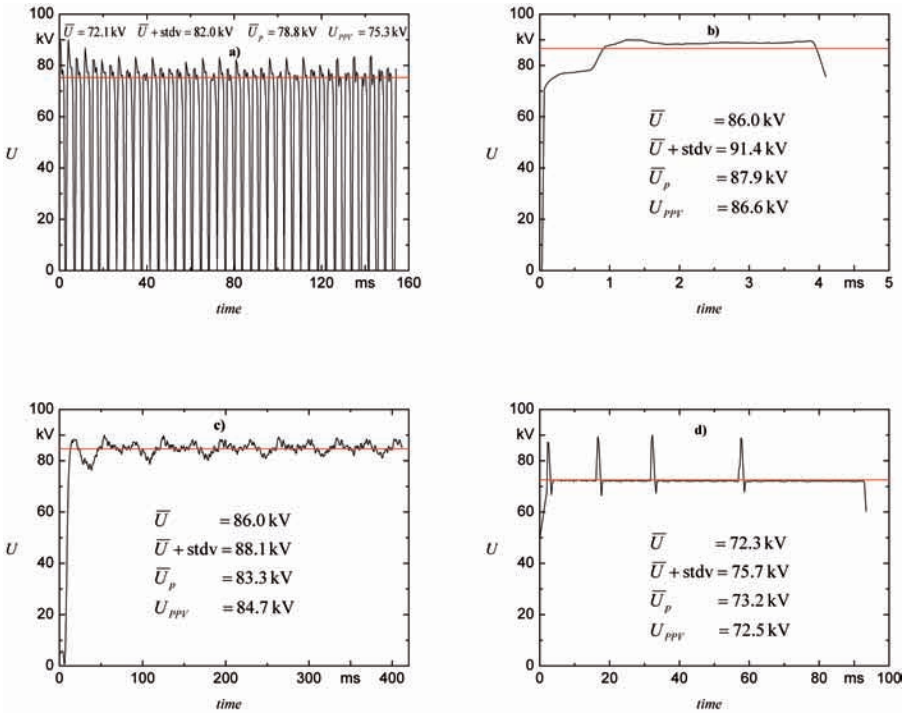

FIG. IV.1. Examples of different waveforms each normalized to 90 kV absolute peak voltage. Factors $\bar{U}$, $\bar{U}_P$ and U_{PPV} are the average, the average peak and the practical peak voltages (marked as red lines), 'stdv' denotes the standard deviation. In all examples, $\bar{U}_P$ is calculated taking into account each local maximum value. Examples (c) and (d) highlight the importance of the definition of a 'peak'.

IV.2. OLD QUANTITIES

The major problem that gave rise to the practical peak voltage is that there is no agreed upon quantity to measure what is designated peak voltage. Voltage is measurable, but when the peak is proclaimed the amount of ripple affects the measurement (see also Fig. IV.1), including the selection of the end point of the measurement. There are many definitions that involve characterization of the X ray tube voltage, the most common being:

(a) Absolute peak voltage, which is the maximum value of the voltage during the exposure;
(b) Average peak voltage, which is the average of all peak values occurring during the exposure;

(c) Effective peak voltage, which is the effective voltage that would give the same image contrast as a constant potential X ray system multiplied by a factor related to the typical shapes of voltage waveforms.

Together with others, some of these quantities are illustrated schematically in Fig. IV.I. For a constant potential, where there is no ripple, all of these quantities are the same. For a uniform ripple, each of these quantities would be different, but the difference becomes more drastic when there is non-uniform ripple [IV.2].

IV.3. PRACTICAL PEAK VOLTAGE

A measurable standard quantity for the X ray tube/generator voltage should have the following characteristics:

(a) Capability to define a reproducible physical method for voltage measurement, including ripple of an X ray generator from the output of the X ray tube;
(b) Ease of measurement technique;
(c) Clinical relevancy of the definition (with regard to image contrast);
(d) Relevancy to technical aspects of the X ray machine and its performance.

The practical peak voltage was designed to conform to the above four characteristics. It was derived by defining that constant voltage which provides in a radiograph the same low level contrast of a given object as that obtained with any arbitrarily selected waveform. The proper definition is entirely electrical. The practical peak voltage is unambiguous and traceable to national electrical standards and is applicable regardless of the nature of ripple. The details of this quantity and its method of determination are given in Section IV.4. In order that there is uniformity in the measurement quantity, it is highly recommended that all measurements be done in terms of practical peak voltage, expressed in kilovolts.

IV.4. DETERMINATION OF THE PRACTICAL PEAK VOLTAGE

For a given probability distribution, $p(U_i)$, for the occurrence of a value of the voltage in the interval $(U_i - \Delta U/2, U_i + \Delta U/2)$, the practical peak voltage, $\hat{U}$, is calculated by:

$$\hat{U} = \frac{\sum_{i=1}^{n} p(U_i) w(U_i) U_i}{\sum_{i=1}^{n} p(U_i) w(U_i)} \tag{IV.1}$$

When U_i is in kilovolts, the weighting function $w(U_i)$ is given by the following formulas:

in the voltage region of $U_i < 20$ kV by:

$$w(U_i) = 0 \tag{IV.2}$$

in the voltage region of 20 kV ≤ U_i < 36 kV by:

$$w(U_i) = \exp\left(aU_i^2 + bU_i + c\right) \tag{IV.3}$$

and in the voltage region of 36 kV ≤ U_i ≤ 150 kV by:

$$w\left(U_i\right) = dU_i^4 + eU_i^3 + fU_i^2 + gU_i + h \tag{IV.4}$$

with constants:

$a = -8.646855 \times 10^{-3}$ $b = +8.170361 \times 10^{-1}$ $c = -2.327793 \times 10^{+1}$
$d = +4.310644 \times 10^{-10}$ $e = -1.662009 \times 10^{-7}$ $f = +2.308190 \times 10^{-5}$
$g = +1.030820 \times 10^{-5}$ $h = -1.747153 \times 10^{-2}$

For the definition, the formula for $\hat{U}$ is generalized by using integral expressions instead of the summations, which, however, does not affect the values for the weighting function.

The above formula and the given values for the parameters *a* to *h* are valid for the application ranges conventional diagnostic, CT, dental and fluoroscopic.

For mammography in the voltage region of $U_i \leq 50$ kV, the formula and the values for the parameters *k* to *o* as given below can be used:

$$w\left(U_i\right) = \exp\left(kU_i^4 + lU_i^3 + mU_i^2 + nU_i + o\right) \tag{IV.5}$$

where:

$k = -2.142352 \times 10^{-6}$ $l = +2.566291 \times 10^{-4}$ $m = -1.968138 \times 10^{-2}$
$n = +8.506836 \times 10^{-1}$ $o = -1.514362 \times 10^{+1}$

NOTE: This formula is only defined for waveforms containing voltage peaks of less than 50 kV.

REFERENCES

[IV.1] KRAMER, H.-M., SELBACH, H.-J., ILES, W.J., The practical peak voltage of diagnostic X-ray generators, Br. J. Radiol. **71** (1998) 200–209.

[IV.2] RANALLO, F.N., The Noninvasive Measurement of X-Ray Tube Potential, Medical Physics Department, PhD Thesis, University of Wisconsin, (1993).

Appendix V

DETERMINATION OF THE HVL

Generally, the HVL of the radiation beam is the thickness of an absorber that attenuates the measured quantity to one half of its initial value. This means that the HVL depends on the measured quantity. The use of different quantities results in different values of the HVL. In this Code of Practice, the air kerma or air kerma rate are used as the quantity for the HVL measurement.

V.1. FIRST AND SECOND HVLs AND HOMOGENEITY COEFFICIENT

The first HVL (HVL_1), is defined as the thickness of the specified material which attenuates the air kerma or air kerma rate in the beam to one half of its original value measured without any absorber. The contribution of all scattered radiation, other than any which might be present initially in the beam concerned, is deemed to be excluded.

Additional layers of attenuators further reduce the measured air kerma. When the beam has passed through a thickness of material corresponding to the sum of the first and second HVLs, the air kerma (air kerma rate) is reduced to one quarter of its initial value. The second HVL (HVL_2) is equal to the difference between the thickness of an absorber necessary to reduce the air kerma (air kerma rate) to one quarter, $d_{1/4}$, and the value of HVL_1:

$$HVL_2 = d_{1/4} - HVL_1 \tag{V.1}$$

The ratio between HVL_1 and HVL_2 is termed the homogeneity coefficient, h:

$$h = \frac{HVL_1}{HVL_2} \tag{V.2}$$

The value of h gives a certain indication about the width of the X ray spectrum. Its value lies between 0 and 1 with higher values indicating a narrower spectrum. Typical values of h for beams used in diagnostic radiology are between 0.7 and 0.9.

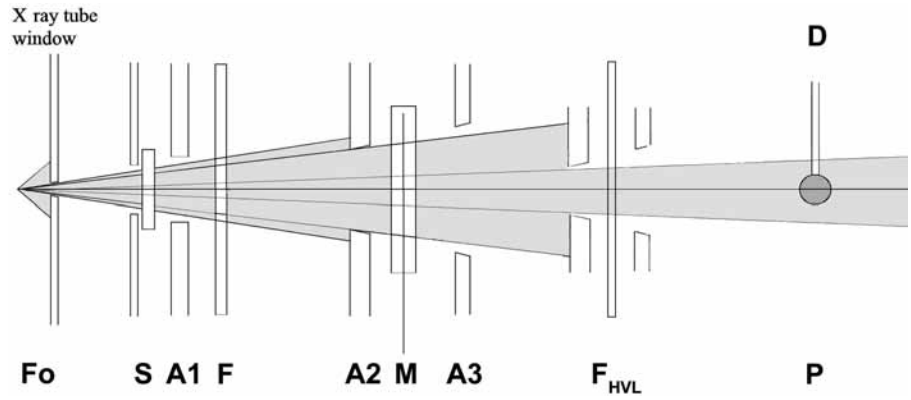

FIG. V.1. Schematic drawing of the HVL measurement set-up, where: Fo is the focal spot; S is the shutter; A1, A2, A3 are apertures; F is added filtration; F_{HVL} is the HVL absorber; M is the monitor chamber; D is the detector; P is the point of test.

V.2. MEASUREMENT SET-UP

The measurement set-up basically does not differ when measuring the HVL in the SSDL or clinic. The procedure used for determining the HVL should follow recommendations given by the ICRU [V.1] and the IAEA [V.2].

The geometry of measurement should be that of a narrow beam. The diameter of the beam should be just sufficient to irradiate the detector completely and uniformly. An unnecessarily large cross-sectional area of the beam will produce additional scattered radiation that will contribute to the signal. When the beam is too narrow, necessary conditions required for measurement of the air kerma may not be fulfilled for some detectors. The aperture in the beam limiting diaphragm should be just large enough to produce the smallest beam covering the measuring chamber. Additional diaphragms should be used to shield the measuring chamber from scattered radiation produced in absorbers.

The experimental set-up for HVL measurements in the SSDL is shown in Fig. V.1. This situation may be difficult to reproduce in clinical situations but physicists should aim at following the above principles.

In principle, the readings of any chamber can be corrected for the effect of the energy dependence of response, which implies that any chamber can be used for the HVL measurement. In practice, this is hardly achievable and only ionization chambers with a negligible energy dependence of the response should be used for HVL measurements. The reference class ionization chambers (see Table 5.2) possess this characteristic and their use is

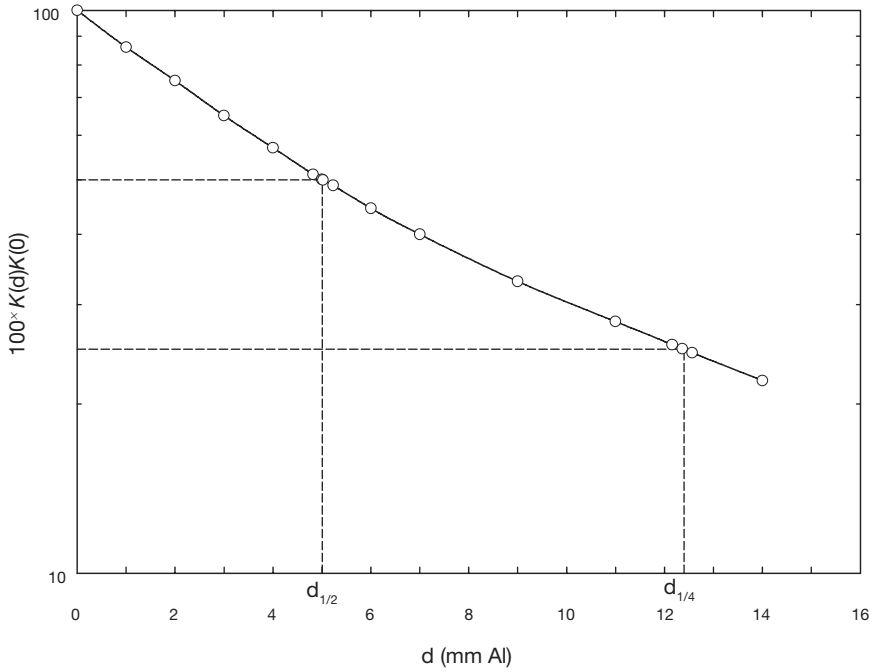

FIG. V.2. Determination of HVL_1 and HVL_2 by the interpolation of measured values of the air kerma.

recommended by this Code of Practice. The ionization chamber should be placed at the point where the HVL is required to be known. Generally, this is a calibration position in the SSDL or a measurement position in the clinical set-up. To avoid differences caused by variations in the output of the X ray tube, it is recommended that the monitor chamber be used and the readings of the measuring ionization chamber normalized with respect to the readings of the monitor. The monitor should be positioned such that its readings are independent of the presence and the thickness of the absorber. This can best be achieved by locating the absorbers equidistant from the monitor chamber and from the detector. The distance from the aluminium absorbers to the detector should be at least five times the diameter of the beam at the detector position.[1] This arrangement ensures that the production of scattered radiation in the absorber does not lead to an unnecessarily large contribution of scattered radiation to the signal of the monitor chamber or the reference chamber.

[1] This may be difficult to achieve in some clinical situations but every effort should be made to fulfil this condition.

If the temperature in the room varies considerably over the period of the measurement, a correction for this influence should be applied. If there are large temperature gradients in the room, separate corrections for the measuring chamber and the monitor may be needed.

The aluminium absorbers should be used for measurements of the HVL in diagnostic radiology. It is recommended that the actual thickness of attenuators be known with an uncertainty not exceeding 10 μm for X rays of 40 kV and above and 5 μm for mammography applications. The purity of the aluminium attenuators should be at least 99.9%.

V.3. MEASUREMENT PROCEDURE AND EVALUATION OF THE MEASUREMENTS

The initial measurement should be the air kerma in the absence of any absorber and this measurement should be repeated as the last measurement after having measured the air kerma for absorbers of various thickness. The air kerma should be measured for several absorber thicknesses close to 50% of the value of the air kerma measured initially without any absorber. If the second HVL is desired, measurements close to 25% should be also performed.

The measured values of the air kerma for various absorbers are plotted versus the absorber thickness on a semi-logarithmic scale (see Fig. V.2). The HVL values are derived by interpolation from the graph. Figure V.2 contains data that describe a complete attenuation curve, although in practice three measurement points around the actual HVL thickness are sufficient for the linear interpolation.

REFERENCES

[V.1] INTERNATIONAL COMMISSION ON RADIATION UNITS AND MEASUREMENTS, Physical Aspects of Irradiation, National Bureau of Standards Handbook 85, Rep. 10b, ICRU, Washington, DC (1964).

[V.2] INTERNATIONAL ATOMIC ENERGY AGENCY, Calibration of Dosimeters Used in Radiotherapy, Technical Reports Series No. 374, IAEA, Vienna (1995).

Appendix VI

APPLICATION OF PATIENT DOSE MEASUREMENTS

VI.1. INTRODUCTION

In medical X ray imaging there are two fundamental reasons for determining patient dose: as a means of setting and checking standards of good practice and as a means of assessing detriment for the purposes of justification and risk assessment. This section therefore discusses the concepts of guidance and reference dose levels and the use of patient dose measurements for the calculation of risk related dosimetric quantities.

VI.2. GUIDANCE LEVELS (DIAGNOSTIC REFERENCE LEVELS)

Diagnostic radiology investigations need to be optimized so that doses received by the patient are not higher than needed to obtain the required diagnostic information. The BSS [VI.1] require the use of guidance levels as part of the optimization of protection of patients in diagnostic radiology. The European Commission's Medical Exposure Directive [VI.2] and the ICRP [VI.3] promote the use of diagnostic reference levels. Examples of the development and use of guidance (reference) levels are given in Ref. [VI.4].

These concepts of guidance/reference levels should not be used in isolation. It is always essential to maintain the appropriate level of image quality required for diagnostic confidence. The BSS require the medical practitioners who prescribe or conduct radiological diagnostic examinations to ensure that the exposure of patients be the minimum necessary to achieve the required diagnostic objective, taking into account norms of acceptable image quality established by appropriate professional bodies and relevant guidance levels for medical exposure. An important tool for optimization is, therefore, the use of guidance levels, which provide guidance of what is achievable with current good practice, but which are to be applied with flexibility to allow higher exposures if these are indicated by sound clinical judgement.

According to BSS requirements, guidance levels should be used by diagnostic radiology practitioners in order that (i) corrective actions be taken as necessary if doses fall substantially below the guidance levels and the exposures do not provide useful diagnostic information and do not yield the

expected medical benefit to patients[1]; and (ii) reviews be considered if doses exceed the guidance levels as an input to ensuring optimized protection of patients and maintaining appropriate levels of good practice. Further, according to the BSS requirements, guidance levels should be derived from wide scale quality surveys, which include entrance surface doses (entrance surface air kerma) and cross-sectional dimensions of the beams delivered by individual facilities for the most frequent examinations.[2] In the absence of wide scale surveys, performance of the equipment should be assessed on the basis of comparison with the guidance levels specified in the BSS.

The ICRP has encouraged [VI.5] "authorized bodies to set diagnostic reference levels that best meet their specific needs and that are consistent for the regional, national or local area to which they apply." A comparative review of the various approaches to guidance and reference levels is given in the same ICRP publication.

VI.3. STOCHASTIC AND DETERMINISTIC EFFECTS

The probability of a cancer resulting from human exposure to ionizing radiation usually increases with increments in dose, probably with no threshold, and in a way that is roughly proportional to dose. This kind of effect is termed stochastic, meaning 'of a random or statistical nature'. If radiation damage occurs in a cell whose function is to transmit genetic information to later generations, any resulting effects are expressed in the progeny of the exposed person. This type of stochastic effect is termed hereditary. If cellular damage does occur and if it is not adequately repaired, it may prevent a cell from surviving or reproducing. If the number of cells lost is large enough, there will be observable harm reflecting a loss of tissue function. The probability of causing such harm will be zero at small doses, but above some level of dose (the threshold) will increase steeply to unity. Above the threshold, the severity of the harm will increase with dose. This type of effect is termed deterministic. Stochastic and deterministic effects are discussed in Ref. [VI.6].

---

[1] The intention of this BSS requirement is to place emphasis on the fact that too low doses may be undesirable if they do not provide the information needed and that overzealous dose reduction may be detrimental to the diagnosis.

[2] The sample of hospitals chosen for the survey, from which guidance (reference) levels will be derived, should be as representative as possible of practice, for example, by including public and private hospitals, large university and small X ray departments, and hospitals in town as well as outside town.

It is normal to assume that the probability of a stochastic effect for a given organ or tissue is proportional to the organ dose, D_T. In most situations, the organ dose is impossible to measure directly. Use is made of conversion coefficients that relate organ dose to measurable quantities. Such conversion coefficients are obtained from measurements using phantoms or Monte Carlo calculations that simulate the X ray source and patient. The latter is the better established approach, is well validated and has the important advantage of flexibility. All of the conversion coefficients presented in this Code of Practice were obtained from Monte Carlo calculations. However, whichever approach is used, the conversion coefficients will be model dependent and will not correspond exactly to any individual patient.

In some situations, a simpler approach may be possible using the mean absorbed dose to the patient, or a region of the patient. This may be estimated using the energy imparted to the patient divided by the mass of the patient or the region of the patient irradiated.

Deterministic effects only occur in diagnostic radiology in special circumstances when the local dose is very high. The most important example is the high skin dose which can arise during interventional procedures using X rays (e.g. Refs [VI.7–VI.10]).

VI.4. ORGAN DOSE

In most situations in diagnostic radiology, it is not possible or practicable to measure organ dose directly. Instead, use is made of tabulated conversion coefficients that relate organ dose to readily measurable quantities such as 'entrance surface dose' (entrance surface air kerma), 'dose–area product' (air kerma–area product) or a 'CT dose index' (CT kerma index).[3] Tables of such conversion coefficients are generally produced using Monte Carlo based computer models. Such models offer a much greater possibility for the simulation of a wide range of examinations and X ray spectra than measurements using anthropomorphic phantoms.

The key features of a Monte Carlo model are the simulation of the radiation field incident on the patient (including field size, direction and X ray spectrum), the simulation of photon transport through the patient and the simulation of the patient. The methodology for the simulation of photon

[3] Quantities in quotes are those used in the original publications; quantities in parentheses are those used in this Code of Practice. The rationale for this choice of quantities is given in Chapter 4.

histories is well established. For the diagnostic energy range, it is sufficient in most cases to assume that energy deposited after a photon interaction is locally absorbed so that organ doses may be estimated by recording the energy depositions that take place when many photon histories are followed. An important exception to this is the energy deposition in the red bone marrow where the range of secondary electrons may be comparable to the size of the marrow cavities. A correction may be applied for this effect [VI.11, VI.12].

Two approaches have been adopted for the simulation of the human body. One is to use a mathematical phantom (also known as a geometrical phantom) in which the body and the organs it contains are constructed as combinations of various geometrical solids. The first such phantom was based on ICRP Reference Man [VI.13] and the formulas governing its construction were published by the Medical Internal Irradiation Dose Committee [VI.14]. Subsequent revisions of this phantom added representations of children. The publication by Cristy [VI.15] provides mathematical equations for five phantoms representing children (neonate and 1, 5, 10 and 15 years old) and an adult phantom. The Cristy phantoms are hermaphrodite but the adult phantom may be used to simulate an adult male and the 15-year old phantom an adult female. The group at the GSF-National Research Center for Environment and Health has developed separate male and female adult mathematical phantoms, Adam and Eva [VI.16]. Mathematical phantoms can be criticised as being unrealistic in terms of organ position and shape.

An alternative approach is to use one or more voxel phantoms based on the anatomy of individuals. Such phantoms may be obtained, for example, from whole body CT or magnetic resonance images, which have been segmented, voxel by voxel, into different organs and tissue types. The most comprehensive series of voxel phantoms has been developed at GSF. Other voxel phantoms have been developed [VI.17–VI.20]. Table VI.1 lists the voxel phantoms developed by GSF and which are based on actual individuals. All of the phantoms are for European individuals except for Otoko (Japan) and the Visible Human (United States of America).

As a result of the statistical nature of Monte Carlo simulations, the organ dose conversion coefficients thus estimated have associated statistical errors. In general, the statistical uncertainties in the doses to organs lying within the radiation field will be less than those for organs lying outside the radiation field. In the latter case, the relative uncertainty will increase with the distance from the edge of the field.

Organ dose conversion coefficients calculated using Monte Carlo techniques have been published by various authors. The most extensive tabulations are those of the CDRH, the GSF and the National Radiological

TABLE VI.1. VOXEL PHANTOMS DEVELOPED AT GSF [VI.21]*

Name	Gender	Age	Type	Mass (kg)	Height (mm)	Voxel size (mm^3)	No. of organs
Baby	Female	8 weeks	Whole body	4.2	570	2.9	56
Child	Female	7 years	Whole body	21.7	1150	19.0	61
Donna	Female	40 years	Whole body, with standardized gastrointestinal tract	79	1700	35.2	62
Helga	Female	26 years	From mid thigh upwards	81 (76.8)	1700 (1140)	9.6	62
Frank	Male	48 years	Torso and head	(65.4)	(965)	2.8	60
Golem	Male	38 years	Whole body	68.9	1760	34.6	121
Otoko	Male		Whole body	65	1700	9.6	122
Standardized gastrointestinal tract	Female		Gastrointestinal tract			2.0	14
Visible Human	Male	38 years	From knees upwards	(87.8) 103.2	(1250) 1800	4.3	131

* All phantoms are based on actual individuals. Where the mass or height are given in brackets, this denotes the values for the phantom, otherwise the values are for the individual.

Protection Board (NRPB)[4] in the UK. In addition, a PC based Monte Carlo computer program is available from the Radiation and Nuclear Safety Authority (STUK) in Finland, which can compute organ doses for user specified radiation fields. This appendix outlines the important features of these data sources. More details can be found in the appendices of Ref. [VI.22] and the original publications.

The choice of tabulation for a particular situation will depend upon data availability and how well the situation modelled matches the situation for which the organ doses are required. All conversion coefficients are beam quality dependent and it will usually be adequate to interpolate linearly between values of the conversion coefficients at different beam qualities.

[4] In 2005, the NRPB became the Radiation Protection Division of the Health Protection Agency (http://www.hpa.org.uk/radiation).

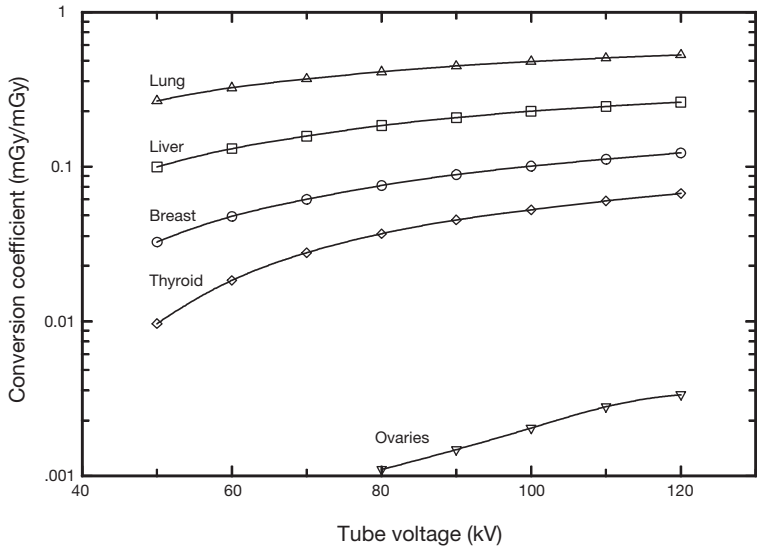

FIG. VI.1. Variation of organ dose conversion coefficients, c_{D_T,K_e}, with tube voltage for lung, liver, breast, thyroid and ovaries. Chest postero–anterior examination. X ray spectra have total filtration of 3 mm Al. Data taken from Hart et al. [VI.23].

Figure VI.1, which is based on Hart et al. [VI.23], illustrates this by showing the variation of selected organ dose conversion coefficients with tube voltage for a chest postero–anterior examination.

It is important to note that the size of the modelled patient, the position and size of the modelled organs and the position and size of the radiation field will not in general match those of the real situation. Significant errors can arise as a consequence. Large errors may arise when the field size used in practice is different to that modelled, or when the beam centre deviates from the one calculated. Whole organs may lie wholly within or partly within the field for one case and wholly outside the field for the other. Table VI.2, taken from Petoussi-Henss et al. [VI.21], demonstrates the differences in organ dose conversion coefficients for a posterior–anterior chest examination at 141 kV when three different GSF phantoms that simulate an adult male are used. The Adam mathematical phantom and the Golem voxel phantom have similar external dimensions, but the coefficients for several organs including lung, liver and thyroid are significantly different, owing to differences in the size, shape and position of the internal structures of the two phantoms. The visible human phantom is much larger than the Golem phantom and comparison of the results for these two phantoms shows that the conversion coefficients in

TABLE VI.2. ORGAN DOSE CONVERSION COEFFICIENTS PER INCIDENT AIR KERMA, C_{D_T,K_i}, CALCULATED FOR TWO VOXEL PHANTOMS AND ONE MATHEMATICAL PHANTOM*

Organ	Organ dose per unit incident air kerma (mGy/mGy)		
	Voxel Golem	Voxel Visible Human	Mathematical Adam
Colon	0.09	0.04	0.008
Testes			
Liver	0.38	0.30	0.27
Lungs	0.57	0.51	0.79
Pancreas	0.27	0.19	0.32
Red bone marrow	0.26	0.21	0.21
Skeleton	0.40	0.33	0.39
Spleen	0.77	0.52	0.39
Small intestine	0.09	0.04	0.01
Stomach wall	0.30	0.24	0.14
Thyroid	0.28	0.18	0.14
Surface (entrance)	1.27	1.40	1.39
Surface (exit)	0.10	0.07	0.09

* Chest posterior–anterior examination; tube voltage: 141 kV; total filtration: 5.7 mm Al; focus image distance: 1500 mm; field size at the image plane: 350 mm × 400 mm. Data taken from Petoussi-Henss et al. [VI.21].

general decrease with increasing patient size, owing to the increased shielding offered to most organs as the body size increases. A detailed discussion of the differences between organ dose conversion coefficients for different phantoms is given in Zankl et al. [VI.24]. These authors also note that the GSF voxel phantoms are based on patients examined in the supine position, whereas some X ray examinations are made with the patient erect. The position of some organs is quite different for the two situations.

VI.4.1. Tabulations of organ dose conversion coefficients for general diagnostic radiology and fluoroscopy

Four handbooks are available from the CDRH, which provide conversion coefficients for the estimation of organ doses in general radiographic and

fluoroscopic examinations. Some of these handbooks present doses in mrad[5] per unit entrance exposure (mrad/R free in air). Such data may be converted to mGy/mGy incident air kerma by division by 876[6] (see also Chapter 3). The handbooks are described below.

Projections common in diagnostic radiology (adults) [VI.25]. Conversion coefficients are provided for the calculation of doses to 7 organs and total trunk tissue for 54 radiographic projections and 12 beam qualities ranging from HVLs of 1.0–6.5 mm Al in steps of 0.5 mm Al. The calculations were made using a modified version of the MIRD-5 phantom [VI.14].

Projections common in paediatric radiology [VI.26]. Conversion coefficients are provided for the calculation of doses to 5 organs and total body for 20 radiographic projections and 3 or 4 beam qualities (HVLs of 2.0, 2.5, 3.0 and 3.5 mm Al) as appropriate to the particular projection. The calculations were made for three sizes of patient: newborn (birth to six months), a one-year old child and a five-year old child.

Upper gastrointestinal fluoroscopic examinations [VI.27]. Conversion coefficients are provided for the calculation of doses to 12 organs and total trunk (excluding lungs and skeletal tissues) for 12 radiographic projections and 3 beam qualities (HVLs of 4.0, 5.0 and 5.5 mm Al). The calculations were made for the GSF mathematical phantoms Adam and Eva.

Fluoroscopic and cineangiographic examination of the coronary arteries [VI.28]. Conversion coefficients are provided for the calculation of doses to 20 organs and entrance skin area of the radiation field for 12 radiographic projections and 3 beam qualities. The calculations were made for the GSF mathematical phantoms Adam (at HVLs of 2.5, 4.0, 5.0 and 5.5 mm Al) and Eva (at HVLs of 2.0, 3.5 and 5.0 mm Al). A correction is described that should be used when the diameter of the field of view differs from that used for the calculation by more than 20%.

[5] 1 rad = 0.01 Gy.

[6] Value appropriate to data used by CDRH.

The GSF calculated conversion coefficients for the estimation of organ doses from incident air kerma for a wide range of exposure conditions for general radiography. Its publications for adults and children are described below.

Common projections in diagnostic radiology (adults) [VI.29]. Conversion coefficients are provided for the calculation of doses to 16 organs, skin entrance surface and skin exit surface for 40 radiographic projections (including techniques for pregnant women). The coefficients for each projection are available for three tube voltages. In each case the total filtration of the X ray beam was 2.5 mm Al. Data are also provided for 28 radiographic projections with technical parameters in accordance with the EC quality criteria guidelines [VI.30]. The calculations were made using the GSF Adam and Eva phantoms.

Common projections in diagnostic radiology (paediatric) [VI.31, VI.32]. Conversion coefficients for the GSF Child voxel phantom and organ doses for the GSF Baby voxel phantom have been published. Data are provided for 16 organs and 5 radiographic projections for the Baby phantom and 10 organs and 6 radiographic projections for the Child phantom. They were calculated for representative exposure settings. Scaling factors may be used to derive values for children of different size to those used in the calculations [VI.33, VI.34].

Two software reports are available from the NRPB that provide comprehensive tabulations of conversion coefficients for the estimation of organ doses for adults and children. The data are provided in digital form for computer input. A helpful feature is that the conversion coefficients are available for both entrance surface dose to air (entrance surface air kerma) and dose–area product (air kerma–area product). The choice between conversion coefficients that can be used to calculate organ dose from entrance surface air kerma or air kerma–area product will depend upon the particular situation. The total energy imparted to the patient (phantom) will increase with increasing field size, but the dose to an organ wholly contained within the radiation field will show a much smaller fractional change. Coefficients normalized to air kerma–area product may be of particular utility for situations such as fluoroscopic examinations where the field size and direction are modified throughout the procedure. These NRPB reports are described below.

Common adult X ray examinations [VI.23, VI.35]. Conversion coefficients are provided for the calculation of doses to 26 organs for 68 radiographic projections and 40 beam qualities (tube voltages of 50–120 kV in steps of 10 kV and total filtrations of 2, 2.5, 3, 4 and 5 mm Al). The conversion coefficients were calculated [VI.11] using a modified version of Cristy's adult phantom [VI.15]. Information provided on backscatter facilitates use with measurements of incident air kerma. A computer program has been developed [VI.36] which can estimate organ doses using the NRPB data tabulation and exposure parameters entered by the user.

Common paediatric X ray examinations [VI.37, VI.38]. Conversion coefficients are provided for the calculation of doses to 26 organs for 18 radiographic projections and 72 beam qualities (tube voltages of 50–120 kV in steps of 10 kV and total filtrations of 2, 2.5, 3, 4 and 5 mm Al, 2 mm Al + 0.1 mm Cu, 2 mm Al + 0.2 mm Cu, 3 mm Al + 0.1 mm Cu and 3 mm Al + 0.2 mm Cu). The conversion coefficients were calculated for modified versions of each of the five Christy child phantoms (neonate and 1, 5, 10 and 15 years old). Information provided on backscatter facilitates use with measurements of incident air kerma. A computer program has been developed [VI.39] which can estimate organ doses using the NRPB data tabulation and exposure parameters entered by the user.

The PC based Monte Carlo computer program (PCXMC) developed by STUK directly calculates organ doses for user specified radiation fields. Its features are described below.

PCXMC – A PC based Monte Carlo program for the calculation of patient dose in medical X ray examinations [VI.40]. This computer program can run on a PC. It is able to calculate organ doses for user specified radiation fields (size, position, angulation and X ray spectrum). The calculations may be made for modified versions of the six Cristy phantoms (five child phantoms and one adult phantom). A useful refinement is the capability to change the mass or the height of the phantoms. In this case, scaling factors are calculated which are used to change all the dimensions of the phantoms. Comparison has been made with the conversion coefficients of Hart et al. [VI.23, VI.38] and good agreement generally obtained.

VI.4.2. Tabulations of organ dose conversion coefficients for CT

Tabulations of organ dose conversion coefficients for use in CT have been provided by the GSF and the NRPB. Both sets of tabulations provide conversion coefficients for a series of CT slices that cover the length of the patient. The features of these tabulations are described below.

Report on organ doses from CT examinations (adults) [VI.41]. Conversion coefficients are provided for the calculation of doses to 21 organs for a series of 10 mm wide CT slices that cover the lengths of the GSF Adam and Eva mathematical phantoms. The conversion coefficients are normalized to the air kerma measured free in air on the axis of the scanner, K_i, thus:

$$D_T = c_{D_T,K_i} K_i \qquad \text{(VI.1)}$$

The conversion coefficients were evaluated for three radiation qualities and for CT scanners without beam shaping filters.

Report on organ doses from CT examinations (paediatric) [VI.42]. Conversion coefficients are provided for the calculation of doses to 23 organs for a series of 10 mm wide CT slices that cover the lengths of the GSF Baby and Child voxel phantoms. The conversion coefficients are normalized to the air kerma measured free in air on the axis of the scanner. The conversion coefficients were evaluated for three radiation qualities, for CT scanners without beam shaping filters and for both 360º and 180º rotation. In the latter case, the calculations were made for anterior radiation incidence only.

Adult CT examinations [VI.43, VI.44]. Conversion coefficients are provided for the calculation of doses to 27 organs for 208 contiguous 5 mm slices which cover the length of a modified adult Cristy phantom. The conversion coefficients were normalized to a CT dose index (see discussion in Section 3.2.1) expressed in terms of the dose to ICRU muscle (kerma in ICRU muscle) measured free in air on the axis of the scanner. This index is related to the CT dose index expressed in terms of dose to air (air kerma) by the ratio of the mass energy absorption coefficients for ICRU muscle [VI.45] and air. The ratio of the mass energy absorption coefficients may be taken to be 1.07 over the range of beam qualities used in CT [VI.46]. The conversion coefficients are

available for 23 different CT exposure conditions (tube voltage, focus to axis distance, and total filtration and beam shaping (or bow tie) filters) in software report SR250, which contains data for four scanners.

Using the above data sets, the organ doses for an axial or a helical examination can be calculated by summing the conversion coefficients for the individual slices, i, of the phantom that lie within the actual scanned volume [VI.47]. The dose, D_T, to a given organ is given by:

$$D_T = \frac{C_{a,100}}{p} \sum_i c_{D_T, C_{a,100}} \qquad \text{(VI.2)}$$

where the CT pitch factor, p, is given by Eq. (3.16). In Eq. (VI.2), the CT air kerma index must correspond to the actual tube current used. If the complete examination is divided into components where the examination parameters are different, then Eq. (VI.2) must be evaluated separately for each component. For the GSF tabulation, the coefficient $c_{D_T, C_{a,100}}$ is numerically equal to c_{D_T, K_i}. However, if the NRPB tabulation is to be used with Eq. (VI.2), a correction is required because of the use of different normalization (see above). For this situation, the tabulated data are multiplied by the ratio of the mass energy absorption coefficients of ICRU muscle and air. As noted above, a value of 1.07 may be used.

Figure VI.2 shows the variation of the conversion coefficients, $c_{D_T, C_{a,100}}$, for ovaries, lung and thyroid along the length of the patient. Each curve shows a peak at the position of the particular organ. The relative magnitudes of the peaks depend upon the thickness and nature of the overlying tissues and the extent of the organs.

Computer programs are available which use the tabulated data to calculate organ doses from knowledge of CT exposure parameters and the body region scanned. Examples include LeHeron [VI.48] and ImPACT [VI.46]. In making such calculations it is important to match the scanner design to that used for the calculation of the conversion coefficients. For example, the shape of the bow-tie filter can have an important influence on organ dose. ImPACT [VI.46] has devised a method of selecting a scanner from the 23 tabulated by Jones and Shrimpton [VI.43, VI.44], which best matches the characteristics of a given modern scanner.

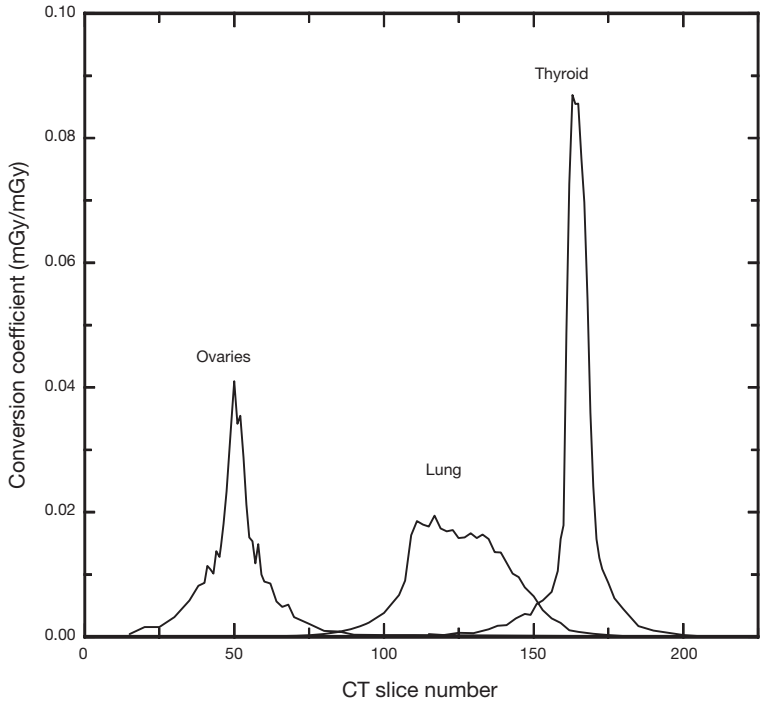

FIG. VI.2. Variation along the length of the patient of organ dose conversion coefficients, $c_{D_{T,Ca,100}}$, per 5 mm CT slice for ovaries, lung and thyroid for a particular CT scanner. Data based on Jones and Shrimpton [VI.43].

VI.4.3. Mean glandular dose

The ICRP [VI.49] recommends the use of the mean (or average) absorbed dose to the glandular tissues within the breast as the risk related quantity for mammography (see Chapter 3). The determination of the mean glandular dose forms part of this Code of Practice. The methodology adopted and the choice of conversion coefficients are discussed in Appendix VII.

VI.4.4. Foetal dose

In diagnostic radiology and interventional procedures using X rays, foetal dose estimation is usually not necessary unless the foetus is in the direct beam [VI.50]. However, occasions may arise where pregnant patients undergo X ray examinations, either intentionally because the examination is required urgently for the management of the patient or inadvertently because the patient was

unaware that she was pregnant at the time of the examination. These exposures can lead to anxiety about possible effects of the dose to the foetus.

Even though the absorbed doses to the conceptus are generally small, such concern may lead to inappropriate suggestions that additional exposures be delayed or withheld or even that the pregnancy should be terminated. However, according to the ICRP [VI.51], foetal doses should not be considered a reason for terminating a pregnancy if they are below 100 mGy.

In early pregnancy, it is straightforward to estimate the dose to the foetus. It can be assumed that the uterine dose is a good estimate of the foetal dose. The conversion coefficients described in Section VI.4 for the estimation of organ dose can therefore be used in combination with an appropriate measured quantity such as incident air kerma. In interpreting this estimate, it is important to remember the limitations of the models used to simulate the patient. In later pregnancy, the mean depth dose of the foetus will be greater and the foetal dose increases with the size of the pregnant uterus because both the focus to skin distance and the uterine depth decrease [VI.52].

Foetal dose varies with the gestational age and is, in general, proportional to it. Adjustments may be made to the foetal dose based on depth dose data [VI.53].

Table VI.3 [VI.50] provides information on typical uterine dose (i.e. foetal dose) from some routine X ray examinations and procedures. If a pregnancy is recognized prior to exposure, tailoring of the examination may reduce the dose below these levels.

After low dose examinations (such as a chest X ray) in which the conceptus is not in the X ray beam, there is no real need for individual foetal dose estimation. However, after high dose abdominal or pelvic procedures (e.g. CT or fluoroscopy), an estimate of the dose and the associated risk to the foetus should be made.

VI.4.5. Skin dose

The assessment of absorbed dose to the most exposed area of the skin is essential in interventional procedures because of the potential for reaching the threshold for deterministic effects in complicated procedures. Knowledge during the procedure of the skin dose is necessary to avoid deterministic effects or to reduce their severity. Knowledge after the procedure of the skin dose is necessary in order to decide which patients require follow-up for potential deterministic effects.

The determination of the skin dose to the most exposed area is not straightforward since exposure parameters and projection angle change during the procedure. The most exposed area cannot be predicted in most cases and

TABLE VI.3. UTERINE (i.e. FOETAL) RADIATION DOSES (WESTERN EUROPEAN COUNTRY)*

Procedure	Mean absorbed dose (mGy)	Highest absorbed dose (mGy)
Conventional diagnostic X ray procedures		
Abdomen	1.4	4.2
Chest	<0.01	<0.01
Intravenous pyelogram (urogram)	1.7	10
Lumber spine	1.7	10
Thoracic spine	<0.01	<0.01
Pelvis	1.1	4
Fluoroscopic procedures		
Barium meal	1.1	5.8
Barium enema	6.8	24
CT		
Head	<0.005	<0.005
Chest	0.06	0.96
Abdomen	8.0	49
Pelvis	25	79
Lumbar spine	2.4	8.6

* NRPB data [VI.50].

even retrospective identification of this area and its dose can be difficult. Methods for determining skin dose for interventional procedures are discussed in Appendix VII.

Values of the dose thresholds for deterministic effects and typical fluoroscopy times for which these thresholds are reached can be found in Ref. [VI.8].

VI.5. ENERGY IMPARTED TO THE PATIENT

The transmission ionization chamber for measurement of the air kerma–area product, P_{KA}, was originally introduced for determination of the energy imparted, $\bar{\varepsilon}$, to the patient [VI.54–VI.56]. The energy imparted to the patient is significant since it is a quantity that is related to the stochastic risk of cancer

induction. Whilst this risk is the sum of organ doses multiplied with their risk coefficients, the energy imparted to the patient is the sum of organ doses multiplied by their masses. Thus, the total risk for cancer induction and the energy imparted to the patient both depend on the irradiated volume of the patient.

If the energy is imparted uniformly to the body, the effective dose, E (see Section 3.3.3), is equal to the mean absorbed dose, $\bar{D} = \bar{\varepsilon}/m$, for the whole body (where m is the mass of the patient). For example, an energy imparted of 1 J gives effective doses of 0.1 Sv and 0.01 Sv for body masses of 10 and 100 kg respectively. When the energy is imparted non-uniformly to the body, the mean absorbed dose, $\bar{D}$, is still closely related to effective dose [VI.57]. If the energy is imparted to a limited part of the body such as the trunk, Wall and Shrimpton [VI.58] suggested using the mean absorbed dose in that body part to approximate the organ doses. For an average adult of 70 kg, the trunk mass of 44 kg was used to estimate the mean of the organ doses in the trunk for examinations involving the upper part of the body.

A conversion coefficient, $c_{\bar{\varepsilon},P_{KA}}$, is needed to convert P_{KA} to the energy imparted, $\bar{\varepsilon}$, to the patient. It is obtained from [VI.59]:

$$c_{\bar{\varepsilon},P_{KA}} = \varepsilon / \int_A K \mathrm{d}A = \frac{aR_f}{\left(\overline{\mu_{tr}/\rho}\right)_{air}} \qquad \text{(VI.3)}$$

where a is the fraction of the beam that is incident on the patient; R_f is the fraction of the radiant energy incident on the patient, which is imparted to the patient (the imparted fraction) and $\left(\overline{\mu_{tr}/\rho}\right)_{air}$ is the mass energy transfer coefficient of air weighted over the energy fluence spectrum of the incident photons.

Shrimpton et al. [VI.60] and Jones and Wall [VI.11] published values of the imparted fraction for examinations of the adult trunk and the entire skull. Persliden and Alm Carlsson [VI.61] calculated values for laterally infinite water slabs. Gibbs [VI.62] derived imparted fractions for dental projections of the head using a CT based female skull model. The imparted fractions for a laterally infinite water slab of 150 mm thickness agree well with those for the trunk and entire skull. Imparted fractions for dental projections are lower owing to the thin body part irradiated in this case.

Conversion coefficients, $c_{\bar{\varepsilon},P_{KA}}$, based on the values of the imparted fraction from Jones and Wall [VI.11] and X ray spectra from Birch et al. [VI.63] for constant potential are shown in Fig. VI.3 for 12 common examinations of the trunk (left) and entire skull (right). The conversion coefficients increase strongly with increasing tube voltage as a result of the energy dependence of $\left(\overline{\mu_{tr}/\rho}\right)_{air}$ (c.f. Eq. (VI.3)). For paediatric patients, conversion coefficients were calculated by Persliden and Sandborg [VI.64] and by Almén and Nilsson [VI.65].

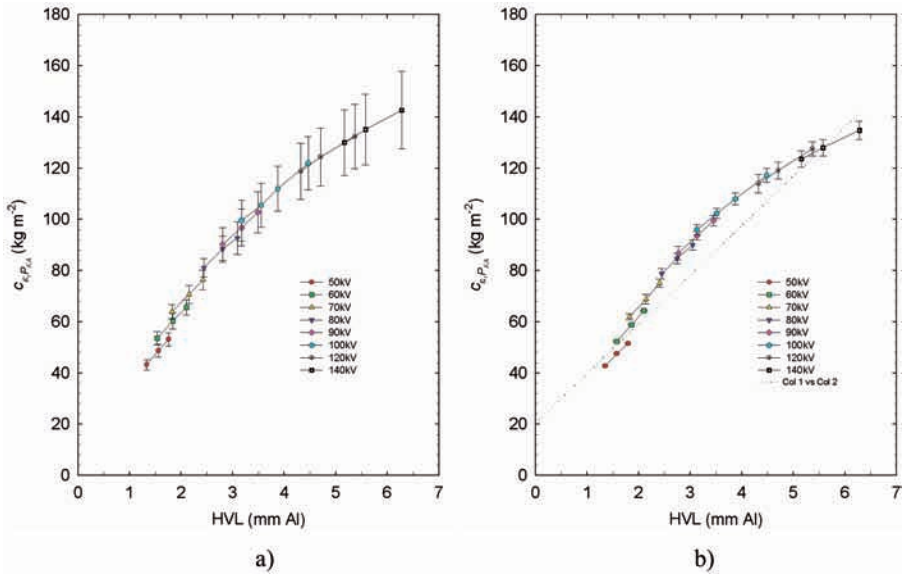

FIG. VI.3. Conversion factor $c_{\bar{\varepsilon},P_{KA}}$ as a function of HVL with tube voltage as the parameter for (a) trunk and (b) skull. The values were derived using imparted fractions from Jones and Wall [VI.11] and constant potential energy spectra from Birch et al. [VI.63]. The entire beam is incident upon the patient, i.e. a = 1 in Eq. (VI.3). The dashed, straight line approximation (b) was used by Stenström et al. [VI.66] for tube voltages <70 kV and intraoral radiography. (After Carlsson and Alm Carlsson [VI.59]).

VI.6. EFFECTIVE DOSE

Effective dose, E, is defined in Chapter 3. The tissue weighting factor, w_T, in the expression for effective dose (Eq. (3.20)) gives the relative contributions to the total detriment from organ or tissue, T, in a uniform whole body irradiation. It follows that the sum of the weighting factors equals one and that effective dose represents the uniform whole body irradiation, which causes the same detriment as an actual non-uniform irradiation with different values for the equivalent doses to the various tissues and organs.

The detriment is calculated as the risk of induction of disease (cancer and hereditary disease), weighted for the severity and taking into account the expected length of life lost to fatal cancer, the morbidity of non-fatal cancer and the severity of hereditary disease (see Table B20 in ICRP 60 [VI.6]). If the equivalent dose (see Section 3.3.2) is fairly uniform over the whole body, the probability of fatal cancer can be calculated using the nominal probability coefficient of 4×10^{-2} Sv^{-1} (radiation workers) or 5×10^{-2} Sv^{-1} (whole

TABLE VI.4. TISSUE WEIGHTING FACTORS

Tissue or organ	Tissue weighting factor (w_T)
Gonads	0.20
Bone marrow (red)	0.12
Colon	0.12
Lung	0.12
Stomach	0.12
Bladder	0.05
Breast	0.05
Liver	0.05
Oesophagus	0.05
Thyroid	0.05
Skin	0.01
Bone surface	0.01
Remainder*	0.05

* ICRP 60 [VI.6] lists the following tissues and organs to be included in the remainder: adrenals, brain, upper large intestine, small intestine, kidney, muscle, pancreas, spleen, thymus and uterus. In those cases in which a single one of the remainder tissues or organs receives an equivalent dose in excess of the highest dose in any of the twelve organs for which a weighting factor is specified, a weighting factor of 0.025 should be applied to that tissue or organ and a weighting factor 0.025 to the average dose in the rest of the remainder tissues or organs.

population). If the distribution of equivalent dose is non-uniform, which is the case in most diagnostic procedures, use of the nominal probability coefficients will be less accurate. The nominal detriment coefficient per unit of effective dose is 5.6×10^{-2} Sv^{-1} (workers) and 7.3×10^{-2} Sv^{-1} (whole population). The weighting factors [VI.6] are given in Table VI.4 and are assumed to be the same for radiation workers and for the whole population.

The United Nations Scientific Committee on the Effects of Atomic Radiation [VI.67] has strongly emphasized that effective dose should not be used directly to estimate detriment from medical exposure, for example, by application of the nominal fatality probability coefficients given by ICRP 60 [VI.6]. Such estimation would be inappropriate, as there are differences in health status, age and sex between the population of patients undergoing

diagnostic procedures and the population for which the nominal coefficients were derived.

Notwithstanding this caveat, effective dose may be used for comparative purposes, for example, between procedures performed with different exposure factors, or carried out in different hospitals or countries, or even for comparing different procedures. It has increasingly been used to estimate the detriment from diagnostic procedures advocated by, for example, the NRPB [VI.68, VI.69] and the ICRP [VI.3]. While the tissue weighting factors (Table VI.4) are not assumed to be different for a patient population, the detriment per unit of effective dose has been adjusted to take the age distribution into account. In the UK, correction factors for this have been estimated and are 0.15 (geriatric patients >70 years), 0.85 (adult patients 16–69 years) and 1.8 (paediatric patients 0–15 years) of that for the whole population [VI.69].

Calculation of effective dose requires knowledge of organ doses and can be derived from the tabulations of organ doses discussed above and the appropriate tissue weighting factors. Extensive tables of conversion coefficients, $c_{E,P_{KA}}$, for adult and paediatric patients are thus available for planar radiography from LeHeron [VI.70] and Hart et al. [VI.35, VI.38] and conversion coefficients, c_{E,K_i}, for male and female adult phantoms from Drexler et al. [VI.29]. Values of the effective dose for planar radiography can also be calculated using the PCXMC computer program [VI.40], referred to previously. For panoramic dental radiology, the conversion coefficient, $c_{E,P_{KA}}$, has been estimated as 0.06 mSv/(Gy·cm^2) by Williams and Montgomery [VI.71].

Conversion coefficients for effective dose in CT examinations can be calculated in the same way as those for planar radiography. Thus, the organ dose conversion coefficients for CT published by the NRPB [VI.43, VI.44] and the GSF [VI.41, VI.42], as discussed in Section VI.4.2, may be used. To facilitate the calculation of effective dose, specific software packages are available which use these conversion factors. For example, the ImPACT CT patient dosimetry calculator [VI.46] uses the NRPB data and CT-Expo [VI.72, VI.73] uses the GSF data. Both packages allow the user to enter actual scan data. Alternatively, but more simply, the CT air kerma–length product, $P_{KL,CT}$, can be used in combination with a rather limited set of conversion coefficients to estimate effective dose [VI.74] for specific CT examinations.

Conversion coefficients, $c_{E,\varepsilon}$, were derived by Huda and Gkanatsios [VI.75] using data from Hart et al. [VI.23] for 68 projections as a function of beam quality (50–120 kV) for a 70.9 kg anthropomorphic phantom. They also derived $c_{E,\varepsilon}$ from Hart et al. [VI.37] for paediatric phantoms of different size. The results show that the conversion coefficient, $c_{E,\bar{D}}$, in most cases deviates from unity within a factor of two (from 0.5 to 2.0). The highest values are

caused by examinations where a radiosensitive organ is situated at shallow depth, e.g. the gonads in the rectum antero–posterior view ($c_{E,\bar{D}} = 6.8$). Values below unity indicate that radiosensitive organs are protected by overlying tissues.

The conversion coefficients cited above have been derived for fixed irradiation geometries (field size and field position in a given examination). Limited information is available on the sensitivity of the conversion coefficients to a number of variations seen in clinical practice. Wise et al. [VI.76] investigated the effect on conversion coefficients $c_{E,P_{KA}}$, c_{E,K_i}, $c_{\varepsilon,P_{KA}}$, c_{ε,K_i} and $c_{E,\bar{D}}$ of up to five factors: tube voltage, field size, field position, phantom size and sex for four radiographic views: chest PA, chest left lateral, lumbar spine antero–posterior and lumbar spine left lateral. While P_{KA} was strongly correlated to the energy imparted to the patient, the correlation to effective dose was considerably weaker. Large uncertainties in effective dose are caused by organs partly irradiated in an examination and sensitive to the exact positioning of the radiation field [VI.77]. Organ doses and consequently effective dose are in addition strongly dependent on the patient model used in the Monte Carlo simulations [VI.21].

In dental radiography, the highest doses are not received in organs with fixed weighting factors (Table VI.4) but in the salivary glands. The salivary glands are not explicitly cited in ICRP 60 as organs of the remainder and the treatment of the doses to salivary glands in calculations of effective dose varies in the literature. According to Lecomber et al. [VI.78], effective dose, excluding the dose to salivary glands, is two to five times lower than effective dose including the salivary glands, as part of the remainder. As a result of the magnitude of the remainder in this situation and the uncertainty in its calculation, Stenström et al. [VI.79] concluded that the energy imparted to the patient should be preferred for risk estimates, a view shared by Huda and Atherton [VI.80] as regards CT examinations.

In conclusion, effective dose is a quantity which allows comparison of different types of examination, use of different equipment and technique factors from a risk point of view and is thus a useful tool for optimizing technique factors and examination methodology. For this application there is no need to quantify the risk coefficients, i.e. the detriment or risk per unit of effective dose. Estimates of risk may on the other hand be valuable for use in cost–benefit analysis (e.g. for a justification of the purchase of dose saving equipment), where the cost may be expressed in terms of lives or money saved per unit of dose averted [VI.68]. It must, however, be kept in mind that the risk coefficients are associated with large uncertainties and that risk estimates have to be handled with appropriate caution. Owing to the dependence of effective dose on the anthropomorphic model used for calculating organ doses, the

energy imparted to the patient or the mean absorbed dose in the patient may serve as an alternative risk related quantity for optimization.

REFERENCES

[VI.1] FOOD AND AGRICULTURE ORGANIZATION OF THE UNITED NATIONS, INTERNATIONAL ATOMIC ENERGY AGENCY, INTERNATIONAL LABOUR ORGANIZATION, OECD NUCLEAR ENERGY AGENCY, PAN AMERICAN HEALTH ORGANIZATION, WORLD HEALTH ORGANIZATION, International Basic Safety Standards for Protection against Ionizing Radiation and for the Safety of Radiation Sources, Safety Series No. 115, IAEA, Vienna (1996).

[VI.2] EUROPEAN COMMISSION, Council Directive 97/43/Euratom of 30 June 1997 on Health Protection of Individuals against the Dangers of Ionizing Radiation in Relation to Medical Exposure, and repealing Directive 84/466/Euratom, Rep. Off. J. Eur. Comm. No. L 180/22-27, EC, Luxembourg (1997).

[VI.3] INTERNATIONAL COMMISSION ON RADIOLOGICAL PROTECTION, Radiological Protection and Safety in Medicine, Publication 73, Pergamon Press, Oxford and New York (1997).

[VI.4] INTERNATIONAL ATOMIC ENERGY AGENCY, Radiological Protection of Patients in Diagnostic and Interventional Radiology, Nuclear Medicine and Radiotherapy (Proc. Int. Conf. Málaga, 2001), IAEA, Vienna (2001).

[VI.5] INTERNATIONAL COMMISSION ON RADIOLOGICAL PROTECTION, Radiation and Your Patient: A Guide for Medical Practitioners, Supporting Guidance 2, Pergamon Press, Oxford and New York (2001).

[VI.6] INTERNATIONAL COMMISSION ON RADIOLOGICAL PROTECTION, 1990 Recommendations of the International Commission on Radiological Protection, Publication 60, Pergamon Press, Oxford and New York (1991).

[VI.7] BERLIN, L., Malpractice issues in radiology: Radiation-induced skin injuries and fluoroscopy, Am. J. Roentgenol. **177** (2001) 21–25.

[VI.8] INTERNATIONAL COMMISSION ON RADIOLOGICAL PROTECTION, Avoidance of Radiation Injuries from Medical Interventional Procedures, Publication 85, Pergamon Press, Oxford and New York (2000).

[VI.9] KÖNIG, T.R., WOLFF, D., METTLER, F.A., WAGNER, L.K., Skin injuries from fluoroscopically guided procedures 2: Review of 73 cases and recommendations for minimizing dose delivered to patient, Am. J. Roentgenol. **177** (2001) 13–20.

[VI.10] KÖNIG, T.R., WOLFF, D., METTLER, F.A., WAGNER, L.K., Skin injuries from fluoroscopically guided procedures 1: Characteristics of radiation injury, Am. J. Roentgenol. **177** (2001) 3–11.

[VI.11] JONES, D.G., WALL, B.F., Organ Doses from Medical X-Ray Examinations Calculated Using Monte Carlo Techniques, Rep. NRPB-R186, National Radiological Protection Board, Chilton (1985).

[VI.12] KING, S.D., SPIERS, F.W., "Photon dosimetry in bone", Dosimetry in Diagnostic Radiology, (FITZGERALD, M., Ed.), Hospital Physicists Association, London (1984) 40–43.
[VI.13] INTERNATIONAL COMMISSION ON RADIOLOGICAL PROTECTION, Reference Man: Anatomical, Physiological and Metabolic Characteristics, Publication 23, Pergamon Press, Oxford and New York (1975).
[VI.14] SNYDER, W.S., FORD, M.R., WARNER, G.G., FISHER, H.L., Jr., Estimates of absorbed fraction for monoenergetic photon sources uniformly distributed in various organs of a heterogeneous phantom, MIRD Pamphlet No. 5, J. Nucl. Med. **10** 3 (1969).
[VI.15] CRISTY, M., Mathematical Phantoms Representing Children of Various Ages for Use in Estimates of Internal Dose, Rep. NUREG/CR-1159, Rep. ORNL/NUREG/TM-367, Oak Ridge National Laboratory, Oak Ridge, TN (1980).
[VI.16] KRAMER, R., ZANKL, M., WILLIAMS, G., DREXLER, G., The Calculation of Dose from External Photon Exposures Using Reference Human Phantoms and Monte Carlo Methods, Part I: The Male (ADAM) and Female (EVA) Adult Mathematical Phantoms, Rep. Bericht S-885, GSF National Research Centre for Environment and Health, Neuherberg (1982).
[VI.17] CAON, M., Voxel-based computational models of real human anatomy: A review, Radiat. Environ. Biophys. **42** (2003) 229–235.
[VI.18] DIMBYLOW, P.J., "The development of realistic voxel phantoms for electromagnetic field dosimetry", Voxel Phantom Development, National Radiological Protection Board, Chilton (1996) 1–7.
[VI.19] XU, X.G., CHAO, T.C., BOZKURT, A., VIP-MAN: An image based whole body adult male model constructed from colour photographs of the visible human project for multi-particle Monte Carlo calculations, Health Phys. **78** (2000) 476–486.
[VI.20] ZUBAL, I.G., et al., Computerized segmented three-dimensional anatomy, Med. Phys. **21** (1994) 299–302.
[VI.21] PETOUSSI-HENSS, N., ZANKL, M., FILL, U., REGULLA, D., The GSF family of voxel phantoms, Phys. Med. Biol. **47** (2002) 89–106.
[VI.22] INTERNATIONAL COMMISSION ON RADIATION UNITS AND MEASUREMENTS, Patient Dosimetry for X Rays Used in Medical Imaging, ICRU Rep. 74, ICRU, Bethesda, MD (2006).
[VI.23] HART, D., JONES, D.G., WALL, B.F., Normalised Organ Doses for Medical X-Ray Examinations Calculated Using Monte Carlo Techniques, Rep. NRPB-SR262, National Radiological Protection Board, Chilton (1994).
[VI.24] ZANKL, M., FILL, U., PETOUSSI-HENSS, N., REGULLA, D., Organ dose conversion coefficients for external photon irradiation of male and female voxel models, Phys. Med. Biol. **47** (2002) 2367–2385.
[VI.25] ROSENSTEIN, M., Handbook of Selected Tissue Doses for Projections Common in Diagnostic Radiology, HHS Publication FDA 89-8031, Center for Devices and Radiological Health, Rockville, MD (1988).

[VI.26] ROSENSTEIN, M., WARNER, G.G., BECK, T.J., Handbook of Selected Organ Doses for Projections Common in Pediatric Radiology, HHS Publication FDA 79-8079, Bureau of Radiological Health, Rockville, MD (1979).

[VI.27] ROSENSTEIN, M., SULEIMAN, O.H., BURKHART, R.L., STERN, S.H., WILLIAMS, G., Handbook of Selected Tissue Doses for the Upper Gastrointestinal Fluoroscopic Examination, HHS Publication FDA 92-8282, Center for Devices and Radiological Health, Rockville, MD (1992).

[VI.28] STERN, S.H., ROSENSTEIN, M., RENAUD, L., ZANKL, M., Handbook of Selected Tissue Doses for Fluoroscopic and Cineangiographic Examination of the Coronary Arteries (in SI units), HHS Publication FDA 95-8289, Center for Devices and Radiological Health, Rockville, MD (1995).

[VI.29] DREXLER, G., PANZER, W., WIDENMANN, L., WILLIAMS, G., ZANKL, M., The Calculation of Dose from External Photon Exposures Using Reference Human Phantoms and Monte Carlo Methods, Part III: Organ Doses in X-Ray Diagnosis (Revised and Amended), Rep. GSF-Bericht 11/90, GSF National Research Centre for Environment and Health, Neuherberg (1990).

[VI.30] EUROPEAN COMMISSION, European Guidelines on Quality Criteria for Diagnostic Radiographic Images in Paediatrics, Rep. EUR 16261, EC, Luxembourg (1996).

[VI.31] ZANKL, M., et al., The construction of computer tomographic phantoms and their application in radiology and radiation protection, Radiat. Environ. Biophys. **27** (1988) 153–164.

[VI.32] ZANKL, M., PETOUSSI, N., VEIT, R., FENDEL, H., "Organ doses for a child in diagnostic radiology: Comparison of a realistic and a MIRD-type phantom", Optimization of Image Quality and Patient Exposure in Diagnostic Radiology (MOORES, B.M., WALL, B.F., ERISKAT, H., SCHIBILLA, H., Eds), British Institute of Radiology, London (1989) 196–198.

[VI.33] VEIT, R., ZANKL, M., Influence of patient size on organ doses in diagnostic radiology, Radiat. Prot. Dosim. **43** (1992) 241–243.

[VI.34] VEIT, R., ZANKL, M., Variation in organ doses in pediatric radiology due to patient diameter, calculated with phantoms of varying voxel size, Radiat. Prot. Dosim. **49** (1993) 353–356

[VI.35] HART, D., JONES, D.G., WALL, B.F., Estimation of Effective Dose in Diagnostic Radiology from Entrance Surface Dose and Dose–Area Product Measurements, Rep. NRPB-R262, National Radiological Protection Board, Chilton (1994).

[VI.36] LEHERON, J.C., XDOSE: A User's Guide, National Radiation Laboratory, Christchurch (1994).

[VI.37] HART, D., JONES, D.G., WALL, B.F., Normalised Organ Doses for Paediatric X-Ray Examinations Calculated Using Monte Carlo Techniques, Rep. NRPB-SR279, National Radiological Protection Board, Chilton (1996).

[VI.38] HART, D., JONES, D.G., WALL, B.F., Coefficients for Estimating Effective Doses from Paediatric X-Ray Examinations, Rep. NRPB-279, National Radiological Protection Board, Chilton (1996).
[VI.39] LEHERON, J.C., CHILDOSE Computer Program, National Radiation Laboratory, Christchurch (1996).
[VI.40] TAPIOVAARA, M., LAKKISTO, M., SERVOMAA, A., PCXMC: A PC-Based Monte Carlo Program for Calculating Patient Doses in Medical X-Ray Examinations, Rep. STUK-A139, STUK, Helsinki (1997).
[VI.41] ZANKL, M., PANZER, W., DREXLER, G., The Calculation of Dose from External Photon Exposures Using Reference Human Phantoms and Monte Carlo Methods, Part VI: Organ Doses from Computed Tomographic Examinations, Rep. Bericht 30/91, GSF National Research Centre for Environment and Health, Neuherberg (1991).
[VI.42] ZANKL, M., PANZER, W., DREXLER, G., Tomographic Anthropomorphic Models, Part II: Organ Doses from Computed Tomographic Examinations in Paediatric Radiology, Rep. Bericht 30/93, GSF National Research Centre for Environment and Health, Neuherberg (1993).
[VI.43] JONES, D.G., SHRIMPTON, P.C., Survey of CT Practice in the UK, Part 3: Normalised Organ Doses Calculated Using Monte Carlo Techniques, Rep. NRPB-R250, National Radiological Protection Board, Chilton (1991).
[VI.44] JONES, D.G., SHRIMPTON, P.C., Normalised Organ Doses for X-ray Computed Tomography Calculated Using Monte Carlo Techniques, Rep. NRPB-SR250, National Radiological Protection Board, Chilton (1993).
[VI.45] INTERNATIONAL COMMISSION ON RADIATION UNITS AND MEASUREMENTS, Radiation Dosimetry: X Rays Generated at Potentials of 5 to 150kV, ICRU Rep. 17, ICRU, Bethesda, MD (1970).
[VI.46] IMPACT, ImPACT CT Dosimetry Calculator, Imaging Performance Assessment of CT Scanners (2002), http://www.impactscan.org
[VI.47] NAGEL, H.D., Radiation Exposure in Computed Tomography: Fundamentals, Influencing Parameters, Dose Assessment, Optimization, Scanner Data, Terminology, CTB Publications, Hamburg (2002).
[VI.48] LEHERON, J.C., CTDOSE Computer Program, National Radiation Laboratory, Christchurch (1993).
[VI.49] INTERNATIONAL COMMISSION ON RADIOLOGICAL PROTECTION, Statement from the 1987 Como meeting of the ICRP, Publication 52, Pergamon Press, Oxford and New York (1987).
[VI.50] NATIONAL RADIOLOGICAL PROTECTION BOARD, Diagnostic Medical Exposures: Advice on Exposure to Ionizing Radiation During Pregnancy, NRPB, Chilton (1998).
[VI.51] INTERNATIONAL COMMISSION ON RADIOLOGICAL PROTECTION, Pregnancy and Medical Radiation, Publication 84, Pergamon Press, Oxford and New York (2000).
[VI.52] TUNG, C.-J., TSAI, H.-Y., Evaluations of gonad and fetal doses for diagnostic radiology, Proc. Natl. Sci. Counc. **23** (1999) 107–113.

[VI.53] OSEI, E.K., DARKO, J.B., FAULKNER, K., KOTRE, C.J., Software for the estimation of foetal radiation dose to patients and staff in diagnostic radiology, J. Radiol. Prot. **23** (2003) 183–194.
[VI.54] CARLSSON, C.A., Integral absorbed doses in roentgen diagnostic procedures, I: The dosemeter, Acta Radiol. **3** (1965) 310–326.
[VI.55] PYCHLAU, H., PYCHLAU, P., Ein Diagnostik-Dosimeter-Grundform und Abwandlung, Fortschr. Roentgenstr. **100** (1964) 177–180.
[VI.56] REINSMA, K., Dosemeters for X-ray diagnosis, Philips Technical Library, Eindhoven (1960) (in Dutch).
[VI.57] ALM CARLSSON, G., CARLSSON, C.A., Relations between effective dose equivalent and mean absorbed dose (energy imparted) to patients in diagnostic radiology, Phys. Med. Biol. **31** (1986) 911–921.
[VI.58] WALL, B.F., SHRIMPTON, P.C., "Deliberations on a suitable quantity and technique for assessing the somatic risk in diagnostic radiology", Patient Exposure to Radiation in Medical X-Ray Diagnosis (DREXLER, G., ERISKAT, H., SCHIBILLA, H., Eds), Rep. EUR 7438, European Commission, Luxembourg (1981).
[VI.59] CARLSSON, C.A., ALM CARLSSON, G., "Dosimetry in diagnostic radiology and computerised tomography", The Dosimetry of Ionizing Radiation (KASE, K.R., BJÄRNGARD, B.E., ATTIX, F.H., Eds), Academic Press, Orlando (1990) 163–257.
[VI.60] SHRIMPTON, P.C., WALL, B.F., JONES, D.G., FISHER, E.S., The measurement of energy imparted to patients during diagnostic X-ray examinations using the diameter exposure–area product meter, Phys. Med. Biol. **29** (1984) 1199–1208.
[VI.61] PERSLIDEN, J., ALM CARLSSON, G., Energy imparted to water slabs by photons in the energy range 5–300 keV: Calculations using a Monte Carlo photon transport model, Phys. Med. Biol. **29** (1984) 1075–1088.
[VI.62] GIBBS, S.J., Vanderbilt University Medical Center, Department of Radiology and Radiological Sciences, personal communication, 1988.
[VI.63] BIRCH, R., MARSHALL, M., ARDRAN, G.M., Catalogue of Spectral Data for Diagnostic X-Rays, Rep. SRS 30, Hospital Physics Association, London (1979).
[VI.64] PERSLIDEN, J., SANDBORG, M., Conversion factors between energy imparted to the patient and air collision kerma integrated over beam area in pediatric radiology, Acta Radiol. **34** (1993) 92–98.
[VI.65] ALMÉN, A., NILSSON, M., Simple methods for the estimation of dose distributions, organ doses and energy imparted in paediatric radiology, Phys. Med. Biol. **43** (1996) 1093–1105.
[VI.66] STENSTRÖM, B., HENRIKSON, C.O., KARLSSON, L., SARBY, B., Energy imparted from intraoral radiography, Swed. Dent. J. **10** (1986) 125–136.
[VI.67] UNITED NATIONS, Sources and Effects of Ionizing Radiation (Report to the General Assembly), Scientific Committee on the Effects of Atomic Radiation (UNSCEAR), UN, New York (2000).

[VI.68] NATIONAL RADIOLOGICAL PROTECTION BOARD, "Patient dose reduction in diagnostic radiology", Documents of the NRPB, Vol. 1, No. 3, Rep. No. 3, NRPB, Chilton (1990).
[VI.69] NATIONAL RADIOLOGICAL PROTECTION BOARD, "Medical exposure: Guidance on the 1990 Recommendations of the ICRP", Documents of the NRPB, Vol. 4, No. 2, Rep. No. 2, NRPB, Chilton (1993).
[VI.70] LEHERON, J.C., Estimation of effective dose to the patient during medical X-ray examination from measurements of dose–area product, Phys. Med. Biol. **37** (1992) 2117–2126.
[VI.71] WILLIAMS, J.R., MONTGOMERY, A., Measurement of dose in panoramic dental radiology, Br. J. Radiol. **73** (2000) 1002–1006.
[VI.72] BRIX, G., et al., Assessment of a theoretical formalism for dose estimation in CT: An anthropomorphic phantom study, Eur. Radiol. **14** (2004) 1275–1284.
[VI.73] STAMM, G., NAGEL, H.D., CT-Expo — ein neuartiges Programm zur Dosisevaluierung in der CT, Fortschr. Roentgenstr. **174** (2002) 1570–1576.
[VI.74] EUROPEAN COMMISSION, European Guidelines for Quality Criteria for Computed Tomography, Rep. EUR 16262, EC, Luxembourg (2000).
[VI.75] HUDA, W., GKANATSIOS, N.A., Effective dose and energy imparted in diagnostic radiology, Med. Phys. **24** (1997) 1311–1316.
[VI.76] WISE, K.N., SANDBORG, M., PERSLIDEN, J., ALM CARLSSON, G., Sensitivity of coefficients for converting entrance surface dose and kerma–area product to effective dose and energy imparted to the patient, Phys. Med. Biol. **44** (1999) 1937–1954.
[VI.77] GOSCH, D., GURSKY, S., Describing the radiation exposure of patients in diagnostic radiology on the basis of absorbed energy, Radiat. Prot. Dosim. **43** (1992) 115–117.
[VI.78] LECOMBER, A.R., YONEYAMA, Y., LOVELOCK, D.J., HOSOI, T., ADAMS, A.M., Comparison of patient dose from imaging protocols for dental implant planning using conventional radiography and computed tomography, Dentomaxillofac. Radiol. **30** (2001) 255–259.
[VI.79] STENSTRÖM, B., HENRIKSON, C.O., KARLSSON, L., SARBY, B., Effective dose equivalent from intraoral radiography, Swed. Dent. J. **11** (1987) 71–77.
[VI.80] HUDA, W., ATHERTON, J.A., Energy imparted in computed tomography, Med. Phys. **22** (1995) 1263–1269.

Appendix VII

BACKGROUND TO THE CODE OF PRACTICE FOR CLINICAL MEASUREMENTS

VII.1. INTRODUCTION

Patient dose determination and dose audits are important tools for quality assurance in medical radiology. In order to document patient exposures, well-defined and easy to use methods of dose measurement are needed. Quality control in medical radiology also requires methods to estimate image quality for optimization of the imaging procedure. The concepts of diagnostic reference (guidance) levels were introduced as a tool to achieve practical optimization [VII.1]. In order to allow for meaningful comparisons between hospitals, nationally and internationally, standardized methods of dose measurement on phantoms and patients are needed. Doses[1] from diagnostic X ray procedures provide by far the largest contribution to the population dose from artificial sources. Since the risk for stochastic effects (induction of cancer and genetic disorders) is believed to be without a threshold, the detriment to the population increases with increasing population dose. Patient dose measurements are therefore becoming increasingly important.

It is preferable to make dose measurements using a phantom to simulate a patient for the control of technical parameters, the comparison of the same system at different times, the comparison of different systems and for optimization. When a phantom is used, the measured dose will depend upon the phantom shape and size and it is essential that the phantom be standardized so that such variations are avoided.

Dose assessments with a phantom cannot provide a direct estimate of the average dose for a given patient population and cannot indicate the dose variations seen in practice because of differences in patient size and composition and in radiographic technique. It is important therefore that any measurements made with phantoms are supplemented by measurements made on patients.

The following discussion presents background material concerning the choice of phantoms and the practical methodology for measurements with phantoms and patient dosimetry used in this Code of Practice.

---

[1] Whenever the terms dose or patient dose are used without qualification, they are used in a generic sense.

VII.2. DESIGN OF PHANTOMS

Standard phantoms should be designed and constructed so that they offer the same primary attenuation and scatter production as the relevant body section(s) of a representative patient over the relevant range of X ray energies used in the clinic. Scatter production may be important in terms of the spectrum of scattered radiation leaving the exit surface of the phantom and/or in terms of the spectrum of backscattered radiation. It is desirable that such phantoms be inexpensive, be constructed from readily available materials of stable and homogeneous composition and be stable dimensionally.

Tissue substitute materials suitable for use in diagnostic radiology are described in ICRU 44 [VII.2]. They include acrylic resins that can be varied in composition to match the properties of particular types of tissue [VII.3, VII.4] and readily available materials such as PMMA (also known as Perspex or Lucite), polystyrene and water.

Sandborg et al. [VII.5] investigated the equivalency of 10 different phantom materials with respect to properties such as contrast, tube loading to maintain a fixed energy imparted to the image receptor, signal to noise and contrast increase as well as dose increase factors using a grid. The thickness of the phantom material corresponding to a given thickness of soft tissue was determined at 100 kV tube voltage. The equivalent thickness was found to depend on the soft tissue thickness and the particular quantity studied. Tissue substitutes 'Mix-D', 'M3' and water showed the closest resemblance to soft tissue while materials without elements of atomic number >6 (polystyrene and paraffin wax) were less good. PMMA was intermediate in performance between these two groups.

ICRU 48 [VII.6] describes, inter alia, phantoms which are suitable for measurements in diagnostic radiology. A wide range of such phantoms is available which are appropriate for various imaging and dosimetric tasks. Some are designed for specific X ray procedures whereas others are of general utility. The latter include anthropomorphic phantoms, constructed from tissue substitute materials sometimes with embedded human bones. Such phantoms often have cavities for the insertion of TLDs and are very useful for detailed studies of the dose distribution within the body.

Simple phantoms can be constructed entirely from PMMA or using PMMA (or polystyrene) as the wall of a box which is filled with water (e.g. Dance [VII.7], ICRU [VII.6] and Martin et al. [VII.8]). They can be of value when measuring incident or entrance surface air kerma. The latter phantoms can also be constructed using a suitable solid substitute for water [VII.8].

Jennings [VII.9] describes a method for designing two component phantoms which can accurately simulate the attenuation and scattering

properties of a given body section. Such phantoms consisting of PMMA and aluminium have been developed by the CDRH for chest (PA), abdomen (AP) and lumbosacral (AP) examinations [VII.10, VII.11] of averaged-sized US patients. They are referred to in the following text as CDRH or FDA/CDRH phantoms.

VII.3. GENERAL RADIOGRAPHY

General radiography refers to a broad range of diagnostic imaging procedures, covering X ray imaging of head, chest, abdomen, extremities, etc. Owing to the broad imaging base, the range of doses received by patients in general radiography is also broad. Some studies [VII.12] show that even now, order of magnitude variations in patient doses are possible for the same diagnostic examinations.

The following discussion presents background material concerning the choice of phantoms for dosimetry in general radiography and the practical methodology used in this Code of Practice for conducting measurements with phantoms and on patients.

VII.3.1. Phantoms

Phantoms of varying degrees of complexity and anatomical accuracy have been used in general radiography. Examples of some of the simpler phantoms are given in Table VII.1.

The CDRH chest phantom [VII.10] is constructed to correspond to an average US citizen in the postero–anterior projection (225 mm thickness) with the AEC determined by detectors placed over the lung field. For systems using field centred detectors, the phantom is too thin and will underestimate the exposure time needed with a real patient. The phantom has a holder for an ionization chamber. It is situated at a distance from the phantom surface (220 mm) sufficient to ensure that the backscatter contribution is less than 2%. Incident air kerma has to be calculated using the inverse square law. The phantom has not been tested under extreme technique conditions, e.g. for tube voltages greater than 150 kV or with primary filtration other than aluminium.

The CDRH abdomen phantom [VII.11] is constructed to correspond to an average US citizen in the antero–posterior projection (230 mm thickness). The accuracy of the phantom to reproduce transmitted primary energy spectra has been tested in the range 90–120 kV. Good matching was achieved for spectra transmitted through both the soft tissue and spinal areas of the

TABLE VII.1. EXAMPLES OF SIMPLE PHANTOMS USED FOR GENERAL RADIOGRAPHY

Phantom	Description	References
CDRH postero–anterior (LucAl) chest phantom	2 pcs 254 mm × 254 mm × 9.5 mm PMMA 1 pc 254 mm × 254 mm × 54 mm PMMA 2 pcs 254 mm × 254 mm × 9.5 mm PMMA 1 pc 254 mm × 254 mm × 1.6 mm Al (type 1100 Al) 1 pc 254 mm × 254 mm × 2.5 mm Al (type 1100 Al) 190 mm air gap	Conway et al. [VII.10]
CDRH antero–posterior (LucAl) abdomen/lumbar spine phantom	*Abdomen section (outside spine insert):* 1 pc 254 mm × 254 mm × 169.2 mm PMMA *Lumbosacral spine section:* 1 pc 254 mm × 254 mm × 168.9 mm PMMA 1 pc 254 mm × 254 mm × 2 mm Al (type 1100 Al) 1 pc 254 mm × 254 mm × 9.5 mm PMMA 1 pc 254 mm × 254 mm × 2.5 mm Al (type 1100 Al) 1 pc 254 mm × 254 mm × 9.5 mm PMMA	Conway et al. [VII.11]
Modified CDRH skull phantom	43 mm PMMA and 5 mm Al placed inside the LucAl chest phantom (the 5 mm Al is in contact with the thinner part of the chest phantom)	Servomaa and Tapiovaara [VII.16]
Modified CDRH thoracic spine phantom	An additional 2.5 mm Al and 95 mm PMMA placed inside the LucAl chest phantom (2.5 mm Al in contact with the thicker part of the chest phantom. The width of the additional part is 100 mm)	Servomaa and Tapiovaara [VII.16]
ICRU head phantom	160 mm × 160 mm × 160 mm PMMA (approx. 6 mm) filled with water Cavities are available for radiation detectors at depths: surface, 40, 80, 120 mm	ICRU [VII.6]
ICRU abdomen phantom	300 mm × 300 mm × 300 mm PMMA (approx. 6 mm) filled with water Cavities are available for radiation detectors at depths: surface, 50, 100, 150, 200, 250 mm	ICRU [VII.6]

TABLE VII.1. EXAMPLES OF SIMPLE PHANTOMS USED FOR GENERAL RADIOGRAPHY (cont.)

Phantom	Description	References
ANSI chest phantom	4 pcs 305 mm × 305 mm × 25.4 mm PMMA 1 pc. 305 mm × 305 mm × 1 mm (type 1100 Al) 1 pc. 305 mm × 305 mm × 2 mm (type 1100 Al) 50.8 mm air gap	ANSI [VII.13] AAPM [VII.14]
Modified ANSI abdomen/ lumbar spine phantom	7 pcs 305 mm × 305 mm × 25.4 mm PMMA 1 pc 70 mm × 305 mm × 4.5 mm (type 1100 Al)	ANSI [VII.13] AAPM [VII.14]
ANSI skull phantom	4 pcs 305 mm × 305 mm × 25.4 cm PMMA 1 pc 305 mm × 305 mm × 1.0 mm (type 1100 Al) 1 pc 305 mm × 305 mm × 2.0 mm (type 1100 Al) 1 pc 305 mm × 305 mm × 50.8 mm PMMA	ANSI [VII.13] AAPM [VII.14]
ANSI extremity phantom	1 pc 305 mm × 305 mm × 25.4 mm PMMA 1 pc 305 mm × 305 mm × 2.0 mm (type 1100 Al)	ANSI [VII.13] AAPM [VII.14]

phantom when compared with measurements on an anthropomorphic phantom consisting of a human skeleton embedded in tissue-simulating plastic. These two areas correspond to the regions of interest over which the AEC detectors integrate. Comparison of the air kerma measured in broad beam conditions behind the two phantoms (with and without the grid) was made for different arrangements of the aluminium and PMMA in the spinal region to obtain a good match at both the soft tissue and the spinal area AEC detectors [VII.11].

Two component phantoms of PMMA and aluminium have also been developed by the American National Standard Institute (ANSI) [VII.13]. Dose measurements obtained with a modified ANSI phantom and the CDRH phantoms have been compared. The incident air kerma obtained with the ANSI phantom was found to be 33% higher than with the CDRH chest phantom but 15% lower than with the CDRH abdomen and lumbar spine phantoms [VII.14]. The patient equivalency of the CDRH phantoms has been established clinically by the US Food and Drug Administration (FDA) and the CDRH and they have been widely used in the US Nationwide Evaluation of X ray Trends (NEXT) surveys [VII.15]. The CDRH chest phantom is also referred to as the 'LucAl' phantom.

Servomaa and Tapiovaara [VII.16] have modified the CDRH chest phantom in order to construct phantoms suitable for skull and thoracic spine (AP) examinations and compared them with an Alderson-Rando male

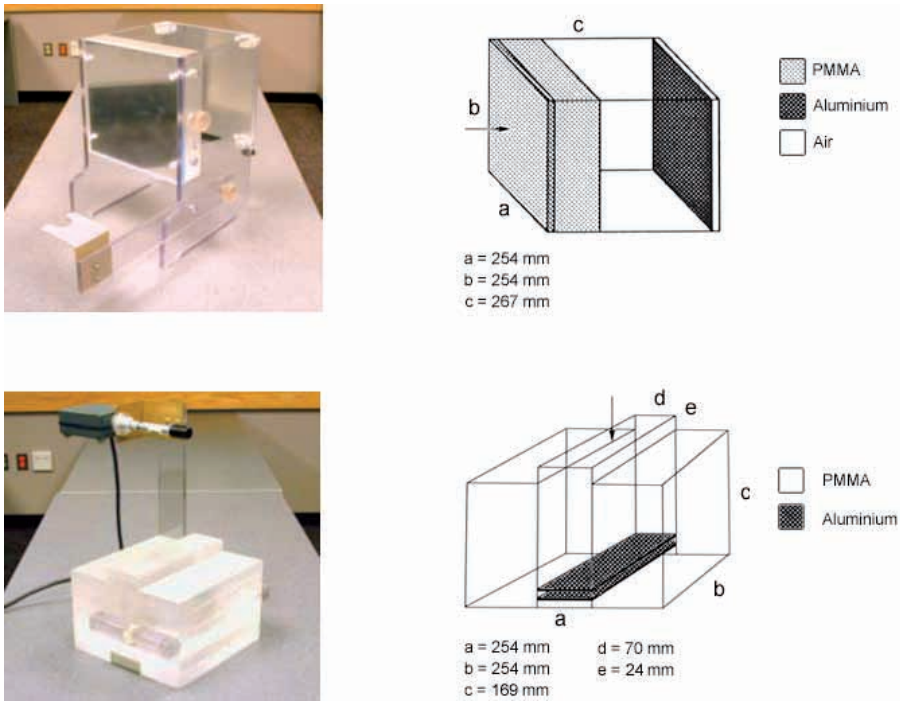

FIG. VII.1. Photographs and drawings of CDRH postero–anterior chest phantom (upper) and CDRH antero–posterior abdomen/lumbar spine phantom (lower) [VII.6].

phantom. Scatter matching was obtained by adjusting the relative positions of PMMA and aluminium so that air kerma values behind the phantoms were the same for both the anthropomorphic and the homogeneous phantoms at defined positions.

For the sake of simplicity, only two common applications, chest (PA) and abdomen (AP), are considered in this Code of Practice. On the basis of the above discussion, the recommended phantoms for the measurement of incident air kerma for these procedures are the CDRH postero–anterior chest and antero–posterior abdomen/lumbar spine phantoms.

Such phantoms may be purchased commercially or manufactured in the hospital workshop. They are illustrated in Fig. VII.1. Construction details are available by contacting the FDA (http://www.fda.gov.cdrh/radhlth/next.html).

VII.3.2. Measurements using phantoms

For general radiography, the incident air kerma is measured for standard phantoms utilizing the X ray technique factors for an average adult patient.

The methodology is described in Section 8.4 for two common imaging tasks: chest and abdomen/lumbar spine. The recommended phantoms for the determination of incident air kerma are the CDRH postero–anterior chest and CDRH antero–posterior abdomen/lumbar spine phantoms discussed above. The methodology can also be applied to other situations where suitable representative phantoms are available.

The procedure for measurement of the incident air kerma is based on the NEXT protocols for the survey of adult chest and abdomen radiography [VII.17, VII.18]. In 2007, these protocols were also available on-line (www.crcpd.org). Protocols describe procedures for capturing data and information which characterize patient exposure and image quality for screen–film radiography systems, computed radiography systems and other digital based X ray imaging systems in the USA. Compared with the NEXT protocols, the procedures described in Section 8.4 only concern the measurement of the incident air kerma, they do not cover procedures for the evaluation of imaging properties.

VII.3.3. Patient dosimetry

For general radiography, the incident air kerma, entrance surface air kerma or air kerma–area product may be used for the routine monitoring of patient dose. The incident air kerma can be determined indirectly with a knowledge of the technique factors (tube voltage, tube loading, focus to skin distance and field size) for each patient undergoing X ray examination. In this approach, the incident air kerma is calculated from these factors using the known output of the X ray equipment for a given tube voltage, tube loading, filtration and focus to skin distance using the inverse square law. If necessary, entrance surface air kerma can then be estimated by applying an appropriate backscatter factor (see Section 8.4). This method, also known as the semi-empirical method, has been adopted by researchers such as Harrison et al. [VII.19] and Heggie [VII.20]. Comparison of dose derived from thermoluminescence measurements and the calculation method have been shown to agree to within ±10% [VII.20, VII.21]. The methodology for the measurement of air kerma product using a KAP meter is discussed in the sections on fluoroscopy (see Section 8.5) and is not repeated for general radiography.

The measurement of entrance surface air kerma, K_e, provides a direct assessment of patient dose. The method described in this Code of Practice uses TLDs attached to the patient's skin to measure the entrance surface air kerma for the chest examination but it may be applied for other situations in general radiography. The measurement technique and protocol are adapted from the

UK's National Protocol for Patient Dose Measurement in Diagnostic Radiology [VII.22].

The TLDs used for the measurement have to be calibrated. The calibration should be carried out at a dose and with an X ray quality typical of those to which the dosimeters will be exposed in the course of the patient dose measurement. The calibration of TLDs is described in Appendix IX.

VII.4. FLUOROSCOPY INCLUDING INTERVENTIONAL PROCEDURES

Fluoroscopy is frequently used to assist in a wide variety of medical diagnostic procedures. More complex examinations also involve the use of fluoroscopic imaging as well as the generation of radiographs of selected anatomical regions. There are many factors that determine the patient dose during fluoroscopy examinations. In addition to the dose mode selected, factors such as the frame rate (for fluorography and pulsed fluoroscopy), the number of radiographs generated, field size and fluoroscopy duration are important. The fluoroscopic equipment is capable of producing very high radiation dose rates and fluoroscopy exposure times are normally measured in minutes. As a result, examinations involving fluoroscopy have radiation doses that may be markedly higher than those encountered in simple radiography.

In interventional procedures, the local skin dose may become very high owing to long periods of fluoroscopy and the high number of frames and this may result in skin burns. Estimation of the entrance surface air kerma on patients during fluoroscopically guided procedures is therefore important. In such procedures, the position of the entrance surface on the patient is not fixed and special methods are required to locate the maximum value of the entrance surface air kerma. Since no standardized method exists, specific recommendations on how to measure the maximum skin absorbed dose in interventional procedures are not given in this Code of Practice but are discussed briefly.

VII.4.1. Measurements using phantoms

Modern fluoroscopy systems employ automatic brightness control to maintain constant brightness of the fluoroscopic image. Therefore, laterally homogeneous phantoms are preferred because of the difficulty of positioning an inhomogeneous phantom so as to achieve reproducible measurements. Suleiman et al. [VII.23] modified the CDRH abdomen/lumbar spine phantom for fluoroscopy applications. The separate 'spine' in the radiographic phantom was removed in order to obtain a laterally homogeneous phantom. Its

cross-sectional area is smaller since fluoroscopic fields are usually smaller than conventional radiographic fields. Martin et al. [VII.8] recommend the use of a rectangular phantom of tissue equivalent material of cross-sectional area 300 mm × 300 mm and thickness 200 mm in accordance with the recommended standard in the UK [VII.24]. The 200 mm thick phantom represents a standard adult. As a substitute, these authors suggest the use of two polycarbonate containers, each 100 mm thick, filled with water. A third container of the same size may be added to simulate a heavier patient. The walls of the container can also be made of PMMA.

Solid PMMA slabs provide an alternative that might be preferred because they are easier to handle. Faulkner et al. [VII.25] recommend the use of a 200 mm PMMA phantom for this purpose. Martin et al. [VII.8] provide a correction factor of 1.22 with which to reduce measurements of the entrance surface air kerma made with a 200 mm PMMA phantom to correspond to measurements using a 200 mm water phantom. The use of this single correction factor will introduce an uncertainty of 10%. These authors also calculated, as a function of tube voltage, the thickness of PMMA that corresponds to 200 mm of water with respect to attenuation. They found that a thickness of 185 mm could be used to simulate 200 mm of water for tube voltages in the range 60–110 kV with an uncertainty of less than 2%. While this is true for the radiation transmitted through the phantom, which controls the function of the automatic brightness control, the backscattering properties of the phantom are also important when entrance surface air kerma rates are measured. A correction for different backscatter factors will be needed. Backscatter factors for water and PMMA are given in Table VIII.1. The table shows that PMMA is a more effective scatterer than water. The quotient, B_{water}/B_{PMMA}, between the backscatter factors for water and PMMA varies in the range 0.92–0.93 for field sizes 200 mm × 200 mm and 250 mm × 250 mm for tube voltages in the range 60–150 kV.

For an under couch installation, a rig is required to support the phantom and allow the dosimeter to be placed in close contact with it. The rig may consist of two PMMA bars of rectangular cross-section, the height of which is just larger than the thickness of the ionization chamber, which is placed under opposite edges of the phantom.

A phantom with a smaller cross-sectional area may be used for measurements on smaller image intensifier fields but the area must be large enough to cover the entire X ray beam at its exit surface with the collimators fully open. The CDRH fluoroscopy phantom [VII.23] has a cross-sectional area of 178 mm × 178 mm. It consists of PMMA and aluminium sheets. The aluminium sheets cover the side of the phantom facing the X ray tube. Since the backscatter from the aluminium is likely to be considerably different from that of water, this

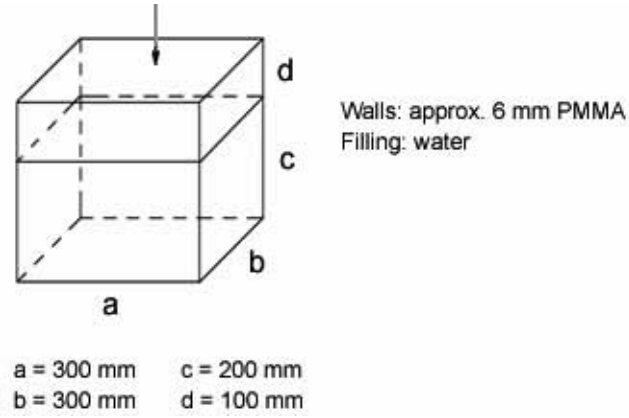

FIG. VII.2. Water phantom for measurements of entrance surface air kerma in fluoroscopy.

arrangement is less satisfactory for measurements of entrance surface air kerma.

To simulate heavier patients, Martin et al. [VII.8] recommend an additional thickness of 100 mm of water be added to the 200 mm standard phantom. It is noted that in order to have a standardized geometry with flexible use of different phantom thicknesses, the 200 mm phantom leaves an air gap between it and the image intensifier (see Chapter 8).

Phantoms recommended for use in fluoroscopy in this Code of Practice include a water phantom of thickness 200 mm and cross-sectional area 300 mm × 300 mm to be used for measurement of entrance surface air kerma in standard conditions. Alternatively, a phantom of 185 mm PMMA can be used. To simulate heavier patients, 100 mm of water should be added to the standard phantom [VII.8] (see Fig. VII.2).

VII.4.2. Patient dosimetry

VII.4.2.1. Fluoroscopy

The air kerma–area product, P_{KA}, offers a convenient quantity for monitoring patient exposure as it reflects changes in both dose rate and beam area which may occur during a procedure. It is closely related to the energy imparted to the patient and effective dose (see Appendix VI) and is thus suitable for comparisons of patient exposures. Its use is therefore recommended in this Code of Practice.

Measurement of P_{KA} can be accomplished using a plane transmission ionization chambers mounted on the collimator housing and covering the whole of the X ray beam. It is noted that the transmission ionization chamber is often called a dose–area product meter, but as the quantity measured is the air kerma–area product, the abbreviation 'KAP' is used here. KAP meters need to be calibrated in situ in the clinic for every X ray stand in order to handle properly the heterogeneous distribution of air kerma in the beam caused by the heel effect and extrafocal radiation. In situ KAP meter calibrations have been described in detail by Carlsson [VII.26], Shrimpton and Wall [VII.27] and Larsson et al. [VII.28, VII.29]. Calibration methods adopted by this Code of Practice are described in Appendix IX.

For use in paediatric radiology, it has been recommended by the European Commission [VII.30] and others [VII.31] that an extra copper filter be added to the conventional filter. The same applies to interventional procedures. A separate calibration needs to be performed for this set-up. The added filter introduces a beam hardening effect that may change the calibration coefficient by as much as 6% at the same tube voltage [VII.32]. In some practices this has been accomplished by placing the extra filter on top of the KAP meter [VII.33]. The signal from the KAP meter will increase more than the signal from the reference chamber owing to the effect of scattered radiation produced in the filter. Larsson [VII.32] showed that the calibration constant decreased by about 10% compared with the value obtained with the copper filter in the position of the holder for the primary filter, 150 mm above the KAP meter.

A portable KAP meter calibrated for transmitted radiation (see Chapters 6 and 7) at an SSDL can also be used for measurements on various X ray machines in the hospital. It is noted that when such a KAP meter is used in an under couch installation, a correction is needed for the attenuation in the table top and possibly backscatter from the patient and table top [VII.34]. The attenuation by the table top can be estimated as 15–30% for beam qualities with an HVL of 2–7 mm Al [VII.35, VII.36].

VII.4.2.2. Interventional procedures

In fluoroscopy guided interventional procedures, the air kerma–area product, P_{KA}, offers a convenient quantity for monitoring patient exposure. However, such procedures may give rise to high skin absorbed doses and monitoring of the skin absorbed dose is important because of the potential for reaching the threshold for deterministic effects. The determination of the dose to the most exposed area is not straightforward since exposure parameters and projection angle change during the procedure and the most exposed area

cannot always be anticipated. In order to estimate the peak skin absorbed dose it is therefore necessary to have a detector that registers the skin dose at many points simultaneously. Such distributions can be obtained using a rectangular array of TLDs attached to the patient's skin with a maximum separation between dosimeters of about 10 mm, which makes the practical application of the technique difficult. Another way is to use a low sensitivity film (commonly used in radiotherapy) positioned close to the patient where the film optical density is calibrated. The optical density of this type of film saturates at a dose of about 1–2 Gy. The method is thus not capable of determining the maximum dose in some cases [VII.37, VII.38]. This drawback can be overcome by using radiochromic film, the sensitivity of which is adequate even for high dose interventional procedures. Giles and Murphy [VII.39] have evaluated the dose characteristics of this material.

A drawback of the dose mapping procedures described above is that they do not give an answer in real time so as to allow possible adjustments of the technique (e.g. changing projection) during the procedure. Real time measurements are possible to perform using real time detectors located on or near the skin but these cannot generally provide complete dose mapping since the number of real time detectors that can be used will be limited. A priori knowledge of the position of the maximum skin absorbed dose would therefore be needed. Since this cannot be known beforehand, the reading from the detector can severely underestimate the maximum skin dose. Real time detectors currently available are MOSFET detectors [VII.40, VII.41] and scintillation detectors consisting of zinc–cadmium [VII.42, VII.43] or aluminium oxide (Al_2O_3:C) [VII.44]. Scintillation detectors are bonded to an optical fibre and both the instantaneous dose rate and the cumulative absorbed dose can be measured.

Two alternative approaches to estimate the maximum possible incident air kerma have also been described. The first method uses measurements at a reference point in the beam, the so-called 'interventional reference point', defined in IEC-60601-2-43 [VII.45] as a point on the central ray of the X ray beam which is 150 mm from the isocentre of the radiological equipment in the direction of the X ray tube. The value of the air kerma at the interventional reference point is inferred from measurements obtained by a detector placed at the beam port (e.g. systems described by Gkanatsios et al. [VII.46] and Cusma et al. [VII.47]). The method does not take into consideration changes of projection during the procedure and the cumulative air kerma at the interventional reference point and thus may overestimate the maximum incident air kerma at any point on the patient. The second method uses measurements of P_{KA} to provide an indication of the maximum possible incident air kerma if the focus to skin distance and field area are recorded during the course of the

procedure. As changes of projection are not noted, this method overestimates the maximum incident air kerma on the patient in a way similar to the method using the interventional reference point.

A method to correlate the maximum skin dose to P_{KA} in coronary angiography examination and percutaneous transluminal coronary angioplasty intervention was published by Hansson and Karambatsakidou [VII.48] and by Sandborg et al. [VII.49] based on studies conducted on an anthropomorphic phantom. They reported conversion coefficients $c_{D_{max},P_{KA}}$ of 3.9 mSv/(Gy·cm^2) and 7.3 mSv/(Gy·cm^2) for coronary angiography and percutaneous transluminal coronary angioplasty, respectively. These conversion coefficients are in reasonable agreement with the results of Vañó et al. [VII.50], who reported values of P_{KA} and maximum skin absorbed doses from a number of hospitals and derived, on the basis of these measurements, conversion coefficients $c_{D_{max},P_{KA}}$ of (3.3 ± 2.1) mGy/(Gy·cm^2) and (6.7 ± 5.7) mGy/(Gy·cm^2) for coronary angiography and percutaneous transluminal coronary angioplasty, respectively (one standard deviation indicated). The large variation in the conversion coefficient, as indicated by the standard deviation, is consistent with the work of Waite and Fitzgerald [VII.51], who did not find any correlation between entrance skin dose and P_{KA} for cardiac percutaneous transluminal coronary angioplasty procedures. They advocate, however, along with Sandborg et al. [VII.49], the use of local P_{KA} values for specific examinations to alert staff to the potential for skin injury. On the contrary, van de Putte et al. [VII.52], in noting that total P_{KA} only gives an approximate indication of the skin dose, recommend direct measurements to monitor skin dose.

A system named CareGraph has been reported by den Boer [VII.53] and this calculates the complete skin dose distribution in real time using a mathematical model, which combines data from a KAP meter with information on changes in the irradiation geometry and exposure parameters during the procedure. This system is no longer available but development in this direction may be foreseen in the future. A review of the methods discussed in this section can be found in Balter et al. [VII.54].

None of the above described direct and indirect methods can presently be regarded as either accurate or well established. They are not, therefore, described in Chapter 8.

VII.5. MAMMOGRAPHY

The ICRP [VII.55] recommends the use of the mean (or average) absorbed dose to the glandular tissues within the breast as the risk related quantity for mammography (see Section 3.3). This recommendation has been

adopted in many national and international protocols and is followed in this Code of Practice.

It is not possible to measure the mean glandular dose directly; it is estimated from measurements of incident air kerma by application of a conversion coefficient (see Section 3.4). In this Code of Practice, the measurement and calculation methodology used generally follows the European protocol [VII.56].

Both the incident air kerma and the conversion coefficient depend upon the beam quality, the thickness of the breast (which is compressed during the exposure) and the breast glandularity. The breast thickness depends upon the radiographic projection and varies within and between populations. For example, in a survey of breast dose for women undergoing breast screening in the UK, Young and Burch [VII.57] found compressed breast thicknesses in the range 10–100 mm and average compressed breast thicknesses of 54 mm and 52 mm for medio-lateral oblique and cranio-caudal projections, respectively. In Malaysia, Jamal et al. [VII.58] reported average values of 46 mm and 38 mm for the compressed breast thickness in the same two projections. Fife [VII.59] has studied the area of the compressed breast. He recorded the width of the breast image and the chest wall to nipple distance and found values of width by breadth ranging from 120 mm × 14 mm to 250 mm × 174 mm with a median value of 180 mm × 81 mm. The study of Wu et al. [VII.60] found that the mean glandular dose decreased by 2% if the breast area was reduced by a factor of three and increased by only 0.6% if the breast area was increased by a factor of 1.5. It follows that the dose measured using a phantom chosen to be representative of a medium-sized breast will only have limited dependence on the cross-sectional area of the phantom.

The glandularity[2] of the breast will vary with the age of the woman, the size of the breast and hormonal status, but there remain wide variations in glandularity for women of a given age and fixed breast size. Breast glandularities have been estimated by several workers including Geise and Palchevsky [VII.61], Heggie [VII.62], Klein et al. [VII.63], Young et al. [VII.64], Beckett and Kotre [VII.65] and Kruger and Schueler [VII.66].

The following discussion presents background material concerning the choice of phantoms for mammography, the practical methodology used in this

[2] Estimates of glandularity will vary depending upon the breast model assumed. Glandularity here is estimated for model breasts that have a surface layer of adipose tissue of fixed thickness and a central region which is a mixture of adipose and glandular tissues. The glandularity is the fraction by mass of glandular tissue in the central region.

TABLE VII.2. PHANTOMS USED FOR BREAST DOSIMETRY

Application or protocol	Phantom construction
UK: Survey by Fitzgerald et al. [VII.68]	40 mm BR12
Germany: DGMP protocol [VII.69]	50 mm PMMA
UK: IPSM (now IPEM) protocol [VII.70–VII.72]	40 mm PMMA (up to 2003), 45 mm PMMA (from 2005)
Sweden: SSI protocol [VII.73]	45 mm PMMA
USA: ACR protocol [VII.74]	e.g. 44 mm. PMMA with 7 mm dental wax layer containing embedded test objects
Europe: European protocol [VII.56] and this Code of Practice	45 mm PMMA

Code of Practice for phantom and patient measurements, the choice of conversion coefficients and the formalism used.

VII.5.1. Measurements using phantoms

VII.5.1.1. Choice of breast phantom

A mammographic phantom should be chosen so that it approximately simulates the properties of a compressed breast in terms of the spectra of primary and scattered radiation that leave its lower surface. If measurements of entrance surface air kerma are to be made, for example, using TLDs, backscattering properties of the phantom material become important. However, the backscatter factors for PMMA and breast tissue are similar [VII.67]. In cases such as this Code of Practice, where a single phantom is used, it is only necessary for the phantom to be representative of a typical patient. It is not the intention that the dose measured with the phantom should be equal to the median or average dose from a survey of patient doses.

Table VII.2 shows some of the phantoms that have been used in national and international breast dosimetry protocols or breast dose surveys. Tissue equivalent materials are available which simulate the adipose and the glandular tissues within the breast [VII.3, VII.4] and it is possible to combine them in appropriate proportions to simulate a breast of any glandularity, for example, fabricated materials, based on the elemental composition of glandular and adipose tissue [VII.2, VII.3, VII.75] commercially available. Glandularity of 50% has in the past been regarded as typical for breasts of average thickness and is much used as a standard composition in breast dosimetry protocols. For

example, the American College of Radiology dosimetry protocol [VII.74] states that a phantom should be used which is approximately equivalent to a 42 mm thick compressed breast of 50% glandularity for X ray beam qualities used for screen–film mammography.

The 1996 European mammographic dosimetry protocol [VII.56] and this Code of Practice follow the above standard composition and use a standard breast 50 mm thick and of 50% glandularity. This breast is approximately simulated by a PMMA phantom 45 mm thick. For practical purposes, the use of PMMA has important advantages. It is cheaper than specially manufactured tissue substitutes and is more readily available. A 45 mm phantom is believed to be better suited than a 42 mm breast equivalent phantom (used for example in the American College of Radiology protocol) for testing X ray systems which offer a range of target/filter combinations, and for testing digital mammography systems [VII.72, VII.76]. The breast phantom to be used when following this Code of Practice is a 45 mm thick PMMA phantom with either a semicircular cross section of radius at least 100 mm or a rectangular cross-section with dimensions equal to or exceeding 150 mm × 100 mm.

Figure VII.3 shows an example of a phantom satisfying these recommendations. The total phantom thickness should be within 0.5 mm of its nominal thickness. Faulkner and Cranley [VII.77] found that a 2% change in the phantom thickness used in the UK mammographic dosimetry protocol caused variations in the estimate of mean glandular dose of +5% and –4%.

If it is required to estimate the incident air kerma and mean glandular dose for other breast thicknesses and compositions, measurements may be repeated using plastic phantoms of other sizes to simulate the breast. Table VII.3 is based on data from Dance et al. [VII.78] and gives equivalent breast thicknesses and glandularities simulated by a range of thicknesses of PMMA. The data are appropriate to a UK screening population of women aged 50–64. The equivalent PMMA thicknesses were determined from a computer model of the breast and imaging system and have been verified by measurement. The equivalence was chosen so that the incident air kerma at the phantom surface is the same as that at the surface of the corresponding breast.[3]

[3] The glandularity indicated by Table VII.3 for a breast 50 mm thick is less than the 50% value used for the standard breast. However, these data are for a particular population of women and may not be appropriate for other populations. The glandularity of 50% falls within the variation seen in practice, its use is well established and no change to the composition of the standard breast has therefore been made for this Code of Practice.

FIG. VII.3. Photograph of a 45 mm thick PMMA phantom for use in breast dosimetry. This particular phantom is comprised of four semicircular slabs of thickness 10 mm and one slab of thickness 5 mm. The slabs have been partially separated for purposes of illustration. The use of a multislab phantom allows the possibility of measurements at thicknesses other than 45 mm. The thickness tolerance specified for the phantom applies to the total thickness and not the thickness of the individual slabs.

VII.5.1.2. Measurement practicalities

The incident air kerma may be obtained using two alternative methods. The preferred method is to measure the air kerma in the absence of the phantom using a diagnostic dosimeter. The alternative method uses a measurement of the entrance surface air kerma using TLDs. The incident air kerma is then calculated by division by an appropriate backscatter factor. The backscatter factors used are those from the European protocol [VII.56].

Owing to the heel effect, the air kerma will vary along the anode–cathode axis of the X ray tube, which in mammography is usually oriented with the anode furthest from the chest wall. Faulkner and Cranley [VII.77] have shown that the air kerma can vary by up to 11.5% as the position of measurement is moved along the anode–cathode axis. It is therefore important to fix the position of measurement, which is taken to be a point 40 mm from the chest wall side of the phantom, centred laterally and at a height of 45 mm above the breast support. The point so-defined is referred to here as the mammographic reference point.

TABLE VII.3. EQUIVALENT THICKNESSES AND GLANDULARITIES OF COMPRESSED BREASTS SIMULATED BY PMMA

PMMA thickness (mm)	Equivalent breast thickness (mm)	Glandularity of equivalent breast (%)
20	21	97
30	32	67
40	45	40
45	53	29
50	60	20
60	75	9
70	90	4
80	103	3

VII.5.2. Patient dosimetry

It is not practical to make direct measurements of incident air kerma for patient exposures using a diagnostic dosimeter. For measurement of entrance surface air kerma, the use of TLDs could be considered, but these can be seen on the mammographic image and their use is not acceptable in some countries. Although TLDs have been used to measure the entrance exposure on 4400 women with various breast thicknesses [VII.79], they have found their greatest use in measurements on phantoms and not on patients. This Code of Practice therefore does not generally recommend the use of TLDs for measurements on patients undergoing mammography. Instead, use is made of the tube current–exposure time product (mA·s) for the patient exposure, which is recorded by the equipment. Knowledge of the X ray tube output (Eq. (3.8)) allows calculation of the incident air kerma. The mean glandular dose for each exposure may then be calculated in accordance with the methodology described below.

For an examination comprising more than one exposure of each breast, the dose to each breast is the sum of the values of the mean glandular dose to each breast from each exposure of that breast. However, when considering the organ dose for risk assessment, it is the mean glandular dose to the breasts that must be considered. This is the average of the mean glandular dose estimates for the left and right breasts.

For large breasts, it may not be possible to image the whole breast in a single exposure. Multiple exposures may therefore be used. In this situation, an approximate value of the dose for each exposure may be obtained by estimating the fraction of the total breast volume that is irradiated. This fraction can be used to scale the value of the mean glandular dose for irradiation of the whole breast. Alternatively, an overestimate of the dose may be made by assuming that the whole breast is irradiated in each exposure. When mammographic magnification views are obtained or stereotactic localization is performed, only part of the breast may again be irradiated. A similar procedure can be followed to estimate the mean glandular dose.

VII.5.3. Mammographic conversion coefficients and dose calculation

VII.5.3.1. Conversion coefficients and formalism

The mean glandular dose, D_G, may be calculated from a measurement of the incident air kerma, K_i, using the relationship:

$$D_G = c_{D_G,K_i} K_i \qquad \text{(VII.1)}$$

The conversion coefficients, c_{D_G,K_i}, may be measured using suitable phantoms, but it is more usual to make use of the results of Monte Carlo calculations. Several authors have made such calculations using simple models of the breast (e.g. Rosenstein et al. [VII.80], Wu et al. [VII.60, VII.81], Boone [VII.82, VII.83], Dance [VII.7], Zoetelief and Jansen [VII.84], Klein et al. [VII.63], Dance et al. [VII.78]). The resulting coefficients depend on the model and input data used. With quite similar models there are differences of the order of 10–15% between the results of different authors. The coefficients themselves depend upon the radiation quality, breast thickness and breast glandularity. A review of breast dosimetry is given by Dance et al. [VII.85]. The influence of model assumptions on the value of the conversion coefficients is discussed in Alm Carlsson and Dance [VII.86] and Zoetelief and Jansen [VII.84].

More recent work [VII.87] has used a voxel phantom to model the breast and spatial distributions of glandular tissue that are quite different to those in the simple breast models. As a consequence, the conversion coefficients found were also significantly different (as much as 59%). However, because the actual spatial distribution of the glandular tissue will vary widely from patient to patient and is, in general, not known, these authors did not suggest that any change be made to the conversion coefficients used for standard mammographic dosimetry.

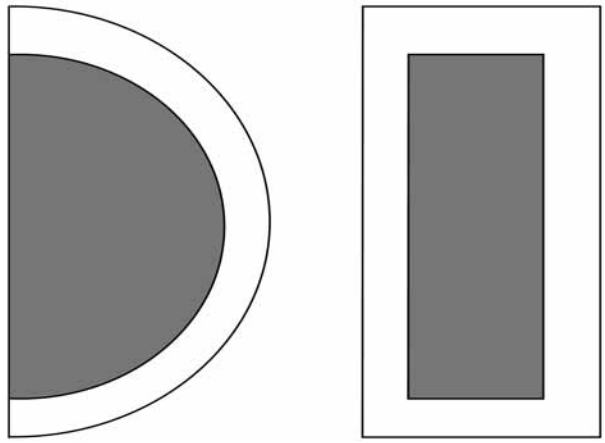

FIG. VII.4. Diagram of breast model used for the Monte Carlo calculations, which simulates the breast in cranio-caudal projection. The left side of the figure shows a horizontal cross-section through the breast model. The central (shaded) region is a uniform mixture of adipose and glandular tissues. The outer (unshaded) region represents the 'adipose shield'. The right side of the figure is a vertical cross-section through the 'chest wall' edge of the breast.

The conversion coefficients used here follow the European guidelines for quality assurance [VII.76][4] and the UK protocol [VII.72] and are based on [VII.7, VII.78]. The simple model used to simulate the breast for their computation is based on a suggestion of Hammerstein et al. [VII.75] and is shown in Fig. VII.4. The compressed breast view is modelled in the cranio-caudal projection as a cylinder of semicircular cross-section of radius 80 mm. It has a central region that is a uniform mixture of adipose and glandular tissues. Surrounding this central region on all sides apart from the chest wall is a layer of adipose tissue of uniform thickness 5 mm.

The conversion coefficients, c_{D_G,K_i}, are quality dependent and are tabulated as a function of the HVL of the X ray spectrum. In the past, mammographic X ray units have been used which have a molybdenum target and

[4] The relationship between the European and US (American College of Radiology) protocols is discussed in the European protocol. The set of mammographic conversion coefficients used in the American College of Radiology protocol is based on the Monte Carlo simulations of Wu et al. [VII.60, VII.81], which use a slightly different model of the breast. Parameterization by Sobol and Wu [VII.88] allows dose estimation for a broad range of clinical conditions.

molybdenum filter. However, equipment with different anode/filter combinations is now used which offers harder spectra for imaging larger breasts and for digital mammography [VII.78, VII.89–VII.91]. Examples include molybdenum/rhodium, rhodium/rhodium or tungsten/rhodium target/filter combinations. Since the publication of the European protocol in 1996, data have been calculated which allow its extension so that it can be used for these newer spectra [VII.78]. A correction factor, *s*, is introduced, which takes a different value for each target filter combination and is unity for the standard molybdenum/molybdenum combination. A constant value of *s* is used for each target/filter combination. This gives rise to an error of no more than 3.6% compared with that arising from the use of an individual factor for each thickness and glandularity. Equation VII.1 becomes:

$$D_{\mathrm{G}} = c_{D_{\mathrm{G}},K_{\mathrm{i}}} s K_{\mathrm{i}} \tag{VII.2}$$

In the practical situation, it is convenient to show the explicit dependence of the conversion coefficient on the breast glandularity, *g*, by writing $c_{D\mathrm{G}g,K\mathrm{i}}$ and to use the formulation:

$$c_{D_{\mathrm{G}g},K_{\mathrm{i}}} = c_{D_{\mathrm{G}50},K_{\mathrm{i}}} c_{D_{\mathrm{G}g},D_{\mathrm{G}50}} \tag{VII.3}$$

Factor $c_{D\mathrm{G}50,K\mathrm{i}}$ is the conversion coefficient for calculating the mean glandular dose for a breast of 50% glandularity (see Table 8.10) and $c_{D\mathrm{G}g,D\mathrm{G}50}$ is given by:

$$c_{D_{\mathrm{G}g},D_{\mathrm{G}50}} = \frac{c_{D_{\mathrm{G}g},K_{\mathrm{i}}}}{c_{D_{\mathrm{G}50},K_{\mathrm{i}}}} \tag{VII.4}$$

The expression for the mean glandular dose for a breast of glandularity, *g*, becomes:

$$D_{\mathrm{G}} = c_{D_{\mathrm{G}50},K_{\mathrm{i}}} c_{D_{\mathrm{G}g},D_{\mathrm{G}50}} s K_{\mathrm{i}} \tag{VII.5}$$

The calculation thus becomes a calculation for a breast of glandularity 50% multiplied by the factor $c_{D\mathrm{G}g,D\mathrm{G}50}$ which corrects for the actual glandularity, *g*. The advantage of this formulation is that for a given glandularity and HVL, the value of $c_{D\mathrm{G}g,D\mathrm{G}50}$ shows little variation with the choice of tube target or filtration. This conversion coefficient is therefore tabulated against just HVL and glandularity (Table 8.11). The error associated with this simplification is of the order of 2% or less [VII.78]. Linear interpolation in the tabulations of

$c_{D_{Gg},D_{G50}}$ in Table 8.10 as a function of glandularity is adequate and will give rise to errors of similar magnitude.

In order to ascertain the conversion coefficients for the estimation of mean glandular dose from the tables provided in Chapter 8, it is necessary to know the HVL, which should be measured. For situations where a measured value is not available, a table of standard HVLs is provided (Table 8.7). The data in the table are based on a survey of 1459 HVL measurements in the UK's national health service breast screening programme [VII.92]. The average values of the measured HVL have been 'fitted' to a straight line as a function of measured tube voltage and the results from the fit tabulated. The fitted values differed from the actual mean values by no more than 1.4% and the standard deviation of the distribution of values for any given target/filter combination and tube voltage was at most 5.5%. This value corresponded to a difference of 5% in the estimated mean glandular dose for the exposure of the 45 mm PMMA phantom.

VII.5.3.2. Dose calculation for measurements with phantoms

As noted above, the breast phantom used in this Code of Practice is a slab of PMMA 45 mm thick, which simulates a 'standard compressed breast' 50 mm thick and of 50% glandularity. However, it is not assumed that the incident air kerma measured with the standard phantom is the same as that which would be obtained for the standard breast. A small correction (about 10%) is applied for this via the conversion coefficient, $c_{D_{G50},K_{i,PMMA}}$ [VII.56]. This coefficient combines the coefficient c_{D_{G50},K_i} (Eq. (VII.5)) and the ratio of the values of the incident air kerma for the standard breast and the standard phantom. The mean glandular dose is thus given by:

$$D_G = c_{D_{G50},K_{i,PMMA}} s K_i \qquad \text{(VII.6)}$$

where K_i in this case is the incident air kerma for exposure of the standard phantom. The coefficient $c_{D_{G50},K_{i,PMMA}}$ is given in Table 8.5.

VII.5.3.3. Dose calculation for patient measurements

In order to apply Eq. (VII.5) for patient measurements, it is necessary to know the incident air kerma, the target/filter combination, tube voltage, HVL and breast glandularity. Usually, the breast glandularity is unknown and an assumption must be made. Two approaches are described in this Code of Practice: (i) the assumption of a fixed glandularity of 50%, so that the value of $c_{D_{Gg},D_{G50}}$ is unity and (ii) the use of average glandularities for particular breast

sizes, which may be obtained from the literature (when appropriate for the population of women being examined) or from local data where these exist.

The assumption of 50% glandularity can give rise to errors for an individual dose estimate of about 10–35%, depending upon breast size and actual glandularity. For example, Young and Burch [VII.57] found that for a population of screened women in the UK, accounting for glandularity variations increased the average value of the mean glandular dose by 11% and 14% for cranio-caudal and medio-lateral oblique views, respectively.

VII.6. CT

In single detector CT, the patient is irradiated with an X ray beam which is fan shaped in the transverse plane but which is collimated in the longitudinal plane so that only a slice through the patient is directly irradiated. For axial CT scanning, the X ray tube rotates about the patient and the tomographic information in the single slice is obtained by reconstruction using the projection data thus obtained. To obtain volume information, sequential slices are taken with the patient couch moving between slices. In helical CT scanning, the tube rotates continuously and the couch moves as the tube rotates. In multislice (multidetector) CT, a bank of detectors is used so that several slices can be taken at the same time. Helical motion can again be used.

Measurements of CT dosimetric quantities are made with a pencil ionization chamber specially designed for such work. Such chambers were first described by Jucius and Kambic [VII.93] and Suzuki and Suzuki [VII.94].[5]

VII.6.1. Special dosimetric quantities for CT

As the irradiation conditions in CT are quite different from those in planar X ray imaging, it is necessary to use special dosimetric quantities and techniques. National and international advice is available on the methodology to be used when estimating CT dose [VII.96–VII.99]; there is variation in the definition of quantities to be used. The CT dosimetric quantities used in this Code of Practice are defined in Section 3.2.7 and comprise the CT air kerma indices $C_{a,100}$ and $C_{PMMA,100}$, the weighted CT air kerma index, C_W, and the CT air

[5] It is also possible to measure CT dosimetric quantities using a stack of TLDs [VII.95]. This is a slow process as the dosimeters have to be individually read out after exposure [VII.96] and is not described. It becomes impractical in the usual situation where a series of measurements are required.

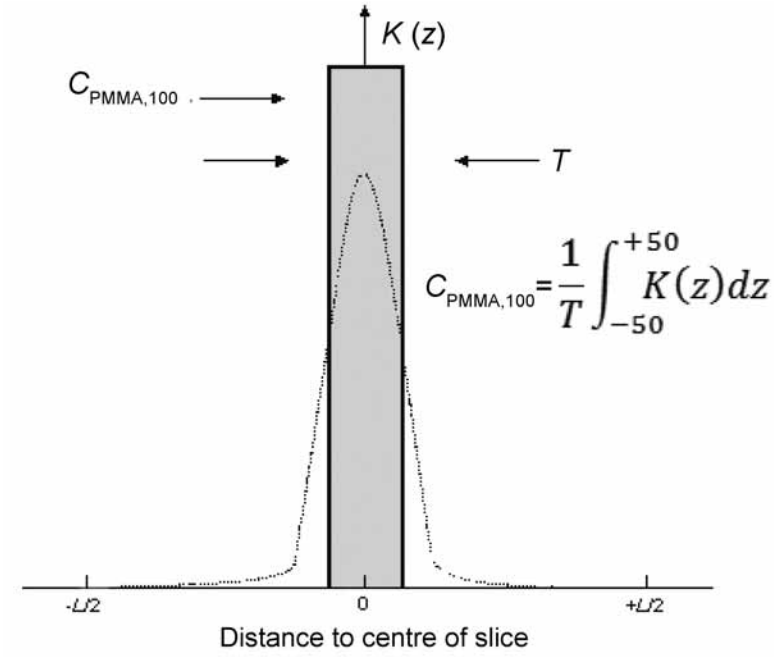

FIG. VII.5. Profile of air kerma, K(z) measured in the standard CT dosimetry phantom along an axis parallel to the CT scanner axis (z) for a single CT slice of nominal width T mm. The CT kerma index $C_{PMMA,100}$ is obtained by integrating the air kerma over a length (L) of 100 mm.

kerma index C_{VOL}, which is derived from C_W for particular patient scan parameters. In addition, the CT air kerma–length product, $P_{KL,CT}$, calculated according to Eq. (3.17) from C_{VOL} and the scan parameters, is used as a measure of the patient dose for a complete procedure.

The index $C_{a,100}$ is measured free in air and the index C_W is derived from measurements of the CT air kerma index $C_{PMMA,100}$ in standard head and body CT dosimetry phantoms [VII.14], based on the methodology described in IEC 60601-2-44 [VII.100] and in European and UK guidance [VII.96, VII.98]. These quantities are defined for a single axial slice and are obtained from integrals of the air kerma along a line parallel to the axis of rotation of the scanner over a length of 100 mm (Eqs (3.11, 3.12) and Fig. VII.5). The CT air kerma index is the height of a rectangular air kerma profile of width equal to the nominal slice width that has the same value as the line integral. This choice of CT air kerma indices has the important practical advantage over those used by the FDA in

the USA [VII.99, VII.101] in that they are easily measured using a readily available CT ionization chamber of length 100 mm.

The CT kerma indices, $C_{a,100}$ and C_W, can both be used for routine quality control. The index $C_{a,100}$ is a coarser indicator of patient dose than C_W, which is measured in a phantom, as it takes no account of the effect of the shaped beam filtration that is present in the scanner [VII.98, VII.102]. However, the procedure for the free in air measurement is simpler and does not require the use of a heavy PMMA phantom.

The weighted CT air kerma index, C_W, is derived from the quantities $C_{PMMA,100,c}$ and $C_{PMMA,100,p}$, which are measured in the centre and peripheral bores of the standard body or head CT dosimetry phantoms, the readings for the four peripheral bores being averaged. The weighted CT air kerma index is an approximation to the average air kerma in the volume of the phantom interrogated by a rotating fan beam of the nominal slice thickness [VII.103]. The more recent C_{VOL} [VII.100, VII.104] is a volume average which takes into account the helical pitch or the axial scan spacing for a patient examination (Eq. (3.15)). Related quantities, ${}_nC_W$ and ${}_nC_{VOL}$, are also used (Eq. (3.15)) in which the indices are normalized to unit tube loading.

The same methodology is used in this Code of Practice for single slice and multislice CT, with the nominal slice thickness being replaced by the sum of the nominal slice thicknesses that are simultaneously irradiated (i.e. by the nominal width of the irradiating beam). However, it should be noted [VII.105] that the use of CT air kerma related quantities may lead to underestimates of patient dose when the total thickness irradiated in a single scanner rotation approaches the length of the CT ionization chamber. As a result of the increasing use of multislice (multidetector) CT, it is possible that additional or different dosimetric quantities will be introduced in due course, which may replace or supplement some of those used here.

It is noted that the quantity 'multiple scan average dose' [VII.106] has also been used for CT dosimetry. This quantity is closely related to the index, C_{VOL}, and is not used in this Code of Practice.

VII.6.2. Measurements using phantoms

Unlike some other areas of dosimetry used in diagnostic radiology, only two phantoms have found common application for standardized dosimetry in CT. These phantoms [VII.14, VII.98–VII.100] are referred to here as the standard head and body CT dosimetry phantoms. They are constructed from PMMA and each is a right circular cylinder. The head and body phantoms have diameters of 160 mm and 320 mm, respectively. Thus, the body phantom presents a cross-section which is larger than that of a typical adult. Each

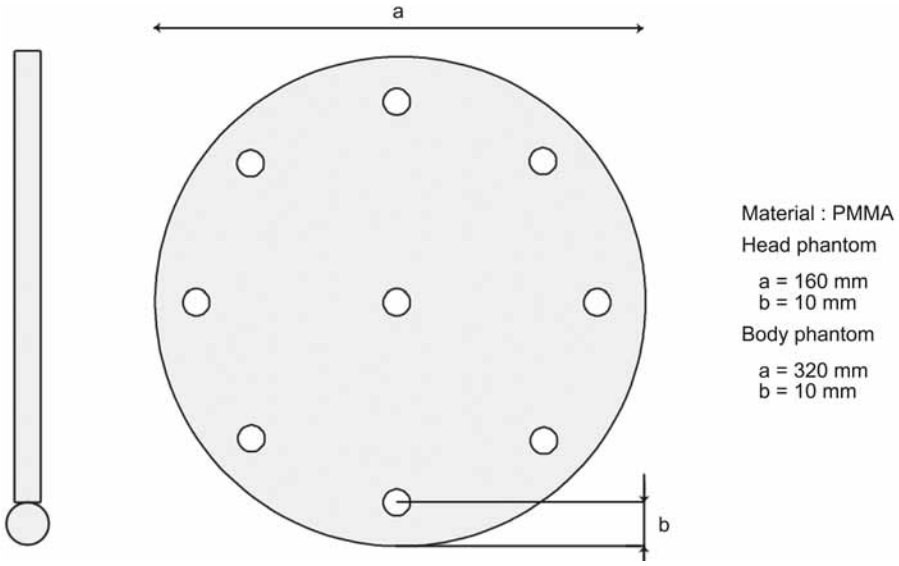

FIG. VII.6. A cross-section through the standard head or body phantom. The small circles indicate the positions of the bores for inserting a CT ionization chamber. A PMMA plug is shown on the left (not to scale).

phantom has a central bore and four peripheral bores (some models have eight peripheral bores) centered 10 mm below the phantom surface for positioning a CT ionization chamber. Plugs of PMMA are provided for each bore so that they may be filled as appropriate during measurements. Figures VII.6 and VII.7 show an outline drawing and photograph of the phantom. The particular example shown in the photograph uses the head phantom as the central portion of the body phantom, thus reducing the weight that needs to be transported when both phantoms are to be used. The required phantoms are, therefore, two right circular cylinders constructed of PMMA, of length at least 140 mm and diameters 160 mm and 320 mm. Each phantom should have a central bore and at least four peripheral bores, each of which is parallel to the axis of the cylinder. The peripheral bores should be spaced 90° apart with centres 10 mm below the phantom surface. Each hole should be suitable for the insertion of a 100 mm long CT ionization chamber.

Such phantoms may be purchased commercially or constructed by the hospital workshop. Many examples of this phantom, including that illustrated, have eight peripheral holes. For such phantoms, alternate peripheral holes are used for the measurement of C_W.

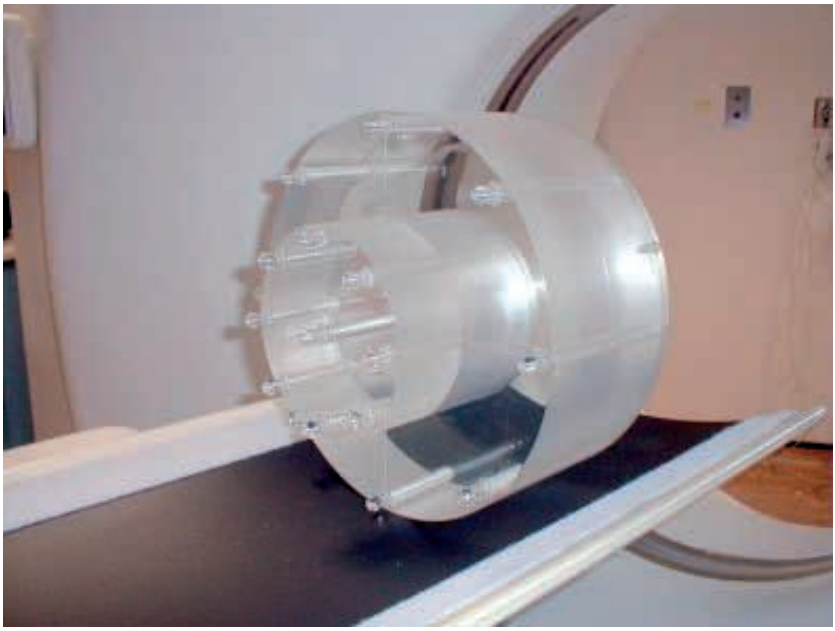

FIG. VII.7. Photograph of typical standard head and body CT dosimetry phantoms. The head phantom is the innermost cylinder (which has been partially removed for clarity) and when surrounded by a PMMA annulus, the body phantom is formed. The phantom illustrated has more chamber holes than are required for the measurements described in this Code of Practice. All the holes are filled with plugs, which may be individually removed to facilitate measurement.

Some scanners display the value of C_W on the operator's console and IEC 60601 Part 2.44 [VII.100] requires C_{VOL} to be displayed. Whilst these are helpful indications, they may only be values typical for the pitch factor selected (for C_{VOL}) and the particular type of scanner. They do not obviate the need to make measurements of C_W using the standard dosimetry phantoms.

Various other phantoms have been used for specific application in CT. Examples include the use of anthropomorphic phantoms for measurements of organ dose with TLDs (e.g. Adams et al. [VII.107], Chapple et al. [VII.108]) and PMMA phantoms differing in size and/or shape from the standard phantoms used for the measurement of air kerma–length product (e.g. Nawfel et al. [VII.109] and Avilés Lucas et al. [VII.110]). For situations where entrance surface air kerma is to be measured using a phantom, it is very important to note that the value of this quantity is strongly dependent upon the distance of the measurement position from the scanner axis. This has been demonstrated

by Avilés Lucas et al. [VII.110, VII.111] for measurements and calculations of the entrance surface air kerma on the anterior surface of a phantom. The effect is due to the beam shaping filter and can give rise to a difference of as much as 35% if measurements on a centred standard body phantom are used to estimate the surface air kerma for a small child centred in the gantry. As a consequence, care must be taken when positioning phantoms to ensure that the vertical position of the anterior surface of the phantom within the gantry matches that of the patient. Indeed, in such a situation it may be helpful to make a series of measurements with different vertical positions of the phantom.

VII.6.3. Patient measurements

In this Code of Practice, the direct measurement of patient dose for CT is not described as there are presently no standardized techniques for such measurements. Instead, the CT kerma index, C_W, measured using the standard dosimetry phantoms is used in combination with the exposure parameters for the scan or scan series to calculate the CT air kerma index, ${}_nC_{VOL}$ (Eq. (3.15)), and hence the CT air kerma–length product, $P_{KL,CT}$, for the whole examination in accordance with Eq. (3.17). As the measurements are made on circular PMMA phantoms which do not match the patient size or composition, the values obtained are only indicative. Nevertheless, this is a suitable quantity for use when setting diagnostic reference (guidance) levels, and dose–length product is used as such in the European guidelines [VII.98].

The weighted CT air kerma index, C_W, can also be used as a reference dose quantity [VII.98] as it is a measure of the average dose within a CT slice. However, the more recently introduced quantity, C_{VOL}, provides a better volume average and may also be used for this purpose. These two quantities are useful for comparisons of generic scan protocols where the scan length is not specified. According to the IEC [VII.100], the value of C_{VOL} (termed '$CTDI_{VOL}$') should be indicated on the CT scanner console. On older scanner models, the value of C_W (termed the 'weighted CT dose index' or $CTDI_W$) may be displayed or there may be no indication of dose apart from the tube current–exposure time product. Whilst the display on the console of C_W or C_{VOL} provides a very useful indication, it does not obviate the need to make measurements of C_W.

A practical approach to the determination of the CT air kerma–length product may be to use the dose–length product displayed on the scanner console (where available). In this case, the user should be aware that this value may have been calculated using generic values of C_W or C_{VOL} and if necessary a correction can be made based on the measured values of C_W and the displayed

weighted CTDI or $CTDI_{VOL}$. If this approach is adopted, it is recommended that the user establishes the method used by the scanner manufacturer for the calculation of the dose–length product. If necessary, an allowance for over scan may need to be added. This approach is not described further in this Code of Practice.

The discussion so far has been concerned with the dose arising from the collection of volume information. However, before the volume information is collected, a scan projection radiograph is taken in order to localize the volume to be examined. The dose arising from the collection of this digital radiograph is often regarded as insignificant since it contributes typically 3% of the dose from the whole examination [VII.112]. For bone densitometry, where only one or two axial scans may be performed, the scan projection radiograph can make a more significant contribution to the total dose. Pelvimetry scans generally involve just a scan projection radiograph. In both the latter situations, it may be necessary to measure the dose arising from the scan. Detailed instructions are not given in Section 8.7 as the measurement of dose for planar radiographs is treated in Section 8.4. However, it is noted that it is possible to use the CT ionization chamber to measure the incident air kerma for the scan projection radiograph [VII.96]. This is done in the absence of patient or phantom using the CT ionization chamber supported at the appropriate height above the couch top and aligned parallel to the axis of rotation of the scanner. The scanner settings should be the same as those for the scan projection radiogaph and the scan length should exceed the length of the ionization chamber (100 mm).

VII.7. DENTAL RADIOGRAPHY

In dental radiography, different types of examination are performed: intraoral and panoramic examinations, cephalometry and CT. In this Code of Practice, two types of dental radiography examination are considered: intraoral (bitewing projections) and panoramic examinations. For cephalometry and CT examinations, the same type of equipment is used as in general radiography and CT in order that the phantoms and measurement methods recommended for these modalities can be applied.

VII.7.1. Measurements using phantoms

For intraoral and panoramic examinations, measurements with phantoms reported in the literature have been made mainly to determine organ doses and effective dose. For this purpose, anthropomorphic phantoms are used with

drilled holes to allow insertion of TLDs. The most commonly used phantoms are the Alderson-Rando phantoms, which are available for both adults and children [VII.113–VII.121]. Dose measurements with other types of physical phantom are generally not performed.

Measurements with anthropomorphic phantoms are not treated in this Code of Practice.

VII.7.2. Patient dosimetry

Measurements made directly on patients are generally not performed in dental radiography. Fixed exposure settings are normally used (possibly using different settings for adults and children) and measurements free in air are sufficient to derive application specific quantities.

For intraoral projections, incident air kerma, K_i, is the recommended quantity. If required, the air kerma–area product, P_{KA}, is readily derived as the product of K_i and beam area since this is well defined by the spacer/director cone. From the experiments performed with anthropomorphic phantoms, K_i and P_{KA} can be related to energy imparted to the patient [VII.118] or effective dose [VII.113–VII.115, VII.118–VII.121]. For special purposes, entrance surface air kerma on patients can be measured in the same way as in general radiography by attaching TLDs to the skin. The corresponding procedures for conducting measurements in general radiography should be followed.

In panoramic radiography, the quantity to use for setting diagnostic reference levels has been debated. The NRPB has suggested the air kerma–length product, P_{KL}, for this purpose and a diagnostic reference value of P_{KL} = 65 mGy·mm [VII.122]. In recent publications, use of the air kerma–area product, P_{KA}, has been suggested [VII.121, VII.123] since this quantity is more closely related to risk and is used within other fields of diagnostic radiology. Reference [VII.121] estimates a conversion coefficient, $c_{E,P_{KA}}$, of approximately 0.06 $mSv \cdot Gy^{-1} \cdot cm^{-2}$ for applications in dental radiography.

Procedures for measurement of P_{KL} are recommended using a cylindrical ionization chamber (e.g. CT chamber) or TLDs. Such measurements have been described for a cylindrical ionization chamber by Isoardi and Ropolo [VII.124] and Perisinakis et al. [VII.125] and for TLDs by Williams and Montgomery [VII.121]. Factor P_{KA} can be easily obtained from the product of P_{KL} and the height, H, of the X ray beam at the secondary collimator. This procedure was adopted in this Code of Practice for patient dosimetry during panoramic examinations.

Future development of digital techniques may lead to the introduction of AEC in dental radiography and call for methods to monitor individual patient exposures. Helmrot and Alm Carlsson [VII.126] have compared measurements

of P_{KA} using a KAP meter and measurements made with a cylindrical ionization chamber. Agreement within 8% was achieved. This work suggests that KAP meters may be used for determining P_{KA} in direct measurements on intraoral and panoramic units. In this case, measurement on patients follows the procedure recommended for fluoroscopy (see Section 8.5).

REFERENCES

[VII.1] INTERNATIONAL COMMISSION ON RADIOLOGICAL PROTECTION, Radiation and Your Patient: A Guide for Medical Practitioners, Supporting Guidance 2, Pergamon Press, Oxford and New York (2001).

[VII.2] INTERNATIONAL COMMISSION ON RADIATION UNITS AND MEASUREMENTS, Tissue Substitutes in Radiation Dosimetry and Measurement, ICRU Rep. 44, ICRU, Bethesda, MD (1989).

[VII.3] WHITE, D.R., The formulation of tissue substitute materials using basic interaction data, Phys. Med. Biol. **22** (1977) 889–899.

[VII.4] WHITE, D.R., MARTIN, R.J., DARLISON, R., Epoxy resin based tissue substitutes, Br. J. Radiol. **50** (1977) 814–821.

[VII.5] SANDBORG, M., ALM CARLSSON, G., PERSLIDEN, J., DANCE, D.R., Comparison of different materials for test phantoms in diagnostic radiology, Radiat. Prot. Dosim. **49** (1993) 345–347.

[VII.6] INTERNATIONAL COMMISSION ON RADIATION UNITS AND MEASUREMENTS, Phantoms and Calculational Models in Therapy, Diagnosis and Protection, ICRU Rep. 48, ICRU, Bethesda, MD (1992).

[VII.7] DANCE, D.R., Monte Carlo calculation of conversion factors for the estimation of mean glandular breast dose, Phys. Med. Biol. **35** (1990) 1211–1219.

[VII.8] MARTIN, C.J., SUTTON, D.G., WORKMAN, A., SHAW, A.J., TEMPERTON, D., Protocol for measurement of patient entrance surface dose rates for fluoroscopic X-ray equipment, Br. J. Radiol. **71** (1998) 1283–1287.

[VII.9] JENNINGS, R.J., Spectrally precise phantoms for quality assurance in diagnostic radiology, Br. J. Radiol. Suppl. **18** (1985) 90–93.

[VII.10] CONWAY, B.J., et al., Beam quality independent attenuation phantom for estimating patient exposure from X-ray automatic exposure controlled chest examinations, Med. Phys. **11** (1984) 827–832.

[VII.11] CONWAY, B.J., et al., Patient-equivalent attenuation phantom for estimating patient exposures from automatic exposure controlled X-ray examinations of the abdomen and lumbo-sacral spine, Med. Phys. **17** (1990) 448–453.

[VII.12] NATIONWIDE EVALUATION OF X-RAY TRENDS (NEXT), Tabulation and Graphical Summary of 2001 Survey of Adult Chest Radiography (2005), http://www.crcpd.org

[VII.13] AMERICAN NATIONAL STANDARDS INSTITUTE, Methods for Sensitometry of Medical X-Ray Screen–Film Processing Systems, Rep. PH2.43, ANSI, New York (1982).
[VII.14] AMERICAN ASSOCIATION OF PHYSICISTS IN MEDICINE, Standardized Methods for Measuring Diagnostic X-ray Exposures, Rep. 31, AAPM, New York (1990).
[VII.15] SULEIMAN, O.H., STERN, S.H., SPELIC, D.C., Patient dosimetry activities in the United States: The nationwide evaluation of X-ray trends (NEXT) and tissue handbooks, Appl. Radiat. Isot. **50** (1999) 247–259.
[VII.16] SERVOMAA, A., TAPIOVAARA, M., Two new patient equivalent phantoms in diagnostic radiology, Radiat. Prot. Dosim. **43** (1992) 229–231.
[VII.17] FOOD AND DRUG ADMINISTRATION, NEXT 2001—Protocol for the Survey of Adult Chest Radiography (2002), http://www.crcpd.org/free_docs.asp
[VII.18] FOOD AND DRUG ADMINISTRATION, NEXT 2002—Protocol for the Survey of A/P Abdomen and Lumbo-Sacral Spine Radiography (2002), http://www.crcpd.org/free_docs.asp
[VII.19] HARRISON, R.M., CLAYTON, C.B., DAY, M.I., OWEN, J.P., YORK, M.F., A survey of radiation doses to patients in five common diagnostic examinations, Br. J. Radiol. **56** (1983) 383–395.
[VII.20] HEGGIE, J.C.P., A survey of doses to patients in a large public hospital resulting from common plain film radiographic procedures, Aust. Phys. Eng. Sci. Med. **13** (1990) 71–80.
[VII.21] MARTIN, C.J., DARRAG, C.L., MCKENZIE, G.A., BAYLISS, A.P., Implementation of a programme for reduction of radiographic doses and results achieved through increases in tube potential, Br. J. Radiol. **66** (1993) 228–233.
[VII.22] NATIONAL RADIOLOGICAL PROTECTION BOARD, National Protocol for Patient Dose Measurements in Diagnostic Radiology, NRPB, Chilton (1992).
[VII.23] SULEIMAN, O.H., et al., Assessing patient exposure in fluoroscopy, Radiat. Prot. Dosim. **49** (1993) 141–143.
[VII.24] INSTITUTE OF PHYSICS AND ENGINEERING IN MEDICINE, Recommended Standards for the Routine Performance Testing of Diagnostic X-Ray Imaging Systems, Rep. 77, IPEM, York (1997).
[VII.25] FAULKNER, K., BROADHEAD, D.A., HARRISON, R.M., Patient dosimetry measurement methods, Appl. Radiat. Isot. **50** (1999) 113–123.
[VII.26] CARLSSON, C.A., Determination of integral absorbed dose from exposure measurements, Acta Radiol. **1** (1963) 433–457.
[VII.27] SHRIMPTON, P.C., WALL, B.F., An evaluation of the Diamentor transmission ionization chamber in indicating exposure–area product (R cm^2) during diagnostic radiological examinations, Phys. Med. Biol. **27** (1982) 871–878.

[VII.28] LARSSON, J.P., PERSLIDEN, J., ALM CARLSSON, G., Ionization chambers for measuring air kerma integrated over beam area: Deviations in calibration values using simplified calibration methods, Phys. Med. Biol. **43** (1998) 599–607.
[VII.29] LARSSON, J.P., PERSLIDEN, J., SANDBORG, M., ALM CARLSSON, G., Transmission ionization chambers for measurements of air kerma integrated over beam area: Factors limiting the accuracy of calibration, Phys. Med. Biol. **41** (1996) 2381–2398.
[VII.30] EUROPEAN COMMISSION, European Guidelines on Quality Criteria for Diagnostic Radiographic Images in Paediatrics, Rep. EUR 16261, EC, Luxembourg (1996).
[VII.31] TAPIOVAARA, M.J., SANDBORG, M., DANCE, D.R., A search for improved technique factors in paediatric fluoroscopy, Phys. Med. Biol. **44** (1999) 537–559.
[VII.32] LARSSON, J.P., Department of Radiation Physics, Linköping University, personal communication, 2004.
[VII.33] GFIRTNER, H., STIEVE, F.E., WILD, J., A new Diamentor for measuring kerma–area product and air kerma simultaneously, Med. Phys. **24** (1997) 1954–1959.
[VII.34] CARLSSON, C.A., ALM CARLSSON, G., "Dosimetry in diagnostic radiology and computerised tomography", The Dosimetry of Ionizing Radiation (KASE, K.R., BJÄRNGARD, B.E., ATTIX, F.H., Eds), Academic Press, Orlando (1990) 163–257.
[VII.35] CARLSSON, C.A., Integral absorbed doses in roentgen diagnostic procedures, I: The dosemeter, Acta Radiol. **3** (1965) 310–326.
[VII.36] HARRISON, D., RICCIARDELLO, M., COLLINS, L., Evaluation of radiation dose and risk to the patient from coronary angiography, Aust. N.Z. J. Med. **28** (1998) 597–603.
[VII.37] GUIBELALDE, E., et al., Practical aspects for the evaluation of skin doses in interventional cardiology using a new slow film, Br. J. Radiol. **76** (2003) 332–336.
[VII.38] VAÑÓ, E., GUIBELALDE, E., FERNANDEZ, J.M., GONZALES, L., TEN, J.I., Patient dosimetry in interventional radiology using slow film systems, Br. J. Radiol. **70** (1997) 195–200.
[VII.39] GILES, E.R., MURPHY, P.H., Measuring skin dose with radiochromic dosimetry film in the cardiac catheterization laboratory, Health Phys. **82** (2002) 875–880.
[VII.40] BOWER, M.W., HINTENLANG, D.E., The characterization of a commercial MOSFET dosemeter system for use in diagnostic radiology, Health Phys. **75** (1998) 197–204.
[VII.41] PEET, D.J., PRYOR, M.D., Evaluation of a MOSFET radiation sensor for the measurement of entrance surface dose in diagnostic radiology, Br. J. Radiol. **72** (1999) 562–568.

[VII.42] HWANG, E., et al., Real-time measurement of skin radiation during cardiac catheterization, Cathet. Cardiovasc. Diagn. **43** (1998) 367–370.
[VII.43] WAGNER, L.K., POLLOCK, J.J., Real-time portal monitoring to estimate dose to skin of patients from high dose fluoroscopy, Br. J. Radiol. **72** (1999) 846–855.
[VII.44] BØTTER-JENSEN, L., AGERSNAP LARSEN, N., MARKEY, B.G., MCKEEVER, S.W.S., Al_2O_3:C as a sensitive OSL dosemeter for rapid assessment of environmental photon dose rates, Radiat. Meas. **27** (1997) 295–298.
[VII.45] INTERNATIONAL ELECTROTECHNICAL COMMISSION, Medical Electrical Equipment—Part 2-43: Particular Requirements for the Safety of X-Ray Equipment for Interventional Procedures, Rep. IEC 60601-2-43, IEC, Geneva (2000).
[VII.46] GKANATSIOS, N.A., HUDA, W., PETERS, K.R., FREEMAN, J.A., Evaluation of an online patient exposure meter in neuroradiology, Radiol. **203** (1997) 837–842.
[VII.47] CUSMA, J.T., BELL, M.R., WONDROW, M.A., TAUBEL, J.P., HOLMES, D.R.J., Realtime measurement of radiation exposure to patients during diagnostic coronary angiography and percutaneous interventional procedures, J. Am. Coll. Cardiol. **33** (1999) 427–435.
[VII.48] HANSSON, B., KARAMBATSAKIDOU, A., Relationship between entrance skin dose, effective dose and dose area product for patients in diagnostic and interventional cardiac procedures, Radiat. Prot. Dosim. **90** (2000) 141–144.
[VII.49] SANDBORG, M., FRANSSON, S.G., PETTERSSON, H., Evaluation of patient and staff absorbed doses during coronary angiography and intervention by femoral and radial artery access routes, Eur. Radiol. **14** (2004) 653–658.
[VII.50] VAÑÓ, E., et al., Skin dose and dose–area product values for interventional cardiology procedures, Br. J. Radiol. **74** (2001) 48–55.
[VII.51] WAITE, J.C., FITZGERALD, M., An assessment of methods for monitoring entrance surface doses in fluoroscopically guided cardiac interventional procedures, Radiat. Prot. Dosim. **94** (2001) 89–92.
[VII.52] VAN DE PUTTE, S., VERHAEGEN, F., TAEYMANS, Y., THIERENS, H., Correlation of patient skin doses in cardiac interventional radiology with dose–area product, Br. J. Radiol. **73** (2000) 504–513.
[VII.53] DEN BOER, A., DE FEIJTER, P.J., SERRUYS, P.W., ROELANDT, J.R., Real time quantification and display of skin radiation during coronary angiography, Circ. **104** (2001) 1179–1784.
[VII.54] BALTER, S., et al., "Techniques to estimate radiation dose to skin during fluoroscopically guided procedures", 44th Ann. AAPM Mtg (PHELPS, B., Ed.), AAPM, College Park, MD (2002).
[VII.55] INTERNATIONAL COMMISSION ON RADIOLOGICAL PROTECTION, Radiological Protection and Safety in Medicine, Publication 73, Pergamon Press, Oxford and New York (1997).

[VII.56] EUROPEAN COMMISSION, European Protocol on Dosimetry in Mammography, Rep. EUR 1626, EC, Luxembourg (1996).
[VII.57] YOUNG, K.C., BURCH, A., Radiation doses received in the UK breast screening programme in 1997 and 1998, Br. J. Radiol. **73** (2000) 278–287.
[VII.58] JAMAL, N., NG, K.-H., MCLEAN, I.D., A study of mean glandular dose during diagnostic mammography in Malaysia and some of the factors affecting it, Br. J. Radiol. **76** (2003) 238–245.
[VII.59] FIFE, I., The physical dimensions of the compressed breast, Br. J. Radiol. **64** (1991) 73–74.
[VII.60] WU, X., BARNES, G.T., TUCKER, D.M., Spectral dependence of glandular tissue dose in screen–film mammography, Radiol. **179** (1991) 143–148.
[VII.61] GEISE, R.A., PALCHEVSKY, A., Composition of mammographic phantom materials, Radiol. **198** (1996) 342–350.
[VII.62] HEGGIE, J.C.P., Survey of doses in screening mammography, Aust. Phys. Eng. Sci. Med. **19** (1996) 207–216.
[VII.63] KLEIN, R., et al., Determination of average glandular dose with modern mammography units for two large groups of patients, Phys. Med. Biol. **42** (1997) 651–671.
[VII.64] YOUNG, K.C., RAMSDALE, M.L., BIGNALL, F., Review of dosimetric methods for mammography in the UK breast screening programme, Radiat. Prot. Dosim. **80** (1998) 183–186.
[VII.65] BECKETT, J., KOTRE, C.J., Dosimetric implications of age related glandular changes in screening mammography, Phys. Med. Biol. **45** (2000) 801–813.
[VII.66] KRUGER, R.L., SCHUELER, B.A., A survey of clinical factors and patient dose in mammography, Med. Phys. **28** (2001) 1449–1454.
[VII.67] KRAMER, R., et al., Backscatter factors for mammography calculated with Monte Carlo methods, Phys. Med. Biol. **46** (2001) 771–781.
[VII.68] FITZGERALD, M., WHITE, D.R., WHITE, E., YOUNG, J., Mammographic practice and dosimetry in Britain, Br. J. Radiol. **54** (1981) 212–220.
[VII.69] DEUTSCHE GESELLSHAFT FÜR MEDIZINISCHE PHYSIK, Praxis der Weichstrahl-dosimetric, Rep. -Bericht 5, DGMP, Cologne (1986).
[VII.70] INSTITUTE OF PHYSICAL SCIENCES IN MEDICINE, The Commissioning and Routine Testing of Mammographic X-Ray Systems, Rep. 59, IPSM, York (1989).
[VII.71] INSTITUTE OF PHYSICS AND ENGINEERING IN MEDICINE, The Commissioning and Routine Testing of Mammographic X-Ray Systems, Rep. 59, IPEM, York (1994).
[VII.72] INSTITUTE OF PHYSICS AND ENGINEERING IN MEDICINE, The Commissioning and Routine Testing of Mammographic X-Ray Systems: A Technical Quality Control Protocol, Rep. 89, IPEM, York (2005).
[VII.73] STATENS STRÅLSKYDDINSTITUT, Kvalitetssäkring för mammografiprestanda-ochkonstanskontroller, Rep. 89-19, SSI, Stockholm (1989) (in Swedish).

[VII.74] AMERICAN COLLEGE OF RADIOLOGY, Mammography Quality Control Manual, ACR, Reston, VA (1999).
[VII.75] HAMMERSTEIN, G.R., et al., Absorbed radiation dose in mammography, Radiol. **130** (1979) 485–491.
[VII.76] EUROPEAN COMMISSION, European Guidelines for Quality Assurance in Mammographic Screening, EC, Luxembourg (2006).
[VII.77] FAULKNER, K., CRANLEY, K., An investigation into variations in the estimation of mean glandular dose in mammography, Radiat. Prot. Dosim. **57** (1995) 405–408.
[VII.78] DANCE, D.R., SKINNER, C.L., YOUNG, K.C., BECKETT, J.R., KOTRE, C.J., Additional factors for the estimation of mean glandular breast dose using the UK mammography dosimetry protocol, Phys. Med. Biol. **45** (2000) 3225–3240.
[VII.79] GENTRY, J.R., DEWERD, L.A., TLD measurements of in vivo mammographic exposures across the United States, Med. Phys. **23** (1996) 899–903.
[VII.80] ROSENSTEIN, M., ANDERSEN, L.W., WARNER, G.G., Handbook of Glandular Tissue Doses in Mammography, Rep. FDA 85-8239, Center for Devices and Radiological Health, Rockville, MD (1985).
[VII.81] WU, X., GINGOLD, E.L., BARNES, G.T., TUCKER, D.M., Normalized average glandular dose in molybdenum target–rhodium filter and rhodium target–rhodium filter mammography, Radiol. **193** (1994) 83–89.
[VII.82] BOONE, J.M., Glandular breast dose for monoenergetic and high-energy X-ray beams: Monte Carlo assessment, Radiol. **213** (1999) 23–37.
[VII.83] BOONE, J.M., Normalized glandular dose (DgN) coefficients for arbitrary spectra in mammography: Computer-fit values of Monte Carlo derived data, Med. Phys. **29** (2002) 869–875.
[VII.84] ZOETELIEF, J., JANSEN, J.T.M., Calculation of air kerma to average glandular tissue dose conversion factors for mammography, Radiat. Prot. Dosim. **57** (1995) 397–400.
[VII.85] DANCE, D.R., SKINNER, C.L., ALM CARLSSON, G., Breast dosimetry, Appl. Radiat. Isot. **50** (1999) 185–203.
[VII.86] ALM CARLSSON, G., DANCE, D.R., Breast absorbed doses in mammography: Evaluation of experimental and theoretical approaches, Radiat. Prot. Dosim. **43** (1992) 197–200.
[VII.87] DANCE, D.R., et al., Breast dosimetry using a high-resolution voxel phantom, Radiat. Prot. Dosim. **114** (2005) 359–363.
[VII.88] SOBOL, W.T., WU, X., Parametrization of mammography dose tables, Med. Phys. **24** (1997) 547–554.
[VII.89] KIMME-SMITH, C.M., SAYRE, J.W., MCCOMBS, M.M., DEBRUHL, N.D., BASSETT, L.W., Breast calcification and mass detection with mammographic anode–filter combinations of molybdenum, tungsten and rhodium, Radiol. **203** (1997) 679–683.

[VII.90] THILANDER-KLANG, A., et al., Influence of anode–filter combinations on image quality and radiation dose in 965 women undergoing mammography, Radiol. **203** (1997) 348–354.
[VII.91] YOUNG, K.C., RAMSDALE, M.L., RUST, A., Dose and image quality in mammography with an automatic beam quality system, Br. J. Radiol. **69** (1996) 555–562.
[VII.92] YOUNG, K.C., Royal Surrey County Hospital, Guildford, private communication, 2003.
[VII.93] UCIUS, R.A., KAMBIC, G.X., Radiation dosimetry in computed tomography, Appl. Opt. Instrum. Eng. Med. **127** (1977) 286–295.
[VII.94] SUZUKI, A., SUZUKI, M.N., Use of a pencil shaped ionization chamber for measurement of exposure resulting from a computed tomography scan, Med. Phys. **5** (1978) 536–539.
[VII.95] PERNIČKA, F., CT dosimetry using TL technique, Radiat. Prot. Dosim. **34** (1990) 271–274.
[VII.96] INSTITUTE OF PHYSICS AND ENGINEERING IN MEDICINE, Measurement of the Performance Characteristics of Diagnostic X-Ray Systems: Computed Tomography X-Ray Scanners, Rep. 32, Part 3, IPEM, York (2003).
[VII.97] AMERICAN ASSOCIATION OF PHYSICISTS IN MEDICINE, Specification and Testing of Computed Tomography Scanners, Rep. 39, AAPM, New York (1993).
[VII.98] EUROPEAN COMMISSION, European Guidelines for Quality Criteria for Computed Tomography, Rep. EUR 16262, EC, Luxembourg (2000).
[VII.99] FOOD AND DRUG ADMINISTRATION, Performance Standards for Diagnostic X-Ray Systems—Computed Tomography (CT) Equipment, Federal Register Rules and Regulations Ed 1/4/00 CFR Part 1020.33, FDA/CDRH, Rockville, MD (2000).
[VII.100] INTERNATIONAL ELECTROTECHNICAL COMMISSION, Medical Electrical Equipment—Part 2-44: Particular Requirements for the Safety of X-Ray Equipment for Computed Tomography, Rep. IEC-60601-2-44—Consol. Ed. 2.1, IEC, Geneva (2002).
[VII.101] FOOD AND DRUG ADMINISTRATION, Diagnostic X-Ray Systems and Their Major Components, Amendments to Performance Standard—Final Rule, 21 CFR Part 1020, FDA/CDRH, Rockville, MD (1984).
[VII.102] SHRIMPTON, P.C., EDYVEAN, S., Report on a round table meeting establishing a survey of standard dosimetry measurements on CT scanners, held at St. George's Hospital, London, 18 April 1997, Br. J. Radiol. **71** (1998) 1–3.
[VII.103] LEITZ, W., AXELSSON, B., SZENDRO, G., Computed tomography dose assessment: A practical approach, Radiat. Prot. Dosim. **57** (1995) 377–380.
[VII.104] MCNITT-GRAY, M.F., Radiation doses in CT, Radiographics **22** (2002) 1541–1553.

[VII.105] INTERNATIONAL COMMITTEE FOR WEIGHTS AND MEASURES, MRA: Mutual Recognition of National Measurement Standards and of Calibration and Measurement Certificates Issued by National Metrology Institutes (1999), http://www.bipm.org/pdf/mra.pdf
[VII.106] SHOPE, T.B., GAGNE, R.M., JOHNSON, G.C., A method for describing the doses delivered by transmission X-ray computed tomography, Med. Phys. **8** (1981) 488–495.
[VII.107] ADAMS, E.J., BRETTLE, D.S., JONES, A.P., HOUNSELL, A.R., MOTT, D.J., Estimation of foetal and effective dose for CT examinations, Br. J. Radiol. **70** (1997) 272–278.
[VII.108] CHAPPLE, C.L., WILLIS, S., FRAME, J., Effective dose in pediatric computed tomography, Phys. Med. Biol. **47** (2002) 107–115.
[VII.109] NAWFEL, R.D., ET, A., Patient and personnel exposure during CT fluoroscopy-guided interventional procedures, Radiol. **216** (2000) 180–184.
[VII.110] AVILÉS LUCAS, P., CASTELLANO, I.A., DANCE, D.R., VAÑÓ, E., Analysis of surface dose variation in CT procedures, Br. J. Radiol. **74** (2001) 1128–1136.
[VII.111] AVILÉS LUCAS, P., DANCE, D.R., CASTELLANO, I.A., VAÑÓ, E., Monte Carlo calculations in CT for the study of the surface air kerma and energy imparted to phantoms of varying size and position, Phys. Med. Biol. **49** (2004) 1439–1454.
[VII.112] SHRIMPTON, P.C., et al., Survey of CT practice in the UK, Part 2: Dosimetric aspects, Rep. NRPB R249, National Radiological Protection Board, Chilton (1991).
[VII.113] COHNEN, M., KEMPER, J., MOBES, O., PAWELZIK, J., MODDER, U., Radiation dose in dental radiology, Eur. Radiol. **12** (2002) 634–637.
[VII.114] HAYAKAWA, Y., KOBAYASHI, N., KUROYANAGI, K., NISHIZAWA, K., Paediatric absorbed doses from rotational panoramic radiography, Dento-Maxillo-Facial Radiol. **30** (2001) 285–292.
[VII.115] LECOMBER, A.R., YONEYAMA, Y., LOVELOCK, D.J., HOSOI, T., ADAMS, A.M., Comparison of patient dose from imaging protocols for dental implant planning using conventional radiography and computed tomography, Dento-Maxillo-Facial Radiol. **30** (2001) 255–259.
[VII.116] LUDLOW, J.B., DAVIES-LUDLOW, L.E., BROOKS, S.L., Dosimetry of two extraoral direct digital imaging devices: New Tom cone beam CT and Orthophos Plus DS panoramic unit, Dento-Maxillo-Facial Radiol. **32** (2003) 229–234.
[VII.117] SCHULZE, D., HEILAND, M., THURMANN, H., ADAM, G., Radiation exposure during midfacial imaging using 4- and 16-slice computed tomography, cone beam computed tomography systems and conventional radiography, Dento-Maxillo-Facial Radiol. **33** (2004) 83–86.
[VII.118] STENSTRÖM, B., HENRIKSON, C.O., KARLSSON, L., SARBY, B., Energy imparted from intraoral radiography, Swed. Dent. J. **10** (1986) 125–136.

[VII.119] STENSTRÖM, B., HENRIKSON, C.O., KARLSSON, L., SARBY, B., Effective dose equivalent from intraoral radiography, Swed. Dent. J. **11** (1987) 71–77.
[VII.120] VISSER, H., HERMANN, K.P., BREDEMEIR, S., KÖHLER, B., Dosismessungen zum Vergleich von konventionellen und digitalen Panoramaschichtaufnahmen, Mund- Kiefer- Gesichstchirurgie **4** 4 (2000) 213–216.
[VII.121] WILLIAMS, J.R., MONTGOMERY, A., Measurement of dose in panoramic dental radiology, Br. J. Radiol. **73** (2000) 1002–1006.
[VII.122] NAPIER, I.D., Reference doses for dental radiography, Br. Dental J. **186** (1999) 392–396.
[VII.123] INSTITUTE OF PHYSICS AND ENGINEERING IN MEDICINE, Guidance on the Establishment and Use of Diagnostic Reference Levels for Medical X-ray Examinations, Rep. 88, IPEM, York (2004).
[VII.124] ISOARDI, P., ROPOLO, R., Measurement of dose–width product in panoramic dental radiology, Br. J. Radiol. **76** (2003) 129–131.
[VII.125] PERISINAKIS, K., DAMILAKIS, J., NERATZOULAKIS, J., GOURTSOYIANNIS, N., Determination of dose–area product from panoramic radiography using a pencil ionization chamber: Normalized data for the estimation of patient effective and organ doses, Med. Phys. **31** (2004) 708–714.
[VII.126] HELMROT, E., ALM CARLSSON, G., Measurement of radiation dose in dental radiology, Radiat. Prot. Dosim. **114** (2005) 168–171.

Appendix VIII

BACKSCATTER FACTORS FOR GENERAL RADIOGRAPHY AND FLUOROSCOPY

The backscatter factor, B, was introduced in Chapter 3. It is the conversion coefficient that relates the incident air kerma, K_i, to the entrance surface air kerma, K_e, thus:

$$K_e = K_i B \qquad \text{(VIII.1)}$$

There are several circumstances where it is necessary to use a backscatter factor to convert from incident air kerma to entrance surface air kerma or vice versa. One example is the situation where measurements of the two quantities need to be compared. A second example is the situation where organ doses are to be calculated using conversion coefficients that are based on incident air kerma, and measurements of entrance surface air kerma are available. This appendix presents the backscatter factors recommended for use in general radiography and fluoroscopy.

The literature contains various sources of backscatter factors which are suitable for use in diagnostic radiology. Some have been measured and others have been calculated using Monte Carlo methods based on homogeneous phantoms or anthropomorphic phantoms. In this Code of Practice, it is recommended that the backscatter factors calculated by Petoussi-Henss et al. [VIII.1] for homogeneous phantoms be used. These data were selected because they have been calculated in terms of air kerma, they cover the necessary range of field sizes and diagnostic spectra (apart from mammography) and they are available for three backscatter materials. In addition, the data have been successfully validated by comparison with the results of Harrison [VIII.2], Bartlett et al. [VIII.3] and Grosswendt [VIII.4].

Table VIII.1 gives the values of the Petoussi-Henss et al. [VIII.1] backscatter factors for field sizes of 100 mm × 100 mm, 200 mm × 200 mm and 250 mm × 250 mm, 21 X ray spectra with X ray tube voltages between 50 kV and 150 kV and for backscattering materials, including water and ICRU tissue of density 1.00 g/cm^3 (elemental composition 10.1% H, 11.1% C, 2.6% N and 76.2% O [VIII.5]). The data for PMMA are included as they may be of value when dosimeters are calibrated with PMMA backscatter present. All the data in the table were calculated at a focus to skin distance of 1000 mm and with a scattering slab of entrance area 300 mm × 300 mm and thickness 150 mm. This thickness provides full backscatter [VIII.6]. Petoussi-Henss et al. [VIII.1] have

TABLE VIII.1. BACKSCATTER FACTORS, *B*, FOR WATER, ICRU TISSUE AND PMMA FOR 21 DIAGNOSTIC X RAY BEAM QUALITIES AND FOR THREE FIELD SIZES AT A FOCUS TO SKIN DISTANCE OF 1000 mm*

Tube voltage (kV)	Filter	Backscatter factor (*B*)									
		Field size	100 mm × 100 mm			200 mm × 200 mm			250 mm × 250 mm		
		HVL (mm Al)	Water	ICRU tissue	PMMA	Water	ICRU tissue	PMMA	Water	ICRU tissue	PMMA
50	2.5 mm Al	1.74	1.24	1.25	1.33	1.26	1.27	1.36	1.26	1.28	1.36
60	2.5 mm Al	2.08	1.28	1.28	1.36	1.31	1.32	1.41	1.31	1.32	1.42
70	2.5 mm Al	2.41	1.30	1.31	1.39	1.34	1.36	1.45	1.35	1.36	1.46
70	3.0 mm Al	2.64	1.32	1.32	1.40	1.36	1.37	1.47	1.36	1.38	1.48
70	3.0 mm Al +0.1 mm Cu	3.96	1.38	1.39	1.48	1.45	1.47	1.58	1.46	1.47	1.59
80	2.5 mm Al	2.78	1.32	1.33	1.41	1.37	1.39	1.48	1.38	1.39	1.50
80	3.0 mm Al	3.04	1.34	1.34	1.42	1.39	1.40	1.51	1.40	1.41	1.52
80	3.0 mm Al +0.1 mm Cu	4.55	1.40	1.40	1.49	1.48	1.50	1.61	1.49	1.51	1.63
90	2.5 mm Al	3.17	1.34	1.34	1.43	1.40	1.41	1.51	1.41	1.42	1.53
90	3.0 mm Al	3.45	1.35	1.36	1.44	1.42	1.43	1.53	1.42	1.44	1.55
90	3.0 mm Al +0.1 mm Cu	5.12	1.41	1.41	1.50	1.50	1.51	1.62	1.51	1.53	1.65
100	2.5 mm Al	3.24	1.34	1.34	1.42	1.40	1.41	1.51	1.41	1.42	1.53
100	3.0 mm Al	3.88	1.36	1.37	1.45	1.44	1.45	1.55	1.45	1.46	1.57

TABLE VIII.1. BACKSCATTER FACTORS, *B*, FOR WATER, ICRU TISSUE AND PMMA FOR 21 DIAGNOSTIC X RAY BEAM QUALITIES AND FOR THREE FIELD SIZES AT A FOCUS TO SKIN DISTANCE OF 1000 mm* (cont.)

Tube voltage (kV)	Filter	Backscatter factor (*B*)									
		Field size	100 mm × 100 mm			200 mm × 200 mm			250 mm × 250 mm		
		HVL (mm Al)	Water	ICRU tissue	PMMA	Water	ICRU tissue	PMMA	Water	ICRU tissue	PMMA
100	3.0 mm Al +0.1 mm Cu	5.65	1.41	1.42	1.50	1.51	1.53	1.64	1.53	1.55	1.66
110	2.5 mm Al	3.59	1.35	1.35	1.43	1.42	1.43	1.53	1.43	1.44	1.55
120	3.0 mm Al	4.73	1.37	1.38	1.46	1.46	1.48	1.58	1.48	1.49	1.60
120	3.0 mm Al +0.1 mm Cu	6.62	1.41	1.42	1.50	1.53	1.54	1.64	1.54	1.56	1.67
130	2.5 mm Al	4.32	1.36	1.36	1.44	1.44	1.45	1.55	1.45	1.47	1.57
150	2.5 mm Al	4.79	1.36	1.36	1.44	1.45	1.46	1.55	1.46	1.48	1.58
150	3.0 mm Al	6.80	1.39	1.39	1.47	1.50	1.51	1.61	1.52	1.53	1.63
150	3.0 mm Al +0.1 mm Cu	8.50	1.40	1.41	1.48	1.53	1.54	1.64	1.55	1.57	1.67

* Data taken from Petoussi-Henss et al. [VIII.1].

demonstrated that backscatter factors calculated at focus to skin skin distances of 500 mm and 1500 mm differ from those calculated for a focus to skin distance of 1000 mm by at most 2–3% and these differences can be ignored. The data in the table are for three different tube filtrations (2.5 mm Al, 3.0 mm Al and 3.0 mm Al + 0.1 mm Cu). Values of the backscatter factor at HVLs between the tabulated points may be obtained by linear interpolation. Data for square fields of areas between 100 mm × 100 mm and 250 mm × 250 mm may also be obtained by linear interpolation. Above the latter field size, the backscatter factor may be assumed to be constant with sufficient accuracy (the largest difference in Table VIII.1 between the backscatter factors for the 200 mm × 200 mm and the 250 mm × 250 mm data is less than 2%). It is suggested that backscatter factors for rectangular fields (of length L and width W) be obtained for the 'equivalent square' field of side L_{equiv} given by Ref. [VIII.7]:

$$L_{equiv} = \frac{2LW}{(L+W)} \qquad \text{(VIII.2)}$$

It should be noted that there are important differences between the backscatter factors for the three materials in the table. The differences vary with field size and X ray spectrum and are the greatest between water and PMMA where they can be as large as 9%. The backscatter factors in the table range between 1.24 and 1.67.

Backscatter factors for mammography are discussed in Section 8.6.

REFERENCES

[VIII.1] PETOUSSI-HENSS, N., ZANKL, M., DREXLER, G., PANZER, W., REGULLA, D., Calculation of backscatter factors for diagnostic radiology using Monte Carlo methods, Phys. Med. Biol. **43** (1998) 2237–2250.

[VIII.2] HARRISON, R.M., Backscatter factors for diagnostic radiology (1–4 mm Al HVL), Phys. Med. Biol. **27** (1982) 1465–1474.

[VIII.3] BARTLETT, D.T., DIMBYLOW, P.J., FRANCIS, T.M., Calculated backscatter from phantoms for dosemeter calibration, Radiat. Prot. Dosim. **32** (1990) 123–125.

[VIII.4] GROSSWENDT, B., Dependence of the photon backscatter factor for water on irradiation field size and source-to-phantom distance between 1.5 and 10 cm, Phys. Med. Biol. **38** (1993) 305–310.

[VIII.5] INTERNATIONAL COMMISSION ON RADIATION UNITS AND MEASUREMENTS, Radiation Quantities and Units, ICRU Rep. 33, ICRU, Bethesda, MD (1980).

[VIII.6] KLEVENHAGEN, S.C., The build-up of backscatter in the energy range 1 mm Al to 8 mm Al HVT, Phys. Med. Biol. **27** (1982) 1035–1043.
[VIII.7] STERLING, S.H., PERRY, H., KATZ, L., Derivation of a mathematical expression for the per cent depth dose surface of cobalt 60 beams and visualization of multiple field dose distributions, Br. J. Radiol. **37** (1964) 544–550.

Appendix IX

FIELD CALIBRATIONS

IX.1. PRINCIPLES OF CROSS-CALIBRATION

Chapter 4 discusses the situations in which the user decides to calibrate the field dosimeter that is subsequently used for the measurement. This is typically done when measuring with KAP meters or TLDs and in situations when more dosimeters are required to cover dosimetry needs in hospitals.

Cross-calibration of a field instrument refers to its comparison in a suitable user's beam of quality, Q_{cross}, against a reference instrument that has already been calibrated at the SSDL. The calibration coefficient of the field instrument is then written as:

$$N_{K,Q_{\text{cross}}}^{\text{field}} = \frac{M_{Q_{\text{cross}}}^{\text{ref}}}{M_{Q_{\text{cross}}}^{\text{field}}} N_{K,Q_0}^{\text{ref}} k_{Q_{\text{cross}}}^{\text{ref}} \tag{IX.1}$$

where 'field' and 'ref' refer to the field and the reference instruments respectively. Factors $M_{Q_{\text{cross}}}^{\text{ref}}$ and $M_{Q_{\text{cross}}}^{\text{field}}$ are the mean values measured with the reference and the field instruments, corrected for the influence of all quantities except that of beam quality. Factors N and k are the calibration coefficient of the reference instrument and the factor correcting for the difference in response between beam qualities Q_0 and Q_{cross}.

The calibration coefficient of the field instrument obtained through cross-calibration in the beam quality, Q_{cross}, can be used only for this beam quality. If the beam quality changes, a new cross-calibration in the new beam quality is required.

It is preferable to use an X ray machine with a sufficiently stable output for calibration. A sufficient number of readings has to be taken for both instruments to reduce standard deviations of the mean values. If the output fluctuates, the readings of dosimeters should be corrected for these fluctuations. One possibility is to use another dosimeter as the beam monitor. This dosimeter should be positioned in the beam so that it does not disturb the measurement.

IX.2. CALIBRATION OF DIAGNOSTIC DOSIMETERS

Calibration of diagnostic dosimeters should be done by the substitution method. Firstly, measurements are made with the reference dosimeter in the beam and then with the dosimeter to be calibrated. A calibration methodology is similar to the methodology described in Chapter 7 for the calibration of dosimeters in the SSDL. The calibration coefficient for the field instrument is calculated using Eq. (IX.1).

When calibrating the KAP meter, the detectors of the reference dosimeter and the KAP meter are irradiated simultaneously.

IX.3. CALIBRATION OF KAP METERS

IX.3.1. General

In the clinic, the KAP meter is mounted on the tube housing. All X rays, both focal and extrafocal, pass through its sensitive volume. Those transmitted through the chamber will, if attenuation in the air can be neglected, pass every plane perpendicularly to the beam central axis downstream of the beam. If the integration of air kerma over beam area is extended over the entire plane, the integral will be invariant with distance from the X ray tube and a geometry independent calibration coefficient can be derived.

Modern X ray diagnostic machines are often equipped with built-in KAP meters. This also includes devices which determine the air kerma–area product on the basis of X ray generator data (tube current and voltage) and the setting of the diaphragm. A hospital typically possesses a number of such machines and it is important that their KAP meters are calibrated for all relevant clinical situations in which the machines are used. The calibration of all KAP meters at the SSDL is not practical and in some cases not even possible. They must be calibrated in situ using a suitable method.

When calibrating the clinical KAP meter, the air kerma–area product should be determined for the X ray beam transmitted through the chamber and incident on the patient. A transmission chamber typically reduces the air kerma by 15–20%. In an under couch installation, the attenuation in the patient couch has to be considered and in situ calibration has to be performed separately for under couch and over couch installations.

In this Code of Practice, two methods of KAP meter calibrations have been adopted. The first method is based on the work of Shrimpton and Wall [IX.1], which uses a diagnostic dosimeter to measure the air kerma at the reference plane with a beam whose area has already been determined. The

second method uses a reference KAP meter calibrated at an SSDL for the calibration of a clinical KAP meter [IX.2, IX.3].

IX.3.2. Calibration using diagnostic dosimeter

The air kerma–area product is determined as the product of the air kerma on the central axis and the nominal beam area. For all clinically relevant radiation qualities, the KAP chamber is exposed for a given, fixed field size and its indication is measured together with the indication of a reference class diagnostic dosimeter positioned in the plane of measurement. A beam area of 100 mm × 100 mm at the position of the diagnostic dosimeter is recommended [IX.4].

IX.3.2.1. Over couch installation

The over couch installation procedure is as follows:

(1) Mount the KAP meter on the tube housing and connect it to a calibrated electrometer. If installations have a built-in KAP meter, then use this internal device.
(2) Place the detector of the calibrated diagnostic dosimeter on the central axis and 200 mm above the couch (table top) to avoid the influence of backscattered radiation. A block of Styrofoam can be used to support the detector (see Fig. IX.1(a)).
(3) Collimate the X ray beam so that its area at the position of the detector is approximately 100 mm × 100 mm.
(4) Expose the detector and the KAP meter using all combinations of tube voltage and total filtration occurring in the clinical applications (beam quality Q).
(5) Register signals from the KAP meter, M_Q^{KAP}, and the reference dosimeter, M_Q^{ref}.

For screen–film systems

(6) Remove the reference chamber and position a screen–film cassette (or a direct film) perpendicular to the central axis at the position of the reference detector.
(7) Expose the screen–film cassette or the film. The maximum optical density must not exceed 0.5.
(8) Develop the film and determine the nominal beam area, A, as the area contained within 50% of the maximum optical density. This can be

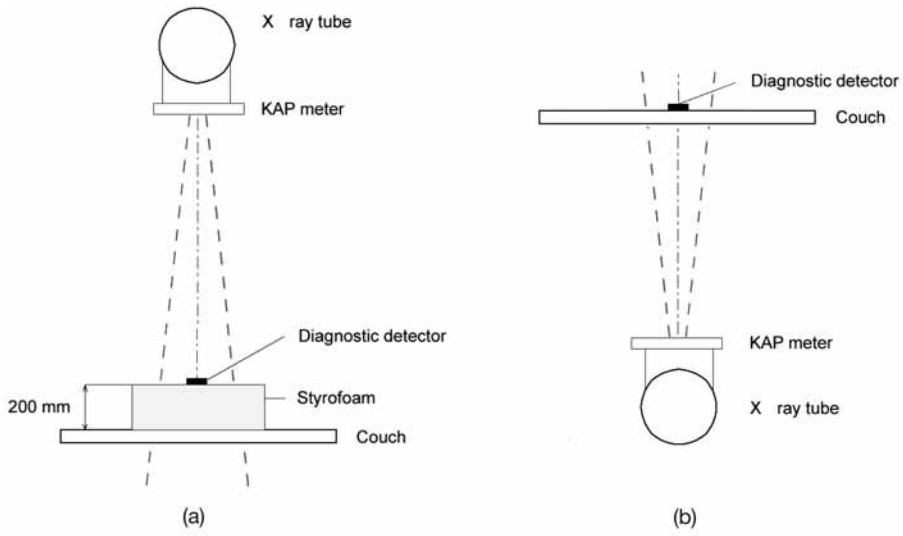

FIG. IX.1. Set-up for KAP meter calibrations: (a) is an over couch installation, Styrofoam being used to support the detector at a distance sufficient to avoid the effect of backscattered radiation, (b) is an under couch installation.

accomplished by using a scanning densitometer and a ruler or using the eye and a ruler.

For computed radiography systems

(6) Remove the reference chamber and position a computed radiography cassette perpendicular to the central axis at the position of the reference detector.
(7) Expose the cassette.
(8) Produce a 'soft' copy of an image and determine the nominal beam area, A, as the area contained within 50% of the maximum pixel value.

The calibration coefficient, $N_{P_{KA},Q}$, is calculated from the readings M_Q^{KAP} and M_Q^{ref} (corrected for air density if necessary) and the measured nominal beam area, A_{nom}, using Eq. (IX.2) that was obtained by modification of Eq. (IX.1). In this equation, N_{K,Q_0}^{ref} and k_Q^{ref} are the calibration coefficient of the reference dosimeter obtained at a beam quality Q_0 and the factor correcting for the difference of the response between beam qualities Q_0 and Q. The calculation applies to both over couch and under couch installations:

$$N_{P_{KA},Q} = \frac{M_Q^{ref}}{M_Q^{KAP}} N_{K,Q_0}^{ref} k_Q^{ref} A_{nom} \quad \text{(IX.2)}$$

IX.3.2.2. Under couch installation

The air kerma–area product, P_{KA}, value should be representative of that in the beam incident on the patient and thus take into account the attenuation in the couch as well as the scatter from the couch that may reach the patient. The couch may reduce P_{KA} by about 15–30% compared with the over couch situation [IX.5]. For under couch calibration of a KAP meter, the detector should be positioned on the table top[1] to reflect the beam attenuation and scattering by the table. The calibration set-up is shown in Fig. IX.1(b). Steps 3–8 as described for the over couch calibration procedure are also followed for the under couch situation.

NOTE: It has been assumed that the energy dependence of the response of the reference class dosimeter is negligible compared with that of the KAP chamber. Given the rather large energy dependence of KAP chambers, this assumption is usually fulfilled.

IX.3.3. Calibration using a reference KAP meter

A reference KAP meter calibrated at an SSDL can be used for the calibration of KAP meters in a hospital. The reference KAP meter should be calibrated for radiation incident on the KAP chamber (see Chapter 7) or, in the case that it is calibrated for transmitted radiation, the correction factor that corrects for the effect of attenuation in the KAP chamber should be supplied by the SSDL. The calibration of the reference KAP meter is required for a range of beam qualities characterized by the value of their HVL. Calibrations between two points can be interpolated to obtain the calibration coefficient for beam qualities available in the hospital. An extrapolation beyond the HVLs in the calibration certificate is not recommended.

Interpolation between two calibration points for the reference KAP meter can be used for a total filtration of up to 3 mm Al, irrespective of the X ray tube voltage. For beams with stronger filtrations, both HVL and the

[1] Many plane parallel detectors require that their entry window be oriented towards the X ray source. This has to be considered when positioning such a detector in the beam.

X ray tube voltage may be required to perform the interpolation. Pöyry et al. provide details on this calibration method [IX.2, IX.6].

IX.3.3.1. Over and under couch installations

A calibration set-up for both installations is the same as those shown in Fig. IX.1(a) and (b) except that the diagnostic detector is replaced by the reference KAP chamber. The calibration procedure described for the diagnostic dosimeter is followed.

The calibration coefficient, $N_{P_{KA},Q}$, is calculated from the readings M_Q^{KAP} and $M_Q^{KAP_{ref}}$ (corrected for air density) using Eq. (IX.3) that was obtained by modification of Eq. (IX.1). In this equation, $N^{ref}_{P_{KA},Q_0}$ is the calibration coefficient of the reference KAP meter obtained at a beam quality Q_0 and k_Q^{ref} the factor correcting for the difference of the response between beam qualities Q_0 and Q, where:

$$N_{P_{KA},Q} = \frac{M_Q^{KAP_{ref}}}{M_Q^{KAP}} N^{ref}_{P_{KA},Q_0} k_Q^{ref} \qquad \text{(IX.3)}$$

IX.4. CALIBRATION OF TLDs

IX.4.1. General

The TLDs should be calibrated against a diagnostic dosimeter using the substitution method. The dosimeters should be encapsulated in the same way as they are when used for measurements. The encapsulation should be thin and should not contain high atomic number elements. Typically, a thin Mylar foil is used to pack dosimeters into sachets. The TLDs are calibrated in terms of the air kerma under free in air geometry. This geometry is achieved by positioning sachets with dosimeters far from any scattering materials. It is recommended that they be attached to a sheet of card or polystyrene. They can also be fixed into a frame using adhesive tape.

The calibration of TLDs should be carried out at an air kerma level and with an X ray quality typical of those to which the dosimeters will be exposed during the course of measurements in the hospital. An incident air kerma of about 5–10 mGy and an X ray spectrum generated at around 80 kV with 3.0 mm Al total filtration will usually be appropriate for most situations. Special attention should be paid to the calibration of TLDs used for measurement of mammography X ray beams.

Various correction factors are needed for the interpretation of measurements made with TLDs, in particular the factor k_Q for correcting the energy dependence of the response of TLDs, the factor k_f for correcting for fading of dosimeters and the factor k_s for correcting for the individual sensitivity of dosimeters. These factors are established as part of the testing of the thermoluminescence system and they have to be re-established each time the parameters of the system that influence the correction factors change (mainly changes in annealing and readout parameters).

A thermoluminescence signal changes over time after the dosimeter's annealing owing to irradiation by background radiation (environmental radiation and radiation in workplaces). The measured signals from irradiated dosimeters should be corrected for this contribution. The value of a background signal can be reduced by keeping the dosimeters in a low background environment (shielding).

Details of measurement procedures with TLDs can be found elsewhere [IX.7].

IX.4.2. Selection of dosimeters

Since not all TLDs are manufactured to have the same efficiency with respect to thermoluminescence, their measured signals differ after irradiation to the same air kerma. A typical batch of TLDs has a variation coefficient of 10–15%. This variation can be reduced to about 1% using appropriate methods.

One possibility is to divide a batch of dosimeters into groups having similar sensitivities. Another possibility is to establish an individual sensitivity factor for each dosimeter in the batch. Both options are described below.

IX.4.2.1. Grouping TLDs

The purpose of grouping TLDs is to select those dosimeters having sensitivities within a given narrow interval. The following procedure can be used:

(1) Check TLDs for mechanical damage. Damaged dosimeters should be removed from the group.
(2) Set aside at least three TLDs to provide a background reading.
(3) Encapsulate dosimeters into sachets and place them into an irradiation position (use free in air geometry).
(4) Select exposure parameters of the X ray machine so that the resulting air kerma of about 5–10 mGy is achieved during the exposure. Expose the dosimeters.

(5) Remove the dosimeter sachets and arrange for the dosimeters to be read. Record the readings M_1, M_2,…., M_n from the exposed dosimeters and the readings M_{01}, M_{02} and M_{03} from the unexposed (background) dosimeters.

Selection

(1) Calculate the mean value of the background reading, $\bar{M}_0$, from background dosimeter readings M_{01}, M_{02} and M_{03} ($\bar{M}_0 = (M_{01} + M_{02} + M_{03})/3$).

(2) Calculate the mean value of background corrected dosimeter readings, $\bar{M}$, where:

$$\bar{M} = \frac{\sum_{i=1}^{n}\left(M_i - \bar{M}_0\right)}{n} \qquad \text{(IX.4)}$$

and standard deviation:

$$s\left(M_i\right) = \frac{\sum_{i=1}^{n}\left(M_i - \bar{M}_0\right)^2}{n-1} \qquad \text{(IX.5)}$$

(3) Identify outliers and remove them from the group. A practical way is to remove dosimeters whose background corrected reading ($M_i - \bar{M}_0$) is outside of the interval ($\bar{M} \pm 3s(M_i)$).

(4) For the remaining dosimeters, calculate the mean value of the background corrected reading. Divide the dosimeters into groups with those in the group having background corrected readings lying within a selected interval. Selecting too narrow an interval will result in a small number of dosimeters in the group. If the interval is too wide, the precision of measurements made with these dosimeters will be lower. The user should select the interval with due regard for the purpose of the measurement. A minimum of three groups should be selected; one group of dosimeters reading around the mean value and the other two groups comprising dosimeters with lower and higher readings.

IX.4.2.2. Group sensitivity factors

Group sensitivity correction factors of the *i*-th group, k_{si}, are calculated as:

$$k_{si} = \frac{\bar{M}}{\bar{M}^i} \tag{IX.6}$$

where the mean value $\bar{M}$ is calculated from readings of dosimeters after removing outliers and $\bar{M}^i$ is the mean value of background corrected readings for the *i*-th group of dosimeters.

IX.4.2.3. Individual sensitivity factors

Individual sensitivity factors of the *i*-th dosimeter, k_{si}, is calculated as:

$$k_{si} = \frac{\bar{M}}{M_i - \bar{M}_0} \tag{IX.7}$$

where the mean value is calculated for the remaining dosimeters after removing outliers.

IX.4.3. Procedure

It is suggested that use be made of dosimeters which have already had their individual sensitivity factors established for calibration of TLDs. The procedure is as follows:

(1) Set the detector of the reference dosimeter into a calibration position and measure the air kerma at the selected tube voltage and primary filtration (beam quality *Q*). The exposure time should be selected so that the resulting air kerma is about 5–10 mGy.
(2) Register the signal from the reference dosimeter, M_Q^{ref}.
(3) Set aside at least three TLDs to provide a background reading.
(4) Select three dosimeters and encapsulate them into a sachet. Position the sachet into the irradiation position.
(5) Expose the TLDs in the same manner as the reference dosimeter.

(6) Remove the sachet and arrange for the dosimeters to be read. Record the readings M_1, M_2 and M_3 from the exposed dosimeters and the readings M_{01}, M_{02} and M_{03} from the unexposed (background) dosimeters.

(7) Calculate the mean value of the background reading, $\bar{M}_0$, from background dosimeter readings M_{01}, M_{02} and M_{03} ($\bar{M}_0 = (M_{01} + M_{02} + M_{03})/3$).

(8) Calculate the mean value of the background corrected dosimeter readings, M_i ($i = 1, 2, 3$), as:

$$\bar{M}_Q = \frac{\sum_{i=1}^{3} k_{si}\left(M_i - \bar{M}_0\right)}{3} \tag{IX.8}$$

where k_{si} is the individual sensitivity factor for the i-th dosimeter.

The calibration coefficient of TLDs, $N_{K,Q}$, is calculated from the reading M_Q^{ref} (corrected for air density) and the mean value of the background corrected reading for TLDs, $\bar{M}_Q$, as:

$$N_{K,Q} = \frac{M_Q^{\text{ref}}}{\bar{M}_Q} N_{K,Q_0}^{\text{ref}} k_{Q_{\text{cross}}}^{\text{ref}} \tag{IX.9}$$

The calibration coefficient can be established each time the beam quality changes. It may be more practical to establish the calibration coefficient (N_{K,Q_0}) for the reference beam quality (Q_0) and factors (k_Q) correcting for changes in beam quality. Equation (IX.10) applies:

$$N_{K,Q} = N_{K,Q_0} k_Q \tag{IX.10}$$

REFERENCES

[IX.1] SHRIMPTON, P.C., WALL, B.F., An evaluation of the Diamentor transmission ionization chamber in indicating exposure–area product (R cm^2) during diagnostic radiological examinations, Phys. Med. Biol. **27** (1982) 871–878.

[IX.2] PÖYRY, P., KOMPPA, T., KOSUNEN, A., "Calibration of dose–area product meters for diagnostic X-ray beams", 39th Ann. Conf. Finn. Phys. Soc. (Proc. Conf. Helsinki, 2005), Finn. Phys. Soc., Helsinki (2005) 247.

[IX.3] PÖYRY, P., KOMPPA, T., KOSUNEN, A., “A tandem calibration method for kerma area product meters”, Quality Assurance and New Techniques in Radiation Medicine (Proc. Conf. Vienna, 2006), IAEA, Vienna.
[IX.4] NATIONAL RADIOLOGICAL PROTECTION BOARD, National Protocol for Patient Dose Measurements in Diagnostic Radiology, NRPB, Chilton (1992).
[IX.5] CARLSSON, C.A., ALM CARLSSON, G., “Dosimetry in diagnostic radiology and computerised tomography”, The Dosimetry of Ionizing Radiation (KASE, K.R., BJÄRNGARD, B.E., ATTIX, F.H., Eds), Academic Press, Orlando (1990) 163–257.
[IX.6] PÖYRY, P., KOMPPA, T., KOSUNEN, A., “X ray beam quality specification for kerma area product meters”, Quality Assurance and New Techniques in Radiation Medicine (Proc. Conf. Vienna, 2006), IAEA, Vienna.
[IX.7] ZOETELIEF, J., JULIUS, H.W., CHRISTENSEN, P., Recommendations for Patient Dosimetry in Diagnostic Radiology Using TLD, Rep. EUR 19604, European Commission, Luxembourg (2000).

GLOSSARY

anode angle. The angle between the directions of the electron beam in an X ray tube and the normal to the anode surface.

automatic exposure control (AEC). A mode of operation of an X ray machine by which the tube loading is automatically controlled and terminated when a preset radiation exposure to the imaging receptor is reached. The tube potential may or may not be automatically controlled.

backscatter factor (*B*). The ratio of the entrance surface air kerma to the incident air kerma.

beam, attenuated. X ray beam exiting the patient or phantom.

beam, unattenuated. X ray beam incident on the patient or phantom.

calibration. A set of operations that establish the relationship between values of quantities indicated by the instrument under reference conditions and the corresponding values realized by standards.

calibration coefficient (*N*). For a detector assembly with an associated measuring assembly, the coefficient that converts the indication, corrected to stated reference conditions, to the conventional true value of the dosimetric quantity at the reference point of the detector. For a detector calibrated on its own without a specified measuring assembly, the coefficient which converts the output (usually current or charge), corrected to reference conditions, to the dosimetric quantity at the reference point of the detector.

calibration of a diagnostic dosimeter. The comparison of the indication of the instrument under test with the conventional true value of the air kerma or air kerma rate with the objective of determining the calibration coefficient.

conditions, reference. For the purposes of this Code of Practice, the reference values for temperature, atmospheric pressure and relative humidity are as follows: ambient temperature: 20°C; atmospheric pressure: 101.3 kPa; relative humidity: 50%.

conditions, standard test. A value (or range of values) of the influence quantities or instrument parameters that are specified for the dosimetry of the radiation fields. It should be noted that the range of values for ambient temperature, atmospheric pressure and relative humidity are as follows: ambient temperature: 15–25°C; ambient pressure: 86–106 kPa; relative humidity: 30–75%. Working outside these ranges may result in reduced accuracy.

detector assembly. Comprises the detector and all other parts to which the detector is permanently attached, excluding the measuring assembly. For a cable connected detector, it includes the stem, the electrical fitting and any permanently attached cable or preamplifier. For a thin window ionization chamber, it includes any block of material in which the ionization chamber is permanently embedded.

detector orientation effect. Change in the response of the detector as the direction of radiation incidence is varied.

dosimeter, diagnostic. Equipment which uses ionization chambers and/or semiconductor detectors for the measurement of air kerma, air kerma length and/or air kerma rate in the beam of an X ray machine used for diagnostic medical radiological examinations.

dosimeter, thermoluminescent. A detector made of a material that emits visible light when heated after irradiation. The amount of light emitted is dependent upon the radiation exposure.

effective dose. The sum over all the organs and tissues of the body of the product of the equivalent dose, H_T, to the organ or tissue and a tissue weighting factor, w_T, for that organ or tissue, where:

$$E = \sum_T w_T H_T$$

The tissue weighting factor, w_T, for organ or tissue T represents the relative contribution of that organ or tissue to the total detriment arising from stochastic effects of uniform irradiation of the whole body.

energy, mean ($\bar{E}$).

$$\bar{E} = \frac{\int \phi_E(E) \left(\mu_{\text{en}}(E) / \rho \right) E^2 \, \mathrm{d}E}{\int \phi_E \left(\mu_{\text{en}}(E) / \rho \right) E \, \mathrm{d}E}$$

where $\phi_E(E)$ is the derivative of the fluence ϕ of the primary photons of energy E with respect to energy E, defined as

$$\phi_E(E) = \frac{\mathrm{d}\phi(E)}{\mathrm{d}E} \quad \text{and} \quad \left(\mu_{\text{en}}(E) / \rho \right)$$

is the mass energy absorption coefficient. In this Code of Practice the mean energy is defined as the energy averaged over the spectral air kerma. Sometimes the average is calculated over the spectral fluence or over the spectral energy fluence. For dosimetric purposes the definition given here is usually the most suitable.

entrance surface air kerma. The air kerma at a point in a plane corresponding to the entrance surface of a specified object, e.g. a patient's breast or a standard phantom. The radiation incident on the object and the backscattered radiation are included.

entrance surface dose. Absorbed dose in air, including the contribution from backscatter, assessed at a point on the entrance surface of a specified object.

exposure parameters. The settings of X ray tube voltage (kV), tube current (mA) and exposure time (s).

guidance level, diagnostic reference level. A level of a specified quantity above which appropriate action should be considered. In some circumstances, action may need to be considered when the specified quantity is substantially below the guidance or reference level.

heel effect. The non-uniform distribution of air kerma rate and of the beam hardness in an X ray beam in planes perpendicular to the beam axis and in the direction cathode to anode.

homogeneity coefficient (h). $h = \dfrac{\mathrm{HVL}_1}{\mathrm{HVL}_2}$

imaging device. A device used for imaging body anatomy. The X ray devices are assumed in this Code of Practice.

incident air kerma. The air kerma at a point in a plane corresponding to the entrance surface of a specific object, e.g. a patient's breast or a standard phantom. Only the radiation incident on the object and not the backscattered radiation is included.

influence quantity. Any external quantity that affects the result of the measurement (e.g. ambient temperature, pressure, humidity, radiation quality).

inherent filtration. The filtration provided by permanent materials through which the radiation beam must pass before emerging from the X ray tube. The definition of the term is found in IEC 61223-3-1:1999 and in IEC 61267:1994. An alternative term 'permanent filtration' defined in IEC 60522:1999 has not been used in this Code of Practice (see permanent filtration).

intrinsic error. The deviation of the measured value (i.e. the indicated value corrected to reference conditions) from the conventional true value of the measurand when the measuring instrument is subjected to a specified reference radiation under specified reference conditions.

intrinsic error, relative. The ratio of intrinsic error to the conventional true value.

ionization chamber. A detector filled with a suitable gas, in which an electric field (insufficient to induce gas multiplication) is provided for the collection of charges associated with the ions and the electrons produced in the sensitive volume of the detector by the ionizing radiation. The ionization chamber includes the sensitive volume, the collecting and polarizing electrodes, the guard electrode (if any), the chamber wall, the parts of the insulator adjacent to the sensitive volume and any necessary build-up caps to ensure electron equilibrium.

ionization chamber, diagnostic field class. A detector used to measure levels of radiation from common medical diagnostic X ray sources in the field and capable of being calibrated to within an uncertainty of 5% (coverage factor $k = 2$) for the conventional X ray range (50–150 kV) or for the mammography range of X ray tube voltages (22–40 kV).

ionization chamber, diagnostic reference class. A detector capable of being calibrated in diagnostic beams (50–150 kV) and in mammography beams (22–40 kV) to within an uncertainty of 3.2% (k = 2) and possessing a record of long term stability of better than 0.5% change per year.

ionization chamber, vented. An ionization chamber constructed in such a way as to allow the air inside the sensitive volume to communicate freely with the atmosphere such that corrections to the response for changes in air density need to be made. Sealed chambers are not suitable for dosimetry in diagnostic radiology because the necessary wall thickness of a sealed chamber may cause an unacceptable energy dependence of the response and because the long term stability of sealed chambers is not guaranteed.

kerma area product. Product of the area of a cross-section of a radiation beam and the average value of a kerma related quantity over that cross-section. This quantity is available clinically either by direct measurement with a KAP meter or by calculator and display on a KAP indicator.

leakage current. Total detector current flowing at the operating bias in the absence of radiation.

linearity, deviation from (δ). Percentage deviation from linearity given by $\delta = 100(mQ/Mq - 1)$, where M and Q refer to the indication and input at a chosen reference point, respectively; m is the indication observed for some other input signal q. For multirange instruments, the above definition is applicable to each range.

mean (average) glandular dose. The mean absorbed dose in the glandular tissue (excluding skin) in a uniformly compressed breast of, for example, 50% adipose, 50% glandular tissue composition. The reference breast thickness should be specified.

measuring assembly. A device for measuring the current or charge from the detector and converting it into a form suitable for display, control or storage.

medical exposure. Exposure applying to patients as part of their own medical diagnosis or treatment, individuals as part of occupational health surveillance, individuals as part of health screening programmes, healthy individuals or patients voluntarily participating in medical or biomedical,

diagnostic or therapeutic programmes and individuals as part of medico-legal procedures.

monitor. An instrument used to monitor the stability of the air kerma rate during irradiation or to compare values of air kerma after successive irradiations.

optical density. The degree of blackening of processed X ray or photographic film. Numerically equal to the decadal logarithm of the ratio of light incident on the film to that transmitted through the film.

patient dose (exposure). A generic term used for a variety of quantities applied to a patient or group of patients. The quantities are related and include absorbed dose, incident air kerma, entrance surface air kerma, etc.

permanent filtration. This term is defined in IEC 60522:1999. The definition is similar to that used for inherent filtration. This Code of Practice uses the term inherent filtration in preference to permanent filtration (see inherent filtration).

phantom. An object used to absorb and/or scatter radiation equivalent to that of a patient and hence to aid estimation of radiation doses and test imaging systems without actually exposing a patient. It may be an anthropomorphic or a physical test object.

point of test. The point at which the reference point of the detector is placed for calibration purposes and at which the conventional true kerma rate is known.

polymethylmethacrylate (PMMA). A polymer plastic commercially available as Perspex or Lucite.

practical peak voltage ($\hat{U}$). Weighted mean of the X ray tube potential according to:

$$\hat{U} = \frac{\int_{U_{\min}}^{U_{\max}} p(U)w(U)U\,\mathrm{d}U}{\int_{U_{\min}}^{U_{\max}} p(U)w(U)\,\mathrm{d}U}$$

where $p(U)$ is the distribution function for the voltage, U, and $w(U)$ is a weighting function, U_{max} is the highest voltage in the interval and U_{min} is the lowest voltage in the interval. The unit of the quantity practical peak voltage is the volt (V). Additional information on the practical peak voltage and the weighting function $w(U)$ is provided in Appendix IV. Using this weighting function, $w(U)$, the practical peak voltage will be defined as the constant potential which produces the same air kerma contrast behind a specified phantom as the non-DC voltage under test.

primary radiation. Radiation emitted by the X ray tube.

radiation effect, deterministic. A radiation effect for which generally a threshold level of dose exists above which the severity of the effect is greater for a higher dose.

radiation effect, stochastic. A radiation effect, generally occurring without a threshold level of dose, whose probability is proportional to the dose and whose severity is independent of the dose.

radiation quality. A measure of the penetrative power of an X ray beam, usually characterized by a statement of the tube potential and the HVL.

reference instrument. A secondary standard calibrated with primary standards by a primary standards laboratory or at an acknowledged reference laboratory that holds appropriate standards. Alternatively, the secondary standards, if they are national standards, may be calibrated by the BIPM in Paris. Where the reference instrument is not a secondary standard, it should be calibrated against a secondary standard.

reference point of a detector. The point of the detector to which the measurement of the distance from the radiation source to the detector at a given orientation refers. The reference point should be marked on the assembly by the manufacturer of the instrument. If this proves impossible, the reference point should be indicated in the accompanying documentation supplied with the instrument.

response. The ratio between the indication of the measuring assembly and the conventional true value of the measured quantity at the position of the reference point in space. The response under reference conditions is the inverse of the calibration coefficient.

response time. The time interval between the instant when a stimulus is subjected to a specified abrupt change and the instant when the indication reaches and remains within specified limits of its final steady value.

s**emiconductor detector.** A device that uses a semiconductor to detect and measure the number of charge carriers set free in the detector by ionizing radiation.

standard breast. A model used for calculations of glandular dose consisting of a 40 mm thick central region comprising a 50:50 mixture by weight of adipose tissue and glandular tissue surrounded by a 5 mm thick superficial layer of adipose tissue. The standard breast is semicircular with a radius of >80 mm and a total thickness of 50 mm.

standard, national. A standard of a particular quantity that is recognized by an official national decision as the basis for fixing the value, in a country, of all other standards of the given quantity.

standard, primary. A standard of a particular quantity which has the highest metrological qualities in a given field.

standard, reference. A standard of a particular quantity available at a given location (organization), from which all measurements made at that location are derived.

standard, secondary. A standard, the value of which is fixed by direct or indirect comparison with a primary standard.

standard, working. A standard that is used for routine calibrations at the calibration laboratory.

standards dosimetry laboratory, primary (PSDL). A laboratory possessing one or more primary standards.

standards dosimetry laboratory, secondary (SSDL). A laboratory possessing one or more secondary standards.

tissue equivalent material. Material which absorbs and scatters a specified ionizing radiation to the same degree as a particular biological tissue.

tissue weighting factor. A dimensionless factor used to weight the equivalent dose in a tissue or organ.

traceability. The property of a result, measurement or standard whereby it can be related to a stated reference (usually a national or international standard) through an unbroken chain of comparisons, all of which have stated uncertainties.

true value. A value which characterizes a quantity perfectly as defined, in the conditions which exist when that quantity is considered**.**

true value, conventional. The value of a quantity which, for a given purpose, may be substituted for the true value. A conventional true value is, in general, regarded as sufficiently close to the true value for the difference to be insignificant for a given purpose.

tube current–exposure time product (mA·s). The product of X ray tube current (mA) and the exposure time in seconds (*s*).

tube loading. The tube current–exposure time product that applies during a particular exposure.

uncertainty of measurement. A parameter, associated with the result of a measurement, that characterizes the dispersion of values that could be reasonably attributed to the measurand.

X ray spectrum. The distribution of the intensity of the X rays (or the number of photons) according to wavelength, frequency or energy.

X ray tube. Vacuum tube designed to produce X rays by bombardment of the anode with a beam of electrons accelerated through a potential difference.

X ray tube shielding. A fixed or mobile panel or housing intended to reduce scattering from the X ray tube.

X ray tube voltage. The potential difference applied between the cathode and the anode of an X ray tube. The X ray tube voltage may vary as a function of time.

X ray tube voltage ripple (*r*). The ratio, expressed as a percentage, defined for a given current by the formula:

$$r = \frac{U_{\max} - U_{\min}}{U_{\max}} 100\%$$

where $U_{\max}$ is the maximum value and $U_{\min}$ the minimum value between which the voltage oscillates.

X ray unit. Assembly comprising a high voltage supply, an X ray tube with its protective housing and high voltage electrical connections.

zero drift. Slow variation with time of the indication of the measuring assembly when the input is short circuited.

zero shift. Sudden change in the scale reading of either polarity of a measuring assembly when the setting control is changed from the 'zero' mode to the 'measure' mode, with the input connected to a detector in the absence of ionizing radiation other than background radiation.

CONTRIBUTORS TO DRAFTING AND REVIEW

Alm Carlsson, G.	Linköping University, Sweden
Angerstein, W.	Consultant, Germany
Arnold, D.	St. George's Hospital, United Kingdom
Collins, L.	Westmead Hospital, Australia
Dance, D.R.	The Royal Marsden NHS Foundation Trust, United Kingdom
DeWerd, L.	University of Wisconsin, United States of America
Drexler, G.	GSF-National Research Center for Environment and Health, Germany
Fransson-Andreo, A.	Karolinska University Hospital, Sweden
Heggie, J.	St Vincents Hospital, Australia
Herrnsdorf, L.	RTI Electronics AB, Sweden
Horáková, I.	National Radiation Protection Institute, Czech Republic
Järvinen, H.	Radiation and Nuclear Safety Authority, Finland
Komppa, T.	Radiation and Nuclear Safety Authority, Finland
Kosunen, A.	Radiation and Nuclear Safety Authority, Finland
Kramer, H.-M.	Physikalisch-Technische Bundesanstalt, Germany
Le Heron, J.	New Zealand Radiation Laboratory, New Zealand
Leitz, W.	Swedish Radiation Protection Authority, Sweden
McLean, I.D.	International Atomic Energy Agency
Meghzifene, K.	The Medical University of Vienna, Austria

Msimang, Z.	Centre for Scientific and Industrial Research, South Africa
Nowotny, R.	The Medical University of Vienna, Austria
O'Brien, M.	National Institute of Standards and Technology, United States of America
Ortiz Lopez, P.	International Atomic Energy Agency
Ng, K.-H.	University of Malaysia, Malaysia
Pernička, F.	National Radiation Protection Institute, Czech Republic
Pöyry, P.	Radiation and Nuclear Safety Authority, Finland
Regulla, D.	GSF-National Research Center for Environment and Health, Germany
Shrimpton, P.	Health Protection Agency, United Kingdom
Smyth, V.	New Zealand Radiation Laboratory, New Zealand
Spelic, D.	Food and Drug Administration, United States of America
Tapiovaara, M.	Radiation and Nuclear Safety Authority, Finland
Unfors, T.	Unfors Instruments AB, Sweden
Vañó, E.	Complutense University, Spain
Wagner, L.	The University of Texas, United States of America
Wall, B.	Health Protection Agency, United Kingdom
Wilson, C.	Medical College of Wisconsin, United States of America
Witzani, J.	BEV—Federal Office of Metrology and Surveying, Austria
Zoetelief, H.	Delft University of Technology, Netherlands

Consultants Meetings

Vienna, Austria: 10–14 May 1999, 6–10 November 2000,
8–12 December 2003, 11–15 July 2005

Research Coordination Meetings

Vienna, Austria: 14–18 May 2001, 13–17 January 2003

This Code of Practice is intended to support those working in the field of diagnostic radiology dosimetry, both in standards laboratories involved in the calibration of dosimeters and also in clinical centres and hospitals where patient dosimetry and quality assurance measurements are of vital concern. As such it covers diverse dosimetric situations corresponding to the range of examinations found clinically and includes guidance on dosimetry for general radiography, fluoroscopy, mammography, computed tomography and dental radiography. The material is presented in a practical way, with guidance worksheets and examples of calculations. More detailed aspects of diagnostic radiology dosimetry are discussed in the appendices.

INTERNATIONAL ATOMIC ENERGY AGENCY
VIENNA
ISBN 92–0–115406–2
ISSN 0074–1914